Techniques to Measure the NC Background in the SNO Experiment

Heidi Heron
St John's College, Oxford

Thesis submitted for the degree of Doctor of Philosophy

Hilary Term 1998

Abstract

The Sudbury Neutrino Observatory (SNO) is a solar neutrino detector which is currently under construction in Sudbury, Canada. This experiment is unique amongst solar neutrino experiments in that it can seperately measure the rate of electron neutrinos which come from the Sun and, via a neutral current (NC) interaction, the total rate of electron, muon and tau neutrinos. This is important because the SNO experiment can therefore show if neutrinos coming from the Sun are oscillating into different flavours before they reach the Earth, irrespective of the total solar neutrino flux.

The observation of neutrino oscillations is of great importance since they require neutrinos to have a small, finite mass. If this is found to be true then the Standard Model of Particle Physics will need to be extended since it assumes all neutrinos to be massless. The reasons for this assumption and the results of several experiments which are trying to observe neutrino masses are discussed.

The best evidence for neutrinos having mass comes from solar neutrino measurements. There have been five experiments to date which have measured the rate of electron neutrinos coming from the Sun. They have all observed a deficit when the measured rate is compared to the rate predicted by solar models. The reasons why this deficit is thought to be most easily explained by neutrino oscillations are presented and the reliability of the results of these five solar neutrino experiments is discussed along with the expected ability of the SNO experiment to show whether or not neutrino oscillations are occuring.

To achieve its objective the SNO experiment has to fully understand any sources of backgrounds to NC neutrino interactions. These backgrounds are primarily caused by the presence of natural radioactivity in the 1000 tonnes of heavy water (or magnesium chloride solution) which makes up the SNO detector target. The existing techniques to measure NC backgrounds are summarised before describing in detail the new radiochemical techniques that had to be developed to enable an assay for the most critical isotope, ^{212}Pb.

A novel procedure to manufacture sources of ^{212}Pb is also explained. These sources were shown, at production, to be free from any long-lived activity and so they can be used within the SNO experiment to calibrate ^{212}Pb extraction efficiencies. Such calibrations are shown to be necessary to ensure an accurate assay of ^{212}Pb and hence an accurate measurement of the most significant component of the NC background in the SNO experiment.

Acknowledgements

The completion of this thesis has been aided by many colleagues both at Oxford University and at the Brookhaven National Laboratory (BNL), New York, USA. At Oxford many thanks go to the SNO Water Group consisting of Neil Tanner, Richard Taplin, Peter Trent, Will Locke, Barrie Knox, George Doucas and latterly Martin Moorhead and Nick Jelley. I have Neil Tanner to thank for being my initial supervisor and providing me with interesting insights into the worlds of Particle Physics and Accountancy. Richard Taplin and Peter Trent offered much helpful advice as well as instruction in various counting techniques and in using ultra-filtration membranes. My first wary steps into using radiochemical techniques were aided by Will Locke, the chemist. Barrie Knox and George Doucas both provided excellent technical advice with Barrie also being a great source of information and assistance. I would also like to thank Martin Moorhead for always showing an interest in this work and for providing much encouragement and advice. Finally, I wish to thank Nick Jelley for his increased interest into the activities of the Water Group and for his willingness to assist in the completion of this thesis.

I would also like to thank the members of the SNO experiment based at Oxford who are not members of the Water Group. These include numerous graduate students with whom I had the pleasure of sharing an office and, in particular, Dave Wark who was a great source of encouragement and gave me an education into the broader aspects of the SNO experiment and numerous other interesting topics.

There have also been many others in the Oxford Physics Department, who are not directly connected to the SNO experiment, who have assisted the completion of this thesis. Firstly, without the assistance of many of the workshop staff it would have been impossible to construct the apparatus needed and so thank go to Mick Williams, Colin Graham, Tony Handford and their colleagues who are too numerous to mention here. Secondly, I must thank Beverly Roger and Del Batts for their patience and assistance in organising the many overseas trips that this research required. Finally, it has to be noted that without the tea-ladies nothing would have been achieved.

Outside of the Oxford Physics Department thanks goes to Richard Darton of the Engineering Department for his advice on Chemical Engineering and Chris Jackson of the Geography Department for analysing stable lead samples.

At BNL much thanks has to go to Keith Rowley, Richard Hahn and John Boger and their technical support staff for their hospitality in assisting me with the latter stages of my research. Particular gratitude goes to Keith Rowley for firstly taking an interest in my research and then being a source of both advice and inspiration during its completion. It was a great pleasure to work alongside a true guru in the world of solar neutrino physics. My time at BNL would not have been possible without the efforts of Richard Hahn who also helped to obtain and count radioactive sources, many thanks. The assistance of John Boger in setting up some $\beta - \alpha$ counters at BNL was invaluable and greatly appreciated.

On a personal level I owe much thanks to my friends and family who have supported me throughout the completion of this research. On a larger scale I thank God for creating everything in this world, including the elusive neutrino, and for giving us minds sufficient to investigate and understand it.

Finally, thanks goes to PPARC for funding this research and the Department of Particle Physics at Oxford University for providing the resources that were needed.

Contents

Chapter 1

Do Neutrinos have Mass?

1.1 Introduction

The existence of neutrinos as light, neutral particles was first postulated by Pauli in 1930 in his now famous letter to a physics meeting in Germany to solve the problem of energy conservation in beta decay [Bro78]. Neutrino physics was born to experimental Particle Physicists in the 1950's by the discovery of the electron anti-neutrino by Reines and Cowan [Cow56]. Since that time there have been many experiments conducted to observe neutrinos. Measurements of the width of the Z^0 mass peak began in 1989 (see [LEP89]) and have since been improved to show without doubt that there are three distinct light neutrinos. These three neutrino flavours match the three families of the other fundamental particles and all of these particles have been incorporated into the Standard Model of Particle Physics which describes how they interact.

The interactions of neutrinos in the Standard Model are governed by the electroweak theory and this theory has been proven to be extremely accurate by numerous experimental results. Neutrinos are assumed by this model to be massless because initial experiments showed that if they do have finite masses they are much much smaller than the masses of the other fermions. A possible theoretical model to account for very small neutrino masses, the see-saw effect, will be summarised in this chapter together with the phenomenon of neutrino oscillations which can occur if neutrinos have a finite mass.

After this theoretical discussion the results of various experiments which are trying to measure neutrino masses will be examined. This will include the results from experiments which can directly measure neutrino masses and experiments which can indirectly determine if neutrinos have a small, finite mass by searching for neutrino oscillations.

1.2 A Theoretical Discussion

1.2.1 Possibilities of Neutrino Masses

In this section there is a brief summary of the mechanisms in the Standard Model which give fermions their masses and of a possible theoretical model which would predict neutrinos having masses very much smaller than the other fermions.

The electroweak Lagrangian is invariant under $SU(2)_L \times U(1)_Y$ and as such mass terms like: $-m\bar{\phi}\phi$, cannot be simply added to the interaction terms in the Lagrangian since this term is not gauge invariant. Fermion masses within the Standard Model are generated by adding to the Lagrangian coupling terms between the fermions and the Higgs doublet. In Equation 1.1 the terms that must be included in the Lagrangian to give the electron its mass are shown.

$$\mathcal{L} = -G_e \left[(\overline{\nu}_e, \overline{e})_L \begin{pmatrix} \phi^+ \\ \phi^0 \end{pmatrix} e_R + \overline{e}_R (\phi^-, \overline{\phi^0}) \begin{pmatrix} \nu_e \\ e \end{pmatrix}_L \right] \tag{1.1}$$

By spontaneously breaking the symmetry only two terms remain in the Lagrangian and these are shown in Equation 1.2 in terms of the vacuum expectation value, v. This procedure of spontaneous symmetry breaking is described in many texts such as [Hal84].

$$\mathcal{L} = -m_e \overline{e} e - \frac{m_e}{v} \overline{e} e h \tag{1.2}$$

The first term in Equation 1.2 generates the electron mass whereas the second term is a coupling term between the electron and the neutral Higgs scalar. Although the Higgs mechanism does allow masses to be generated for all the fermions it does not predict what these masses will be.

The Standard Model does not generate neutrino masses, by choice, simply by not including the existence of right handed neutrinos. This prevents the coupling to the Higgs doublet which was used above to generate the electron mass. The Standard Model can be extended to include right handed neutrinos which would allow neutrino masses to be generated in the same way as the other fermions in the Standard Model. Unfortunately by using the same mechanism to generate neutrino mass it is difficult to understand the difference between the very small mass of neutrinos, if indeed they have a mass at all, and the masses of the other fermions.

There is a theoretical model which generates very small neutrino masses and this starts from the fact that, unlike all the other fermions, neutrinos do not carry any electromagnetic charge.

All of the fermions in the Standard Model are assumed to be Dirac particles which can be described by four component spinors consisting of the two spin states of the particle and its anti-particle. It is obvious that by using a Lorentz transformation the helicity of a particle can be changed, however the electric charge is invariant. This means that if one observes a charged particle in one frame by boosting to another frame one might see a different helicity but it will always be a particle not an anti-particle.

It can be seen that there is an ambiguity if the original particle is an uncharged massive neutrino since the particle in the new frame can be either a neutrino of opposite helicity or an anti-neutrino of opposite helicity since there is no charge conservation to prevent the latter occurring. If this latter does occur the neutrino is its own anti-particle, called a Majorana particle, and then it can be completely described by a two component spinor.

By adding to the Standard Model right-handed neutral fields for each charged lepton: N_{lR}, we can develop a full theory which encompasses the possibility of both Dirac and Majorana neutrinos. The most general gauge invariant Lagrangian which gives mass terms for N generations of neutrinos, in the Majorana basis of field and conjugate field, is given in Equation 1.3, as explained in [Moh91].

$$-\mathcal{L} = \frac{1}{2} \left(\overline{\nu}_L \overline{\widehat{N}}_L \right) \begin{pmatrix} \mathbf{0} & \mathbf{M} \\ \mathbf{M^T} & \mathbf{B} \end{pmatrix} \begin{pmatrix} \widehat{\nu}_R \\ N_R \end{pmatrix} + h.c. \tag{1.3}$$

The off diagonal terms given by the $N \times N$ matrices $\mathbf{M}$ and $\mathbf{M^T}$ are called the Dirac mass terms and the values of these terms come from the Higgs mechanism as has already been discussed. The diagonal term, the matrix $\mathbf{B}$, is called the Majorana mass term and it couples the right handed neutrino fields. This coupling is gauge invariant because the N_{lR} and its conjugate field, $\widehat{N}_{lL}$ are both invariant under $SU(2)_L \times U(1)_Y$. This kind of term for the charged leptons would violate electromagnetic gauge symmetry whereas for neutrinos it only leads to the violation of B-L number (Baryon number - Lepton number). Such a violation can be permitted since it does not effect any of the dynamics of the Standard Model.

If just one generation of neutrinos is considered the matrices: $\mathbf{M}$ and $\mathbf{B}$, reduce to simple numbers: M and B. It is then relatively easy to find expressions for the eigenvalues of the mass matrix and the

results are shown in Equation 1.4 together with approximate values for the two masses when it is assumed that $B \gg M$.

$$m_\nu = \frac{1}{2}\left(\sqrt{B^2 + 4M^2} \pm B\right) \Rightarrow m_1 \simeq \frac{M^2}{B} \quad ; \quad m_2 \simeq B \tag{1.4}$$

The value of M is generated by the Higgs mechanism as was discussed above and so it would be expected to be of the same order as the masses of the other fermions in that generation, say a few GeV at most. The value of B is expected to be at energies of Grand Unified Theories, say 10^{15}GeV, since there is no known mechanism to break the symmetry of right-handed neutrinos in the Standard Model. Hence, the assumption that $B \gg M$ is reasonable.

The mass generating mechanism explained above is called the 'see-saw mechanism'. It generates a hierarchy of three very light left-handed neutrinos at the expense of the production of three extremely heavy right-handed neutrinos by allowing the violation of B-L number and the existence of Majorana neutrinos.

1.2.2 Vacuum and Matter Enhanced Neutrino Oscillations

If neutrinos do have finite masses there is no reason for the mass eigenstates to be the same as the three flavour eigenstates. Indeed it is well known that in the quark sector the weak eigenstates are rotated with respect to the strong eigenstates and values for the mixing angles between the three generations have been measured by numerous experiments.

If a similar behaviour is true in the lepton sector, which requires the violation of leptonic charge conservation within families, then neutrino mixing can occur. This means that there is a finite probability that a neutrino of certain flavour will, after a period of time, oscillate into a different flavour.

The probability of an electron neutrino oscillating into a different neutrino as it travels a distance, R, in vacuum can be determined by evolving the flavour eigenstates in time. An expression for this probability for the simple case of just two neutrino flavours is given in Equation 1.5 in terms of a mixing angle, θ, and an oscillation length, $L = 4\pi E_\nu / \Delta m^2$.

$$P(\nu_e \rightarrow \nu_x) = 1 - \sin^2 2\theta \sin^2(\pi R/L) \tag{1.5}$$

Although Equation 1.5 is true for neutrinos which travel through a vacuum, the simple formula has to be altered when the neutrinos travel through matter since the electron neutrinos behave differently in matter to muon and tau neutrinos because they can undergo charged current scattering as well as neutral current scattering. The effect of matter on neutrino oscillations was first investigated by evaluating the Hamiltonian for the scattering and adding it to the Hamiltonian generating the equations of motion in a vacuum by Wolfenstein [Wol78]. This alters the survival probability of an electron travelling through constant density matter to the expression given in Equation 1.6 which is taken from [Ros87]. This expression is a function of parameters whose definitions are given in Equation 1.7 in terms of the weak coupling constant, G_F, and the density of electrons in the matter, N_e.

$$P(\nu_e \rightarrow \nu_x) = 1 - \sin^2 2\theta_M \sin^2(\pi R/L_M) \tag{1.6}$$

$$\begin{aligned} \sin^2 2\theta_M &= sin^2 2\theta/[sin^2 2\theta + (L/L_0 - \cos 2\theta)^2] \quad ; \quad L = 4\pi E_\nu/\Delta m^2 \\ L_M &= L/[sin^2 2\theta + (L/L_0 - \cos 2\theta)^2]^{1/2} \quad ; \quad L_0 = 2\pi/\sqrt{2} G_F N_e \end{aligned} \tag{1.7}$$

The main difference that occurs by adding the matter interactions is that the matter mixing angle, θ_M, is dependent upon a function of the vacuum mixing angle, the density of electrons in the matter and the energy of the neutrinos. This means that even for very small vacuum mixing angles the effect on neutrino survival probabilities can be very large for certain energy neutrinos.

The effect of matter oscillations is even more complicated in the case where the density of the matter traversed by the neutrinos is not constant, for example in the case of neutrinos propagating from the interior to the exterior of the Sun. In 1985 Mikheyev and Smirnov found that neutrino oscillations in variable density matter could be enhanced and this is called the MSW effect [Mik85]. They found that for some neutrino energies it is possible to have complete conversion of electron neutrinos to muon or tau neutrinos.

1.3 Experimental Measurements

1.3.1 Direct Limits on Neutrino Masses

Limits upon the masses of neutrinos have been obtained directly by various experimental methods. The tightest upper limits on the mass of the electron neutrino, m_{ν_e}, come from the measurements of tritium beta decay spectra. There have been numerous limits placed on $m^2_{\nu_e}$ by fitting the energy dependence of Kurie plots for tritium decay, however the derived results may not be entirely reliable due to unknown systematics. The most recent published limits on the electron neutrino mass from tritium beta decay experiments are given in Equation 1.8.

$$m_{\nu_e} < 5.6eV(95\%CL\ MAINZ)[\text{Bon96}] \quad ; \quad m_{\nu_e} < 3.9eV(95\%CL\ TROITSK)[\text{Lob96}] \tag{1.8}$$

The limits in Equation 1.8 are for the mass of the electron neutrino independent of whether neutrinos are Dirac or Majorana particles. Upper limits for the mass of a Majorana electron neutrino, $m^M_{\nu_e}$, can be found by measuring the rate of neutrinoless double beta decay. There are several candidate atoms from which these decays could be observed and there are a number of experiments searching for evidence of neutrinoless double beta decay using these atoms, see Figure 10 of [Kla96]. To date, no evidence of neutrinoless double beta decay has been found which means that there is, as yet, no evidence of that neutrinos are Majorana particles. However, the measured limits on the half-lives of these decays allow corresponding limits to be calculated for the mass of Majorana neutrinos and the best limit at present is produced by the Heidelberg-Moscow experiment, which uses ^{76}Ge. This result is given in Equation 1.9.

$$m^M_{\nu_e} < 0.46eV(90\%CL)[\text{Bau97}] \tag{1.9}$$

The best limit for the mass of the muon neutrino is obtained by momentum analysis of pion decay and the most recent published limit is given in Equation 1.10.

$$m_{\nu_\mu} < 170keV(90\%CL)[\text{Ass96}] \tag{1.10}$$

The LEP accelerator has provided the means to place bounds upon the tau neutrino mass by reconstructing tau decays to pions. There are four published limits from the three LEP experiments: ALEPH, DELPHI and OPAL and these limits are shown in Equation 1.11, as taken from [Pas97].

$$\begin{aligned} m_{\nu_\tau} < 23.1MeV(95\%CL\ ALEPH\ 5\pi^\pm/5\pi^\pm\pi^0) \quad ; \quad m_{\nu_\tau} < 25.7MeV(95\%CL\ ALEPH\ 3\pi^\pm) \\ m_{\nu_\tau} < 29.3MeV(95\%CL\ DELPHI\ 3\pi^\pm) \quad ; \quad m_{\nu_\tau} < 35.3MeV(95\%CL\ OPAL\ 3\pi^\pm) \end{aligned} \tag{1.11}$$

Alongside these direct, experimental bounds it is possible to place bounds on neutrino masses by considering primordial nucleosynthesis since neutrino masses affect predictions of primordial helium abundance by altering the rate of reactions holding the neutrons and protons in equilibrium.

These predicted bounds are functions of the number of extra neutrino species during nucleosynthesis given by: $\Delta N_\nu = N_\nu - 3$. Assuming massless electron neutrinos and the weak bound that $\Delta N_\nu < 1$, bounds on Majorana and Dirac neutrino masses can be calculated and are given in Equation 1.12, as taken from [Fie97].

$$\begin{array}{lll} m_\nu^D > 25MeV & ; \quad m_{\nu_\tau}^D < 0.37MeV & ; \quad m_{\nu_\mu}^D < 0.31MeV \\ m_\nu^M > 32MeV & ; \quad m_{\nu_\tau}^M < 0.95MeV & ; \quad m_{\nu_\mu}^M < 0.95MeV \end{array} \tag{1.12}$$

These limits are not compatible with the tightest upper mass limits for the tau neutrino mass as given in Equation 1.11. To produce an agreement between the experimental bound and the nucleosynthesis bound the mass of the tau neutrino must lie below about 1MeV [Ell96].

In summary, the measured limits on neutrino masses together with the bounds due to nucleosynthesis show that if neutrinos do have a mass then it is extremely small when compared to the other fermions in its generation and this is a possible motivation for the see-saw mechanism as was described in the last section.

One final severe constraint for the mass of stable neutrinos can be made if it is assumed that the mass density of the universe is less than the critical density, as is favoured by theories of cosmological inflation. This limit is derived from General Relativity and is given in Equation 1.13 where it is assumed that the present Hubble expansion rate, H_0, is about $50\text{kms}^{-1}\text{Mpc}^{-1}$.

$$m_\nu < 92H_0^2 \times 10^{-4}eV \simeq 23eV \text{[Ell96]} \tag{1.13}$$

1.3.2 Searches for Neutrino Oscillations

Introduction

There have been many experiments searching for neutrino oscillations in a number of different parameter regions since an observation of neutrino oscillations would be evidence that neutrinos possess a small but finite mass. It can be seen from Equation 1.5 on page 3 that depending upon the energies of the neutrinos involved and the distance through which they propagate different vacuum mixing angles can be investigated. There are three main sources of neutrinos: neutrinos produced by terrestrial sources including nuclear reactors and man-made neutrino beams, neutrinos produced in the atmosphere by cosmic rays scattering off nuclei and finally, neutrinos produced in the fusion reactions of the Sun.

The oscillation length, L, for vacuum neutrino oscillations was given in Equation 1.5 on page 3 as a function of the energy of the neutrinos involved, E_ν, and the squared mass difference between the two neutrino mass eigenstates undergoing the oscillations, Δm^2. It is therefore possible to determine the region of Δm^2 values to which a particular experiment is sensitive. The formula given in Equation 1.14 gives the value of Δm^2 in eV^2 as a function of the distance from the source of the neutrinos, R in metres, and the energy of the neutrinos, E_ν in MeV.

$$\Delta m^2(eV^2) = \frac{2.5E_\nu(MeV)}{R(metres)} \tag{1.14}$$

Using this formula it can be calculated that, due to the high energies of man-made neutrinos and the low distances involved in most terrestrial experiments, accelerator and reactor experiments can investigate neutrino oscillations if Δm^2 is greater than about $1eV^2$. It can also be calculated that atmospheric neutrino experiments can investigate neutrino oscillations if Δm^2 lies between about $10^{-1}eV^2$ and $10^{-4}eV^2$. Finally, due to the very large distances involved, it can be calculated that solar neutrino experiments can investigate vacuum oscillations if Δm^2 lies between about $10^{-10}eV^2$ and $10^{-11}eV^2$. However, since solar neutrinos have to propagate through the Sun it is necessary to take into account the matter enhancement

of the oscillations. If the MSW effect is occurring this means that solar neutrino experiments can actually investigate neutrino oscillations with a much larger range of Δm^2 since the electron density in the Sun varies considerably.

The present status of neutrino oscillation searches in each of these Δm^2 ranges are discussed separately in the following three sections. All of these experiments either search for the appearance of neutrino flavours known not to be initially present or they search for the disappearance of neutrino flavours known to be initially present.

Terrestrial Neutrino Oscillations

As has already been discussed, experiments searching for terrestrial neutrino oscillations can be divided into accelerator and reactor based experiments. The reactor experiments generally start from a known flux of electron anti-neutrinos and measure the final flux which reaches the detector placed some distance away to search for any $\overline{\nu_e} \rightarrow \overline{\nu_x}$ oscillations. Accelerator based experiments generally start from a beam of muon neutrinos or anti-neutrinos and then search for any tau or electron neutrinos or anti-neutrinos. Such accelerator experiments can therefore search for either $\nu_\mu(\overline{\nu_\mu}) \rightarrow \nu_\tau(\overline{\nu_\tau})$ or $\nu_\mu(\overline{\nu_\mu}) \rightarrow \nu_e(\overline{\nu_e})$ oscillations or both depending upon the actual detector.

To date there have been no $\nu_\mu(\overline{\nu_\mu}) \rightarrow \nu_\tau(\overline{\nu_\tau})$ oscillations observed and exclusion limits have been set on combinations of Δm^2 and $\sin^2 2\theta$ by numerous experiments. Recently, two experiments running at CERN, Geneva, called NOMAD and CHORUS have set limits of $\sin^2 2\theta_{\mu\tau} < 3.4 \times 10^{-3}$ and $\sin^2 2\theta_{\mu\tau} < 3.5 \times 10^{-3}$ respectively for large values of Δm^2, see [Mez97] and [Esk97] respectively. These two experiments are both situated about 800 metres from a source of 25GeV muon neutrinos but they differ considerably in their detectors. The CHORUS experiment uses a target of nuclear emulsion which has high resolution so that the 1.5 millimetre decay length of the tau lepton produced by tau neutrino interactions can be observed. The NOMAD experiment has an active target made from drift chambers and together with tracking systems it can distinguish different neutrino interactions by their kinematics. In this way the NOMAD experiment can search for $\overline{\nu_\mu} \rightarrow \overline{\nu_e}$ oscillations as well as $\overline{\nu_\mu} \rightarrow \overline{\nu_\tau}$ oscillations and its exclusion limits for $\overline{\nu_\mu} \rightarrow \overline{\nu_e}$ oscillations are discussed below.

Perhaps the most startling occurrence in the search for neutrino oscillations in the recent past came with the announcement by the LSND experiment in 1995 of a signal consistent with $\overline{\nu_\mu} \rightarrow \overline{\nu_e}$ oscillations [Ath96]. The LSND experiment is a large scintillation detector situated 30 metres away from a beam stop of pions at the Los Alamos Meson Physics Facility, USA. The LSND experiment is designed to detect the production of electron anti-neutrinos from a beam of muon anti-neutrinos. The parameter space of the LSND allowed region is shown in Figure 1.1 together with the most recent exclusion limits from four other experiments. One further exclusion region that can be added to this plot comes from the results of the Bugey short-baseline reactor experiment which excludes $\overline{\nu_\mu} \rightarrow \overline{\nu_e}$ oscillations above about $\sin^2 2\theta = 0.04$ [Ach95] .

The exclusion limits in Figure 1.1 come from the NOMAD experiment which has already been discussed, the currently operational KARMEN experiment and two older experiments: BNL 776 and CCFR. The first of these older experiments, BNL 776, published its results in 1992 using a large fiducial mass electromagnetic calorimeter and a muon spectrometer placed 1 kilometre from the source of a ν_μ beam at the Brookhaven National Laboratory, USA [Bor92]. The second experiment, CCFR, published its results in 1995 using a coarse grained calorimeter situated at Fermilab, USA [McF95].

The exclusion limit shown in Figure 1.1 from the KARMEN experiment is important because this experiment is very similar to the LSND experiment in that it is a highly segmented liquid scintillation detector searching for the appearance of $\nu_e(\overline{\nu_e})$ from a beam of $\nu_\mu(\overline{\nu_\mu})$. The KARMEN experiment is currently operating at the Rutherford Appleton Laboratory (RAL), UK. The KARMEN detector underwent an upgrade in 1996 which means that within the next few years it should be able to fully

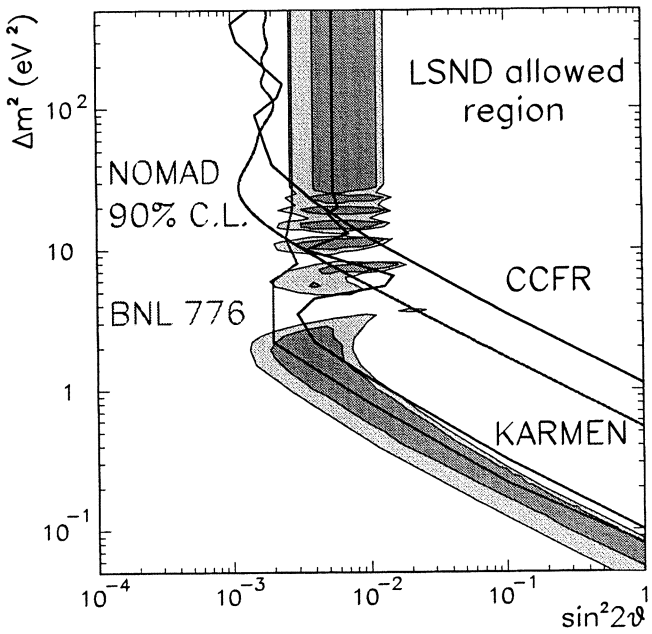

Figure 1.1: *The LSND allowed region for $\overline{\nu_\mu} \rightarrow \overline{\nu_e}$ oscillations together with the current exclusion limits from four experiments. This plot was taken from [Mez97].*

Experiment Name	Exposure in kilotonne years	Number of events	Ratio of Ratios: $R = (\mu/e)_{DATA}/(\mu/e)_{MC}$	Ref
NUSEX	0.74	50	$0.96^{+0.32}_{-0.28}$	[Agl89]
Frejus	2.0	200	1.00±0.15±0.08	[Dau95]
Soudan-II	3.2	~200	0.61±0.15±0.05	[Kaf97]

Table 1.1: *The measurements of atmospheric neutrinos using iron calorimetric detectors. The only currently operating experiments is the Soudan-II experiment which can be seen to have produced a result for R significantly different to unity, unlike the other two experiments.*

investigate the region favoured by the LSND signal and so should be able to confirm or deny this hint of neutrino oscillations [Eit97].

The LSND experiment has continued to refine its own analysis and has recently completed an analysis into $\nu_\mu \rightarrow \nu_e$ oscillations and they report observing a signal consistent with their original claim of $\overline{\nu_\mu} \rightarrow \overline{\nu_e}$ oscillations [Ath97].

Atmospheric Neutrino Oscillations

Since the mid 1980's there have been a number of experiments detecting the number of muon and electron neutrinos produced when cosmic rays scatter in the atmosphere. Although the absolute fluxes of these neutrinos are not well known in theory, the ratio of the number of muon neutrinos produced to the number of electron neutrinos produced is thought to be known quite accurately. Experiments have therefore been measuring a, so called, 'ratio of ratios' given by R which is the measured ratio of muon neutrinos to electron neutrinos divided by the rate that the experiment would expect to see if the theoretical predictions are correct. The measured values of R are shown in Tables 1.1 and 1.2 where the experiments have been divided into the two types of detector that have been used to date.

Experiment Name	Exposure in kilotonne years	Number of events	Ratio of Ratios: $R = (\mu/e)_{DATA}/(\mu/e)_{MC}$	Ref
IMB	7.7	610	0.54±0.05±0.11	[Bec92]
Kamiokande (sub-GeV)	8.3	528	0 .62±0.06±0.06	[Ino97]
Kamiokande (multi-GeV)	6/8.2	233	$0.57^{+0.08}_{-0.07}$±0.07	[Ino97]
Super-K (sub-GeV)	20.1	1453	0.64±0.04±0.05	[Nak97]
Super-K (multi-GeV))	20.1	444	0.60±0.05±0.05	[Nak97]

Table 1.2: *The measurements of atmospheric neutrinos using large water Čerenkov detectors. The only currently operating experiment is the Super-K experiment and it can be seen that all of these experiments and the analysis of both low and high energy events are in good agreement with a value of R of around 0.6.*

The results show that there has been some disagreement between the different experiments. The water Čerenkov detectors have consistently shown a deficit whereas the iron calorimetry experiments have not. However, the currently operating experiments all measure a value for R of around 0.6 which is very different to the expected value of 1. This low value of R could be an indication of $\nu_\mu \rightarrow \nu_\tau$ oscillations since these could decrease the number of muon neutrinos by increasing the number of tau neutrinos which would have not been detected. It is necessary to invoke $\nu_\mu \rightarrow \nu_\tau$ oscillations instead of $\nu_\mu \rightarrow \nu_e$ oscillations since a long base-line reactor experiment, the Chooz experiment, has already searched the favoured parameter space for the latter type of neutrino oscillations and has found no signal [Apo97].

Further evidence for neutrino oscillations comes from the fact that in both the Kamiokande and Super-K experiments it was observed that there was a dependence of R with the zenith angle, the angle between the neutrino direction and the perpendicular direction out of the earth from the detector. This effect, called the 'up/down asymmetry', could be caused by neutrino oscillations since neutrinos coming through the earth have very different path lengths to those coming straight from the atmosphere. The recent results of the Super-K experiment for this effect produce a good fit to $\nu_\mu \rightarrow \nu_\tau$ oscillations with $\Delta m^2 = 5 \times 10^{-3} eV^2$ and $\sin^2 2\theta = 1.0$ [Nak97].

In the future, long-baseline accelerator experiments will be able to investigate this region of parameter space and so provide independent evidence as to whether or not neutrino oscillations are the cause of the low value of R which have been measured.

Solar Neutrino Oscillations

There are two main fusion processes which occur in the Sun which generate neutrinos and energy: the p-p and CNO cycles and in Table 1.3 there is a list of some of the details of the electron neutrinos produced by these cycles. The main energy producing reactions in the Sun are from the p-p cycle and they can be summarised by the reaction shown in Equation 1.15.

$$4p + 2e^- \rightarrow \alpha + 2\nu_e + 4\gamma \quad Q = 26.7 MeV \tag{1.15}$$

This equation shows that two electron neutrinos are released with about every 26MeV of energy. This allows an estimate of the number of electron neutrinos produced by the Sun can be made by using the measured luminosity of the Sun. However, to search for neutrino oscillations it is necessary for the flux of electron neutrinos to be determined accurately. This is done by building solar models which describe the reactions taking place and model the transport of both energy and elements within the Sun. There have been several solar models suggested and these differ in the details of neutrino predictions. It should be noted that these models are in good agreement when they calculate the flux of p-p neutrinos since

Chain name	Individual reactions	Neutrino production:		
		Name	Energy (MeV)	Flux ($cm^{-2}s^{-1}$)
p-p I	$p+p \rightarrow {}^2H + e^+ + \nu_e$ $p+e^- + p \rightarrow {}^2H + \nu_e$ ${}^2H + p \rightarrow {}^3He + \gamma$ ${}^3He + {}^3He \rightarrow \alpha + 2p$	p-p pep	$\leq$0.420 1.442	$5.91^{+0.06}_{-0.06} \times 10^{10}$ $1.40^{+0.01}_{-0.03} \times 10^8$
hep	${}^3He + p \rightarrow {}^4He + e^+ + \nu_e$	hep	$\leq$18.8	$\sim 10^4$
p-p II	${}^3He + {}^4He \rightarrow {}^7Be + \gamma$ ${}^7Be + e^- \rightarrow {}^7Li + \nu_e$ ${}^7Li + p \rightarrow 2\alpha$	^{7}Be	0.86 (90%) 0.38 (10%)	$4.64^{+0.28}_{-0.32} \times 10^9$ $5.15^{+0.31}_{-0.36} \times 10^8$
p-p III	${}^7Be + p \rightarrow {}^8B + \gamma$ ${}^8B \rightarrow {}^8Be^* + e^+ + \nu_e$ ${}^8Be^* \rightarrow 2\alpha$	^{8}B	$\leq$15	$6.62^{+0.93}_{-1.13} \times 10^6$
CNO	${}^{12}C + p \rightarrow {}^{13}N + \gamma$ ${}^{13}N \rightarrow {}^{13}N + e^+ + \nu_e$ ${}^{13}C + p \rightarrow {}^{14}N + \gamma$ ${}^{14}N + p \rightarrow {}^{15}O + \gamma$ ${}^{15}O \rightarrow {}^{15}N + e^+ + \nu_e$ ${}^{15}N + p \rightarrow {}^{12}C + \alpha$ ${}^{15}N + p \rightarrow {}^{16}O + \gamma$ ${}^{16}O + p \rightarrow {}^{17}F + \gamma$ ${}^{17}F \rightarrow {}^{17}O + e^+ + \nu_e$ ${}^{17}O + p \rightarrow {}^{14}N + \alpha$	^{13}C ^{15}O ^{17}F	$\leq$1.2 $\leq$1.73 $\leq$1.74	$6.18^{+1.05}_{-1.24} \times 10^8$ $5.45^{+1.04}_{-1.20} \times 10^8$ $6.48^{0.97}_{1.23} \times 10^6$

Table 1.3: *The energy and flux of electron neutrinos produced by the fusion reactions in the Sun. The fluxes are from the 1995 Bahcall and Pinsonneault solar model [BP95] and the other details about the neutrinos are taken from [Bah89].*

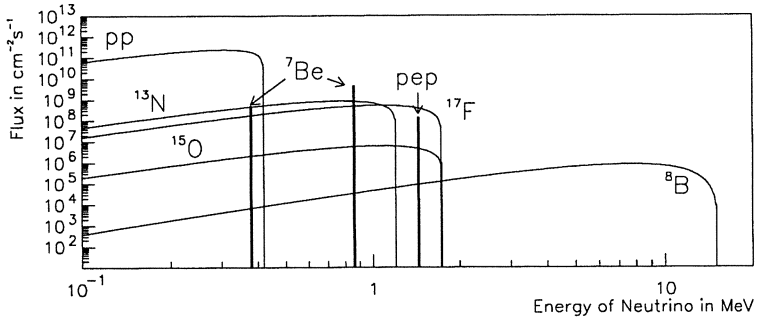

Figure 1.2: *The energy spectrum of solar neutrinos reaching the earth normalised to the fluxes given by the 1995 solar model of Bahcall and Pinsonneault [BP95]. The neutrino fluxes from continuum sources are given in units of the number of neutrinos per square centimetre per second per MeV. The neutrino fluxes from line sources are given in units of the number of neutrinos per square centimetre per second.*

this rate is strongly constrained by the luminosity of the Sun. The solar model most widely accepted as accurate, and which will be used in the rest of this thesis, is the 1995 solar model of Bahcall and Pinsonneault [BP95]. This model includes heavy element diffusion which earlier models did not include and has been shown to compare very favourably with the most recent helioseismology results, see [Bah96].

The fluxes of the different solar neutrinos as given by this solar model are listed alongside the neutrino reactions in Table 1.3 and are displayed in Figure 1.2 to show the complete electron neutrino energy spectrum produced by the Sun.

As of 1996 there were four operating solar neutrino detectors which used three different targets to detect the neutrinos: chlorine, water and gallium. These different detectors have both different cross-sections for detecting neutrinos and different energy thresholds which means that their expected detection rate needs to be calculated individually. The results of solar neutrino experiments are often expressed in terms of solar neutrino units where 1 SNU is 10^{-36} events per second per target atom. These rates are predicted by the solar model for each solar neutrino detector by convolving calculated fluxes with the appropriate cross-sections for electron neutrinos interacting in the particular target while taking into account the energy threshold of the detector. The results of the solar neutrino experiments, as of 1996, are shown and compared to the solar model predictions in Figure 1.3 taken from [Bah97].

It is clear that all four experiments have measured smaller rates of electron neutrinos than the rates predicted by the solar model. The overall deficit as measured by each experiment is roughly the same and so naively one could simply say that the solar model overestimates the flux of neutrinos by a factor of about three. This simplistic solution does not fit the data because the different experiments are sensitive to the neutrinos coming from the different fusion reaction in the Sun, as can be seen in Figure 1.3. A direct comparison of the rate measured by the chlorine and water experiments suggests that there is no flux of pep, ^{7}Be or CNO neutrinos. Furthermore, the results of the gallium experiments show that their measured rate is fully accounted by the predicted flux of p-p neutrinos. This result is almost independent of the solar model used since, as has already been noted, the flux of p-p neutrinos is strongly constrained by the measured luminosity of the Sun. The gallium experiments therefore also seem to indicate that there is no flux of ^{7}Be neutrinos coming from the Sun. However, ^{8}B neutrinos are observed in the water experiment and so this apparent deficit of ^{7}Be neutrinos is extremely hard to explain using standard physics.

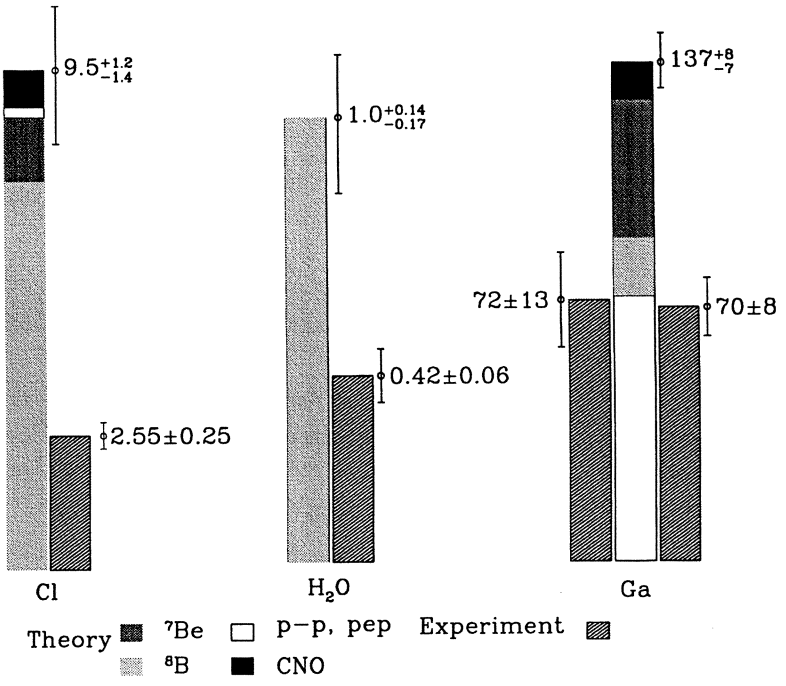

Figure 1.3: *This figure shows the measured rates of solar neutrinos in solar neutrino units (SNU) for four experiments using three different targets. These rates are taken from [Enq96] and [Nak97] and are compared to the rates in SNU predicted by the 1995 solar model of Bahcall and Pinsonneault [BP95]. The different shading in the predicted rates indicates the sources of the neutrinos that are expected to be detected. This figure is taken from [Bah97].*

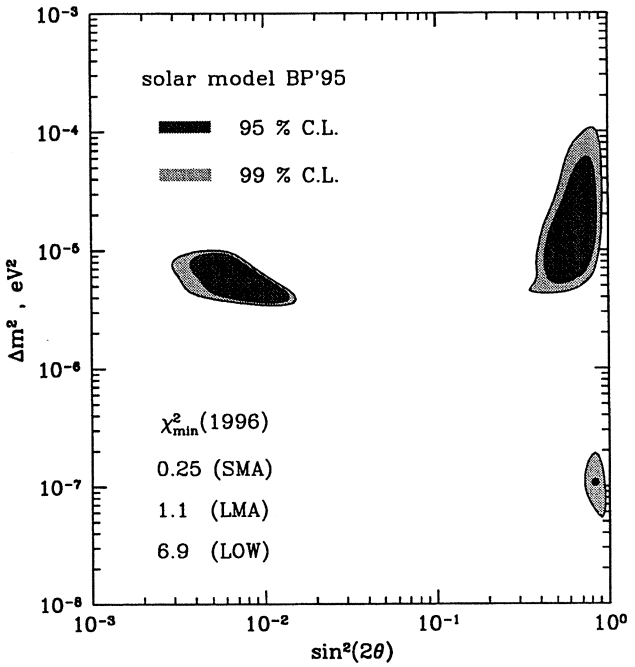

Figure 1.4: *The allowed MSW solutions to the solar neutrino problem, as taken from [Bah97]. This figure uses the the predictions of the 1995 solar model of Bahcall and Pinsonneault [BP95] and the measured rates taken from [Enq96] and [Nak97]. The small mixing angle solution (SMA) has* $\sin^2 2\theta = 8.7 \times 10^{-3}$ *and* $\Delta m^2 = 5.0 \times 10^{-6} eV^2$. *The large mixing angle solution (LMA) has* $\sin^2 2\theta = 0.63$ *and* $\Delta m^2 = 1.3 \times 10^{-5} eV^2$. *The low solution (LOW) has* $\sin^2 2\theta = 0.83$ *and* $\Delta m^2 = 1.1 \times 10^{-7} eV^2$.

There have been attempts to reconcile all of these results by changing the solar model but these have found that the probability of a standard-physics solution is less than 2% if the luminosity constraint is retained and less than 4% if the luminosity constraint is abandoned, see [Hee96]. However, this deficit of solar neutrinos can easily be accounted for if neutrinos have a small, finite mass and undergo $\nu_e \rightarrow \nu_x$ oscillations. In particular, the matter enhanced oscillations suggested by the MSW effect produces survival probabilities for electron neutrinos which vary in energy. It is therefore quite possible for the MSW effect to produce an extremely low flux of ^{7}Be electron neutrinos while keeping an observable flux of ^{8}B electron neutrinos. Figure 1.4 shows the best fit MSW solutions to the solar neutrino data as of 1996. This figure was taken from [Bah97]. It should be noted that the experimental results can also be explained by vacuum neutrino oscillations with no matter enhancement but this gives a worse fit and requires very large mixing angles of $\sin^2 2\theta > 0.6$.

1.4 Conclusions

In this chapter the present experimental results relating to the question of whether or not neutrinos have mass has been summarised. To date no direct evidence of massive neutrinos has been found and limits on these masses are always being reduced by better experimentation. There is however a lot of indirect evidence that neutrinos have mass and this comes from the observed hints of neutrino oscillations.

The only direct neutrino oscillation observation is claimed by the LSND collaboration but this needs to be confirmed by another experiment, probably KARMEN, before it will be considered as evidence for neutrino mass. There are two indirect observations of neutrino oscillations and these come from the need to explain an observed deficit in both atmospheric and solar neutrinos. Although recent results from the Super-K experiment are confirming a problem with atmospheric neutrinos this problem is not as convincing as the solar neutrino problem. This is because two previous atmospheric neutrino experiments, NUSEX and Frejus, did not observe the problem. Only with the results of future long-baseline accelerator experiments will the hint of neutrino oscillations in atmospheric neutrinos be proven.

The strongest evidence to date for neutrino oscillations, and hence that neutrinos have a small but finite mass, comes from the measured deficit in the number of neutrinos coming from the Sun. In this chapter it was explained why the combination of the results of the four solar neutrino experiments operational in 1996 makes it virtually impossible to explain the deficit using standard physics. However, neutrino oscillations via the MSW effect can easily account for the observed results.

It seems that the only way to account for the combined results of these solar neutrino experiments, within the realms of standard physics, is if one of these experiments has produced an inaccurate result. In the next chapter this possibility will be examined by discussing the details of the three different techniques that have been used to detect solar neutrinos to date.

Finally, it is interesting to note that the see-saw theory which was described in this chapter can generate a neutrino mass hierarchy with the correct structure needed to give solutions to the hints of neutrino oscillations suggested by the atmospheric and solar neutrino problems. However, it should be noted that it is impossible to solve both of these problems and account for the LSND result with neutrino oscillations without invoking oscillations to non-interacting, sterile neutrinos. It is possible to account for all three of these effects by extending the see-saw mechanism and by the addition of three sterile neutrinos but this could just be the case of adding enough free parameters to fit all of the data [Chu98].

Chapter 2

The Solar Neutrino Experiments

2.1 Introduction

Since the 1960's there have been three different techniques used to detect solar neutrinos, these involve targets of chlorine, gallium and water. In the last chapter the results of these experiments as of 1996 were given and it was explained that, unless one of the measurements was inaccurate, the combined results are a very good indication that solar neutrinos undergo neutrino oscillations. In this chapter the details of these experimental techniques and the most recent results of the experiments that have used them will be discussed in order to verify this conclusion. Finally attention will move from presently operational solar neutrino experiments to a future experiment due to commence operation in April 1998.

This experiment, the Sudbury Neutrino Observatory, is a unique solar neutrino experiment because it can detect electron neutrinos by a charged current (CC) interaction and the total sum of electron, muon and tau neutrinos by a neutral current (NC) interaction. This means that the SNO experiment can prove whether or not the electron neutrinos produced by the Sun are oscillating into muon or tau neutrinos before reaching the Earth. It will also be explained that, to be able to prove that these neutrino oscillations are occurring, the SNO experiment needs to have methods to measure the amount of natural radioactivity within its detector target and some of these methods will be described.

2.2 The First Solar Neutrino Experiment

In 1958 it was realized that neutrinos could be produced in the sun via the infrequent inverse beta decay of both ^{7}Be and ^{8}B, as was shown in Table 1.3 on page 9. This led to several initial attempts to measure solar neutrinos since the flux from ^{8}B was predicted to be reasonably high. These attempts, led primarily by F.Reines, were all foiled by large backgrounds, as described in eg [Rei64]. However it should be noted that these initial experiments were actually pilot experiments of those in preparation today. The first experiment which actually measured the rate of electron neutrinos coming from the Sun used the inverse beta decay reaction given in Equation 2.1.

$$\nu_e + {}^{37}Cl \rightarrow e^- + {}^{37}Ar \quad (E_\nu > 0.814MeV) \tag{2.1}$$

The reason for choosing this reaction is that the ^{37}Ar produced by the neutrino interaction can be quantitatively retrieved from a liquid source of chlorine by purging the liquid with an inert gas. Furthermore, ^{37}Ar decays by electron capture with a 35.2 day half-life by emitting 3 to 4 Auger electrons whose total energy is 2.82keV. This means that after retrieving the ^{37}Ar it is possible to measure it using low background proportional counters.

A collaboration from Brookhaven National Laboratory (BNL), New York, USA, led by R.Davis designed an experiment which used 615 tonnes of tetrachloroethylene [Dav68]. The argon removal system involved purging the tank for 20 hours with helium. Any tetrachloroethylene in this helium was removed using absorbers and finally any argon collected was removed using a liquid nitrogen cooled charcoal trap. The argon was then purified using smaller charcoal traps and a gas chromatography column to remove heavy radioactive gases such as ^{222}Rn which would lead to counting backgrounds. Finally, the purified argon was mixed with a counting gas, consisting of 90% argon and 10% methane, and placed into a 0.5 millilitre miniature proportional counter for measurement. These counters were calibrated using an external source of ^{55}Fe which produces an escape peak at 2.93keV, just above the signal from ^{37}Ar.

To calibrate the efficiency of the collection procedure a known amount of an isotopically pure argon isotope, alternating between ^{36}Ar and ^{38}Ar, was added to the tank before each solar neutrino exposure. The recovery of this carrier was determined after the counting time of 200-400 days by analysing the gas in the counter by mass spectroscopy. These calibrations always showed a carrier recovery greater than 90%. A final calibration of this solar neutrino experiment was made by mixing 500 atoms of ^{37}Ar directly to the target and these were also recovered with a good yield.

In a small scale experiment, performed both at BNL by H.Ruiz and R.Davis and in Russia, some tetrachloroethylene labelled with ^{36}Cl was added to a tank of tetrachloroethylene and the ^{36}Ar was recovered. Measurements using neutron activation showed that both groups obtained excellent yields.

As with all solar neutrino experiments the possible background producing mechanisms needed to be understood, measured and subtracted from the total number of events. One of the main backgrounds was the cosmic ray production of ^{37}Ar and so for this reason the collaboration constructed the experiment down a deep mine in South Dakota, the Homestake Gold Mine. It is from the name of this mine that the solar neutrino experiment gained its name: the Homestake experiment. The cosmic ray background was measured separately and found to produce 0.047±0.011 atoms of ^{37}Ar each day as compared to the few atoms of ^{37}Ar produced each day by solar neutrinos [Dav97]. Other sources of backgrounds were those found in the counters but these were minimised by using pulse rise-time cuts and energy cuts.

This experiment is no longer taking data but after about 25 years of running the neutrino flux was measured to be relatively constant at 2.54±0.20 SNU [Lan96]. This can be compared to the 1995 Bahcall and Pinsonneault solar model prediction, which includes theoretical errors on the calculated cross-section of inverse beta decay on chlorine, of $9.5^{+1.2}_{-1.4}$ SNU [BP95]. The Homestake experiment therefore detected about a quarter of the neutrinos expected and there is no reason to think that this measurement is incorrect since it was shown that argon in the detector was always extracted with a good yield.

The Homestake experiment was not sensitive to p-p neutrinos whose flux is most accurately predicted by solar models and so other experiments which have a lower energy threshold were devised and these are explained in the next section.

2.3 The Gallium Experiments

The next radiochemical solar neutrino experiments used inverse beta decay on a gallium target, as shown in Equation 2.2 since it has an energy threshold lower than the 0.42MeV maximum energy of p-p solar neutrinos.

$$\nu_e + {}^{71}Ga \rightarrow e^- + {}^{71}Ge \quad (E_\nu > 0.233MeV) \tag{2.2}$$

The ^{71}Ge produced by interactions of neutrinos in the gallium can be collected quantitatively by radiochemical techniques for measurement by small, low-background proportional counters since it decays by electron capture with a 11.4 day half-life emitting a 1.17keV gamma ray from the L-peak and a 10.37keV gamma ray from the K-peak. To be able to detect a sufficient number of low energy neutrinos

it was calculated that about 30 tonnes of gallium would be required and methods to extract germanium from this quantity of gallium had to be developed, in fact two such methods were developed [Bah78].

The first of these methods started with a target of metallic gallium and this was used by the SAGE experiment [Abd94]. The germanium can then be extracted into an acidic solution containing hydrogen peroxide by vigorous mixing and concentrated as germanium tetrachloride using a stream of helium.

The second of these methods to extract germanium from 30 tonnes of gallium started from a target of 8M gallium chloride mixed with 2M hydrochloric acid and this was used by the GALLEX experiment [Ans92]. The germanium can then be extracted from this mixture as germanium tetrachloride by purging with nitrogen gas.

In both experiments after the germanium has been extracted as germanium tetrachloride in nitrogen or helium, it has to be purified and concentrated so that it can be measured for ^{71}Ge decays by a miniature, low background proportional counter. The first stage of this concentration uses water absorbers to collect the germanium tetrachloride into a 40 litre volume. This 40 litres is then acidified to 8.5M hydrochloric acid to make the germanium tetrachloride volatile so that it can be extracted and collected, as in the previous stage, into a 1 litre volume. This 1 litre is acidified again and a solvent-solvent extraction carried out using 500 millilitres of carbon tetrachloride. The germanium is then back-extracted from the organic phase using 50 millilitres of low tritium water. Finally, by adding 50 millilitres of a pH 10 solution containing 0.3 grams of sodium borohydride the counting gas, germane (GeH_4), is generated. This germane gas is then purified using water traps and a gas chromatography column before being added to a counting gas with some xenon to increase detection efficiency and transferred into a proportional counter.

These gallium experiments found a background in the proportional counters caused by ^{222}Rn but this could be removed by fitting counting results to the energy of ^{71}Ge decays and its 11.4 day half-life. These experiments also found a background due to the production of radioactive germanium by cosmic rays and so the experiments were operated in underground laboratories like the Homestake experiment. The GALLEX collaboration chose the Gran Sasso National Laboratory in Italy whereas the SAGE collaboration chose the Baksan Neutrino Observatory in Russia. Both experiments had to take steps to deal with a high initial background during their construction in the early 1990's caused by the cosmogenic production of long-lived germanium isotopes in the gallium.

As for the Homestake experiment, a carrier of different germanium isotopes was always used to determine the overall efficiency of recovering germanium in each exposure. However, these experiments also used many more calibrations to verify their results. Both the SAGE and GALLEX experiments used an intense neutrino source to verify the overall efficiency of the experiments in detecting neutrinos independently of theoretical cross-sections. The chosen neutrino source was ^{51}Cr which decays with a 28 day half-life by electron capture emitting neutrinos with energies of 0.426, 0.431, 0.746 and 0.751MeV which are all detectable by inverse beta decay on ^{71}Ga. The results of these calibrations are shown in Table 2.1.

The GALLEX experiment stopped taking data in January 1997 and after this date carried out a further calibration by adding a known amount of ^{71}As to the target solution. This isotope beta decays to ^{71}Ge with a 2.72 day half-life and so the recovery of minute quantities of germanium actually produced in the gallium could be measured and these results are also shown in Table 2.1.

These calibration results show that both gallium detectors were performing as expected and so their solar neutrino measurements must be considered to be accurate. The solar neutrino measurements made by the SAGE and GALLEX experiments during different time periods are shown in Table 2.2 where their average results are compared to the solar model prediction. It can also be seen that the solar neutrino measurements, in particular from the GALLEX experiment, do vary between different time periods however this effect has been studied by the collaboration and they have found that the individual

Experiment Name	^{71}Ge Extraction Calibrations:		
	^{51}Cr Source	^{71}As Source	Ref
SAGE	$0.97^{+0.13}_{-0.12}$	-	[Gav97]
GALLEX	$1.01^{+0.12}_{-0.11}$	0.999±0.012 ; 1.001±0.012	[Cri97]
	$0.84^{+0.12}_{-0.11}$	1.005±0.012 ; 0.996±0.013	

Table 2.1: *The results for calibrations using a ^{51}Cr source of neutrinos and an ^{71}Ar source of ^{71}Ge. These results are given as ratios of the amount of ^{71}Ge recovered to the expected amount of ^{71}Ge produced.*

Experiment Name	Solar Neutrino Rate in SNU:			
	Measurements	Average	Ratio to[BP95]	Ref
SAGE	81^{+20}_{-18} ; 70^{+13}_{-11} ; 65^{+22}_{-13}	70±8	0.51±0.07	[Gav97]
GALLEX	$83.4^{+18.5}_{19.5}$; $75.9^{+10.5}_{-10.7}$	76±8	0.55±0.12	[Cri97]
	$53.9^{+11.0}_{-11.0}$; $117.0^{+12.0}_{-12.0}$			

Table 2.2: *The final results of the GALLEX experiment and the most recent preliminary results of the SAGE experiment. The 1995 Bahcall and Pinsonneault theoretical prediction for the solar neutrino rate in these two experiments is 137^{+8}_{-7} SNU [BP95].*

results are totally consistent with a statistical distribution about a constant production rate. Overall both the SAGE and GALLEX experiments have detected about half the solar neutrinos that the solar model predicted.

The results of these gallium experiments are very compelling evidence for a solar neutrino deficit, much more so than the results of the Homestake experiment, for two reasons. Firstly, the two experiments were carried out independently with different analysis and different initial radiochemical techniques and yet the experiments show excellent agreement on the rate of solar neutrinos. Secondly, these experiments were extremely well calibrated particularly by using a source of neutrinos and so there seems to be no argument that these experiments could determine how many neutrinos they were detecting.

Since these gallium experiments are sensitive to p-p neutrinos their result suggests that the solar neutrino deficit is not caused by errors in the predictions of the solar models since the predicted rate of p-p neutrinos is strongly constrained by the luminosity of the Sun.

There are future plans for other radiochemical experiments with an even lower energy threshold but in the next two sections discussions will concentrate on the other class of solar neutrino detectors, the large water Čerenkov detectors.

2.4 The Light Water Čerenkov Detectors

Other operating solar neutrino experiments are not radiochemical in how they detect neutrinos but they do depend upon radiochemical techniques to reduce and measure backgrounds caused by natural radioactivity. The method for the detection of neutrinos is to detect the Čerenkov light caused by neutrinos scattering off electrons in a large target of water. This method allows real time measurements of neutrinos and provides some directional information about where the neutrinos came from. This directional information allows solar neutrinos to be extracted from other backgrounds such as are caused by natural radioactivity and cosmic rays. The backgrounds due to natural radioactivity, particularly radon gas, increase rapidly at low energy and therefore create an artificial energy threshold in the Čerenkov detectors.

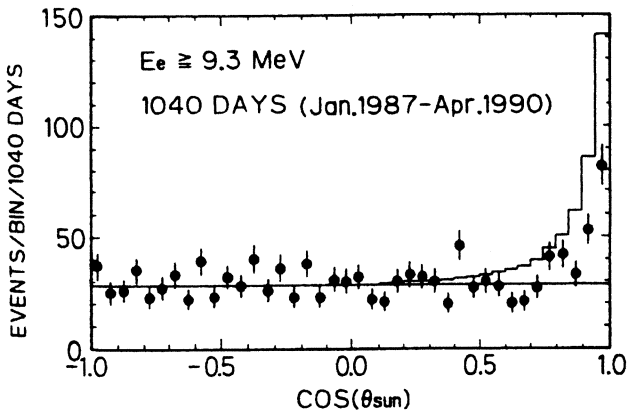

Figure 2.1: *The distribution in* $\cos\theta_{sun}$ *for the initial results from the Kamiokande detector as taken from [Hir90]. The excess of events coming from the Sun, at* $\cos\theta_{sun} = 1.0$*, can be clearly seen above the constant background caused by spallation. It can also be seen that the total number of neutrino events in this peak is much lower than the solar model prediction as of 1990 which is shown by the histogram.*

Experiment	Flux($10^6 cm^{-2} s^{-1}$)	Ratio to [BP95]
Kamiokande	2.80±0.19±0.33	0.42±0.06
Super-K	$2.37^{+0.06\ +0.09}_{-0.05\ -0.07}$	$0.358^{+0.017}_{-0.013}$

Table 2.3: *The final result of the Kamiokande experiment and the most recent results of the Super-K experiment for the flux of* ^8B *solar neutrinos. The 1995 Bahcall and Pinsonneault solar model theoretical prediction for the flux of* ^8B *neutrinos is* $6.62^{+0.93}_{-1.13} \times 10^6 cm^{-2} s^{-1}$ *[BP95].*

The first solar neutrino detector of this kind was converted from a proton decay experiment sitting in the Kamioka mine in Japan. This experiment, the Kamiokande detector [Hir88] had a total target volume of about 3000 tonnes of H_2O viewed by 950 twenty inch photo-multiplier tubes. By using a fiducial volume of 680 tonnes and an anti-coincidence veto, external backgrounds could be reduced and solar neutrinos detected. In 1990 the Kamiokande experiment gave results showing the first directional dependence of neutrinos with the position of the Sun. These initial results, for neutrinos with energies greater than 9.3MeV, are reproduced in Figure 2.1 which is taken from [Hir90]. The threshold of the Kamiokande experiment was reduced as the experiment continued to a final value of 7.0MeV but this experiment could only ever measure ^{8}B neutrinos. The Kamiokande detector was calibrated for energy using 9MeV gamma rays from neutron capture on nickel and 30MeV electrons from muon decay. The final results for the detection of ^{8}B neutrinos are given in Table 2.3 where they are compared to the prediction of the 1995 Bahcall and Pinsonneault solar model [BP95] and show a clear deficit of solar neutrinos of just over one half.

The success of the Kamiokande experiment has led to the construction of a larger experiment, called Super-K, in the same mine in Japan in order to obtain better statistics and a lower energy threshold [Suz94]. This new detector has a total volume of 32,000 tonnes of water which is observed by 11,000 twenty inch photo-multiplier tubes. There is, as there was for Kamiokande, an anti-coincidence detector composed of 1900 eight inch photo-multiplier tubes to allow the detector to veto external backgrounds. The fiducial volume of the detector is 22,500 tonnes of water, a factor of thirty times the fiducial volume of Kamiokande.

The flux of ^{8}B solar neutrinos, as measured by the Super-K experiment between June 1996 and October 1997 is given in Table 2.3 where it can be seen to be in complete agreement with the final result of the Kamiokande experiment.

The high statistics of the Super-K experiment allows measurements not only of the rate of solar neutrinos but the measurement of any time variation of this rate and of any variation in the energy spectrum of the ^{8}B neutrinos as compared to the predictions of solar models. The measurement of any time variation is important because the MSW effect predicts, for certain parameters, a difference in the electron neutrino rate between neutrinos arriving in the detector during the night and during the day. This, so called, 'day/night effect' is caused by the regeneration of neutrinos in the earth via the MSW effect. At present the data is consistent with no such effect and so this excludes certain MSW solutions to the solar neutrino problem.

The measurement of the ^{8}B energy spectrum is also important because the MSW effect predicts an energy dependence to the probability of electron neutrino conversion. However, to make the most use of energy spectrum information it is essential that the threshold for the Super-K experiment is as low as possible. At present the energy threshold of the Super-K detector is 6.5MeV which is a little lower than the final threshold achieved by the Kamiokande experiment. This threshold is dominated by ^{222}Rn in the water and radioactivity in the glass of the photo-multiplier tubes. The measured energy spectrum has so far been found to be consistent with that predicted by solar models. However by using an electron linear accelerator, which produces mono-energetic electrons in the range 5 to 16MeV, a more precise energy calibration of the detector can be made. This together with more statistics will mean that the Super-K experiment will soon be able to make deductions based upon the observed energy spectrum.

The results of the Kamiokande and Super-K experiments have both shown that they can identify solar neutrinos by looking for their directional dependence with the Sun. They have also measured a similar rate of solar neutrinos which is much lower than that predicted by the solar models. In the future the Super-K experiment may be able to determine an energy distortion of the ^{8}B spectrum which would point even more strongly to neutrino oscillations.

There seems to be no reason to doubt the results of any of the solar neutrino experiments to date. All of the detectors have been well understood and, in particular, the gallium experiments have been extremely well calibrated. This means that, as was suggested in the last chapter, their combined results are strong evidence that neutrino oscillations are occurring when neutrinos travel from the Sun to the Earth. However, the only way to prove that neutrino oscillations are occurring is to detect the muon and tau neutrinos that are expected to be produced by such oscillations. The solar neutrino experiment discussed in the next section is the only solar neutrino experiment which has the capability to detect muon and tau neutrinos separately from electron neutrinos.

2.5 The Sudbury Neutrino Observatory

2.5.1 A Description of the Experiment

The Sudbury Neutrino Observatory (SNO) is presently completing the construction of a large Čerenkov detector similar to the Super-K detector. The important difference between these two experiments is that the SNO detector uses heavy water as its neutrino target instead of the light water used in the Super-K detector. The use of a deuterium target to detect solar neutrinos was first tried by T.L.Jenkins in 1962 but the results were limited by backgrounds. In 1985 H.H.Chen discussed the possibility of using neutrino interactions on deuterium to distinguish between electron neutrinos and muon or tau neutrinos [Che85]. In 1987 this idea led to a proposal for the construction of the SNO detector 2 kilometres underground in a mine in Sudbury, Ontario, Canada [McD87]. A schematic diagram of this experiment is shown in Figure 2.2 where it can be seen that the neutrino target of 1000 tonnes of heavy water will be suspended in an acrylic sphere in about 8000 tonnes of light water. This light water provides shielding for the detector from natural radioactivity in the cavity walls. Neutrino interactions within the target are observed by 9500 eight inch photo-multiplier tubes positioned on a geodesic sphere submerged in the light water and encircling the acrylic vessel.

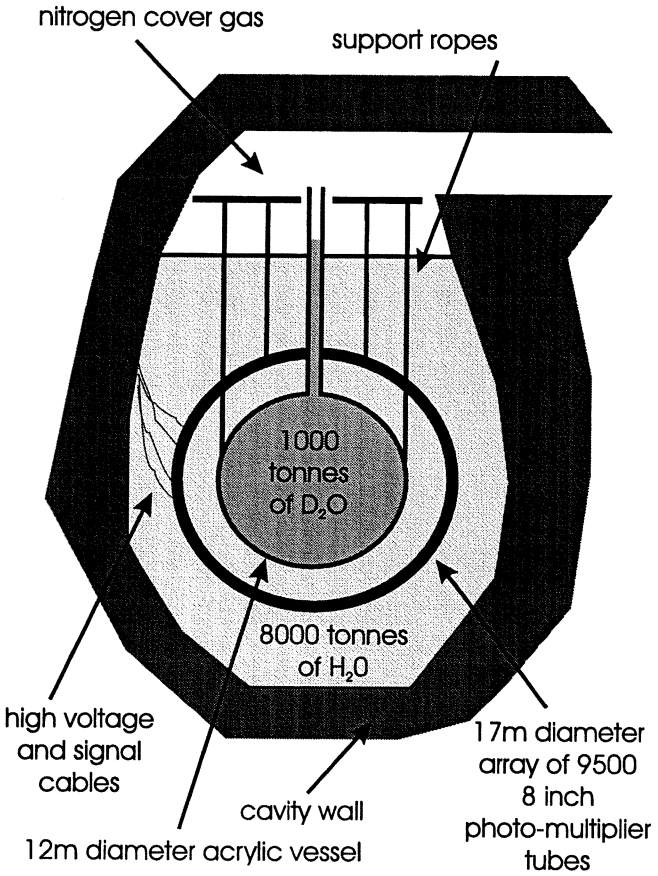

Figure 2.2: *A schematic diagram of the Sudbury Neutrino Observatory. This diagram does not show the many connections which allow both the light and heavy water to be circulated through purification and extractive assay systems.*

Interaction:		Scenario:		
Name	Reaction	SSM	SSM/3	MSW
Charged Current (CC)	$\nu_e + d \rightarrow p + p + e^-$	8832	2944	3400
Elastic Scattering (ES)	$\nu_x + e^- \rightarrow \nu_x + e^-$	1206	402	535
Neutral Current (NC)	$\nu_x + d \rightarrow n + p + \nu_x$	2413	804	2413

Table 2.4: *The neutrino interactions in the SNO detector together with the expected number of events for different situations in a year of taking data assuming the presence of 2 tonnes of magnesium chloride in the heavy water. These expected rates are taken from [Lyo97] and assume a threshold of about 6MeV (60 photo-multiplier tube hits) and a 7 metre fiducial volume. The MSW rates are for the most likely solution whereas the SSM is the expected rate if the solar model is correct.*

The important neutrino interactions which will occur within the SNO experiment are listed in Table 2.4 together with the expected number of events for one year of running in different scenarios. The SNO experiment, like the Super-K experiment, can investigate any MSW distortions of the ^{8}B energy spectrum via the charged current interaction. However, unlike the Super-K experiment, the SNO experiment can separately measure the total rate of electron, muon and tau neutrinos via the neutral current (NC) interaction and the rate of electron neutrinos via the charged current (CC) interaction. This is important because it can be seen from Table 2.4 that the CC/NC ratio can distinguish between an overall factor of three reduction in the number of neutrinos predicted by the solar model and the occurrence of matter enhanced neutrino oscillations. It should be noted that if the electron neutrinos are oscillating into sterile neutrinos then it will be very hard for the SNO experiment to show that neutrino oscillations are occurring.

The three interactions that are listed in Table 2.4 are detected by different methods in the SNO detector. The charged current (CC) and electron scattering (ES) interactions can be easily detected by observing the Čerenkov light from the electron that is either produced or given energy in a scattering. The two interactions can be distinguished because the ES interactions have a greater directional dependence than the CC interactions with the position of the Sun. The important neutral current (NC) interaction is not measured directly by the production of Čerenkov light instead the neutron has to be detected and this can be done by using one of two methods.

The first method is to add about 2 tonnes of magnesium chloride to the heavy water and detect the gamma cascade caused by the thermal capture of the neutron on the chlorine. The light produced by this interaction is more isotropic than the Čerenkov light generated by both the CC and ES interactions and it has been shown that this makes it possible to distinguish NC interactions from CC and ES interactions by considering the angular distribution of the hit pattern produced by the photo-multiplier array [Bri96]. The second method to detect the neutrons produced in NC interactions is to add discrete ^{3}He proportional counters directly into the detector. These neutral current detectors (NCD's) are suspended in an array within the 1000 tonnes of heavy water so that neutrons produced in this volume can be detected. The NCD's are more difficult to add and remove from the detector than the magnesium chloride but they do provide a method of making simultaneous, independent measurements of the CC and NC rates. It is envisaged that both of these methods will be used in the SNO experiment at different times.

2.5.2 Backgrounds to the SNO Detector

The threshold of the SNO experiment is determined by the amount of natural radioactivity in the materials which make up the detector. At present it is expected that the threshold will lie at about 6MeV and this value was used in Table 2.4 to calculate the expected neutrino event rates within the detector. External backgrounds due to cosmic rays are not a problem for the SNO experiment due to the position of the detector 2 kilometres underground in one of the deepest mines in the northern hemisphere. The light water shielding also greatly reduces backgrounds due to high energy gamma decays in the cavity walls. Unfortunately the SNO experiment is especially sensitive to natural radioactivity within the heavy water itself since this not only increases the threshold of the detector it also adds a background which mimics NC neutrino interactions. This is because natural radioactivity produces high energy gamma rays and these can photo-disintegrate the deuterium to produce a neutron as is shown in Equation 2.3.

$$\gamma + d \rightarrow d + n \quad (E_\gamma > 2.223 MeV) \tag{2.3}$$

There are two naturally occurring sources of high energy gamma rays and these are in the decay chains of thorium and uranium and the details of these decay chains are shown in Figures 2.3 and 2.4. The thorium decay chain produces a NC background because every decay of ^{208}Tl releases a gamma of 2.615MeV. The uranium decay chain produces a NC background through decays of ^{214}Bi either directly or via ^{210}Tl. In total about 2.2% of ^{214}Bi decays release gammas with energies higher than 2.223MeV.

It has been calculated that to ensure that the NC background is less than one tenth of the expected NC neutrino signal the amount of thorium and uranium in equilibrium with all of their daughters in the heavy water has to be limited to less than 3.7×10^{-15} grams of ^{232}Th per gram of heavy water and less than 4.5×10^{-14} grams of ^{238}U per gram of heavy water [McD87]. The higher limit for ^{238}U is primarily due to the different branching ratios in the two decay chains to the high energy gamma decays and this means that the SNO experiment is roughly ten times more sensitive to isotopes from the thorium decay chain than isotopes from the uranium decay chain.

It is interesting to note that these extremely low limits for the amount of radioactivity in the heavy water would probably be exceeded by the addition of just one gram of mine dust to the entire 1000 tonnes of heavy water.

In order for the SNO experiment to be confident about accurately measuring the rate of NC neutrino interactions it is essential that the amount of natural radioactivity in the heavy water is kept to these extremely low levels. It is therefore necessary to have techniques which have the sensitivity to be able to measure natural radioactivity in the heavy water down to these extremely low levels and these will be discussed in the next section.

2.5.3 Measuring the NC Background

Recent Monte-Carlo studies have shown that by examining the angular distributions of low energy events in the SNO detector it is possible to extract information about the amount of uranium and thorium in the heavy water [Xin98]. This will be a valuable technique to measure the NC background but it is essential to determine the NC background by a variety of methods. The only other way to measure the natural radioactivity in the heavy water is to extract the radioactivity and then count it in a separate low-level detector.

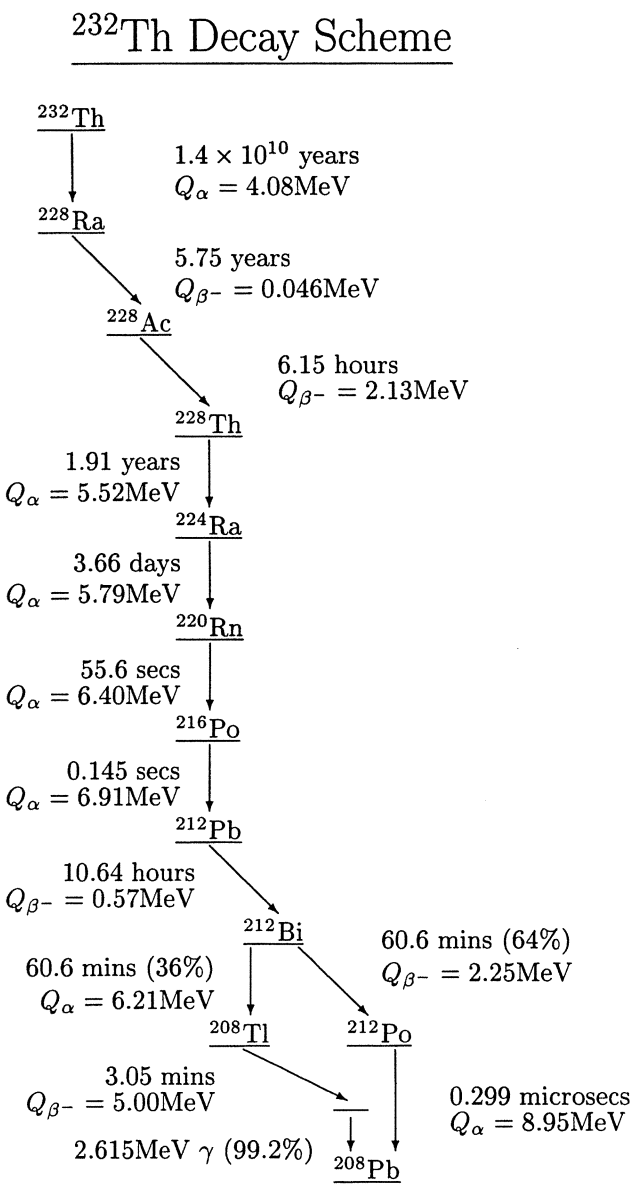

Figure 2.3: *The thorium decay chain including half-lives and Q-values taken from [Fir96].*

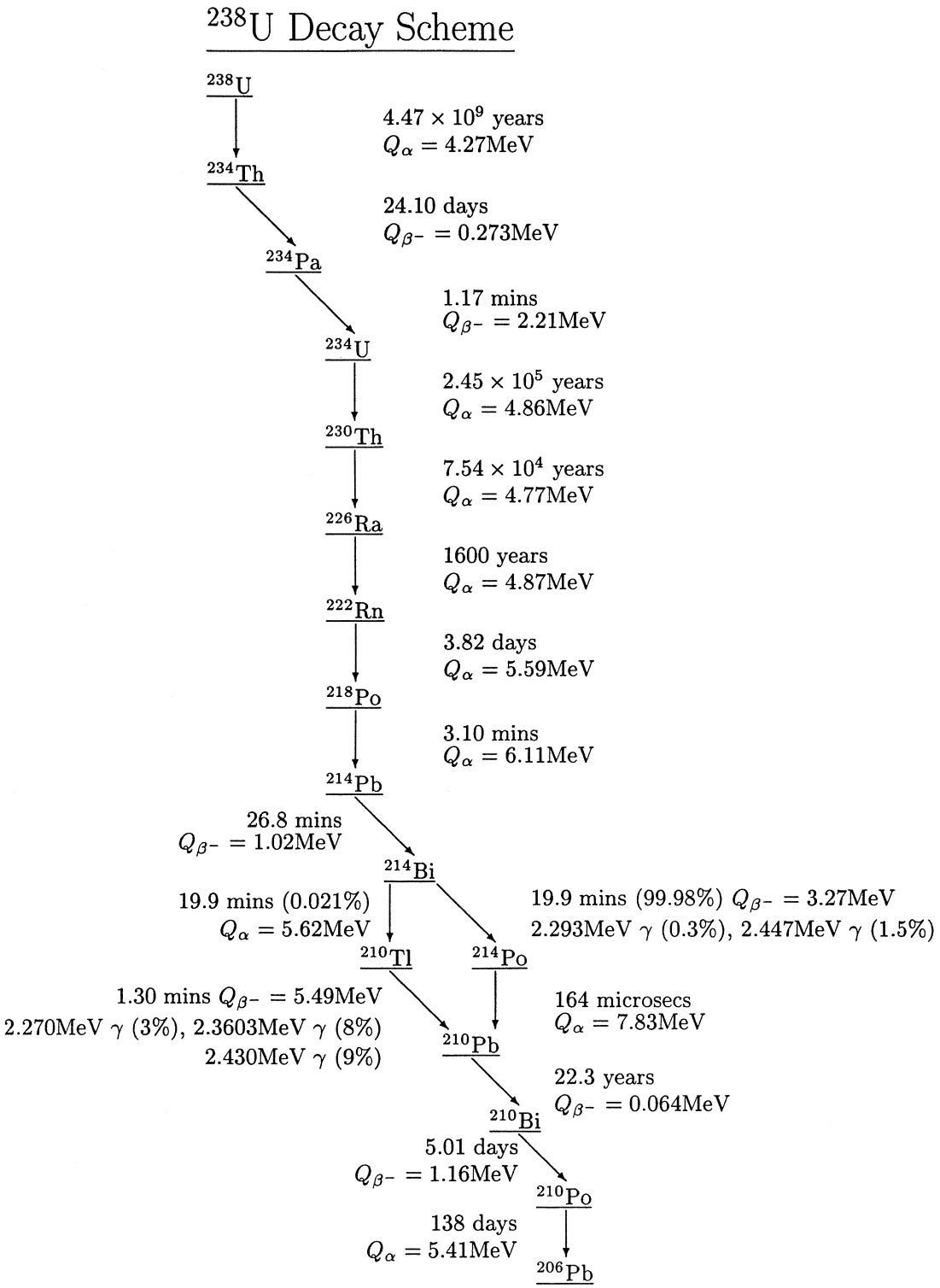

Figure 2.4: *The uranium decay chain including half-lives and Q-values taken from [Fir96].*

There are several extractive radiochemical techniques, called 'assays', that have been developed to carry out this task and these will be summarised below. More details about these techniques can be found in [Nob96].

- A large Reverse Osmosis unit (R/O):

  The R/O unit passes the pure heavy water through a membrane under high pressure. Any contaminants remain on the input side of the membrane, in the concentrate stream, while the pure water passes through the membrane into the permeate stream. The concentrate stream is then sent to a second unit and the concentrate from that unit into a third. In this way any contaminants in the heavy water can be concentrated into just 300 millilitres which can be assayed by various techniques depending upon the exact contaminant, radioactive or non-radioactive, involved.

  This technique has already been operating at the SNO experiment and does provide a very effective concentration of contaminants within the heavy water including lead isotopes. However, this technique cannot be used when the magnesium chloride is present because the R/O unit will then also remove the salt.

- MnO_x coated beads:

  The MnO_x ion-exchange material is very effective at extracting radium isotopes from both pure water and salt solutions. The method of extraction is to coat acrylic beads with the ion-exchange material and pass the heavy water through several 1 litre columns of these beads. In this way ^{224}Ra from the thorium decay chain and ^{226}Ra from the uranium decay chain can be extracted from the heavy water. The extracted radium is measured by drying the columns and counting the radon which emanates from the beads using electrostatic counters. The overall efficiency using this process for detecting radium is quoted to be 6% for ^{224}Ra and 24% for ^{226}Ra [Nob96] . The lower efficiency for ^{224}Ra is primarily due to a lower emanation efficiency for ^{220}Rn due to its shorter half life.

- Monitor Degasser:

  This is a system that assays the amount of ^{222}Rn removed from the heavy water by a LiquiCel. A LiquiCel contains hollow fibres through which nitrogen gas is pumped in the opposite direction to the flow of heavy water. In this way gases in the heavy water diffuse through the large surface area of the fibres into the nitrogen gas flow. The radon in this gas flow is frozen out using a liquid nitrogen cooled trap and reduced in volume so that it can be transferred to a 15 millilitre Lucas Cell which is then measured for activity using a photo-multiplier tube. The amount of ^{222}Rn extracted from a known volume of heavy water can then be evaluated by fitting counts to its 3.82 day half-life.

The usefulness of these three techniques in measuring the NC background can be evaluated by examining the two decay chains which are shown in Figures 2.3 and 2.4. It has already been noted that the background producing, high energy gamma decays lie at the bottom of the two decay chains. To be able to measure the amount of these isotopes in the heavy water the SNO experiment needs to measure the presence of isotopes above these decays within the decay chains. Since ^{226}Ra and ^{228}Th have very long half-lives there is no point in assaying isotopes above these isotopes in the decay chains. This means that there are just two long-lived isotopes that it would be useful to assay in the ^{238}U decay chain and these are: ^{226}Ra and ^{222}Rn. In the ^{232}Th decay chain there are three isotopes that it would be useful to assay and these are: ^{228}Th, ^{224}Ra and ^{212}Pb.

Another important feature of both decay chains is the presence of radon isotopes: ^{220}Rn in the thorium decay chain and ^{222}Rn in the uranium decay chain. These isotopes are important because there are many materials which emanate radon and so it is quite possible that there will be a disequilibrium within both decay chains due to an excess of radon. (There are other mechanisms for generating disequilibria in the decay chains and these will be discussed in the next chapter.) This means that to be able to determine the NC background caused by isotopes from the uranium decay chain it is essential that a method exists to assay ^{222}Rn. The radon isotope in the thorium decay chain, ^{220}Rn, is itself short-lived and so its effects have to be monitored by its only long-lived daughter, ^{212}Pb. To be able to determine the NC background caused by isotopes from the thorium decay chain it is essential that a method exists to assay ^{212}Pb.

The Monitor Degasser is specifically designed to assay the amount of ^{222}Rn in the heavy water which means that the NC background caused by the uranium decay chain can be expected to be well determined. However it should be remembered that the SNO experiment is ten times more sensitive to decays from isotopes of the thorium decay chain than from isotopes of the uranium decay chain. Unfortunately the systems that have been described are not optimised to measure ^{212}Pb. In fact only the R/O system has the capability to measure ^{212}Pb and it cannot be used when the magnesium chloride has been added since it would then remove the salt. This means that the present assay systems are unlikely to be able to determine the NC background caused by the thorium decay chain.

2.6 Conclusions

In this chapter all of the solar neutrino experiments, their radiochemical techniques and their solar neutrino measurements have been discussed. These experiments use well understood detectors, especially the well calibrated gallium experiments, and there seems to be no reason to suspect that the observed deficits in any of the experiments is in error. However, in order to prove that these deficits are caused by neutrino oscillations the results of the Sudbury Neutrino Observatory are needed.

The SNO experiment can measure the rate of electron neutrinos and can compare it to the total rate of electron, muon and tau neutrinos using the neutral current (NC) interaction of neutrinos on deuterium. Unfortunately there is a background to NC neutrino interactions which is caused by natural radioactivity in the heavy water. It is therefore essential that the amount of isotopes from both the thorium and uranium decay chains within the heavy water is kept to extremely low levels. Furthermore it is essential that the SNO experiment has methods which are sensitive enough to measure these low levels of radioactivity.

In the last section the methods that have already been developed to measure the amount of natural radioactivity in the heavy water were discussed. These methods can measure the amount of ^{222}Rn in the heavy water which should allow the NC background caused by isotopes from the uranium decay chain to be determined. However, these systems do not provide a method to determine the NC background caused by isotopes from the thorium decay chain since they cannot measure the amount of ^{212}Pb in all of the running conditions of the SNO experiment, particularly when the magnesium chloride has been added. The SNO experiment is actually ten times more sensitive to the decays of isotopes in the thorium decay chain than from those in the uranium decay chain and so an assay for ^{212}Pb has to be developed.

In the next chapter a new assay system will be described which is designed to assay the amount of ^{212}Pb in the heavy water, even if the magnesium chloride has been added, and so should allow the SNO experiment to determine NC background caused by isotopes from the thorium decay chain.

Chapter 3

The Hydrous Titanium Oxide Seeded Ultra-Filtration System

3.1 Introduction

In the previous section it was discussed how the SNO experiment intends to measure the total rate of electron, muon and tau neutrinos that come from the Sun by the important neutral current (NC) interaction. It was also explained that a background to these NC interactions is caused by high energy gamma rays which are produced by the naturally occurring radioactivity of the uranium and thorium decay chains.

The radiochemical assay systems that have already been developed were discussed in the last chapter and are predominantly useful for measuring the contribution to the NC background caused by the presence of isotopes from the uranium decay chain in the heavy water. In this chapter the hydrous titanium oxide (HTiO) seeded ultra-filtration (SUF) assay system will be described. This assay system was developed for the SNO experiment by members of the Oxford Water Group to provide a radiochemical assay for isotopes from the thorium decay chain. Importantly this system is designed to assay ^{212}Pb in the heavy water even when magnesium chloride is present which is when the R/O assay system is inoperable.

In this chapter the physical and chemical properties of this system are described and then this system is modelled to determine the accuracy to which it can be expected to calculate the contribution to the NC background due to the presence of ^{212}Pb in the heavy water of the SNO experiment.

3.2 An Assay System for the Thorium Decay Chain

3.2.1 Introduction to Delayed Coincidence Scintillation Counting

The activity of ^{212}Pb that it is hoped will be in the heavy water can be calculated from the upper limit for the amount of thorium in the heavy water which will produce neutrons at a rate equal to about one tenth of the rate with which they are expected to be produced by NC neutrino interactions. This was quoted in the last chapter to be 3×10^{-15} grams of ^{232}Th per gram of heavy water. If it is assumed that the thorium decay chain is in equilibrium, this limit is equivalent to an activity of about 1 decay per day per tonne (1ddt) of any isotope within the decay chain. Due to the 10.6 hour half-life of ^{212}Pb, this means that in the entire 1000 tonnes of heavy water there is expected to be no more than about 600 atoms of ^{212}Pb. To assay such minute quantities of ^{212}Pb in the heavy water a new, efficient, low background counting technique needed to be developed and this was done by Dr R.K.Taplin in 1994.

The technique is that of delayed coincidence scintillation counting and details of it can be found in Chapter 4 of [Tap95b] and in Appendix D of this thesis. In the ^{232}Th decay chain there is a delayed $\beta - \alpha$ coincidence caused by the short-lived ^{212}Po isotope which can be seen in Figure 2.3 on page 24 to decay with a 300 nanosecond half-life. This decay produces an 8.78MeV alpha particle which is preceded by a beta decay from ^{212}Bi which has a Q-value of 2.25MeV. Scintillation counting together with pulse shape discrimination allows signals caused by alpha particles to be distinguished from those caused by gamma and beta particles. This allows a coincidence requirement to be made which requires two signals to be recorded in about 1 microsecond with the second signal having been caused by an alpha particle. This coincidence requirement virtually eliminates background coincidences being mistaken for real $\beta - \alpha$ coincidences. The measured background of the $\beta - \alpha$ counters developed at Oxford for measuring isotopes from the thorium decay chain is less than 1 decay per day which is at least an order of magnitude lower than the signals expected to be measured from the SNO experiment. The efficiency of the $\beta - \alpha$ counters developed at Oxford for measuring decays of ^{228}Th, ^{224}Ra and ^{212}Pb from the thorium decay chain is about 50%.

There is a similar delayed $\beta - \alpha$ coincidence that can be used to measure the activity of ^{226}Ra and ^{222}Rn in the ^{238}U decay chain. This coincidence is caused by the ^{214}Po isotope whose decay can be seen in the ^{232}U decay chain shown in Figure 2.4 on page 25. The half-life of ^{214}Po is 164 microseconds which is much longer than the 300 nanosecond half-life of ^{212}Po and so $\beta - \alpha$ coincidences from the uranium and the thorium decay chains can be easily distinguished.

The measured background of the $\beta - \alpha$ counters developed at Oxford for measuring isotopes from the uranium decay chain is higher than that for measuring isotopes from the thorium decay chain, at around a few decays per day, due to the longer coincidence time. However, this background is still at least an order of magnitude lower than the signals expected to be measured from the SNO experiment since the detector is ten times less sensitive to the decays of isotopes from the uranium decay chain than from the thorium decay chain. The efficiency of the $\beta - \alpha$ counters developed at Oxford for measuring decays of ^{222}Rn and ^{226}Ra from the uranium decay chain is about 60%.

This counting technique is used to measure small amounts of activity in up to 12 millilitre aqueous samples by mixing them with 40 millilitres of a scintillator cocktail called Optiphase HiSafe 3[1] and detecting signals on a 2 inch photo-multiplier tube. Although the scintillator cocktail is reasonably tolerant concerning chemical consistency of these 12 millilitre samples it is known that they need to have an acid and salt content less than about 1M in concentration.

To use these low background counters to assay the activity in the heavy water, activity first has to be extracted from large volumes of the heavy water and then concentrated into suitable 12 millilitre aqueous samples. The aim of the radiochemical extraction system developed by the Oxford Water Group is to perform this extraction and concentration and the methods by which this will be done are explained in the next two sections.

3.2.2 Extracting Radioactivity from the Heavy Water

In the last chapter it was explained that, due to its short-lived radon parent, the most important isotope to assay in the thorium decay chain is ^{212}Pb. Unfortunately, ^{212}Pb only has a half-life of 10.6 hours and so an extractive assay for this isotope has to be completed in a time not longer than a few tens of hours. To ensure that enough ^{212}Pb is extracted in this short time any assay system has to work using high flow rates. In order to achieve this a system was designed which would pump the heavy water past an ion-exchange material trapped on the inside of ultra-filtration fibres. This method is called seeded ultra-filtration (SUF) by the Oxford Water Group however this term is a little misleading since it actually

[1] Optiphase HiSafe 3 scintillation cocktail can be purchased from Wallac at 20 Vincent Avenue, Crownhill Business Centre, Milton Keynes, MK8 0AB.

refers to the recirculation of a suspension of ion-exchange material not a fixed coating as is used in this situation.

The ion-exchange material used by this system is hydrous titanium oxide (HTiO). This material was selected because it was known that HTiO extracts lead, radium and thorium from both pure water and solutions of magnesium chloride. The HTiO material was investigated in some preliminary experiments for use in the SNO experiment and these showed very promising results, see [How94] and Chapter 5 of [Tap95b].

The ultra-filtration membranes on which this HTiO will be coated have been chosen so that two such membranes connected in parallel to form a pair can pass a flow rate of 200 litres per minute. This flow rate allows the whole 1000 tonnes of heavy water to be processed in a time comparable to the half-life of ^{224}Ra, or about 120 tonnes in a time comparable to the half-life of ^{212}Pb. The chosen membranes are 4 foot long Amicon H26MP01-43 cartridges, each of which has a 0.1 micron pore size and a 2.4 square metre surface area[2].

Two of these membranes will be coated with 0.1 to 0.5 grams of titanium per square metre of membrane in the form of HTiO using the Elution Rig which will be situated in the surface chemistry laboratory at the SNO experiment. Before a coated membrane can be put into the heavy water the HTiO needs to be deuterated and this will be done using a separate rig to displace the hydrogen with deuterium under gravity. The membranes then have to be kept wet while they are transfered underground. Here they will be connected into the SUF Rig so that the heavy water can flow through the two membranes in parallel at the high flow rate. This unit of two HTiO coated membranes operating in parallel is called a parallel pair of membranes.

After the completion of an assay the membranes will be removed from the SUF Rig and sealed for transportation above ground to the surface chemistry laboratory. Here, they will be reconnected as a parallel pair on the Elution Rig and will undergo further chemical processing using light water.

In the next section some of the details of these further chemical processes will be described, however the full operational details of both the Elution Rig and the SUF Rig can be found in [Moo96].

3.2.3 The Elution and Secondary Concentration Procedures

The HTiO ion-exchange material was known not only to extract lead, radium and thorium very efficiently, even from solutions of magnesium chloride, but it was also known that these ions could then be retrieved from it using mineral acid washes. This method, called eluting, allows radioactive isotopes from the heavy water to be extracted onto membranes and then transferred into about 15 to 20 litres of light water mineral acid.

Some initial work showed that radium extracted onto HTiO can be eluted with about 90% efficiency by washing with 0.03M nitric acid for about 15 minutes [Her93]. This acid is not strong enough to remove very much of any lead and thorium extracted onto the HTiO, however lead and thorium can be eluted from HTiO with about a 95% efficiency by washing with 0.5M hydrochloric acid for 20 minutes [Tap96]. These two elutions will be carried out sequentially using the Elution Rig by circulating 15 to 20 litres of the required acid through a pair of membranes used in an extraction for the desired amount of time.

In the last section the $\beta - \alpha$ delayed coincidence scintillation counting technique was described and it was explained that these counters can measure tiny levels of activity in 12 millilitre aqueous samples. A further stage of chemical processing, the secondary concentration, is therefore required to extract natural radioactivity from the 15 to 20 litres of light water acid into 12 millilitre samples suitable for $\beta - \alpha$ counting.

[2]Amicon membranes are sold by: Millipore (UK) Ltd, The Boulevard, Blackmoor Lane, Watford, Hertfordshire, WD1 8YW.

The secondary concentration for radium will be carried out by treating the eluate with HTiO once again, at a much smaller scale. This will be done by adding about 3 milligrams of titanium, in the form of titanium chloride or titanium sulphate, to the 15 to 20 litre eluate and then raising the pH of the solution to about 8 or 9. At this pH the titanium is precipitated as HTiO which extracts any radium present. The HTiO and radium can then be collected on a Media-Kap 10 filter[3] which has a surface area of 0.015 square metres and a pore size of 0.2 microns. The HTiO on one of these filters can be eluted using two or three samples of 4 millilitres of 0.5M hydrochloric acid by leaving each sample in the filter for several minutes. In this way any ^{224}Ra or ^{226}Ra extracted from the heavy water can be collected into a 12 millilitre sample which is ready to be measured for activity on a $\beta - \alpha$ counter. Experimental results by Dr P.T.Trent have shown that such a secondary concentration procedure for radium is about 75% efficient [Tre96].

Unfortunately, the procedure used for radium cannot also be used for the secondary concentration of lead and thorium because, unlike the 0.03M nitric acid, the 0.5M hydrochloric acid dissolves a large proportion of the HTiO. It has been found that a 20 minute elution with 0.5M hydrochloric acid dissolves over 80% of the titanium originally coated into the membranes [Tap96]. This large amount of titanium cannot all be collected on a Media-Kap 10 filter after being precipitated as HTiO as the amount exceeds the capacity of the filter.

The use of a shorter elution time using 0.5M hydrochloric acid has been shown to reduce the amount of titanium dissolution without greatly reducing the efficiency for eluting lead and thorium. For example, a 5 minute elution with 0.5M hydrochloric acid gives elution efficiencies for lead and thorium of 85% and 65% respectively and it dissolves only about 20% of the titanium [Tap96].

This smaller amount of titanium is still too much to be collected on a Media-Kap 10 filter after precipitation but it could be collected on a medium size filter. This medium filter can then be eluted to return the lead and thorium into an acid solution, however the volume of acid required to do this is greater than the 12 millilitres that can be measured by a single $\beta - \alpha$ counter. The solution could be measured using a number of $\beta - \alpha$ counters but this will reduce sensitivity because counting backgrounds will be higher.

The repetition of HTiO extractions and elutions on progressively smaller sized filters should make it possible to end up with a 12 millilitre volume. Unfortunately, the details of this procedure are dependent upon the amount of titanium in the initial eluate of the SUF membranes. Also, the procedure is inefficient since each extraction and elution stage, including the final Media-Kap stage, is expected to be only about 80% efficient. This means that, for lead, the procedure would give a combined elution and secondary concentration efficiency of only 54% using one intermediate sized filter and only 44% using two intermediate sized filters. The efficiencies for thorium are expected to be even lower since elution efficiencies for thorium are generally lower than for lead.

The development of an alternative, efficient method for the secondary concentration of lead and thorium which is not dependent upon the amount of titanium in the initial eluate of the SUF membranes is clearly needed. In Chapters 5-7 of this thesis there are details of the research that has been conducted to develop such an alternative method.

[3]Registered Trade Mark of MICROGON CAT. #:ME2M-100-18S which are sold by Spectrum, Laguana Hills, CA and their distributors.

3.3 Simulating the Capability of the HTiO SUF Assay System

3.3.1 Introduction

In the last section it was explained that the HTiO ion-exchange material will be coated on two SUF membranes which will be connected in the form of a parallel pair to allow high flow rates of heavy water to be processed. The extraction of ^{228}Th, ^{224}Ra and ^{212}Pb by a single, small scale SUF membrane has been investigated both experimentally and theoretically, see Chapter 5 and Appendix D of [Tap95b].

It was found that when ^{224}Ra extracted on an HTiO coated SUF membrane decays it does not usually produce an atom of ^{212}Pb extracted onto the same membrane. This effect, called 'radon breakthrough', is caused by the ^{224}Ra first decaying to ^{220}Rn which dissolves in the water flow and only decays to ^{212}Pb, with a 55 second half-life, after the water has passed through the membrane.

Because of this effect the HTiO SUF assay system is designed to use two parallel pairs of SUF membranes connected in series with a one tonne decay tank in between. The volume of this decay tank has been chosen so that the residence time of water flowing at 200 litres per minute is 5 minutes. This corresponds to about five half-lives of ^{220}Rn, thus ensuring that almost all of the ^{220}Rn decays to ^{212}Pb before the water enters the second membrane when the decay tank is present.

To calculate the activity of ^{212}Pb in the heavy water by measuring the activity of ^{228}Th, ^{224}Ra and ^{212}Pb on each membrane pair after an extractive assay it is necessary to understand the effect of radon breakthrough in a double membrane system. In the rest of this chapter this will be done by mathematically modelling the HTiO SUF assay system.

3.3.2 Notation and Definitions

A schematic of the double membrane system including the decay tank between the two membrane pairs is shown in Figure 3.1 along with the notation that will be used in modelling this system. The number of atoms of each isotope on each membrane pair are given by: N_i^{M1} and N_i^{M2}, where i stands for thorium, radium or lead. The rate of flow of atoms per hour for each isotope into each membrane pair are given by: R_i^{F1} and R_i^{F2}, and the rate of flow of atoms per hour for each isotope out of each membrane pair are given by: R_i^{P1} and R_i^{P2}.

In order to model the characteristics of this double membrane system a number of parameters have to be defined and estimated. This is done below using the same convention as was used in Appendix D of [Tap95b] and experimental values taken from small scale systems as detailed in Chapter 5 of [Tap95b].

- α_{Th}, α_{Ra} and α_{Pb}: The respective probabilities that an atom of thorium, radium or lead in the heavy water is extracted onto a parallel pair of HTiO coated membranes when a flow rate of 200 litres per minute is maintained. These probabilities are all expected to be about 0.9 meaning that the extraction efficiency of a pair of HTiO coated SUF membranes for thorium, radium and lead is 90%.

- ϵ: The probability that the decay of a ^{224}Ra atom, which has already been extracted onto a membrane pair, leads to an atom of ^{212}Pb being captured on the same membrane pair. Small scale experiments have shown that ϵ takes a value of around 0.25 which corresponds to 75% radon breakthrough.

- μ: The probability that the $(1-\epsilon)$ atoms of ^{212}Pb which are produced by decays of ^{224}Ra on the first membrane pair but are not captured by it, can be extracted by the second membrane pair. If it is assumed that the loss of ^{212}Pb is entirely due to radon breakthrough then the value of μ can be calculated from the residence time between the two membrane pairs. With no decay tank this

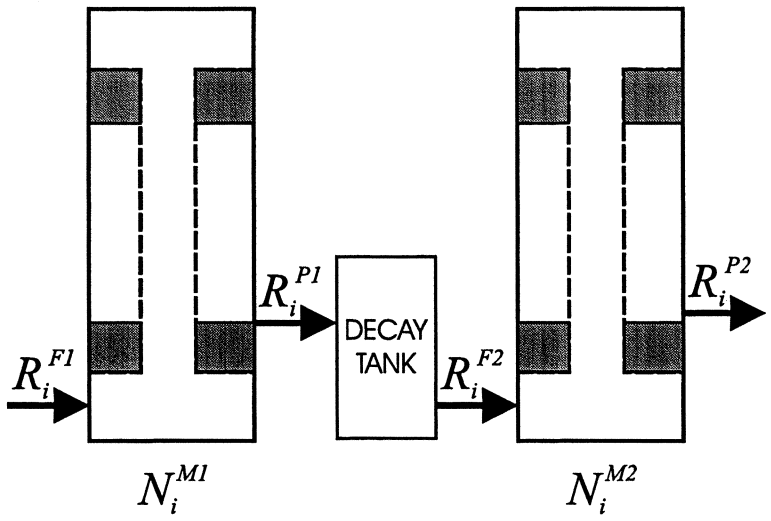

Figure 3.1: *This is a schematic of the double membrane system used by the SUF HTiO system. In this diagram each membrane shown represents a parallel pair of SUF membranes. The R's denote the rates of flow of atoms per hour and the N's denote the numbers of atoms on the membranes. The subscript, i stands for the three important long-lived isotopes in the ^{232}Th decay chain: ^{228}Th,^{224}Ra and ^{212}Pb.*

is estimated to be about 3.4 seconds which means that 4% of the ^{220}Rn will have decayed to ^{212}Pb before the second membrane pair, making $\mu = 0.04$. With the one tonne decay tank the residence time is increased to about 303 seconds which means that 98% of the ^{220}Rn will have decayed to ^{212}Pb before the second membrane pair, making $\mu = 0.98$. To a good approximation therefore, without a decay tank: $\mu = 0$, and with a one tonne decay tank: $\mu = 1$.

- δ: This represents the same loss as ϵ but for the thorium-radium system. It is the probability that the decay of a ^{228}Th atom, which has already been extracted onto a membrane pair, leads to an atom of ^{224}Ra being captured on the same membrane pair. It is expected that there will be no loss mechanism in this system and so δ will have a value of 1. However, this loss has not been investigated experimentally and it is possible that effects such as nuclear recoil may slightly reduce this value.

- η: This variable is the same as μ but for the thorium-radium system. There is no reason to expect this variable to take any value other than 1 and in all calculations it will take this value. However, it is included in algebraic expressions in order to preserve the symmetry between the thorium-radium and radium-lead systems.

Using the definitions above, and by assuming that each membrane pair behaves identically, a number of first order, coupled differential equations can be written down to describe the double membrane system when extracting the three long-lived isotopes in the ^{232}Th decay chain: ^{228}Th, ^{224}Ra and ^{212}Pb, from the heavy water of the SNO detector. These equations all involve the decay constants of ^{228}Th, ^{224}Ra and ^{212}Pb (λ_{Th}, λ_{Ra} and λ_{Pb}) whose values are listed in Equation 3.1.

$$\lambda_{Th} = 4.14 \times 10^{-5} hr^{-1} \quad ; \quad \lambda_{Ra} = 7.89 \times 10^{-3} hr^{-1} \quad ; \quad \lambda_{Pb} = 6.54 \times 10^{-2} hr^{-1} \tag{3.1}$$

The first equations which can be derived are for the atoms of ^{228}Th, ^{224}Ra and ^{212}Pb on each membrane pair after a time, t, of passing heavy water through them. These are shown in Equations 3.2, 3.3 and 3.4 where $j = 1, 2$ denotes the first or second membrane pairs. These equations are given in terms of the rates of flow of atoms into the membrane, the extraction efficiencies and the loss parameters.

$$\frac{dN_{Th}^{Mj}(t)}{dt} = \alpha_{Th} R_{Th}^{Fj}(t) - \lambda_{Th} N_{Th}^{Mj}(t) \qquad j = 1, 2 \tag{3.2}$$

$$\frac{dN_{Ra}^{Mj}(t)}{dt} = \alpha_{Ra} R_{Ra}^{Fj}(t) - \lambda_{Ra} N_{Ra}^{Mj}(t) + \delta \lambda_{Th} N_{Th}^{Mj}(t) \quad j = 1, 2 \tag{3.3}$$

$$\frac{dN_{Pb}^{Mj}(t)}{dt} = \alpha_{Pb} R_{Pb}^{Fj}(t) - \lambda_{Pb} N_{Pb}^{Mj}(t) + \epsilon \lambda_{Ra} N_{Ra}^{Mj}(t) \quad j = 1, 2 \tag{3.4}$$

The feed rate of flow of ^{228}Th atoms into the second membrane pair, R_{Th}^{F2}, is constant in time and an expression for it is given in Equation 3.5. The feed rate of flow of ^{224}Ra and ^{212}Pb into the second membrane pair, R_{Ra}^{F2} and R_{Pb}^{F2}, are not constant in time as they depend on the activity of their parent isotope extracted onto the first membrane pair. Expressions for these can be found in terms of the rate of flow of atoms into, and the number of atoms on, the first membrane pair by taking into account the values of the parameters μ and η and these expressions are given in Equations 3.6 and 3.7.

$$R_{Th}^{F2} = (1 - \alpha_{Th}) R_{Th}^{F1} \tag{3.5}$$

$$R_{Ra}^{F2}(t) = (1 - \alpha_{Ra}) R_{Ra}^{F1} + \eta(1 - \delta) \lambda_{Th} N_{Th}^{M1}(t) \tag{3.6}$$

$$R_{Pb}^{F2}(t) = (1 - \alpha_{Pb}) R_{Pb}^{F1} + \mu(1 - \epsilon) \lambda_{Ra} N_{Ra}^{M1}(t) \tag{3.7}$$

Instead of writing equations in terms of the number of atoms on a membrane or in the flow of water, it is often more useful to express them in terms of activities. These activities can be easily obtained from the number of atoms by multiplying by the decay constant for that particular isotope. This change of notation is shown in Equation 3.8 where the activities of each isotope on each membrane pair are given by: A_i^{M1} and A_i^{M2}, and the feed activity flow rates of each isotope into each membrane are given by: F_i^{F1} and F_i^{F2}.

$$\begin{aligned} A_i^{M1}(t) &= \lambda_i N_i^{M1}(t) \quad ; \quad A_i^{M2}(t) = \lambda_i N_i^{M2}(t) \\ F_i^{F1} &= \lambda_i R_i^{F1} \equiv F_i \quad ; \quad F_i^{F2}(t) = \lambda_i R_i^{F2}(t) \qquad i = Th, Ra, Pb \end{aligned} \tag{3.8}$$

It will be assumed that the feed activity flow rates of each isotope into the first membrane pair are constant in time during an assay. This is shown by redefining the F_i^{F1}'s to be the constant: F_i's, as is also shown in Equation 3.8.

3.3.3 A Computer Simulation of a Single Extraction

In Section A.2 in the Appendix starting on page 139 the full solutions of the equations given in the last section are derived. These expressions are somewhat difficult to analyse directly and so a simple FORTRAN simulation program was written in order to investigate the behaviour of the activity of ^{228}Th, ^{224}Ra and ^{212}Pb on each membrane pair during extractions.

This program allowed the values for the parameters describing the system to be varied along with the feed activities of ^{228}Th, ^{224}Ra and ^{212}Pb within the heavy water. The values of the parameters were chosen to be the expected values given by small scale experiments, as were listed in the last section. This means that the extraction probabilities were assumed to be 0.9, the radon breakthrough parameter was assumed to be 0.25 and no other losses were assumed.

Three situations with different feed activity flow rates were assumed. In the first of these situations, Situation A, it will be assumed that there is the same activity of ^{228}Th, ^{224}Ra and ^{212}Pb in the heavy water, ie radioactive equilibrium. The activity of these isotopes in the heavy water will be assumed to be that which produces neutrons at a rate equal to about one tenth of the rate that they are expected to be produced by NC neutrino interactions. In Section 3.2.1 on page 29 it was explained that this corresponds to an activity of ^{228}Th, ^{224}Ra or ^{212}Pb in the heavy water of 1 decay per day per tonne of heavy water (1ddt). At a flow rate of 200 litres per minute this activity gives a flow rate of activity of 0.5 decays per hour, per hour of water flow into the first pair of membranes. Therefore in Situation A the feed activity flow rates of ^{228}Th, ^{224}Ra and ^{212}Pb (F_{Pb}, F_{Ra} and F_{Th}) will all take the value of 0.5.

There are two obvious physical situations which could cause a steady state disequilibrium between the isotopes of the ^{232}Th decay chain in the heavy water and these situations will be labelled Situation B and Situation C. In these situations it will be assumed that the minimum activity of any isotope in the heavy water is at the 1ddt level and that an assumed excess of a particular isotope will mean that its activity will be at the 5ddt level. These levels have been arbitrarily chosen however they are not thought to be unrepresentative of the conditions that will be found in the SNO experiment. In Situation B it will be assumed that thorium and lead are coming out of the heavy water and adhering to surfaces within the heavy water circulation system. This effect, called 'plating', will reduce the activity of ^{212}Pb and ^{228}Th in the heavy water and create an excess of ^{224}Ra. Therefore in Situation B, while F_{Pb} and F_{Th} will both take the value of 0.5, the value of F_{Ra} will be increased to 2.5. In Situation C it will be assumed that there is a fixed source of ^{224}Ra or ^{228}Th emanating ^{220}Rn into the heavy water which will produce an excess of ^{212}Pb in the heavy water. Therefore in Situation C, while F_{Ra} and F_{Th} will both take the value of 0.5, the value of F_{Pb} will be increased to 2.5.

Using these values for the feed activity flow rates, and the values for the parameters which have already been discussed, the amount of activity of each isotope on each membrane pair was calculated every two hours for a 100 hour extraction using the simulation program. The resulting activities were written as HBOOK[4], ntuple files and plotted using PAW[5] as shown in Figure 3.2.

It can be seen from this figure that the activity of ^{228}Th on the first and second pairs of membranes is linear in time which is to be expected due to the long, 1.91 year half-life of ^{228}Th. It can also be seen that the ^{228}Th activity on the second membrane pair is ten times less than that on the first. This is because the second membrane pair can only extract from the 10% that the first membrane failed to extract. It is clear that by taking the ratio of the activity on the second membrane pair as compared to the first, it is possible to gain some knowledge of the extraction efficiency for that isotope. The calculation of extraction probabilities from final membrane activities is discussed more fully in Section 3.3.5 starting on page 40.

The activity of ^{224}Ra on the first membrane pair is, like the ^{228}Th activity, ten times the activity on the second however there is a slight non-linear time dependence caused by the extraction times being comparable to the 87.8 hour half-life of ^{224}Ra. The excess of ^{224}Ra introduced in Situation B can be clearly seen at all times on both membrane pairs.

[4]HBOOK, CERN Program Library entry Y250.

[5]PAW:Physics Analysis Workstation, CERN Program Library entry Q121.

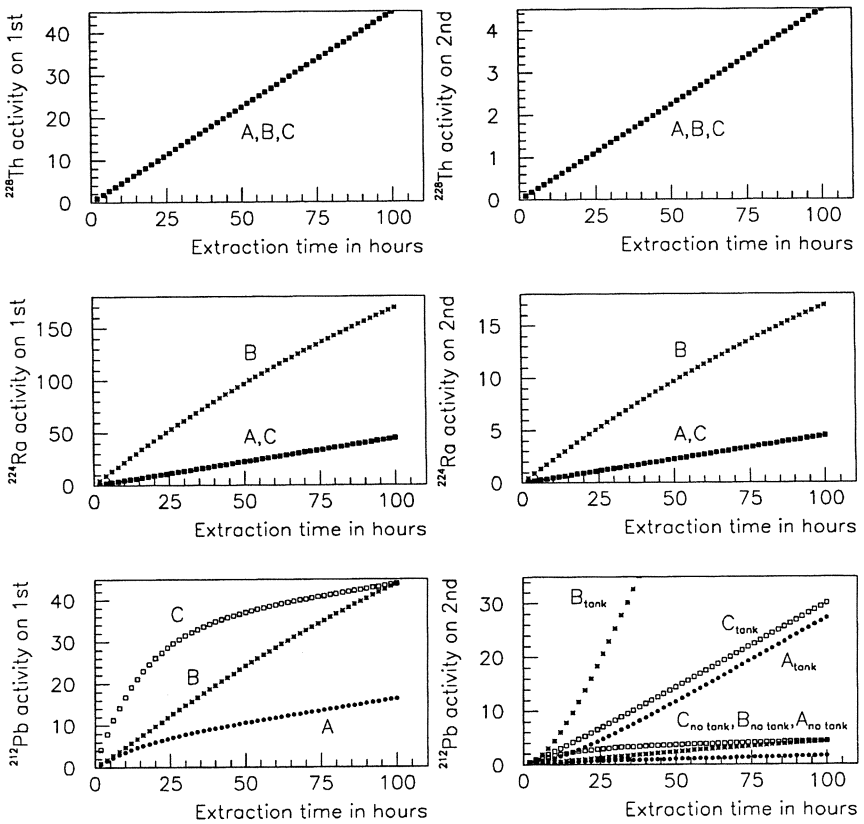

Figure 3.2: *Simulations of the activity of ^{228}Th, ^{224}Ra and ^{212}Pb in decays per hour expected on the first and second membrane pairs in the HTiO SUF assay system for different extraction times. The extraction probabilities for ^{228}Th, ^{224}Ra and ^{212}Pb were all assumed to be 0.9, the radon breakthrough parameter was assumed to be 0.25 and no other losses were assumed. In Situation A (shown by circles) equilibrium feed activities at the 1ddt level were assumed. In Situation B (shown by stars) the case of a ^{224}Ra excess was assumed. In Situation C (shown by empty squares) the case of a ^{212}Pb excess was assumed. The final plot shows the ^{212}Pb activity in decays per hour expected on the second membrane pair and this depends upon whether or not the 1 tonne decay tank is present and so both situations were calculated and are displayed.*

The plots showing the activities of ^{212}Pb on the first and second membrane pairs are the most interesting. With small extraction times the activity of ^{212}Pb on each membrane pair is representative of the activity of ^{212}Pb in the heavy water but with extraction times long compared to the 10.6 hour half-life of ^{212}Pb, the activity of ^{212}Pb on each membrane pair is greatly effected by the activity of ^{224}Ra extracted by that membrane pair. Indeed, in Situation B, where there is an excess of ^{224}Ra, the activity of ^{212}Pb on the first membrane pair is always almost entirely dominated by the activity of ^{224}Ra on that membrane pair.

The activity of ^{212}Pb on the second membrane pair clearly shows the combined effect of radon breakthrough and a decay tank. Without a decay tank the activity of ^{212}Pb on this membrane pair is again always one tenth of the activity on the first membrane pair in each of the three situations. However, when the decay tank is present the ^{212}Pb activity on the second pair of membranes is much higher. This is caused by the extraction of ^{212}Pb produced by decays of ^{224}Ra on the first membrane pair but which are not captured by it due to radon breakthrough. When there is an excess of ^{224}Ra in the heavy water, in Situation B, it can be seen that the activity of ^{212}Pb on the second pair of membranes is actually greater than that on the first pair for extraction times longer than about 15 hours.

The differences between Situation A, when there is equilibrium, and Situation C, where there is an excess of ^{212}Pb, can be clearly seen at all times.

3.3.4 The Decontamination Factor for ^{212}Pb in Different Situations

The HTiO SUF system has been designed primarily as an assay system, however its characteristics as a purification system can also be investigated. An extractive purification system can be described by its decontamination factor (DF) for a particular component. This is defined to be the amount of a component which enters the system divided by the amount which leaves it. The DF for ^{212}Pb for a single HTiO SUF membrane at different times when extracting from a solution in radioactive equilibrium has been shown to depend upon the amount of radon breakthrough, see Appendix D of [Tap95b].

The DF for ^{212}Pb of the HTiO SUF system has to take into account the two pairs of parallel membranes and the possible presence of a 1 tonne decay tank. An expression for the ^{212}Pb activity flowing out of the second pair of membranes as a function of time can be derived and this is shown in Equation 3.9. An expression giving the DF for ^{212}Pb at an instant in time, t hours after the start of an extraction, can be found by substituting into Equation 3.9 the expression for the feed flow of activity into the second membrane pair, as given in Equation 3.7 on page 35. The final expression for $DF_{Pb}(t)$ is given in Equation 3.10.

$$R_{Pb}^{P2}(t) = (1-\alpha_{Pb})R_{Pb}^{F2}(t) + (1-\epsilon)\lambda_{Ra}N_{Ra}^{M2}(t) + (1-\mu)(1-\epsilon)\lambda_{Ra}N_{Ra}^{M1}(t) \tag{3.9}$$

$$\frac{1}{DF_{Pb}(t)} = \frac{R_{Pb}^{P2}(t)}{R_{Pb}^{F1}(t)} = (1-\alpha_{Pb})^2 + \frac{(1-\epsilon)\lambda_{Pb}}{F_{Pb}}[A_{Ra}^{M1}(1-\alpha_{Pb}\mu) + A_{Ra}^{M2}] \tag{3.10}$$

It is obvious that the DF for ^{212}Pb is decreased if ϵ is small meaning that there is a large amount of radon breakthrough. The DF for ^{212}Pb is also decreased if μ is small which is the case if there is no decay tank present. These effects are caused by a large proportion of ^{212}Pb produced by decays of ^{224}Ra on the first membrane pair passing through both membrane pairs and back into the heavy water.

The simulation program discussed in the last section was used to calculate the DF for ^{212}Pb of the HTiO SUF system every two hours for 100 hour extractions. These extractions used the same values for the parameters and feed activities as were used in the last section for the three different feed activity situations. The DF for ^{212}Pb was calculated for extractions with the one tonne decay tank present and for those without a decay tank and the results are compared graphically in Figure 3.3.

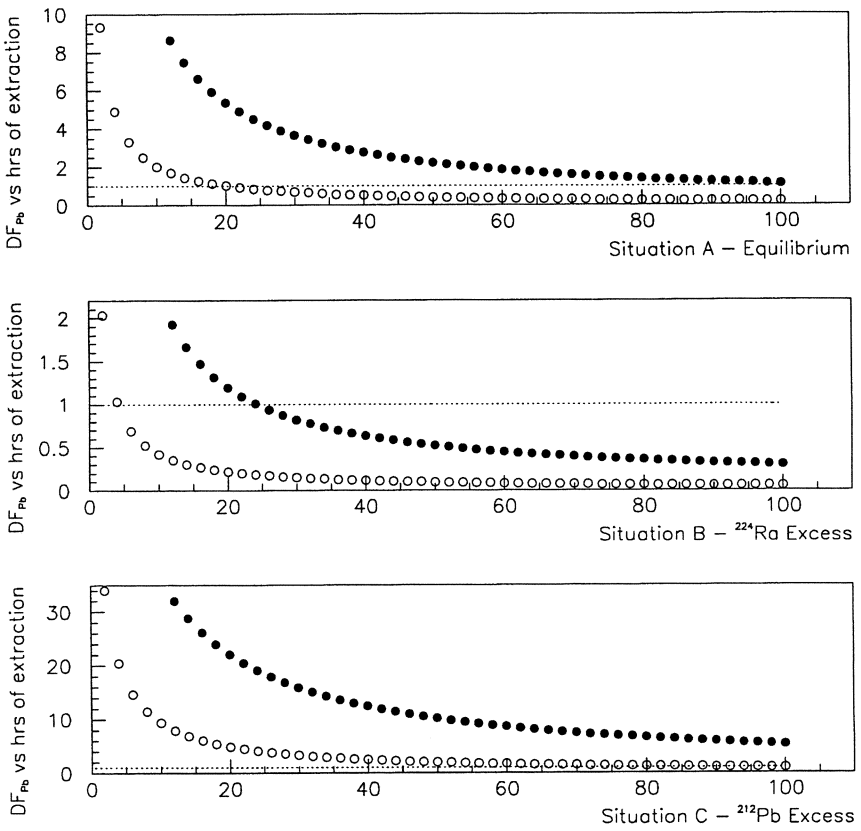

Figure 3.3: *The variation of the decontamination factor for ^{212}Pb with the length of time of an extraction from the heavy water for the three feed situations of radioactive equilibrium at the 1ddt level (Situation A), a ^{224}Ra excess (Situation B) and a ^{212}Pb excess (Situation C). The full circles are the calculated values for DF_{Pb} when a decay tank is present and the empty circles are when there is no decay tank. The horizontal lines given in dots show a value of DF_{Pb} equal to one. When the calculated value for DF_{Pb} crosses this line the amount of ^{212}Pb flowing out of the double membrane system becomes larger than the amount entering the system at that particular time.*

It is clear from examining Figure 3.3 that, as expected, the DF for ^{212}Pb is always higher with a decay tank than without. It is however interesting to note that in certain circumstances the DF for ^{212}Pb actually drops below 1 which means that at that point in time there is more ^{212}Pb flowing out of the second membrane pair than which enters the first membrane pair. In Situation B, where ^{212}Pb plating is assumed to be high creating an excess of ^{224}Ra, this effect is a little artificial since the ^{212}Pb is likely to plate out shortly after the system. However, even when the isotopes are in equilibrium at the 1ddt level, in Situation A, without a decay tank the DF for lead drops below 1 after an extraction time of only 20 hours. The fact that the DF for ^{212}Pb drops below 1 after a certain extraction time does not mean that the integrated effect of the assay is to add ^{212}Pb to the detector but it does mean that for long assays the extraction system can start to become a source of ^{212}Pb which could pass into the SNO detector and increase the NC background at particular times. To ensure that this does not happen extraction times should be kept short and a decay tank should be used.

3.3.5 Modelling Assays Using the HTiO SUF Assay System

A computer model of the HTiO SUF double membrane system was developed using as a basis the simulation program which was discussed in Section 3.3.3 on page 35. This program was changed so that instead of calculating the activities of the three isotopes on the two membrane pairs for just one extraction it could calculate the activities for many such extractions each with different values for the feed activities and parameters.

In the HTiO SUF system the ^{228}Th, ^{224}Ra and ^{212}Pb on each membrane pair after the end of an extraction have to be removed and concentrated into small volumes so that they can be measured by the $\beta - \alpha$ delayed coincidence scintillation counters. The method to do this for radium was discussed in Section 3.2 on page 29. It was also explained that new techniques have to be developed to perform the secondary concentration of lead and thorium. In this model it will be assumed that new techniques exist and that they give efficiencies similar to the already developed secondary concentration procedure for radium.

To be able to analyse and estimate the accuracy to which this system can be expected to calculate the feed activities of ^{228}Th, ^{224}Ra and, especially, ^{212}Pb it is necessary to model these chemical processing and counting techniques while including any sources of uncertainty. It is envisaged that the two main sources of uncertainties are the accuracy to which the efficiency of the secondary processing and counting is known and the statistical $\sqrt{N}$ error on the number of counts that are eventually expected to be measured. The details of how this modelling was performed is given in Section A.3 in the Appendix starting on page 140. The modelling assumes that the overall concentration and counting efficiency is 35% for ^{224}Ra and ^{212}Pb, and 25% for ^{228}Th. The lower overall efficiency for ^{228}Th is assumed because of its lower elution efficiency. This modelling assumes that the actual efficiencies in each secondary concentration are within 10% of these true values indicating a 10% systematic error.

In the SNO experiment the activity of each isotope in the heavy water and some of the parameters which describe the HTiO SUF system will need to be calculated from the measured activities of ^{212}Pb, ^{224}Ra and ^{228}Th on the membrane pairs after an assay. In the following discussion it will be explained how this can be done. It was noted in Section 3.3.3 on page 36 that the ratio of the activity of an isotope on the second membrane pairs compared to the first gives knowledge of the extraction efficiency of the membrane pairs for that isotope. In fact for ^{228}Th the extraction probability, α_{Th}, can be exactly calculated from these activities alone using the expression given in Equation 3.11. Using this calculated value for the extraction probability, α_{Th}, the feed activity flow rate of ^{228}Th, F_{Th}, can be calculated using the expression given in Equation 3.12. In this equation the approximation given is valid for all assay times that will be used in the SNO detector since $\lambda_{Th}t$ is very small for assays lasting only a few days.

$$\alpha_{Th} = 1 - \frac{A_{Th}^{M2}}{A_{Th}^{M1}} \tag{3.11}$$

$$F_{Th} = \frac{A_{Th}^{M1}}{\alpha_{Th}} \frac{\lambda_{Th}}{(1 - e^{-\lambda_{Th}t})} \cong \frac{A_{Th}^{M1}}{\alpha_{Th}t} \tag{3.12}$$

The activity of ^{228}Th in the heavy water can be easily deduced from the calculated value of F_{Th} by knowing the average rate at which the heavy water was pumped through the system during the assay.

Similar expressions to those shown in Equations 3.11 and 3.12 can be used to calculate the extraction probabilities and feed activity flow rates for ^{224}Ra and ^{212}Pb, if assay times used are much shorter than their respective half-lives. If longer assay times are used then it becomes necessary to take into account the effects due to the decays of parent isotopes and in particular the effect of radon breakthrough. The exact expressions for α_{Ra}, α_{Pb}, F_{Ra} and F_{Pb} including all of these effects are given in Section A.4 in the Appendix starting on page 142.

Situation Name:	Description of System:	Feed Activity Flow Rates:			Parameters and Efficiencies:		
		F_{Th}	F_{Ra}	F_{Pb}	δ	ϵ	α_{Th}, α_{Ra} and α_{Pb}
A	Equilibrium	0.4-0.6	0.4-0.6	0.4-0.6	0.9-1.0	0.1-0.4	0.75-0.95
B	^{224}Ra excess	0.4-0.6	2.0-3.0	0.4-0.6	0.9-1.0	0.1-0.4	0.75-0.95
C	^{212}Pb excess	0.4-0.6	0.4-0.6	2.0-3.0	0.9-1.0	0.1-0.4	0.75-0.95

Table 3.1: *The initial ranges of the feed activity flow rates, the two loss parameters: δ and ϵ, and the extraction efficiencies: α_{Th}, α_{Ra} and α_{Pb}, which were used by the computer model for the three different feed activity situations which were discussed in Section 3.3.3 on page 36.*

Unfortunately these exact expressions are in terms of the values of the loss parameters δ and ϵ and it is impossible to measure the values of these parameters for the HTiO SUF assay system without adding long-lived activity to the SNO detector. The effect of any losses in the thorium-radium system, given by δ, can be decoupled from calculating the activity of ^{224}Ra in the heavy water by using assay times of less than about 30 hours since for these times the terms involving δ are only minor corrections. However, the effect of radon breakthrough cannot be decoupled from calculating the activity of ^{212}Pb in the heavy water since assay times short compared to the 10.6 hour half-life of ^{212}Pb will not extract enough activity to be measurable. There is a solution to this difficulty and that is to calibrate the extraction efficiency of ^{212}Pb by the HTiO SUF assay system. This can be done using stable lead or a source of ^{212}Pb which has been separated from its long-lived parents. In the rest of this analysis it will be assumed that such a calibration has taken place and that the extraction efficiency for ^{212}Pb is known to within 10% of its true value in any particular assay. Using this known value of α_{Pb} the value of ϵ can be calculated in each assay from the activities of the isotopes on the membrane pairs after an assay using the expression given in Equation A.18 on page 143.

3.3.6 The Capability of a Single Assay in Different Situations

The computer model which was described in the last section was used to calculate the accuracy to which the activity of ^{212}Pb in the heavy water can be calculated using the HTiO SUF assay system. This was done by simulating many such assays and comparing the calculated values of variables, such as the feed activity flow rate of ^{212}Pb, with the true values that the simulation used. The difference between the calculated and true values as a fraction of the true value was calculated so that distributions for many assays could be generated. The width of these distributions gives the average percentage error to be expected when that variable is calculated by a single assay during the operation of the SNO experiment.

The variation of the percentage error on calculating the activity of ^{212}Pb in the heavy water with different assay times is shown in Table 3.2. These results were achieved by taking values for the feed activity flow rates from those given in Table 3.1 for Situation A which assumes rough equilibrium at the 1ddt level and assuming the presence of a decay tank and a 10% accurate calibration for the ^{212}Pb extraction efficiency.

It can be seen that the variation of the error with assay time is not large but it does indicate that assays of between 10 and 15 hours are optimal. The increased error for short assays is due to an increase in the statistical error on the number of ^{212}Pb counts measured whereas the increase in error for longer assay times is due to additional errors introduced by terms involving the radon breakthrough parameter. To maximise the assay time while keeping the error on calculating the activity of ^{212}Pb in the heavy water as low as possible the best assay time is 15 hours and this time will be used as standard for every short assay in the rest of this analysis.

Time of Assay:	5hrs	10hrs	15hrs	20hrs	30hrs
Error on ^{212}Pb Activity:	38%	34%	34%	36%	42%

Table 3.2: *The percentage error on calculating the activity of ^{212}Pb in the heavy water using a single, short assay of different assay times. These assays assumed values for the feed activities and parameters taken from the ranges given in Table 3.1 for the situation of rough equilibrium at the 1ddt level, the presence of a decay tank and a 10% accurate calibration for the ^{212}Pb extraction efficiency.*

The distributions produced for all of the variables that can be calculated by 15 assays are shown in Figure 3.4 for the case of rough equilibrium at the 1ddt level assuming the presence of a decay tank and a 10% accurate calibration for the ^{212}Pb extraction efficiency. The percentage errors in the calculated values for these variables can be taken from these plots, as has already been explained, and they are given in Table 3.3. Also given in Table 3.3 are the similar results obtained when the feed activities are taken from the ranges shown in Table 3.1 for the situations of a ^{224}Ra excess (Situation B) and a ^{212}Pb excess (Situation C).

The results of Table 3.3 show that the feed activities of ^{228}Th and ^{224}Ra can always be calculated to within about 10% of the true values. This error is dominated by the 10% systematic error which was assumed on the knowledge of the chemical processing and counting efficiencies. These results also show that by using the double membrane system it is possible to self-calibrate the extraction efficiencies for ^{228}Th and ^{224}Ra to within 4-6% of their true values.

The error in calculating the feed activity of ^{212}Pb can be seen to be about 35% when there is equilibrium within the decay chain at the 1ddt level of activity. This error is dominated by the large, statistical error on the number of counts measured for ^{212}Pb samples. When there is five times more ^{212}Pb present in the heavy water, which is the case in Situation C, the error in calculating the activity of ^{212}Pb in the heavy water decreases by a factor of about $\sqrt{5}$ to 15%, as would be expected.

Unfortunately the results of Table 3.3 also show that if there is an excess of ^{224}Ra in the heavy water the activity of ^{212}Pb in the heavy water can be calculated less accurately. This is due to large correction terms involving the poorly calculated radon breakthrough parameter, ϵ.

This parameter can be seen from the results given in Table 3.3 to be very poorly calculated in all situations even when a calibration for the lead extraction efficiency is assumed and a decay tank is present. This is due to the very low statistics that are involved in ^{212}Pb assays. However, except for the case of a ^{224}Ra excess this large uncertainty in the amount of radon breakthrough is not a major error in the calculation of the ^{212}Pb activity in the heavy water since the correction terms are usually small.

The fact that the amount of radon breakthrough does not seem to be very well calculated led to an investigation to determine whether or not the one tonne decay tank is useful when performing short assays using the HTiO SUF assay system and this is discussed below.

Without the presence of a one tonne decay tank it is still possible to calculate the amount of radon breakthrough in the SUF assay system using the expression given in Equation A.18 on page 143 but such calculations are extremely inaccurate. This is because without a decay tank it is virtually impossible to know whether the ^{212}Pb activity on the first membrane pair has been extracted from the heavy water or has been caused by a proportion of ^{224}Ra decays. Only by collecting a known portion of the ^{212}Pb lost from the first membrane pair on the second membrane pair, by the use of a one tonne decay tank, can the amount of radon breakthrough be calculated with any real accuracy. In fact without a decay tank it is more accurate to assume reasonable limiting values for the amount of radon breakthrough and accept the systematic errors that this produces. To investigate the size of this systematic error a simple analysis of short assays without a decay tank present was completed.

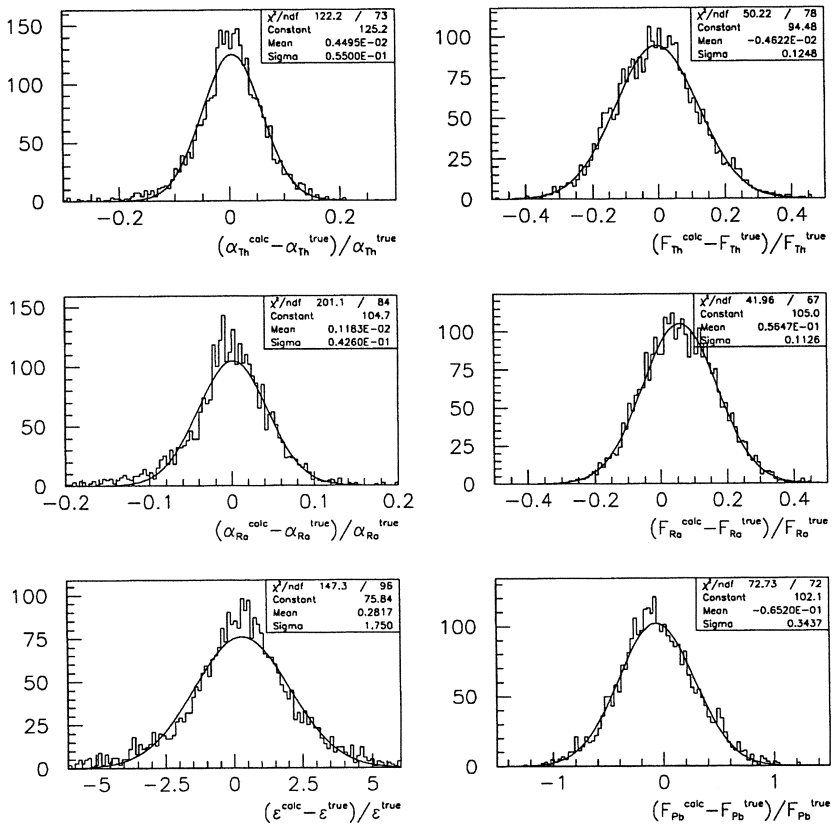

Figure 3.4: *Distributions showing the results of calculating feed activity flow rates and parameters by a model of the HTiO SUF assay system. These results are for 15 hour assays assuming the presence of a decay tank and a calibration for the lead extraction efficiency of 10% accuracy. The feed activity flow rates and parameters were taken from the ranges given in Table 3.1 on page 41 for the situation of rough equilibrium at the 1ddt level, Situation A.*

Situation:		Probabilities:		Loss Param:	Feed Activities:		
Name	Description	α_{Th}	α_{Ra}	ϵ	F_{Th}	F_{Ra}	F_{Pb}
A	Equilibrium	6%	4%	170%	12%	11%	34%
B	^{224}Ra excess	6%	3%	90%	12%	9%	69%
C	^{212}Pb excess	6%	4%	350%	12%	11%	15%

Table 3.3: *A summary of the accuracy to which the feed activities of ^{212}Pb, ^{224}Ra and ^{228}Th in the heavy water and the parameters which describe the system can be expected to be calculated in different feed activity situations as described in detail in Table 3.1 on page 41. These results were calculated using single 15 hour assays assuming the presence of a decay tank and a calibration for the lead extraction efficiency of 10% accuracy.*

In this analysis ϵ is chosen to have a lower limit of 0.0 which is a physical bound and an upper limit of 0.5 which is expected to be a reasonable bound based on the results of small scale experiments. The calculated ^{212}Pb activities using these limiting values of ϵ and no decay tank are compared to the true values for many short assays in Figure 3.5. Superimposed onto each plot are the results found by using a decay tank and calculating ϵ.

These plots show that by removing the decay tank and assuming limiting values for ϵ, the distributions for the calculated feed activity flow rates of ^{212}Pb are systematically shifted in one direction or the other. This is because if ϵ is underestimated then the activity of ^{212}Pb in the heavy water is calculated to be higher than the actual value whereas if ϵ is overestimated then the opposite effect occurs. These shifts in the peaks of the distributions must be interpreted as systematic errors and therefore must be added in quadrature to the statistical error given by the mean width of the two distributions to give overall errors for calculating the activity of ^{212}Pb in the heavy water without a decay tank. These errors are summarised for each of the three feed activity situations and compared to the error found when a decay tank is used and ϵ is calculated in Table 3.4.

The results in this table show that there is very little difference in the overall error on calculating the activity of ^{212}Pb in the heavy water by single 15 hour assays when using a decay tank or by assuming limiting values of radon breakthrough. Only when there is a large excess of ^{224}Ra in the heavy water is the error caused by not having a decay tank very much larger than when using one. However, it may be possible to more accurately calculate the amount of radon breakthrough using the decay tank by combining the results of two assays of different times and this will be discussed in the next section.

3.3.7 The Benefits of Combining the Results of Two Assays

It will be possible to use the HTiO SUF assay system to perform not only single short assays but to perform two consecutive assays of different times. This allows the possibility of not only calculating the amount of radon breakthrough more accurately but it also might allow any losses within the thorium-radium system to be identified.

The computer model used in the previous section was made to assume the presence of a decay tank and a 10% accurate calibration for the extraction efficiency of ^{212}Pb. This model was then developed to combine the results of two assays, assumed to be identical apart from their duration, in order to most accurately calculate the activities in the heavy water and the parameters which describe the system. The exact expressions which were used in these calculations are given in Section A.4 in the Appendix starting on page 142.

In the last section it was found that 15 hours is the best assay time to most accurately calculate the activity of ^{212}Pb in the heavy water by a single, short assay and so it was decided that one of the assays would retain this time. The other assay was chosen to have a longer time of 70 hours so that the combined assay time of 85 hours would process the entire 1000 tonnes of heavy water.

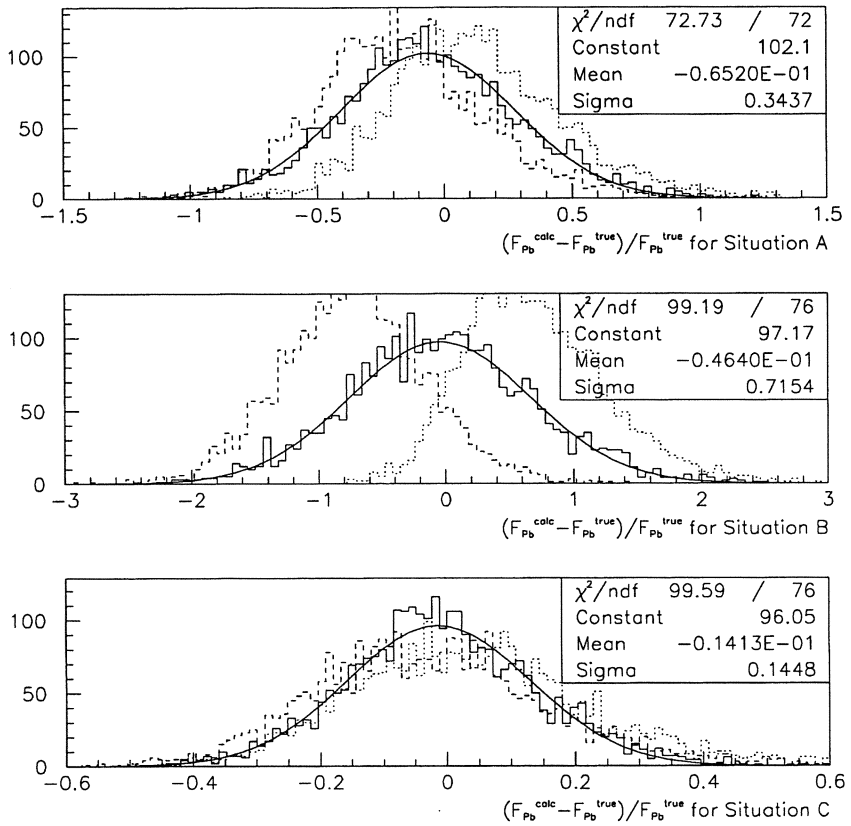

Figure 3.5: *These three plots show distributions of the calculated values for the feed activity flow rate of ^{212}Pb compared to the true values for 15 hour assays in each of the three feed situations as described in Table 3.1 on page 41. The solid histograms with the fitted results give the distributions when a decay tank is present and ϵ is calculated. The dotted and dashed histograms give the distributions when no decay tank is present which means that ϵ cannot be calculated with any degree of accuracy and so it is assumed to take the limiting values of 0.0 and 0.5 respectively.*

Situation:		Overall Errors on ^{212}Pb Activity:	
Name	Description	With Tank	Without Tank
A	Equilibrium	34%	$31\%^{+12\%}_{-18\%} = 34\%$
B	^{224}Ra excess	72%	$54\%^{+67\%}_{-73\%} = 88\%$
C	^{212}Pb excess	14%	$18\%^{+2\%}_{-2\%}$=18%

Table 3.4: *A summary of the accuracy to which the activity of ^{212}Pb in the heavy water can be expected to be calculated using a single 15 hour assay in the three feed activity situations as described in Table 3.1 on page 41. When a decay tank is present the error is purely statistical whereas when there is no decay tank limiting values for ϵ of 0.0 and 0.5 have to be assumed and this leads to additional systematic errors which have to be combined in quadrature with the statistical error to give the overall error.*

The distributions produced for all of the variables that can be calculated by combining the results of two assays are shown in Figure 3.6 for the case of rough equilibrium at the 1ddt level assuming the presence of a decay tank and a 10% accurate calibration for the ^{212}Pb extraction efficiency. The percentage errors in the calculated values for these variables can be taken from these plots, as has already been explained, and they are given in Table 3.5. Also given in Table 3.5 are the similar results obtained when the feed activities are taken from the ranges shown in Table 3.1 for the situations of a ^{224}Ra excess (Situation B) and a ^{212}Pb excess (Situation C).

The results in Table 3.5 can be compared to the results in Table 3.3 to see that, in general, smaller errors can be achieved by combining the results of two assays than can be achieved using a single, short assay. The activity of ^{228}Th and ^{224}Ra in the heavy water and the extraction efficiencies of these isotopes can be calculated more accurately due to lower statistical counting errors since more activity of each isotope is extracted by a longer assay. Also, by combining the results of two assays it can be seen that the error in calculating δ would probably be low enough to determine if there are any significant losses in the thorium-radium system.

The activity of ^{212}Pb in the heavy water can be calculated slightly more accurately by combining the results of a 15 hour assay and a 70 hour assay when there is a ^{224}Ra excess if a one tonne decay tank is used. This is due to a more accurate calculation of the amount of radon breakthrough which can also be seen in Table 3.5. It may be possible to gain more information on the amount of radon breakthrough by combining the results of other assays, in particular short assays with and without the decay tank, however there was insufficient time to investigate this.

3.4 Conclusions

In this chapter the operation of the HTiO SUF assay system has been described as it is expected to be used in the SNO experiment. This assay system has been specifically designed to assay isotopes from the ^{232}Th decay chain, and in particular ^{212}Pb, both in pure heavy water and when magnesium chloride has been added. This assay technique together with those described in the last chapter should enable the SNO experiment to calculate the amount of natural radioactivity in the heavy water in all operational modes.

The majority of this assay system has been developed but there is the need for more efficient methods to perform the secondary concentration of thorium and particularly of lead. These methods must be able to extract lead and thorium efficiently from up to 20 litres of 0.5M hydrochloric acid, containing large quantities of titanium, into a 12 millilitre sample suitable for measurement by a $\beta-\alpha$ delayed coincidence scintillation counter. The development of such new methods is discussed in Chapters 5-7 of this thesis.

If it is assumed that such methods are available then the expected accuracy to which the HTiO SUF assay system can calculate the activity of ^{212}Pb, ^{224}Ra and ^{228}Th in the heavy water can be found by modelling the system. The HTiO SUF assay system is designed to be virtually self-calibrating by operating two parallel pairs of extraction membranes in series. This means that the extraction efficiencies for ^{228}Th and ^{224}Ra can be calculated to within a few percent of their true values by a single assay. Also, the activity of ^{228}Th and ^{224}Ra in the heavy water can be calculated by a single assay as accurately as the secondary concentration efficiencies are known.

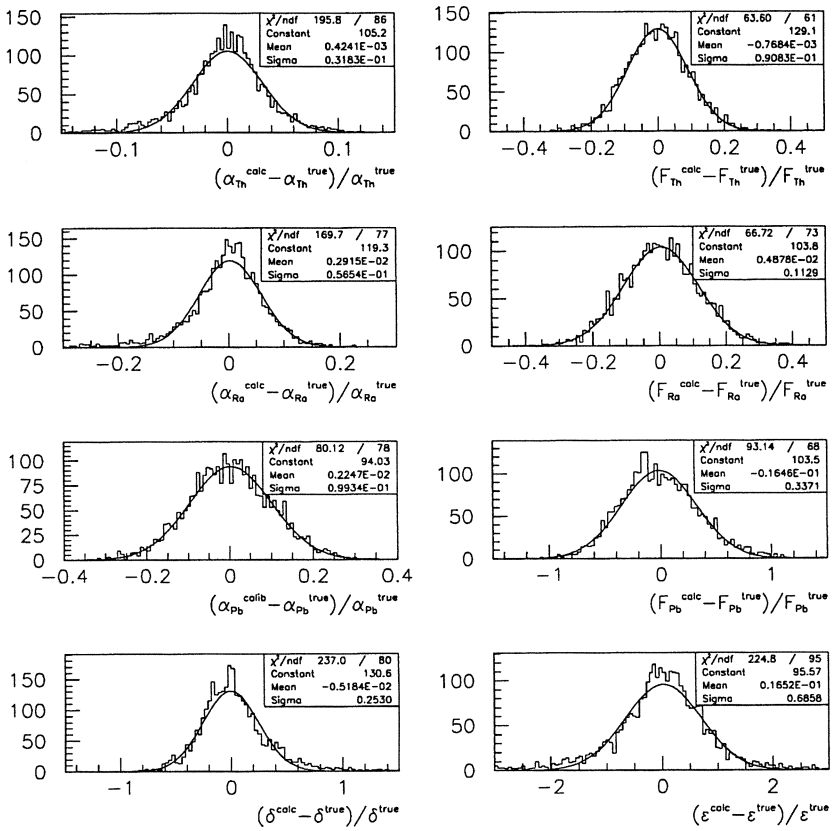

Figure 3.6: *Distributions showing the results of calculating feed activity flow rates and parameters by a model of the HTiO SUF assay system. These results are obtained by combining the results of a 15 hour assay with a 70 hour assay assuming the presence of a decay tank and a calibration for the lead extraction efficiency of 10% accuracy. The feed activity flow rates and parameters were taken from the ranges given in Table 3.1 on page 41 for the situation of rough equilibrium at the 1ddt level, Situation A.*

Situation:		Probabilities:		Loss Params:		Feed Activities:		
Name	Description	α_{Th}	α_{Ra}	ϵ	δ	F_{Th}	F_{Ra}	F_{Pb}
A	Equilibrium	3%	6%	69%	25%	9%	11%	34%
B	^{224}Ra excess	3%	4%	57%	74%	9%	9%	62%
C	^{212}Pb excess	3%	6%	83%	25%	9%	11%	18%

Table 3.5: *A summary of the accuracy to which the feed activities of ^{212}Pb, ^{224}Ra and ^{228}Th in the heavy water and the parameters which describe the system can be expected to be calculated in different feed activity situations as described in detail in Table 3.1 on page 41. These results were calculated by combining the results of a 15 hour assay with a 70 hour assay assuming the presence of a decay tank and a calibration for the lead extraction efficiency of 10% accuracy.*

The activity of ^{212}Pb in any system is complicated due to its short lived radon parent, ^{220}Rn. In the HTiO SUF assay system this isotope produces an effect, called 'radon breakthrough', which means that to calculate the activity of ^{212}Pb in the heavy water it is necessary to perform a calibration for the lead extraction efficiency. Unlike for ^{224}Ra or ^{228}Th the extraction efficiency of the HTiO SUF assay system for ^{212}Pb can be calibrated without adding any long-lived activity to the detector by using either stable lead or specially manufactured ^{212}Pb sources which are free from any other activity. The details of a procedure to manufacture such sources are given in Chapter 4 of this thesis.

Using such a calibration means that the activity of ^{212}Pb in the heavy water can be calculated by a single assay lasting 15 hours but its accuracy is limited by statistical counting errors. If there is radioactive equilibrium within the ^{232}Th decay chain in the heavy water, at the level of 1ddt, the activity of ^{212}Pb can be calculated by the results of a single assay to within 35% of the true value. By performing one such assay every week for three months the average activity of ^{212}Pb in the heavy water during this time can therefore be calculated to within 10% of the true value. This corresponds to an error of 1% on calculating the NC neutrino interaction rate in the SNO detector providing that all of the ^{212}Pb in the detector is found to be in the heavy water.

Unfortunately if the ^{228}Th, and particularly the ^{212}Pb, is not all in the heavy water but has adhered itself to surfaces the situation is much more complicated. This, so called 'plating', effect will mean that there is an excess of ^{224}Ra in the heavy water which makes calculations of the activity of ^{212}Pb in the heavy water less accurate. Also, this effect means that it will be difficult to relate the activity of ^{212}Pb in the heavy water to the amount of NC background in the SNO experiment. It is clear that more research will be needed if this scenario is found to be true in the SNO detector.

The usefulness of a one tonne decay tank situated between two parallel pairs of membranes in the HTiO SUF assay system has also been investigated. This decay tank is present in order to enable the second membrane pair to extract any ^{212}Pb lost by radon breakthrough from the first. It has been found that although its use in single 15 hour assays is somewhat limited its presence is important to be able to calculate the amount of radon breakthrough in the system by combining the results of two assays. The decay tank is also useful to prevent the HTiO SUF system from adding ^{212}Pb back into the heavy water at the end of long assays.

The rest of this thesis explains the research that was carried out into completing the HTiO SUF assay system by developing secondary concentration procedures for ^{212}Pb and ^{228}Th. In the next chapter a procedure to manufacture sources of ^{212}Pb which can be used to calibrate this assay system is detailed.

Chapter 4

A ^{212}Pb Calibration Source for the SNO Experiment

4.1 Introduction

In the last chapter it was found that the HTiO SUF assay system will need to be calibrated for the ^{212}Pb extraction efficiency. This calibration could be performed using stable lead since this contains no long-lived activity and it is expected that any ^{212}Pb present would behave in the same way as the carrier. Indeed in the research detailed in Chapters 4-7 of this thesis stable lead is used to measured the ^{212}Pb extraction efficiency of certain systems. However, there are some concerns over using stable lead as a calibration source for the SUF HTiO assay system and this is because the amount of stable lead that has to be used is much larger than the few hundred of atoms of ^{212}Pb that it is hoped will be present in the heavy water of the SNO detector. A particular concern in using stable lead as a calibration source in the heavy water itself is that lead could plate out on surfaces within the heavy water circulation system. It is unclear whether milligram quantities of stable lead will behave in the same way as a few hundred atoms of ^{212}Pb in this plating process.

The ideal calibration source for ^{212}Pb would be a source of ^{212}Pb itself which has been shown to have been separated virtually entirely from its long-lived thorium parent, ^{228}Th. During 1997 research was conducted both at Oxford University and at the Brookhaven National Laboratory (BNL), New York, USA into a novel technique which separates ^{212}Pb from from both ^{224}Ra and ^{228}Th to a very high degree of cleanliness. At BNL these cleanliness measurements were made using alpha counting techniques with the assistance of Dr R.Hahn.

In this chapter are both details of a procedure to manufacture sources of ^{212}Pb free from ^{224}Ra and ^{228}Th and results of measuring the cleanliness of sources manufactured using this procedure. The ^{212}Pb sources that were produced in the experiments detailed in this chapter were used along with stable lead in experiments detailed in Chapters 6 and 7 to calibrate ^{212}Pb extractions.

4.2 Existing Calibration Sources and Possible Extensions

The use of hydrous titanium oxide (HTiO) to separate radium from thorium was observed by Dr R.Taplin and Dr M.Moorhead of Oxford University in 1995. Solutions of ^{224}Ra which contained less than 0.5% of its parent, ^{228}Th were successfully produced [Tap95a]. Unfortunately the use of such ^{224}Ra sources as calibration sources for its daughter, ^{212}Pb, in the SNO experiment is not feasible since the only way of measuring a ^{224}Ra solution for any ^{228}Th contamination is to leave the ^{224}Ra to decay away with its 3.66 day half-life and measure any remaining long-lived activity. This means that the cleanliness of any ^{224}Ra solution can only be determined after it has been used and this allows the possibility of a serious ^{228}Th contamination should the chemical process not be carried out correctly. Furthermore, the use of ^{224}Ra to calibrate systems for ^{212}Pb is somewhat limited since the ^{212}Pb that is produced by decays of ^{224}Ra would be present for many days making frequent calibrations impossible.

The 10.6 hour half-life of ^{212}Pb itself makes it a much better calibration source, if it can be separated from both ^{224}Ra and ^{228}Th since in only a few days any activity introduced would be reduced by several orders of magnitude. Calibration sources of ^{212}Pb have another major advantage over ^{224}Ra sources and this is due to the fact that the alpha peaks from the daughters of ^{212}Pb are well separated in energy from the peaks of ^{228}Th and ^{224}Ra. This means that it is possible to measure the cleanliness of a ^{212}Pb source as it is produced rather than after all the ^{212}Pb activity has decayed away. This technique is not successful for sensitively measuring the purity of ^{224}Ra solutions because of the overlap in energy between the alpha decays of ^{228}Th and ^{224}Ra. For a typical alpha spectrum of ^{228}Th in equilibrium with its daughters and other details of the alpha counting used in this chapter see Appendix C.

The literature suggests many possible methods to separate ^{212}Pb from its parents, these being: reversed-phase chromatography [Sěb74], anion exchange resin [Atc87], high performance liquid chromatography [AlM88] and amalgam exchange [Qur67]. All of these techniques produce ^{212}Pb sources of high cleanliness but the procedures are rather complicated and often use specialised equipment.

By examining the decay chain of ^{228}Th, which is shown in Figure 2.3 on page 24, it is clear that the presence of the short-lived radon isotope between ^{224}Ra and ^{212}Pb in the decay chain provides a possible separation method for ^{212}Pb. The use of ^{220}Rn to produce sources of ^{212}Pb is also found in the literature but again very complicated, specialised equipment is used, see [Nor91]. In the next section a much simpler procedure using ^{220}Rn to manufacture ^{212}Pb sources which are free from ^{224}Ra and ^{228}Th is detailed.

4.3 The Procedure to Manufacture ^{212}Pb sources which are free from ^{224}Ra and ^{228}Th

The procedure to manufacture ^{212}Pb sources that are free from ^{228}Th and ^{224}Ra contamination is divided into four stages. The first stage uses the HTiO method already mentioned which produces ^{224}Ra solutions containing less than 0.5% ^{228}Th. The second stage is to then immobilise this ^{224}Ra (or some ^{228}Th) on plastic beads coated with manganese dioxide (MnO_2) which are known to have good efficiencies both for extracting radium and for emanating ^{220}Rn, see Chapter 5 of [Fer92]. The third stage is the actual emanation of the ^{220}Rn which is achieved by pumping air through a small cell packed with the MnO_2. Finally, the ^{220}Rn is trapped using a simple coil of tubing and the ^{212}Pb produced by its decay is collected by washing this tubing with dilute acid.

The first stage of separating the ^{224}Ra from the ^{228}Th provides an extra separation by removing any ^{228}Th from the ^{212}Pb generating apparatus. This is useful for safety purposes to reduce risks of unforeseen possible contamination but it was not found to increase the cleanliness of the ^{212}Pb sources that were produced and so it can be considered as an optional stage.

The experimental details of these four stages are given below:

1. The Production of a ^{224}Ra source free from ^{228}Th (OPTIONAL):

   Starting from an acidic source of ^{228}Th in equilibrium with its daughters, a source of ^{224}Ra separated from the ^{228}Th can be produced by adding a small amount of titanium chloride or titanium sulphate, precipitating the titanium as HTiO at pH 4 and filtering the solution using a 0.2 micron filter. At pH 4 the HTiO very efficiently extracts thorium but it does not extract very much radium and so the solution left after filtering typically has a ^{228}Th contamination of less than 0.5% [Tap95a].

   It should be noted that the extraction efficiency of HTiO for radium varies considerably between virtually 0% at pH 4 to about 60% at pH 5 and so care must be taken when increasing the pH of the acidic ^{228}Th solution to ensure that the final pH of the solution is nearer pH 4 than 5. If the pH ends up being too high then it is necessary to re-acidify the solution to a pH of less than 1 to remove the radium from the HTiO before proceeding to raise the pH again.

2. Immobilising the ^{224}Ra or ^{228}Th on MnO_2 Coated Beads:

   An immobilised source of ^{220}Rn can be prepared from either a ^{224}Ra solution produced using the HTiO method, or a solution of ^{228}Th with a pH between 4 and 5, by adding a small quantity of MnO_2 coated acrylic resin beads and leaving the solution to mix for a few minutes. The MnO_2 is virtually 100% efficient at extracting radium under these conditions and extracts about 25-35% of any thorium which is present. These MnO_2 beads can be removed from the solution using a coarse filter and then they should be dried for several days in air or for several hours in an oven at 60-80°C to prepare the beads for emanation.

3. The Emanation of ^{220}Rn:

   To efficiently emanate ^{220}Rn from the small sample of MnO_2 beads they need to be placed into a small cell which has a large aspect ratio to increase the surface area of the beads which is in contact with the circulating air. The ^{220}Rn can then be emanated with an efficiency of around 50% by pumping air through the cell at a flow rate equal to more than 100 cell volumes per minute. The air containing the ^{220}Rn should be passed through a 0.1-0.2 micron filter to remove any MnO_2 fines before any other processing.

4. The Trapping of the ^{220}Rn and the Collection of the ^{212}Pb:

   The ^{220}Rn which is emanated from the MnO_2 cell decays to ^{212}Pb with a 55.6 second half-life and so the ^{220}Rn can be trapped by passing the air out of the MnO_2 cell into a coil of tubing which has a large enough volume to contain the air coming from the cell for a few minutes, ie a few half-lives of ^{220}Rn. In order to prevent the loss of any ^{212}Pb which stays entrained in the flow of the air, the output from this coil of tubing can be fed back to the input to the MnO_2 cell and this pumping circuit run as a closed loop.

   By emanating for several hours the ^{212}Pb has time to build up on the inside of the coil of tubing and it can then be collected by washing the tubing with a suitable amount of 0.5M hydrochloric acid for several minutes. The ^{212}Pb solution which is produced is virtually free from any ^{224}Ra or ^{228}Th.

In Section 4.5 it will be shown that this overall procedure manufactures sources of ^{212}Pb with an activity of about 20-30% of the activity on the MnO_2 cell during the emanation. It will also be shown that the ^{228}Th contamination of these sources has been measured, after the ^{212}Pb had decayed, to be less than 1 part in 10,000 using $\beta - \alpha$ counters whose operation is described in Section 3.2.1 on page 30 and in Appendix D. More importantly the ^{228}Th contamination of these sources has been measured, at production, using alpha counting to be less than 0.3%.

4.4 The Experimental Evaluation of the Individual Stages of the Procedure

4.4.1 General Comments on the Procedure

Several experiments were carried out both at Oxford and at BNL to produce ^{212}Pb sources by the procedure outlined in the previous section and then to measure the contamination of ^{228}Th in these produced sources. In all of these experiments the starting solution was dilute nitric acid containing about 700 becquerels of ^{228}Th in equilibrium with its daughters. In experiments CLS4-9, which were carried out at Oxford, the first stage of producing a ^{224}Ra solution free from ^{228}Th was included. This was done using a small volume of a titanium chloride or titanium sulphate solution and a 0.2 micron Media-Kap 10 filter. The actual amount of titanium added was 3 milligrams which was achieved by taking a tenth of a millilitre of a solution of the titanium salt which contained 0.15 grams of the salt in each millilitre of solution and was hence called a 15% weight to volume (w/v) solution. In experiments CLS10 and BCL1, carried out at Oxford and BNL respectively, this first stage was omitted and instead the MnO_2 was loaded directly with a ^{228}Th solution which had been made to have a pH between 4 and 5. The ^{212}Pb sources manufactured in experiments CLS11-12 and BCL2-8 used the MnO_2 cells which had been made in experiments CLS10 and BCL1 respectively, since these cells contained ^{228}Th activity and so were a constant source of ^{220}Rn. The MnO_2 acrylic resin beads that were used in all of these experiments were purchased from Seakem[1].

The efficiencies in the HTiO extractions, the MnO_2 extractions and the ^{220}Rn emanation were all measured using gamma counting as discussed in Appendix B. The measurements were not only of solutions made up in standard counting bottles but also included measurements of the activity contained in the Media-Kap filter and the MnO_2 cell. To ensure that the different geometry of the filter and cell did not effect the counting rate, for a given amount of activity contained within them, a brief investigation was performed. At Oxford the measured activity of the filter and cell, after an extraction, was compared to the loss of activity from a solution which was measured using the standard geometry counting bottles. In the case of a Media-Kap filter the ratio of these two numbers was measured to be 0.99±0.03 and for the cell used at Oxford it was 0.94±0.05. This shows no significant difference between measuring activity in a standard counting bottle, in a Media-Kap filter and in the MnO_2 cells used at Oxford.

At BNL the measured activity of the MnO_2 cell was compared to the measurement of a known source at two very different distances from the gamma detector. Since these two ratios were very similar this again indicated that there was no significant difference between measuring activity in a standard counting bottle and in the MnO_2 cells used at BNL.

The amount of dry beads containing MnO_2 used in each experiment was 0.25 millilitres, or 0.2 grams. At Oxford, after an extraction, these beads were dried in air for several hours before being dried in an oven at 60-80°C for about 24 hours. At BNL the MnO_2 was simply dried in air for several days. After being dried the MnO_2 was used to make up a cell for ^{220}Rn emanation. The cells used at Oxford were constructed differently to the cell used at BNL and the design of both are shown in Figure 4.1. The main difference between the cells used at Oxford and the one used at BNL was that the latter was made from glass which made it easier to fill with MnO_2 and more robust.

At both Oxford and BNL a very similar pumping circuit was used to collect the ^{212}Pb and a diagram of this is shown in Figure 4.2. A constant flow of air of 30 millilitres per minute around the circuit was obtained using a peristaltic pump and this produced a flow of air of 120 bed volumes per minute through the 0.25 millilitre MnO_2 cell. In Oxford, the coil of tubing was made from 6 millimetre diameter PVC

[1]Seakem Instruments Ltd, Canada. Lot: 86HX005-11

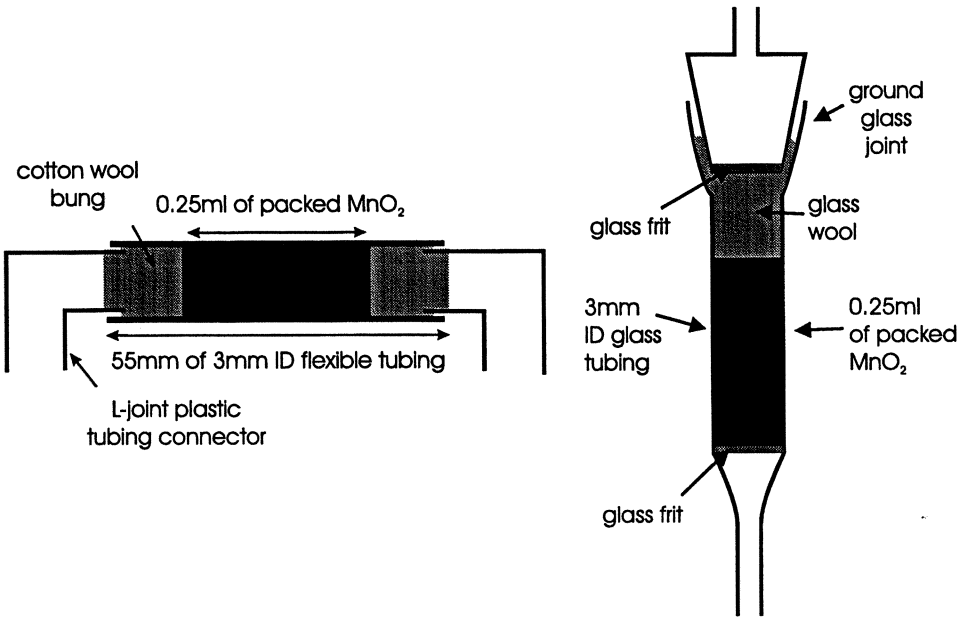

Figure 4.1: *The design of the MnO_2 cells used at Oxford (left) and the MnO_2 cell used at BNL (right).*

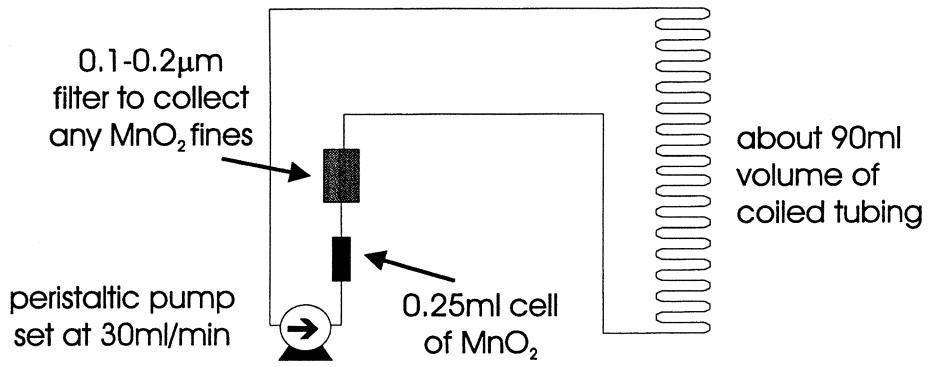

Figure 4.2: *Apparatus for the emanation of ^{220}Rn.*

tubing wrapped around into about a 20 centimetre diameter coil. At BNL it was made from about 4 millimetre diameter glass tubing formed into about a 10 centimetre diameter coil. Normally the ^{212}Pb was left to accumulate for about 24 hours in the coil of tubing before being washed from the coil using a suitable volume of 0.5M hydrochloric acid which was left to circulate in the tubing for at least several minutes at a flow rate of 30 millilitres per minute.

In the following sections the individual stages of the procedure, as detailed in Section 4.2, are evaluated.

4.4.2 The Production of a ^{224}Ra source free from ^{228}Th

The measured extraction efficiencies of HTiO for thorium, radium, lead and bismuth are given in Table 4.1 together with the measured pH of the solution during the extraction. These extraction efficiencies are calculated both from looking at the fitted amount of each isotope extracted onto the Media-Kap filter (appearance) and the fitted amount of each isotope which was lost from the aqueous solution (disappearance).

Exp. Name	pH	Efficiency by Appearance:				Efficiency by Disappearance:			
		^{212}Bi	^{212}Pb	^{224}Ra	^{228}Th	^{212}Bi	^{212}Pb	^{224}Ra	^{228}Th
CLS4	4.9	123±18%	84±5%	70±3%	98±2%	99±17%	100±6%	60±4%	100±3%
CLS5	4.0	112±11%	92±5%	34±2%	107±2%	100±11%	100±6%	1±3%	99±3%
CLS6	4.4	107±10%	87±4%	32±2%	96±2%	100±10%	100±6%	19±3%	99±4%
CLS7	4.0	122±11%	124±9%	36±3%	112±3%	99±9%	100±8%	8±4%	100±3%
CLS8	4.4	123±14%	107±6%	53±4%	118±2%	98±11%	100±6%	41±5%	100±3%
CLS9	4.5	111±8%	105±6%	61±4%	107±5%	100±8%	99±7%	37±5%	99±5%

Table 4.1: *Efficiency measurements for the extraction of HTiO from solutions of pH4-5. The results for experiment CLS9 have been taken directly from the results of the fits shown in Figure 4.3. The efficiencies measured by appearance examined the fitted amount of each isotope extracted onto the Media-Kap filter whereas the efficiencies measured by disappearance examined the fitted amount of each isotope which was lost from the aqueous solution. It can be seen that these two methods do not always give the same values and this is discussed in the text. The more reliable efficiencies, as measured by disappearance, are plotted against the pH of the solution during the extraction in Figure 4.4.*

The errors on the efficiencies in Table 4.1 are the statistical errors based on the errors produced by fitting the activity of each sample measured at different times after it was produced, to the initial activities of ^{212}Bi, ^{212}Pb , ^{224}Ra and ^{228}Th. An example of such a fit for measurements in experiment CLS9 is shown in Figure 4.3. The functional form to which the measured count rates were fit is given in Equation 4.1 with definitions in Equations 4.2, 4.3, 4.4 and 4.5. In these equations $P1, P2, P3$ and $P4$ are the initial activities of ^{212}Bi, ^{212}Pb, ^{224}Ra and ^{228}Th respectively. The derivation and explanation of these expressions can be found in Appendix B.

$$decay\ \ rate = \mathcal{W}e^{-\lambda_{Bi}t} + \mathcal{X}\alpha e^{-\lambda_{Pb}t} + \mathcal{Y}\beta\gamma e^{-\lambda_{Ra}t} + \mathcal{Z} \tag{4.1}$$

$$\lambda_{Bi} = 6.86 \times 10^{-1} hr^{-1} \quad ; \quad \lambda_{Pb} = 6.54 \times 10^{-2} hr^{-1} \quad ; \quad \lambda_{Ra} = 7.89 \times 10^{-3} hr^{-1} \tag{4.2}$$

$$\alpha = \frac{\lambda_{Bi}}{\lambda_{Bi}-\lambda_{Pb}} = 1.11 \quad ; \quad \beta = \frac{\lambda_{Bi}}{\lambda_{Bi}-\lambda_{Ra}} = 1.01 \quad ; \quad \gamma = \frac{\lambda_{Pb}}{\lambda_{Pb}-\lambda_{Ra}} = 1.14 \tag{4.3}$$

$$\mathcal{Z} = P4 \quad ; \quad \mathcal{Y} = P3 - P4 \quad ; \quad \mathcal{X} = P2 - P3\gamma + P4(\gamma - 1) \tag{4.4}$$

$$\mathcal{W} = P1 - P2\alpha + P3\gamma(\alpha - \beta) + P4(\beta\gamma - \alpha(\gamma - 1) - 1) \tag{4.5}$$

From looking at the results in Table 4.1 it is clear that there are some disagreements between the extraction efficiencies as derived from appearance and disappearance measurements. It is interesting to note that the efficiencies as measured by disappearance are consistently lower than those measured by appearance and this indicates that the differences are not due to losses of activity on apparatus. It is possible that the reason for the differences is uncertainties in measuring the total volume of the solution before filtration. If this is the case, the efficiencies as measured by disappearance are the most reliable since in this calculation any error in the measured total volume of the solution cancels. These, more reliable, efficiencies are shown graphically in Figure 4.4 plotted against the measured pH of the solution during the extraction. The pH meter was not well calibrated during these experiments and so a reasonable systematic error of 0.1 pH units has been included in this figure.

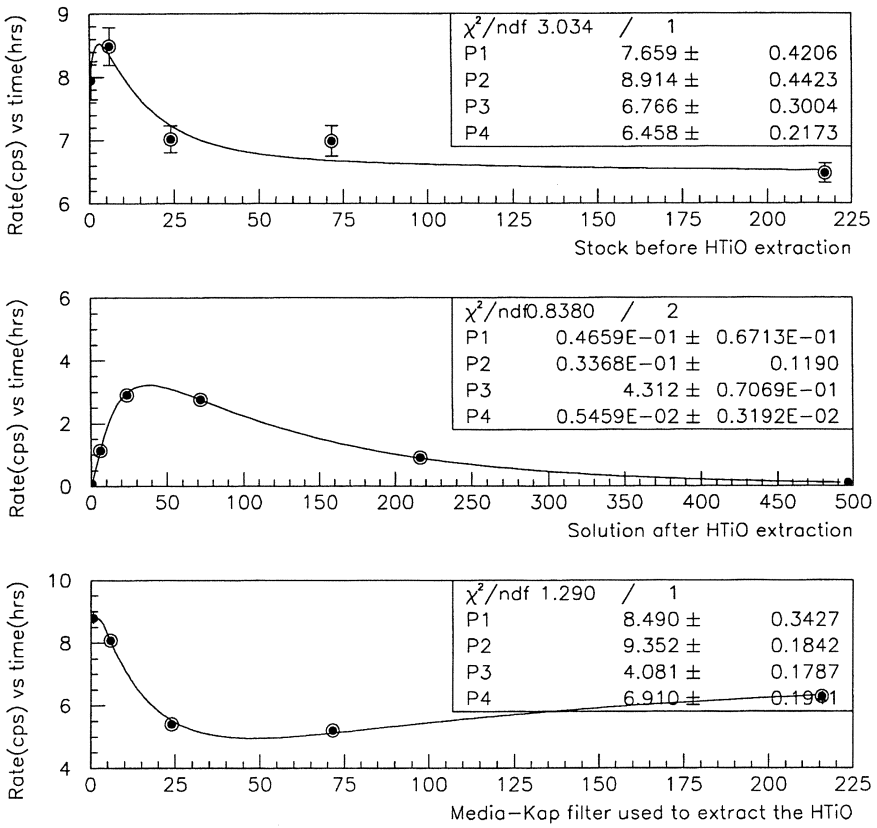

Figure 4.3: *An example of fitting the gamma counting measurements for experiment CLS9. The top plot shows the measurements of the solution at pH 4 just prior to the removal of the precipitated HTiO, the middle plot shows the measurements of the solution after the HTiO had been removed and the bottom plot shows the measurements of the Media-Kap filter which performed the filtration. The fitted parameters are to the initial activities, in counts per second, of the following isotopes in the* ^{232}Th *decay chain: P1=*^{212}Bi*, P2=*^{212}Pb*, P3=*^{224}Ra *and P4=*^{228}Th*. (See Appendix B for details.)*

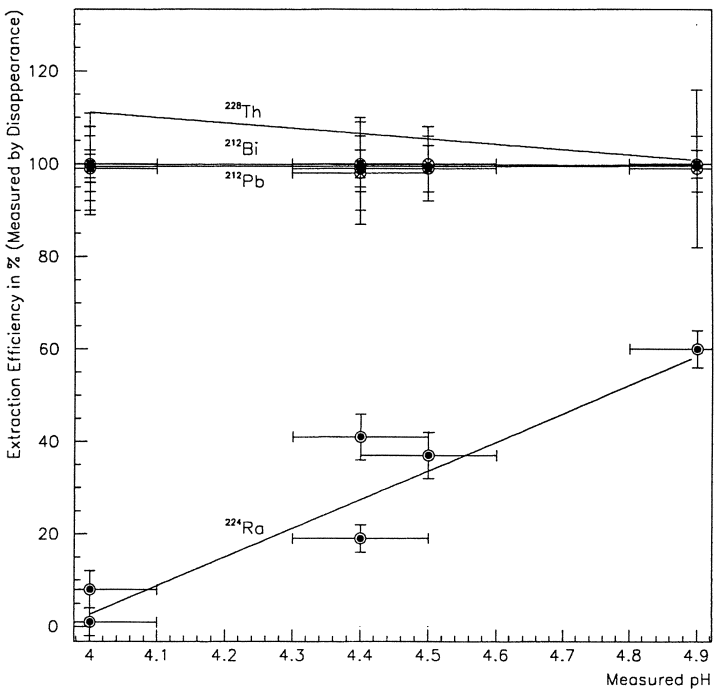

Figure 4.4: *The extraction efficiency of HTiO for ^{228}Th, ^{224}Ra, ^{212}Pb and ^{212}Bi plotted against the measured pH of the solution. These efficiencies were calculated by measuring the disappearance of activity from the solution and are taken directly from Table 4.1.*

The plots shown in Figure 4.4 show that ^{228}Th, ^{212}Pb and ^{212}Bi are all extracted at about 100% efficiency in the pH range of 4.0 to 4.9 whereas ^{224}Ra is extracted only slightly at pH 4.0 but about 60% at pH 4.9. The seemingly linear relationship between the pH and the extraction efficiency for ^{224}Ra is in agreement with that discussed in the literature, see Figure 5.7 of [How94]. Despite the different strength solutions of ^{224}Ra which were produced in these experiments, each solution was found to contain less than 1% (95% CL) of ^{228}Th contamination by gamma counting the solution after all the ^{224}Ra had decayed away.

A brief investigation into an alternative method of producing ^{224}Ra solutions which contain very small quantities of ^{228}Th was conducted at Oxford. This alternative method was to extract ^{224}Ra from a source of ^{228}Th so immobilised that the ^{228}Th was not removed. In this way the ^{224}Ra grows back into the source, due to the radioactive decays of ^{228}Th, and so can be extracted again at a later date. This repeated extraction of an isotope while leaving the parent isotope unaffected is called 'milking' and it is useful because no long-lived radioactive waste has to be generated. One technique by which this can be achieved is to extract ^{228}Th into an organic phase using a solvent-solvent extraction and then to back-extract ^{224}Ra produced by the decays of the ^{228}Th into an aqueous phase.

The literature suggests that trioctylphosphine oxide (TOPO) is a reagent which extracts thorium with a very high efficiency from solutions that are 1M in nitric acid but it does not form a complex with radium [Whi61]. Therefore, an organic phase consisting of a 0.1M solution of TOPO in cyclohexane was used to extract a few kilobecquerels of ^{228}Th from a 1M nitric acid solution and then, after leaving it for 11 days, the organic phase was shaken with an equal volume of 0.1M nitric acid in an attempt to back-extract ^{224}Ra. The 0.1M nitric acid solution was found to extract about 50% of the ^{224}Ra which had been in the organic phase and it contained less than 1.7% ^{228}Th (95% CL).

This single experiment seems to indicate a possible alternative method of producing ^{224}Ra solutions containing very small amounts of ^{228}Th, without generating large quantities of radioactive waste, however further systematic studies are obviously required before confidence can be placed in this technique.

4.4.3 Immobilising the ^{224}Ra or ^{228}Th on MnO_2 Coated Beads

The extraction efficiency of radium by MnO_2 from solutions with a pH between 4 and 5 was measured by the disappearance of ^{224}Ra from the aqueous solution in many experiments and it was found to be consistently around 100% with an error of just a few percent.

As was noted in Section 4.4.1 experiments CLS10 and BCL1 omitted the first stage of the procedure and loaded the MnO_2 with a ^{228}Th solution which had a pH of between 4 and 5. It was therefore possible in these two experiments to measure the extraction efficiency for MnO_2 of thorium, radium, lead and bismuth by observing the disappearance of these isotopes from the solution.

The plots in Figure 4.5 show the measurements from experiment CLS10, conducted at Oxford, of the aqueous solution before and after the addition of the MnO_2 and the results of fitting these measurements to the initial activities of ^{212}Bi, ^{212}Pb, ^{224}Ra and ^{228}Th. From these fitted activities extraction efficiencies can be calculated and these are given in Table 4.2 along with similar calculations performed on measurements taken in experiment BCL1 which was conducted at BNL.

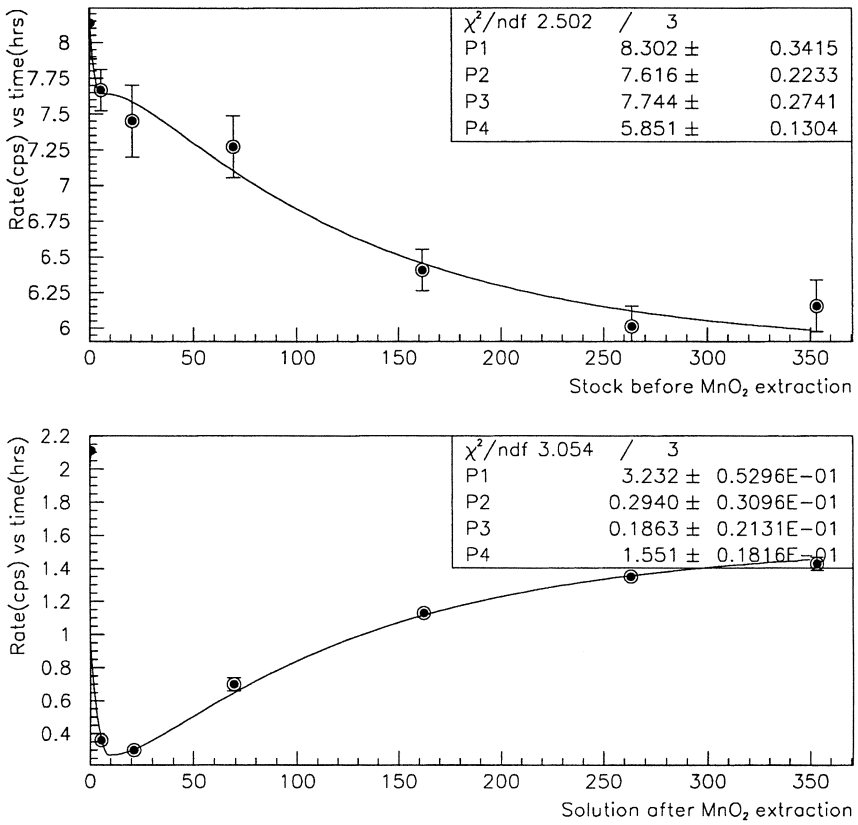

Figure 4.5: *The fitted gamma counting measurements for the MnO_2 extraction in experiment CLS10. The top plot shows the measurements of the solution just prior to the addition of the MnO_2 and the bottom plot shows the measurements of the solution after the MnO_2 had been removed. The fitted parameters are, as before, to the initial activities, in counts per second, of the following isotopes in the ^{232}Th decay chain: P1=^{212}Bi, P2=^{212}Pb, P3=^{224}Ra and P4=^{228}Th.(See Appendix B for details.)*

Exp Name	Extraction efficiency of MnO_2:			
	^{212}Bi	^{212}Pb	^{224}Ra	^{228}Th
CLS10	60±5%	96±4%	98±5%	73±3%
BCL1	76±3%	96±11%	95±13%	73±2%

Table 4.2: *The extraction efficiencies by MnO_2 at pH 4-5 deduced from the observed loss of activity from the aqueous solution. The values for experiment CLS10 are taken directly from Figure 4.5. A discussion in the text explains why the extraction efficiency for ^{228}Th is actually only about 25-35%.*

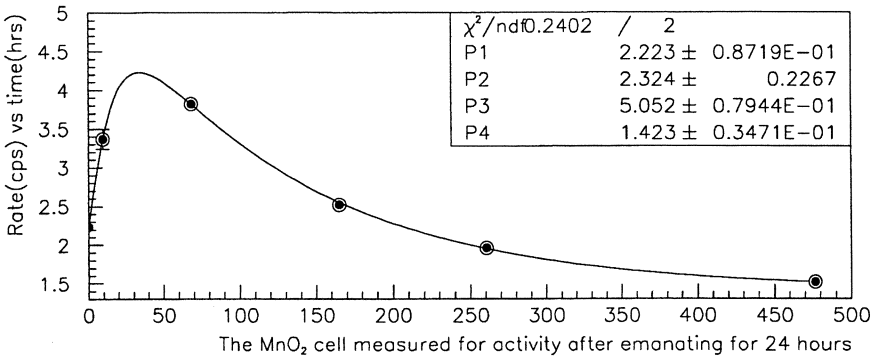

Figure 4.6: *The fitted gamma counting measurements for the MnO_2 cell in experiment CLS10 after 24 hours of emanation. Again, the fitted parameters are to the following isotopes in the ^{232}Th decay chain: P1=^{212}Bi, P2=^{212}Pb, P3=^{224}Ra and P4=^{228}Th. (See Appendix B for details.)*

Unlike in the previous section it was not possible to measure the extraction efficiency for ^{212}Bi and ^{212}Pb by the appearance of activity on the MnO_2 cell since the MnO_2 beads took several hours to dry before the cell could be made up. However, it was possible to measure the cell for ^{224}Ra and ^{228}Th activity and although the amount of ^{224}Ra activity on the cell did seem to be in agreement with the amount that had disappeared from the solution, the amount of ^{228}Th activity on the cell appeared to be somewhat lower than expected. The activity of ^{228}Th extracted by the MnO_2 in experiment CLS10 can be seen from Figure 4.6 to be 1.42±0.03 counts per second whereas from Figure 4.5 the activity of ^{228}Th that disappeared from the solution can be calculated to be 4.4±0.1 counts per second. A similar loss of ^{228}Th was measured in experiment BCL1 where only about half of the expected ^{228}Th activity was actually found on the cell. It must therefore be concluded that some ^{228}Th was lost on apparatus during the extraction and that the true extraction efficiency of ^{228}Th by MnO_2 from a solution of pH between 4 and 5 is only about 25-35%. These losses on apparatus could have been due to the thorium plating on surfaces which is known to occur from solutions with a high pH.

4.4.4 The Emanation of ^{220}Rn

The effect of pumping air through a cell of MnO_2 which has extracted some ^{224}Ra and some ^{228}Th can be seen in Figure 4.6 where the measurements of the activity of the cell used in experiment CLS10 are plotted against the time after a 24 hour emanation. The disequilibrium between the isotopes above and below ^{220}Rn can be clearly seen and the fact that initially there was half as much ^{212}Bi and ^{212}Pb as ^{224}Ra indicates an emanation efficiency of around 50%. This means that about half of the ^{220}Rn atoms produced in the cell are displaced from it by the flow of air before they have time to decay to ^{212}Pb.

If the emanation rate of ^{220}Rn atoms from the MnO_2 cell is assumed to be constant during the emanation process then Equation 4.6 gives a relationship between the deposition rate of ^{212}Pb in atoms per second, R, and the number of atoms of ^{212}Pb on the tubing, $N(t)$, after a time, t, of uninterrupted emanation.

$$\frac{dN(t)}{dt} = R - \lambda_{Pb} N(t) \tag{4.6}$$

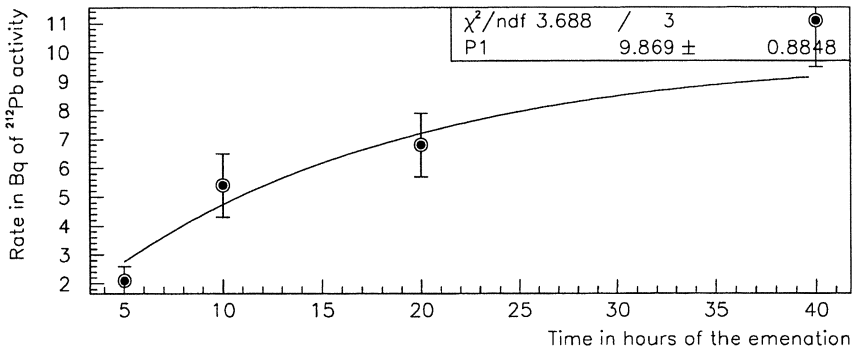

Figure 4.7: *The amount of ^{212}Pb collected from the coil of tubing plotted against different times of emanation. The fit is to a constant deposition rate of ^{212}Pb in the tubing as given in Equation 4.7 and the result is 10±1 atoms of ^{212}Pb deposited per second.*

By assuming that initially the tubing is free from ^{212}Pb a solution to Equation 4.6 can be found and this is given in Equation 4.7 where $A_{Pb} = \lambda_{Pb}N(T)$, is the activity of ^{212}Pb in the tubing immediately after T hours of uninterrupted emanation.

$$R = A_{Pb}(1 - e^{-\lambda_{Pb}T})^{-1} \tag{4.7}$$

An experiment was conducted to determine whether or not this relationship between the recovered activity and the emanation time was followed. This experiment involved using the MnO_2 cell of experiment CLS10 after it had been left for several weeks so that the ^{224}Ra activity, and hence the production of ^{220}Rn, of the cell would remain constant over several days. The cell was then left in the pumping circuit to emanate ^{220}Rn for 5, 10, 20 and 40 hour periods. At the end of each period the tubing was washed with 0.5M hydrochloric acid and the initial activity of the recovered ^{212}Pb was measured by gamma counting.

The results of this experiment, along with the statistical errors of the fitted initial amount of ^{212}Pb, are shown graphically in Figure 4.7 where they are fitted to the expression in Equation 4.7. Despite the large errors it seems clear that the time dependence of the amount of ^{212}Pb recovered as a function of the emanation time is in agreement with the expression given in Equation 4.7. It can therefore be concluded that, approximately, the emanation of ^{220}Rn remains constant over a period of at least a few days.

The emanation efficiencies for all of the ^{212}Pb sources produced at Oxford and BNL are given in Table 4.3. It should be noted that experiment BCL5 was different from all of the other experiments in that the volume of the coil of tubing used was only 30 millilitres and it was expected to trap only about half of the ^{220}Rn that was normally trapped in the 90 millilitre coil. (This expectation is explained in the next section.)

For those experiments where the pumping circuit was run according to the procedure in Section 4.4.1 on page 52 the emanation efficiencies can be seen to vary from about 30% to 70% and these differences are assumed to be due to differences in the drying and packing of the MnO_2 beads. In experiments which used the same cell the variation in emanation efficiency was typically much smaller: 56±5% for the cell made in experiment CLS10, and 59±9% for the cell made in experiment BCL1.

Exp.	Activity of cell	Emanation Eff	Collection Eff	^{212}Pb Activity	Overall Eff
CLS4	53±1Bq	47±8%	~70%	6.4±0.2Bq	12%
CLS5	380±20Bq	31±8%	~80%	43±2Bq	11%
CLS6	235±35Bq	35±11%	~80%	47±2Bq	20%
CLS7	220±10Bq	58±6%	84±2%	49±2Bq	22%
CLS8	155±5Bq	33±4%	~80%	30±1Bq	19%
CLS9	205±5Bq	65±4%	~80%	37±1Bq	18%
CLS10	595±10Bq	54±5%	81±2%	153±7Bq	26%
CLS11	179±5Bq	53±2%	69±3%	24±1Bq	13%
CLS12	165±4Bq	62±4%	~70%	26±1Bq	16%
BCL1	306±8Bq	71±4%	77±1%	116±2Bq	38%
BCL2	275±7Bq	52±3%	68±1%	73±1Bq	27%
BCL5	239±3Bq	39±2%	72±2%	33±3Bq	14%
BCL7	239±3Bq	52±3%	80±1%	48±1Bq	20%
BCL8	239±3Bq	60±3%	79±1%	78±2Bq	33%

Table 4.3: *The efficiencies and activities measured in experiments which manufactured sources of ^{212}Pb. The experiments labelled CLS were conducted at Oxford whereas the experiments labelled BCL were conducted at BNL. The cell used in experiments CLS11 and 12 was the one that was produced in experiment CLS10 and the cell used in experiments BCL2, 5, 7 and 8 was the one that was produced in experiment BCL1. The smaller amount of ^{212}Pb recovered in experiment BCL5 was expected and is explained in the text. In this table the loss of ^{212}Pb due to decays between stopping the pumping and counting the source has been taken into account.*

Washing time	Measurements of Collection Efficiency:		
10 minutes	69±3%(CLS11)	72±2%(BCL5)	
30 minutes	77±1%(BCL1)	80±1%(BCL7)	79±1%(BCL8)
60 minutes	84±2%(CLS7)	81±2%(CLS10)	68±1%(BCL2)

Table 4.4: *The measured collection efficiency for ^{212}Pb after leaving 0.5M hydrochloric acid circulating in the coil of tubing for different times.*

4.4.5 The Trapping of the ^{220}Rn and the Collection of the ^{212}Pb

The ^{212}Pb that was deposited in the coil of tubing was recovered by rinsing with 0.5M hydrochloric acid at a flow rate of about 30 millilitres per minute. The volume of acid that was used to wash the tubing was chosen to be most suitable for the counting technique which was to be used. Hence at Oxford 50 millilitres was used which was then measured initially for activity using gamma counting whereas at BNL only about 10 millilitres were used to produce a more concentrated ^{212}Pb source for alpha counting. It was found that changing the volume of the acid does not noticeably alter the collection efficiency.

The time that the acid was left to circulate within the tubing was varied between 10 and 60 minutes. The efficiency of the collection process was measured by washing the coil of tubing twice and examining the ratio between the amount of ^{212}Pb found in the first wash compared to that found in the second wash. The measured efficiencies after different washing times are listed in Table 4.3 and they seem to imply an increase in efficiency from 70%, when using a washing time of 10 minutes, to 80% when using 30 minutes or more. The result for experiment BCL2 does not seem to be in agreement with the rest of the results and the reason for this is unclear.

Coil Order	Measured ^{212}Pb : Activity	Distribution	Volume of Coil	Residence Time of Coil	Calculated ^{212}Pb Distribution
1st	51±1Bq	100%	25ml	50 seconds	100%
2nd	29±1Bq	57±2%	26ml	52 seconds	55%
3rd	12±1Bq	24±2%	20ml	40 seconds	24%

Table 4.5: *The results of experiment BCL4 which, after a usual emanation procedure, divided the 90 millilitre coil into three coils and then measured the amount of ^{212}Pb deposited in each small coil. The calculated activity that is expected in each coil uses the fact that the rate of flow of air was 30 millilitres per minute and that ^{220}Rn has a 55.6 second half-life.*

A further experiment, experiment BCL4, was performed to try to determine the distribution of the deposition of ^{212}Pb in the 90 millilitre coil after a usual ^{220}Rn emanation. This was done by dividing the 90 millilitre coil into three separate coils of about 30 millilitres each before collecting and measuring the amount of ^{212}Pb in each small coil. The results of these measurements are shown in Table 4.5 along with the results of calculating the expected deposition distribution of ^{212}Pb between the three coils. To perform this calculation the first step was to determine the distribution of ^{220}Rn decays between the three coils by taking into account the 55.6 second half-life of ^{220}Rn, the 30 millilitre per minute flow rate through the coils and the volume of each coil. Knowing the distribution of ^{220}Rn decays and by assuming that a constant fraction of the ^{212}Pb produced from decays of ^{220}Rn is deposited on the tubing at the place where it is produced, the expected distribution of ^{212}Pb between the three coils can be calculated. A comparison of the measured distribution to the expected distribution shows very good agreement. In the second coil 57±2% of the activity in the first coil was collected which compares well to the 55% which was calculated, and in the third coil 24±2% of the activity was collected which, again, compares well to the 24% which was calculated. This is good evidence that most of the ^{212}Pb is deposited on the tubing where the ^{220}Rn decays.

While emanating ^{220}Rn from the MnO_2 cells, as described in Section 4.4.1 on page 52, a more standard procedure to collect the ^{212}Pb produced by the ^{220}Rn decays was investigated. In experiments BCL3 and BCL6 conducted at BNL, the ^{220}Rn emanated from the MnO_2 cell was fed into a filter and then into two, 20 millilitre bubblers in series each of which was filled with 0.5M hydrochloric acid. The amount of ^{212}Pb collected in each bubbler after about 24 hours of emanation was found to be very small. In fact the overall efficiency of producing ^{212}Pb into the combined 40 millilitres of both bubblers was measured to be just 3% in experiment BCL3 and 5% in experiment BCL6. These efficiencies are about an order of magnitude lower than the efficiencies measured when a coil of tubing was used to trap the ^{220}Rn and collect the ^{212}Pb. Therefore the use of bubblers was not investigated further.

4.5 The Overall Evaluation of the Procedure to Manufacture ^{212}Pb Sources

4.5.1 The Overall Efficiency of the Procedure

The overall efficiencies of producing each ^{212}Pb source are shown in Table 4.3 by comparing the amount of ^{212}Pb collected with the measured activity of the MnO_2 cell during the emanation. It is clear that this overall efficiency is less than the result of simply multiplying the emanation efficiency by the collection efficiency and so there must be a further unidentified loss of ^{212}Pb in the production process. One possibility, already mentioned and the reason for usually running the pumping circuit in a closed loop, is that when the ^{220}Rn decays some of the ^{212}Pb atoms produced do not deposit onto the tubing but remain in the flow of air. This ^{212}Pb was not found to deposit in the filter of the circuit and, since all the other surfaces and volumes in the circuit are small compared to the 90 millilitre coil, it must be assumed that this ^{212}Pb remains in the air and is flushed away from the circuit when the collection of the ^{212}Pb commences. One other possible loss is that some of the ^{212}Pb deposits out on the tubing in such a way that 0.5M hydrochloric acid does not remove it. This possibility could be verified by varying the type of acid used to wash the tubing and measuring if any further ^{212}Pb is collected but unfortunately there was insufficient time to carry out such experiments.

Interestingly it can be seen that, for the ^{212}Pb sources manufactured at Oxford, the average overall efficiency is 17±5% which is about half that which would have been expected from combining the measured emanation and collection efficiencies. However, for the ^{212}Pb sources manufactured at BNL, the average overall efficiency is 30±8% which is about two thirds of that which would have been expected. This difference between the efficiency of producing ^{212}Pb sources at the two different institutes could be due to the differences between the coil of tubing used at BNL and that which was used at Oxford. It has already been noted that the coil at BNL was made from smaller diameter glass tubing than the plastic tubing used at Oxford. This smaller tubing might encourage more ^{212}Pb to deposit from the flow of air than the larger tubing or it could be that ^{212}Pb adheres more readily to glass than to plastic. Either of these effects could explain the differences in the overall efficiency of manufacturing a ^{212}Pb source at the two institutes.

The ^{212}Pb sources that were manufactured in the experiments listed in Table 4.3 were all measured for ^{228}Th contamination but two very different techniques for measuring this contamination were used at the two different institutes. At Oxford any ^{228}Th contamination was measured using $\beta - \alpha$ counters by allowing the ^{212}Pb in the source to decay away and then measuring any residual, long-lived, activity. At BNL any ^{228}Th contamination was measured, at production, by examining the alpha spectrum of the ^{212}Pb source. These different techniques and the results they produce will be discussed in the sections below.

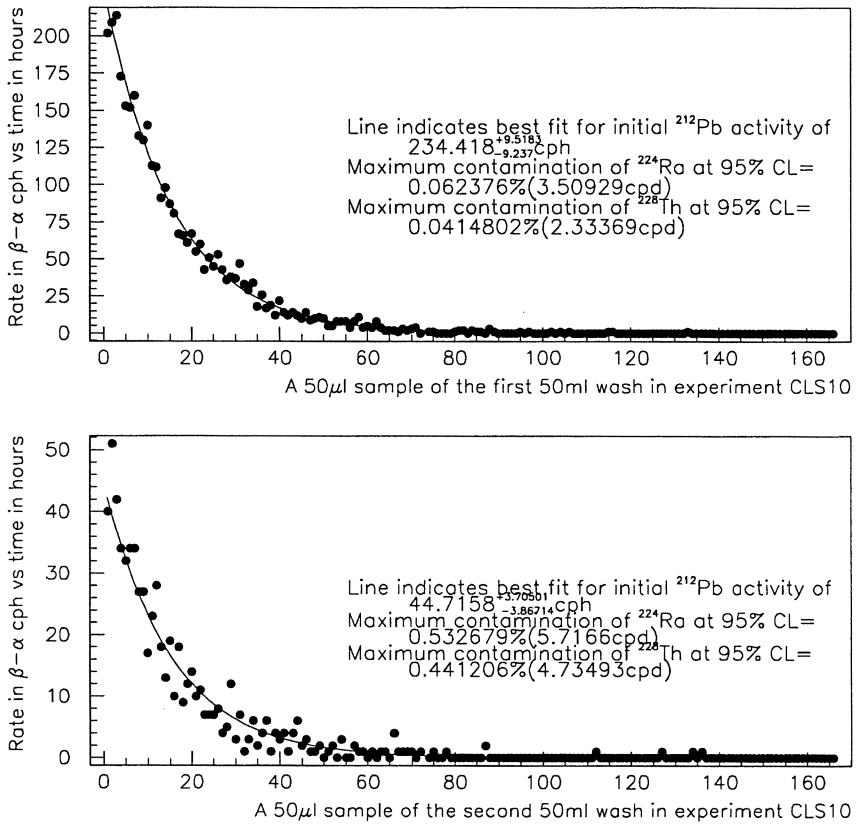

Figure 4.8: *The fitted $\beta - \alpha$ counting measurements of two 60 minute washes of the coil of tubing in experiment CLS10. The collection efficiency can be calculated to be 81±2% by comparing the amount of ^{212}Pb collected in the first wash to that collected in the second. The results shown on the plots use the fitting technique explained in Appendix D.*

4.5.2 Cleanliness Measurements using $\beta - \alpha$ Scintillation Counting at Oxford

A small sample of each ^{212}Pb source produced at Oxford was measured for activity using the $\beta - \alpha$ delayed coincidence scintillation counters, the details of which have already been discussed in Section 3.2.1 on page 30 with more details in Appendix D. The results of a typical measurement are shown in Figure 4.8. This figure shows the number of measured $\beta - \alpha$ counts against the time in hours of the measurement for two sequential washes of the coil of tubing in experiment CLS10. The results of the fits displayed on the plots are for the ^{212}Pb activity and the 95% upper level confidence limits for the ^{224}Ra and ^{228}Th contamination of the source. The ratio of the ^{212}Pb activity in the first wash compared to the second wash gives the collection efficiency to be 81±2% as is listed in Table 4.3. The result of counting 50 microlitres from the first 50 millilitre wash in experiment CLS10 for 160 hours is that the ^{228}Th contamination of the source can be limited to less than 0.04%. In fact, a much tighter limit of the ^{228}Th contamination in this ^{212}Pb source was found by counting a larger volume, 10 millilitres, of the source at least two weeks after its production. This result is listed in Table 4.6 along with similar measurements of 10 millilitres of all of the ^{212}Pb sources produced at Oxford.

Exp. No.	Initial ^{212}Pb of source	Max ^{228}Th in source:	
		Activity	% of ^{212}Pb activity
CLS4	6.4±0.2Bq	0.33±0.06mBq	<0.008%
CLS5	43±2Bq	0.82±0.12mBq	<0.003%
CLS6	47±2Bq	< 0.54mBq	<0.002%
CLS7	49±2Bq	<0.41mBq	<0.002%
CLS8	30±1Bq	0.38±0.08mBq	<0.002%
CLS9	37±1Bq	0.31±0.07mBq	<0.002%
CLS10	153±7Bq	0.20±0.06mBq	<0.0003%
CLS11	24±1Bq	<0.45mBq	<0.002%
CLS12	26±1Bq	0.93±0.15mBq	<0.005%

Table 4.6: *The results of measuring the ^{212}Pb sources manufactured at Oxford for ^{228}Th contamination. Each of these limits were found by measuring 10 millilitres of each 50 millilitre source on a $\beta - \alpha$ counter for several days at least two weeks after the production of the source.*

It can be seen that all of the ^{212}Pb sources manufactured at Oxford had a ^{228}Th contamination of less than 1 part in 10,000. Since the measured ^{228}Th backgrounds do not change considerably in consecutive runs and in particular show no sign of a build up in later sources it seems unlikely that the small ^{228}Th background is being produced by the emanation of the MnO_2. All of the ^{212}Pb sources manufactured at Oxford were produced in a laboratory which has residual ^{228}Th backgrounds from previous high activity experiments and so it seems more likely that this residual activity is the cause of the measured ^{228}Th background.

The results in Table 4.6 also show no difference in the ^{228}Th background between experiments CLS10-12 and CLS4-9 which is evidence that the initial ^{224}Ra separation from ^{228}Th is not required to produce sources of ^{212}Pb free from ^{228}Th. However, as has already been mentioned, it is obviously beneficial to have more than one separation stage between the ^{212}Pb and the ^{228}Th when a contamination of ^{228}Th would be disastrous.

4.5.3 Cleanliness Measurements using Alpha Counting at BNL

The ^{212}Pb sources that were produced at BNL were measured for any ^{228}Th contamination immediately after production by alpha counting a 400 microlitre sample from each source for about 15 hours. These alpha sources were prepared on platinum disks by Dr R.Hahn of BNL and measured as described in Appendix C. The alpha spectrum generated by the ^{212}Pb source manufactured in experiment BCL2 is compared to an alpha spectrum generated by an equilibrium source of ^{228}Th in Figure 4.9. It can be seen from this figure that none of the alpha peaks from isotopes above ^{212}Pb in the decay chain are visible in the ^{212}Pb source.

It should be noted that the alpha spectrum from the ^{212}Pb source produced in experiment BCL5 was different to those produced in the other four experiments due to the appearance of large, low energy tails to the alpha peaks. This effect was probably caused by an increase in the amount of scattering of the alpha particles due to more impurities in the source. It is reasonable to expect more impurities to be found in the ^{212}Pb source manufactured in experiment BCL5 because this was the only experiment which did not run the pumping circuit in a closed loop. It is quite possible that the large volumes of air which were pumped into the coil of tubing deposited not only ^{212}Pb but also impurities since this air was not filtered in any way.

Exp No	Net Number of Counts in:			Branching Ratio	
	5.55-5.65MeV	5.70-5.83MeV	5.92-6.14MeV	5.6MeV	5.8MeV
BCL1	47	72	3420	1.4%	2.1%
BCL2	47	61	5093	0.9%	1.2%
BCL7	75	59	5306	1.4%	1.1%
BCL8	86	84	6973	1.2%	1.2%
			Average:	1.2±0.2%	1.4±0.5%

Table 4.7: *The measurement of the relative branching ratios of two small ^{212}Bi peaks in the alpha spectra from the ^{212}Pb sources manufactured in experiments BCL1, 2, 7 and 8. The branching ratios are all given with respect to the two main unresolved ^{212}Bi peaks at 6.09MeV and 6.05MeV.*

The ^{212}Pb sources manufactured in all the experiments, except experiment BCL5, produced alpha spectra with such good resolution that two tiny peaks were visible at around 5.6MeV and 5.8MeV and for the source manufactured in experiment BCL2 these can be seen in Figure 4.9. These peaks were identified as being alpha decays from ^{212}Bi. A measurement was made of their branching ratios, as a percentage of the number of counts in the two main unresolved ^{212}Bi peaks, and the results are given in Table 4.7. Previous, more accurate, measurements of the alpha decays of ^{212}Bi are listed in [Fir96] and these show that there are actually three ^{212}Bi peaks at 5.607MeV, 5.626MeV and 5.768MeV with branching ratios, as percentages of the branching ratio to the two main unresolved ^{212}Bi peaks, of 1.23%, 0.17% and 1.84% respectively. The results of the present measurement can be seen to be in good agreement with these values.

Limits on the amount of ^{228}Th in each source manufactured at BNL were made by measuring the total number of counts in two energy regions around known alpha peaks in the ^{228}Th spectrum and allocating these counts to that alpha decay. The two energy regions that were selected were, firstly around the main ^{228}Th peaks (5.00MeV-5.50MeV) and secondly, around the ^{220}Rn and the ^{216}Po peaks (6.15MeV-7.00MeV). In order to produce contamination levels as a percentage of the ^{212}Pb activity remaining after the alpha counting, the ^{212}Pb activity was deduced by measuring the net number of counts in both the two main unresolved ^{212}Bi peaks and the ^{212}Po peak. The results of these measurements for all of the ^{212}Pb sources manufactured at BNL are given in Table 4.8.

The results in this table show a much higher ^{228}Th limit for the source manufactured in experiment BCL5 which can be explained by the increased scattering observed in the alpha spectrum. This is because the low energy tail of the two unresolved ^{212}Bi peaks is pushed into the energy region around the ^{228}Th peaks. The close proximity of the ^{228}Th peaks to the ^{212}Bi peaks is one of the reasons for also considering the energy region around the ^{220}Rn and the ^{216}Po peaks to monitor contamination since they are well separated in energy from both the ^{212}Bi and ^{212}Po peaks. It can be seen from Table 4.8 that the limit to the amount of ^{220}Rn in the source manufactured in experiment BCL5 is very similar to those in the other sources which is good evidence that the source does not actually contain any more ^{228}Th.

Since it is very hard to think of a mechanism which would allow ^{228}Th and not ^{224}Ra (hence ^{220}Rn) to be in a ^{212}Pb source manufactured by the procedure explained in this chapter, the 0.2% upper limit to the amount of ^{220}Rn contamination in each source can probably also be assumed to be an upper limit to the amount of ^{228}Th. However, by directly measuring any ^{228}Th contamination using the good resolution alpha spectra it can be seen that ^{212}Pb sources of around a few hundred millibecquerels were made which contained less than 0.3% ^{228}Th. The fact that the ^{228}Th in the sources can be measured down to this sort of level before they are used is a major achievement and means that these ^{212}Pb sources provide a very promising method for calibrating systems in the SNO experiment.

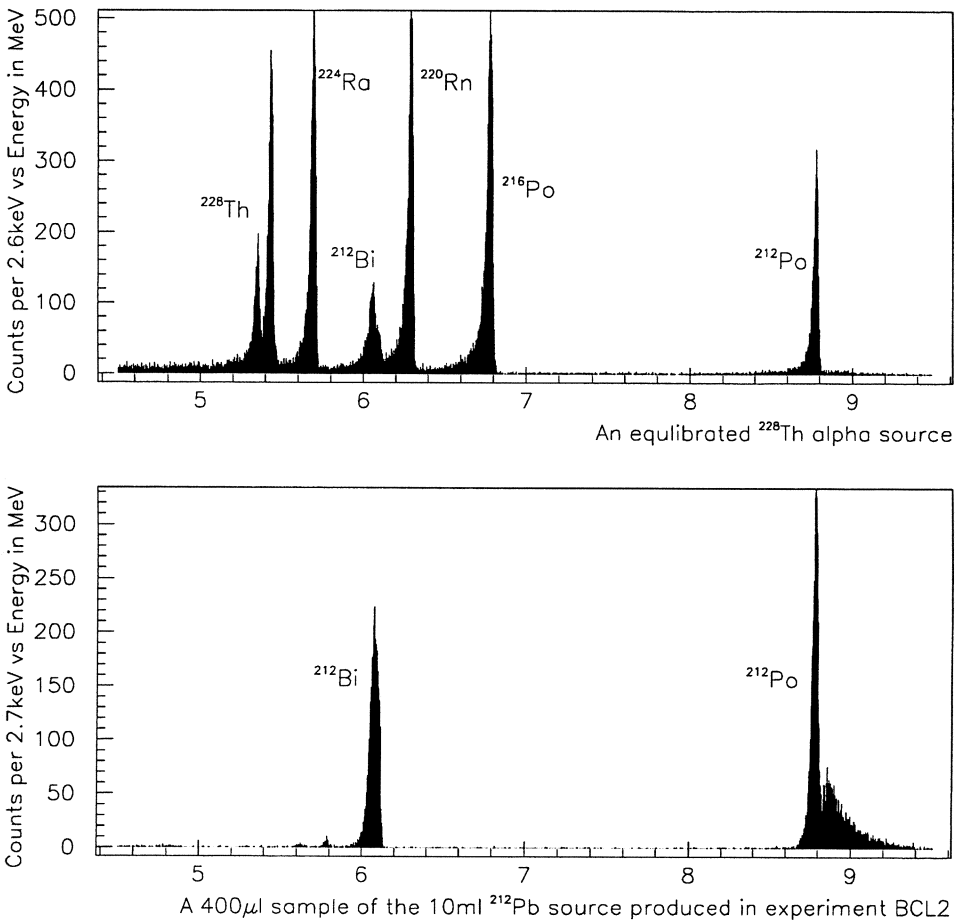

Figure 4.9: *The top alpha spectrum is that which was generated by a source of* ^{228}Th *in equilibrium with all of its daughters. The lower alpha spectrum is that which was generated by a 400 microlitre sample of the* ^{212}Pb *source manufactured in experiment BCL2. It can be seen that the peaks of* ^{228}Th, ^{224}Ra, ^{220}Rn *and* ^{216}Po *are not present in the lower alpha spectrum indicating only the presence of* ^{212}Pb. *The pile up of counts on the high energy side of the* ^{212}Po *peak in the lower spectrum is due to* $\beta - \alpha$ *coincidences since the alpha source was positioned extremely close to the detector to increase efficiencies. Finally, the very small peaks at around 5.6MeV and 5.8MeV are alpha decays from* ^{212}Bi *which have very low branching ratios. These peaks are analysed in Table 4.7 and discussed in the text.*

Exp. No.	Final ^{212}Pb Activity	Max ^{228}Th in source:		Max ^{220}Rn in source:	
		Activity	as % of ^{212}Pb	Activity	as % of ^{212}Pb
BCL1	0.34Bq	0.77mBq	0.23%	0.47mBq	0.14%
BCL2	0.48Bq	0.98mBq	0.20%	0.63mBq	0.13%
BCL5	0.43Bq	2.2mBq	0.51%*	0.67mBq	0.16%
BCL7	0.48Bq	1.3mBq	0.27%	0.51mBq	0.11%
BCL8	0.58Bq	1.4mBq	0.24%	0.63mBq	0.11%

Table 4.8: *The results of measuring the ^{212}Pb sources manufactured at BNL for ^{228}Th and ^{220}Rn contamination. The limits were found by alpha counting 400 microlitres of each source for about 15 hours and measuring the total number of counts in energy windows around the known alpha peaks of ^{228}Th as is discussed in the text. In experiment BCL5 the higher limit for ^{228}Th contamination, which is marked with an asterisk, is discussed in the text as probably being due to the poor quality of the alpha source.*

4.6 Conclusions

In the last chapter it was explained that it is important to be able to calibrate the entire HTiO SUF assay system for ^{212}Pb without adding long-lived activity to the SNO detector. In Section 3.2.1 on page 29 it was explained that the amount of long-lived thorium decay chain activity in the heavy water has to be less than 1 decay per day per tonne (1ddt) in order to produce neutrons at a rate less than about one tenth of the rate that they are expected to be produced by NC neutrino interactions. It is reasonable to insist that any calibration source to be used directly in the heavy water of the SNO experiment must be shown, before use, to produce less that 0.1ddt of ^{228}Th if it is completely mixed with the 1000 tonnes of heavy water. This corresponds to sources being shown to contain less than about 1 millibecquerel of ^{228}Th before they can be used.

In this chapter a procedure for manufacturing sources of ^{212}Pb free from ^{224}Ra and ^{228}Th has been developed and tested with excellent results. The upper limit on the amount of ^{228}Th in such sources was measured to be as low as 1 part in 10,000 by counting the sources for activity after the ^{212}Pb had decayed away. More importantly, using alpha counting, the amount of ^{228}Th in a ^{212}Pb source ready to be used has been measured to be less than 0.3%. Using this 0.3% upper level ^{228}Th contamination limit it can be calculated that up to about 300 millibecquerels of such a ^{212}Pb source can be added to the heavy water without adding more than 1 millibecquerel of ^{228}Th.

These ^{212}Pb sources can be used to calibrate any extractive water system in SNO that is sensitive to ^{212}Pb, including the HTiO SUF assay system, and are used to calibrate ^{212}Pb extractions in Chapters 6 and 7 of this thesis. By adding such sources to the heavy water in the SNO detector at different places before the extractive water systems it may also be possible to determine whether or not lead plating is occurring. The importance of being able to investigate plating effects was discussed in the last chapter.

An interesting use of ^{212}Pb sources would be to add them directly to the 1000 tonnes of heavy water in the acrylic vessel. It has been calculated that for every 470 decays of ^{208}Tl in the SNO detector one neutron will be produced [McD87]. This means that a 300 millibecquerel source of ^{212}Pb added to the acrylic vessel would generate about 30 neutrons in the first 24 hours after it was added to the detector and this would just be noticeable above the neutrino signal which is expected to produce about 10 neutrons a day. However with more research, and by producing stronger ^{212}Pb sources, it is expected that tighter upper limits on the amount of ^{228}Th in the ^{212}Pb sources can be measured and hence it may be possible to add stronger sources of ^{212}Pb to the detector. If such sources were added to the heavy water in the acrylic vessel it would allow investigations both into the mixing of the heavy water and also into the effectiveness of other background analysis techniques which were described in Chapter 2.

Chapter 5

The Secondary Concentration of ^{212}Pb and ^{228}Th from the SUF Eluate

5.1 Introduction

In Chapter 3 it was explained that an efficient method for the secondary concentration of lead and thorium from the SUF eluate is needed to complete the HTiO SUF assay system for the SNO experiment. This method has to satisfy the following requirements:

1. These procedures have to extract and concentrate minute quantities of ^{212}Pb and ^{228}Th from a volume of up to 20 litres of 0.5M hydrochloric acid into just 12 millilitres of aqueous solution which can be measured by a $\beta - \alpha$ delayed coincidence scintillation counter. Furthermore, the procedure for ^{212}Pb has to be completed within about an hour or losses due to the 10.6 hour half-life of ^{212}Pb will begin to be important.

2. The procedures have to be unaffected by the large quantities of titanium that it is expected will be present in the 20 litres due to the dissolution of the HTiO ion exchange material in 0.5M hydrochloric acid.

In this chapter are the details of many experiments designed to evaluate the suitability of the method of solvent-solvent extraction to perform the secondary concentration of lead and thorium from the SUF eluate. Firstly these experiments were conducted using small volumes and large quantities of ^{212}Pb and ^{228}Th, then they used large volumes and finally they used amounts of ^{212}Pb and ^{228}Th similar to the extremely small amounts that it is hoped will actually be present in the SUF eluate.

During these experiments it proved necessary to develop methods both to back-extract the lead and thorium from the organic phases used in the solvent-solvent extractions, and to provide a final concentration to the required 12 millilitres. Finally, different techniques to perform large volume solvent-solvent extractions were investigated and a 8 litre Prototype Rig was constructed and evaluated.

All of the experiments detailed in this chapter were carried out at Oxford University during 1995.

5.2 Theoretical Possibilities for the Secondary Concentration of ^{212}Pb and ^{228}Th

5.2.1 A Possible Extraction Method

Solvent-solvent extraction is the process by which metal ions are extracted from an aqueous phase into an organic phase. A concentration from an aqueous sample can thus be obtained by extracting into an organic phase of a smaller volume.

This method of extraction works by using reagents which combine with metal cations to produce molecules that are preferentially soluble in the organic phase. These reagents are often very selective as to which cations they combine with and hence systems can be formed not only to extract certain metal ions but also to separate them.

Solvent-solvent extractions are actually a better extraction system than the one used for the secondary concentration of ^{224}Ra since in the latter case, unlike in the former, there is a precipitation stage which could give difficulties of contamination due to co-precipitation.

Any solvent-solvent extraction can be characterised by a distribution ratio. This is a stoichiometric ratio of the concentration of a component in the organic phase compared to the amount in the aqueous phase irrespective of the species of the extracted component. If all the chemical reactions involved in an extraction are known this ratio can be calculated, and it can also be measured by experiment.

In batch solvent-solvent extraction Equation 5.1 gives an expression for the percentage extraction efficiency of a component from an aqueous phase into the organic phase, E, in terms of the distribution ratio, D, the volume of the aqueous phase V and the volume of the organic phase v. The ratio of the aqueous phase volume to the organic phase volume, V/v is often called the phase volume ratio.

$$E(\%) = 100 \times \left(1 + \frac{1}{D}\frac{V}{v}\right)^{-1} \tag{5.1}$$

In simple systems the distribution ratio is the same as the distribution coefficient, K, obtained by examining the chemical reactions involved in the extraction. However, when reactions are going on within the different phases themselves the distribution ratio and coefficient are not necessarily equal.

Many solvent-solvent extractions have distribution ratios large enough that good efficiencies can be obtained even when phase volume ratios of as much as twenty are used. Since the SUF eluate may be as large as 20 litres it seems unlikely that a solvent-solvent extraction by itself will produce a 12 millilitre aqueous sample that can be measured by a single $\beta - \alpha$ counter. There are many known techniques, specific to different reagents, to back-extract (or strip) metal ions from an extraction reagent in an organic phase into an aqueous phase and these techniques together with possible extraction reagents for both lead and thorium are listed in the following section and the most promising reagents are selected.

5.2.2 Possible Extraction Reagents

For Lead Extraction:

Possible reagents for the solvent-solvent extraction of lead were obtained by consulting, amongst other sources, the National Academy of Sciences report on the Radiochemistry of Lead [Gib61]. The following is a summary of possible extraction reagents for lead:

- Cupferron

  Using isoamyl alcohol as the solvent, lead can be separated from other elements using cupferron by varying the pH of the solution. However, lead can only be extracted if the pH of the aqueous phase is about 3. The 20 litres of SUF eluate is produced to be 0.5M in hydrochloric acid (a pH of 0.3) and increasing its pH to around 3 is not a desirable alternative since this would involve the careful addition of about 10 moles of alkali which would also generate a large amount of heat. Therefore this reagent was not selected for further study.

- 2-Thenoyltrifluoroacetone

  This reagent is widely used in the separation of metal ions but lead is only extracted from solutions with pH greater than 4 and so again it was not selected for further study.

- Dithizone

  Lead dithizone is selectively extracted into organic solvents. Unfortunately lead is only extracted with dithizone from solutions with a pH above 3 and so this system was not selected for further study.

- Diethyldithiocarbamic acid and related compounds

  Diethyldithiocarbamic acid uses a similar method to that of dithizone but it reacts with more elements and has a more limited pH range of extraction of its complexes and so it is generally less useful than dithizone for separating lead from other elements. However, the lead complex can be extracted from 0.5M hydrochloric acid.

  The diethyldithiocarbamic acid can be generated in two different ways. Firstly, sodium diethyldithiocarbamate can be dissolved in an aqueous phase and then itself and the lead complex extracted into an organic phase, or secondly, an organic diethyldithiocarbamate compound can be dissolved directly into the organic phase. This latter approach is most suitable when extracting from acidic aqueous phases. Two available compounds have been used in the past which dissolve directly into an organic phase. These are:

  - Ammonium pyrrolidinedithiocarbamate (APDC)
  - Diethylammonium diethyldithiocarbamate (DDDC)

  The first of these compounds is generally more stable in acidic conditions than the second but it is also less soluble in organic solvents. The solubility issue of the reagents is discussed alongside the selection of a suitable solvent in the next section.

  A very efficient method for back-extracting lead from both APDC and DDDC can be found in [Mag81] which involves adding a small volume of concentrated nitric acid to the organic phase, mixing for several minutes and then rinsing the lead out with water.

For Thorium Extraction:

Possible reagents for the solvent-solvent extraction of thorium were obtained by consulting, amongst other sources, the National Academy of Sciences report on the Radiochemistry of Thorium [Hyd60]. The following is a summary of possible reagents for the extraction of thorium:

- Tributyl phosphate (TBP)

  This reagent successfully extracts thorium only from high molarity nitric acid solutions or ones which also contain large quantities of calcium nitrate. Altering the chemical consistency of the SUF eluate by such margins would require large quantities of chemicals so this reagent was not considered for further study.

- Trioctylphosphine oxide (TOPO)

  Thorium is very highly extracted using this reagent from nitric acid solutions, particularly if the nitric acid molarity is as much as 1M but unfortunately it does not extract from 0.5M hydrochloric acid solutions. The addition of 20 moles of nitric acid to each SUF eluate before processing would be very impractical and so this reagent is not really suitable for use in the secondary concentration of thorium. [1]

- Di-(2-ethylhexyl)phosphoric acid (HDEHP)

  This is an acidic ester of orthophosphoric acid and it is a reagent specifically designed for the extraction of thorium. It is known that it extracts thorium with a high partition coefficient from hydrochloric acid solutions of virtually all molarities, to a lesser or greater extent.

A number of methods to back-extract thorium from HDEHP were found in the literature and these include using 6M hydrochloric acid [Sat68] or 2M ammonium carbonate [Sha77].

5.2.3 Possibilities for Organic Solvents

An organic solvent was required to perform the solvent-solvent extractions and at first it was hoped for simplicity that the same solvent could be used for both lead and thorium. Firstly, the solvent had to be safe to use from both a toxicity and a flamability standpoint which ruled out most usual solvents such as carbon tetrachloride, toluene and chloroform. Secondly, the solvent had to dissolve or mix with the selected extraction reagents and be compatible with the strong acids used in the back-extraction procedures.

The HDEHP reagent was found to be readily miscible in a number of safe organic solvents, however DDDC and APDC were not found to be readily soluble in these solvents. For example, kerosene was tested for DDDC solubility and even after leaving for several hours an insufficient amount of DDDC was dissolved to perform lead extractions. Due to this solubility difficulty the DDDC compound was chosen for use in preference to the APDC compound since the latter was found to have an even lower solubility.

A safe solvent, investigated for use and found to dissolve a suitable amount of DDDC, was di-isopropyl napthalene (DIN) which is the base of the scintillator cocktail used by the $\beta - \alpha$ counters. Unfortunately this solvent could not be used in the back-extraction of lead as concentrated nitric acid was found to decompose the solvent leaving unknown residues.

[1] Some small scale feasibility tests were conducted using TOPO by adding nitric acid to the aqueous phase before extractions and good efficiencies for thorium were obtained, however no efficient back-extraction method was found and so these tests were discontinued.

After a considerable search a suitable solvent was found which would dissolve good quantities of DDDC and was stable in the presence of concentrated acids. This solvent was 2-pentanone, a long chain ketone. Unfortunately 2-pentanone was not found to have very good separation characteristics from water and so another ketone with a longer chain length was sought. A solvent, 2-octanone, was found to dissolve good quantities of DDDC, to be stable in the presence of concentrated acids and found to have excellent separation characteristics from water. Further characteristics of 2-octanone are that it has a high flash-point, is available from chemical suppliers at a fairly low cost and it has low toxicity.

Therefore 2-octanone was chosen to be used as the solvent in lead extractions and it was also used initially for thorium extractions until it was found that kerosene had to be used to allow the back-extraction of the thorium (see Section 5.4.5).

5.2.4 The Theory of the Selected Chemical Extractions

The chemical mechanisms by which the selected reagents extract lead or thorium have been studied in the literature. Below is a brief summary of the chemical reactions involved in these extractions and an indication of their extraction abilities, as determined by other authors.

- The diethyldithiocarbamate extraction of lead, eg DDDC:

  When the DDDC is dissolved in an organic phase it forms diethyldithiocarbamate ions which have the following chemical formula: $(C_2H_5)_2NCS(S-)$. When shaken with an acid solution, the diethyldithiocarbamate ions are converted to diethyldithiocarbamic acid which reacts with Pb(II) ions. This reaction requires two acid molecules per Pb(II) ion and produces two hydrogen ions which are released into the aqueous phase. The distribution coefficient for this process is given by:

  $$K = \frac{[(Pb - complex)]_O[H^+]_A^2}{[Pb^{2+}]_A[DDDC]_O^2}$$

  Where the square brackets denote the molar concentration of that species in the organic (O) or aqueous (A) phase.

  The lead diethyldithiocarbamate molecule can be hydrolysed using a strong acid into carbon disulphide and an amine which releases Pb(II) ions back into the aqueous phase and this is the recommended back-extraction method as is described in Section 5.2.2 on page 71. Lead has been extracted from a solution at pH 4.5 and then back-extracted with virtually 100% overall efficiency using a few percent weight to volume (w/v) solution of DDDC [Mag81].

  One concern about the suitability of DDDC for extracting from 0.5M hydrochloric acid is the instability of the diethyldithiocarbamic acid formed but the literature indicates that DDDC can be used to extract lead from aqueous solutions up to about 1M in hydrochloric acid [Bod60]. Indeed, when equal phase volumes of DDDC in carbon tetrachloride and 1M hydrochloric acid are mixed together it requires 20 minutes of mixing to reduce the concentration of the dithiocarbamate ion in the organic phase by a factor of two [Bod59]. It should be noted that this characteristic time for decomposition is dependent upon the solvent used since it depends upon the distribution coefficient of the DDDC reagent between the organic and aqueous phases. However, it would seem likely that mixing times of the order of a few minutes can easily be tolerated when using other solvents, including 2-octanone, and this is all that is required to extract lead.

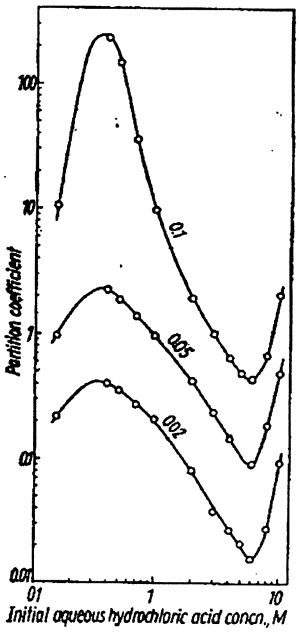

Figure 5.1: *This figure is taken from [Sat68] and it shows a log-log plot of the variation of partition coefficient with hydrochloric acid concentration in the extraction of thorium by solutions of HDEHP in kerosene. The numerals on the curves indicate the molar HDEHP concentration. The decrease of the partition coefficients for all HDEHP molarities at about 6M hydrochloric acid indicates a possible back-extraction method.*

- The extraction of thorium using di-esters of orthophosphoric acid, eg HDEHP:

  The reagent HDEHP is a di-ester of orthophosphoric acid and it has the following chemical formula: $(C_8H_{17}O)_2PO(OH)$. When thorium is extracted by such a reagent the hydrogen ion of the phosphate group is replaced with a fraction of the thorium ion. The dominant reaction requires three HDEHP molecules per Th(IV) ion and it produces four hydrogen ions which are released into the aqueous phase. The distribution coefficient for this dominant reaction is given by:

  $$K = \frac{[Th - complex]_O[H^+]_A^4}{[Th^{4+}]_A[HDEHP]_O^3}$$

  In fact the chemical reactions are more complicated than this dominant reaction and the distribution ratio has been found to include another term involving the concentration of other anions in the aqueous phase [Pep60].

  The measured partition coefficient for thorium extractions using HDEHP from solutions of hydrochloric acid is shown in Figure 5.1 which contains a plot taken from [Sat68]. This figure indicates that good extraction efficiencies are possible when extracting from 0.5M hydrochloric acid and that back-extractions using 6M hydrochloric acid may be possible.

5.3 An Introduction to Experimental Techniques

5.3.1 Methods of Assay

In order to determine the efficiency of lead and thorium extractions and back-extractions it was necessary to have techniques to assay these elements. There were two techniques available at Oxford which could measure ^{212}Pb and ^{228}Th. Firstly, there were the $\beta - \alpha$ delayed coincidence scintillation counters whose operation has already been explained in Section 3.2.1 on page 30 and are also discussed in Appendix D. Unfortunately the $\beta - \alpha$ counters developed at Oxford could not be used to measure samples of 2-octanone and so their use in researching solvent-solvent extractions was quite limited. The second counting technique available was that of gamma counting using a Ge(Li) detector and details of this can be found in Appendix B. The sensitivity of the Ge(Li) counter is much lower than that of the $\beta - \alpha$ counters and so kilobecquerel quantities of ^{212}Pb and ^{228}Th have to be used to measure efficiencies. However, it was not expected that there would be any difference between measuring efficiencies using kilobecquerel or millibecquerel amounts of ^{212}Pb and ^{228}Th but this is investigated briefly in Section 5.7.1 which starts on page 86.

The Ge(Li) detector allows the measurement of any liquid sample and in particular both organic and aqueous samples can be measured. At first the counting bottles were washed in acid and re-used but experiments showed that this did not remove all traces of ^{228}Th which therefore introduced some cross-contamination of experimental results. The effected results were discounted and new, clean bottles were used for all other experiments in order to eliminate this problem.

Unless otherwise stated statistical errors on counting measurements were about 10% and estimates of the initial amounts of ^{212}Pb, ^{224}Ra and ^{228}Th in each sample were made by counting each sample at certain times after the experiment was performed. In later experiments a best fit of such measurements was used to determine initial activities more precisely. Both of these techniques are described in detail in Appendix B.

5.3.2 Sources of Chemicals

The acids and chemicals used in the experimental investigation detailed in this thesis were all purchased from standard chemical suppliers. The DDDC reagent and the 2-octanone (98%) were purchased from Aldrich[2] whereas the HDEHP was purchased from Sigma[3] and the kerosene (as heavy distillate) was purchased from Merck[4].

It should be noted that the HDEHP used in all of the experiments was not purified as was suggested in the literature. This process was omitted to allow for easier experimentation and initial results showed that good extraction efficiencies could be obtained from the reagent used straight from the bottle. (The discussion in Section 5.7.3 on page 91 mentions some possible problems that could result.)

In order to measure extraction efficiencies a spike of ^{228}Th in equilibrium with all of its daughters, including ^{212}Pb, was added to aqueous phases just prior to extractions. This was taken from a 300 becquerel per millilitre stock solution of ^{228}Th in 1M nitric acid which itself had been diluted from a ^{228}Th source purchased from Amersham[5].

[2] Aldrich Chemical Co, The Old Brickyard, New Road, Gillingham, Dorset, SP8 4BR

[3] Sigma Chemical, Fancy Road, Poole, Dorset, BH12 4XA

[4] Merck Ltd, Hunter Boulevard, Magna Park, Lutterworth, Leicestershire, LE17 4XN

[5] Amersham International PLC, White Lion Road, Amersham, Bucks, HP7 9LL

5.4 Small Scale Feasibility Studies using Solvent-Solvent Batch Extraction

5.4.1 Introduction and General Procedure

The reagents selected and examined in previous sections were tested experimentally for extraction and back-extraction efficiencies initially by using just 0.5 litres of aqueous phase. This volume was chosen primarily for practical purposes and it means that the experiments in this section were all carried out at about one fortieth of the scale of the volumes needed for the secondary concentration from the SUF eluate. For all of the experiments this aqueous phase was made chemically similar to the SUF eluate by making it 0.5M in hydrochloric acid and by adding several milligrams of titanium.

All of the extractions in this section were carried out in a 1 litre separating funnel by allowing the phases to mix for a certain amount of time. This mixing was achieved either by tilting the separating funnel by hand a number of times, 10 tilts being carried out in approximately 1 minute, or by mechanically shaking the funnel for a number of minutes. The phases were then allowed to separate, which took only a few minutes, before the aqueous phase was removed and the less dense organic phase collected.

A sample of the aqueous phase was taken before and after each extraction for gamma counting so that extraction efficiencies calculated by measuring the appearance of activity in the organic phase could be checked by comparing them to the disappearance of activity from the aqueous phase.

In the following sections the results of small scale batch experiments using DDDC and HDEHP are listed along with some more specific experimental details.

5.4.2 The Extraction and Back-Extraction of ^{212}Pb using DDDC

The details of several small scale batch solvent-solvent extractions using a solution of DDDC in 2-octanone are given in Table 5.1. Alongside each description of the extraction is the overall extraction efficiency for ^{212}Pb as determined by gamma counting. The gamma counting results also showed that the DDDC reagent did not extract any ^{224}Ra or ^{228}Th which is what one would expect from the literature.

The results in Table 5.1 show that overall extraction efficiencies for lead of about 60-80% can be obtained using a solution of DDDC in 2-octanone when phase volume ratios of around 50 are used. This overall efficiency is the combination of two or three extractions each using a small organic volume and a very short amount of contact time, typically only a minute or two. This efficiency was lower than that

Exp no	Conc in w/v of DDDC	Volume of Org	Time of Ext	Number of Ext	Extraction Efficiency in %
CEL5	sat sol	10ml	20 tilts	2	79
CEL6	2%	5ml	20 tilts	2	63
CEŁ7	2%	15ml	20 tilts	2	70
CEL9	sat sol	8ml	20 tilts	3	72
CEL10	sat sol	8ml	20 tilts	3	77

Table 5.1: *The results of extraction experiments using a solution of DDDC in 2-octanone. The concentration of DDDC is expressed as a weight to volume percentage in the 2-octanone solvent and the saturated solution which was used was estimated to be about 2.5% w/v ie 25 milligrams per millilitre. The overall extraction efficiency is the combined efficiency of all of the individual extractions carried out in each experiment. The aqueous phase used in each of these experiments was 0.5 litres of 0.5M hydrochloric acid.*

which had been expected from the literature however it was considered sufficient for the needs of the SNO experiment. An indication that it was not the chemistry of the extraction that was failing comes from the fact that the results for the experiments are all quite similar despite varying the organic phase volume and the number of extractions. These lower efficiencies can be explained if the organic phase was not completely collected after each extraction which was possible in these experiments because the apparatus was not well rinsed.

For most of the extraction experiments a back-extraction was also carried out. This involved adding a certain volume of concentrated nitric acid to the organic phases of all of the extractions mixed together and shaking the result on a mechanical shaker for a number of minutes. The aqueous phase was then rinsed with a volume of water and separated from the organic phase for gamma counting. The details of these back-extractions and the results that they gave are given in Table 5.2.

The results show that the back-extraction technique works well, being about 60-80% efficient at stripping the lead from the DDDC in the organic phase into a small aqueous volume of high acid strength. Again, these efficiencies are lower than those seen in the literature and they can be explained by inadequate rinsing of the apparatus leading to an incomplete collection of the aqueous phase.

Combining the extraction and back-extraction efficiencies gives an overall efficiency of only 40-60% but it was expected that this could be increased by optimising the techniques involved.

5.4.3 The Extraction and Back-Extraction of ^{228}Th using HDEHP

The details of several small scale batch solvent-solvent extractions using a solution of HDEHP in 2-octanone and kerosene are given in Table 5.3. Alongside each description of the extraction is the overall extraction efficiency for ^{228}Th as determined by gamma counting.

Experiment CPEL3 was an attempt to combine the lead extraction and the thorium extraction and so the organic phase was also saturated with DDDC. Although the ^{228}Th extraction was unaffected by the DDDC there was no observable ^{212}Pb extraction and it is unclear exactly why this was true but it could have been due to the decomposition of the DDDC since the HDEHP reagent itself is acidic.

The results in Table 5.3 show that good extraction efficiencies for ^{228}Th using HDEHP in 2-octanone and kerosene can be achieved when phase volume ratios of around 50 are used. This efficiency does not seem to be increased by increasing the number of extractions, however there is a correlation between the efficiency and the length of contact time in the extraction. Experiments PEL4, 5 and 9 all have notably higher extraction efficiencies than the other experiments and it can be seen that these experiments all used more than 10 minutes extraction time in comparison to the much smaller times used in the other experiments. Hence it would seen that extraction times of at least 10 minutes are needed to efficiently extract ^{228}Th using HDEHP.

The details and results of several attempts to back-extract thorium from HDEHP are shown in Table 5.4. Firstly, it can be seen that thorium cannot be back-extracted from HDEHP using strong nitric acid. Also, back-extractions using 6M hydrochloric acid are unsuccessful when 2-octanone is the solvent. However, the results of experiments PEL7 and 9 show that when kerosene is used as the solvent variable back-extraction efficiencies into 6M hydrochloric acid can be achieved as had been indicated in [Sat68].

Exp no	Total Org Vol	Vol of HNO_3	Time of Shaking	Vol of H_2O	Back-Extraction Efficiency in %
CEL6	30ml	0.2ml	10mins	10ml	65
CEL7	60ml	0.6ml	20mins	10ml	81
CEL9	60ml	0.6ml	20mins	6ml	64
CEL10	60ml	0.6ml	20mins	10ml	83

Table 5.2: *The results of back-extracting ^{212}Pb from DDDC in 2-octanone using concentrated nitric acid.*

Exp no	HDEHP Conc	Volume of Org	Time of Ext	Number of Ext	Extraction Eff in %
PEL1	1.5M in 2-octanone	10ml	20 tilts	2	57
PEL3	1.5M in 2-octanone	10ml	20 tilts	3	58
CPEL3	1.5M in 2-octanone	10ml	2mins	3	64
PEL4	1.5M in 2-octanone	8ml	10mins	3	85
PEL5	1.5M in 2-octanone	8ml	5mins	3	58
PEL7	0.1M in kerosene	10ml	15mins	2	89
PEL9	0.05M in kerosene	15ml	30mins	2	71

Table 5.3: *The results of extraction experiments using a solution of HDEHP in 2-octanone. The overall extraction efficiency is the combined efficiency of all of the individual extractions carried out in each experiment. Experiment CPEL3 was an attempt to combine a ^{228}Th extraction with a ^{212}Pb extraction and so the organic phase was also saturated with DDDC. The aqueous phase used in each of these experiments was 0.5 litres of 0.5M hydrochloric acid.*

Exp no	HDEHP Conc	Total Org Vol	Method for Back-extraction	Back-Extraction Efficiency in %
PEL3	1.5M in 2-octanone	60ml	+3ml conc HNO_3 for 20mins then H_2O rinse	0
CPEL3	1.5M in 2-octanone	60ml	+3ml conc HNO_3 for 20mins then H_2O rinse	0
PEL5	1.5M in 2-octanone	60ml	2×(20ml 6M HCl shaken for 5mins)	0
PEL7	0.07M in kerosene	30ml	30ml 6M HCl shaken for 20mins	31
PEL9	0.05M in kerosene	30ml	30ml 6M HCl shaken for 30mins	100

Table 5.4: *The results of back-extracting ^{228}Th from HDEHP using concentrated nitric acid and 6M hydrochloric acid.*

5.4.4 Titanium Extraction Results

Some samples from lead extractions were analysed for titanium using a spectrophotometric technique as detailed in [How94]. Less than 1% of the titanium initially present was found in any back-extracted lead sample and the titanium content of the aqueous phase remained the same before and after lead extractions. This indicates that DDDC does not extract titanium and that extractions and back-extractions using DDDC are not only insensitive to the amount of titanium in the SUF eluate but they also separate the ^{212}Pb from the titanium.

Samples from experiments PEL4 and PEL5 of the last section, which involved the HDEHP extraction of thorium, were also analysed spectrophotometrically for titanium and in this case some titanium extraction was observed at an efficiency of about 40% but this did not interfere with the ^{228}Th extraction. Furthermore, measurements of back-extracted thorium solutions using the 6M hydrochloric acid showed that less than 1% of the titanium present in the initial aqueous phase makes its way into the back-extraction solution. Therefore HDEHP could be used to separate ^{228}Th from the titanium excess in the SUF eluate.

In conclusion, both DDDC and HDEHP were seen to extract ^{212}Pb and ^{228}Th from a titanium excess into solutions which do not contain titanium and so it is likely that these techniques will still work even if the amount of titanium in the SUF eluate varies considerably.

5.4.5 Conclusions of Feasibility Studies

The results given in the previous sections show that the chosen reagents for the extraction of thorium and lead are suitable. Using a solution of DDDC in 2-octanone ^{212}Pb can be efficiently extracted from a 0.5M hydrochloric acid containing titanium and back-extracted into a smaller aqueous volume. Using a solution of HDEHP in kerosene the same can be achieved for ^{228}Th. In the next section these extraction systems are further investigated in experiments which start from 2 litres of 0.5M hydrochloric acid.

5.5 Medium Scale Studies Using Continuous Extraction Techniques

5.5.1 The Need for a Third Stage for Extractions from the SUF Eluate

Unfortunately if the lead and thorium extraction and back-extraction procedures which were investigated in the last section are used to extract from 20 litres of SUF eluate they would produce aqueous phases which are too acidic and too large to be measured directly by a single $\beta - \alpha$ counter. Therefore it became clear that a further, final concentration stage had to be developed.

In the last section results showed that virtually no titanium remains in the back-extracted solutions after HDEHP and DDDC extractions. This means that it is now possible to use the hydrous titanium oxide (HTiO) ion-exchange method, as is used in the secondary concentration of radium, to perform a final concentration stage. The details of the procedure used for the secondary concentration of radium is given in Section 3.2.3 on page 31.

In the experiments in this section such an HTiO stage is used, in conjunction with a solvent-solvent extraction and back-extraction, to concentrate the ^{212}Pb and ^{228}Th from 2 litres of a liquid chemically similar to the SUF eluate into a 12 millilitre sample.

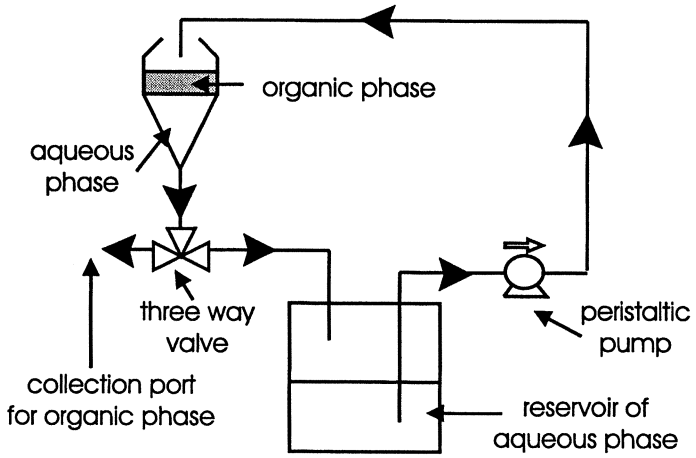

Figure 5.2: *Apparatus for continuous solvent-solvent extractions.*

5.5.2 The Method of Continuous Extraction for Large Volumes

The method of solvent-solvent batch extraction, as used so far, is unsuitable for much larger volumes since large separating funnels are difficult to purchase and become unwieldy to shake. A different approach to perform the extraction was developed and this was to pump the more dense aqueous phase onto the top surface of a layer of an organic phase thereby allowing it to pass through the organic layer under gravity. The advantages of this form of continuous extraction are that the pumping rate can be standardised and, if small enough droplets are produced, one would expect good contact between the two layers.

Some experiments using 2 litres of aqueous phase were performed using the apparatus as shown in Figure 5.2. For each experiment, one extraction at a time was carried out by injecting a volume of organic phase into the separating funnel and spraying the aqueous volume onto it at a rate of about 1 litre per minute.

In each of the three experiments the number of extractions was varied but all of the organic volumes were combined before the ^{212}Pb and ^{228}Th were back-extracted according to the methods determined in the previous section.

Each back-extracted acidic solution was then concentrated using an HTiO extraction and elution stage. This involved adding a tenth of a millilitre of a 15% w/v titanium tetrachloride solution and increasing the pH of the solution to around 8 or 9 using sodium hydroxide. This precipitates the titanium as HTiO which extracts any lead, radium and thorium in the solution. The HTiO in this solution was then collected on a Media-Kap 10 filter and eluted using 3 samples of 4 millilitres of 0.5M hydrochloric acid. In experiment CC5 each acid sample was left in contact with the HTiO for just a few minutes whereas in the other two experiments each sample was left for 10 minutes.

Although the final solution produced was suitable for measurement by a $\beta - \alpha$ counter they were in fact measured by gamma counting along with other samples from the experiment so that extraction, back-extraction and final HTiO stage efficiencies could all be calculated.

To measure efficiencies using gamma counting a ^{228}Th spike of a few kilobecquerels in equilibrium with its daughters was added to the aqueous phase before extractions. In other respects this aqueous phase was chemically similar to the SUF eluate.

Exp No.	Extraction Procedure:	Procedure Efficiencies in %:			Overall Efficiency in %
		Extraction	Back-Ext	HTiO	
CC5	2×(50ml of 1% w/v DDDC in 2-oct) Each left pumping for 20 minutes	16±2	89±9	67±7	10±1
CC6	2×(50ml of 2% w/v DDDC in 2-oct) Each left pumping for 8 minutes	61±10	96±8	81±8	48±8
CC8	4×(50ml of 2% w/v DDDC in 2-oct) Each left pumping for 8 minutes	108±22	57±6	69±9	42±9

Table 5.5: *Results for the three stage secondary concentration of ^{212}Pb from 2 litres of mock SUF eluate.*

5.5.3 Summary of ^{212}Pb Three Stage Concentration Experiments

The extractant used in these experiments was a 1% or 2% w/v solution of DDDC in 2-octanone and the back-extraction method used a volume of concentrated nitric acid equal to one hundredth of the total organic phase volume. This acid was added to the organic phase and the mixture shaken for 10 minutes before standing for 10 minutes and washing the ^{212}Pb out with a few hundred millilitres of water. Table 5.5 shows the ^{212}Pb efficiency for each of the three stages along with the overall efficiency for each of the three experiments. The results and the errors, as given in this table, were obtained by fitting several gamma counting measurements of samples taken at different times after the experiment to give the initial activities of ^{212}Bi, ^{212}Pb, ^{224}Ra and ^{228}Th in each sample as is explained in Appendix B.

The results of experiment CC5 show a much lower extraction efficiency for ^{212}Pb than the other experiments and this must have been due to the longer mixing time that was used. This experiment indicates that the DDDC reagent in 2-octanone suffers from decomposition when it is left mixing in 0.5M hydrochloric acid for times of 20 minutes or more. This can be compared to the 20 minute half-life of DDDC in carbon tetrachloride when mixed with an equal volume of 1M hydrochloric acid (see Section 5.2.4 on page 73).

It is clear that with four extractions of 50 millilitres for 8 minutes each, good overall lead extraction efficiencies of virtually 100% can be achieved. Furthermore, good back-extraction efficiencies of 90-100% efficiency were obtained in the first two experiments. This back-extraction efficiency is larger than those measured in the last section which is presumed to be due to using a larger relative volume of water to rinse out the nitric acid which minimises the effect of losses in its collection. It is unclear why the back-extraction efficiency in experiment CC8 was smaller than in the other two experiments but it may have been due to the larger organic volume that was used.

The results in Table 5.5 also show that the HTiO stage worked very well and gave efficiencies of about 60-80%. It can be noted that the efficiency of this stage did not alter between the experiments which used 10 minutes for each elution (experiments CC6 and CC8) and the one which used only a few minutes (experiment CC5). It can therefore be deduced that the elution of lead from HTiO takes only a few minutes when using 0.5M hydrochloric acid.

5.5.4 Summary of ^{228}Th Three Stage Concentration Experiments

The extractant used in these experiments was a solution of HDEHP in kerosene of varying molarity. The back-extraction method used was to shake the organic phase with an equal volume of 6M hydrochloric acid for 30 minutes. In each of the three experiments the organic phase was diluted to 200 millilitres with kerosene and so the HDEHP molarity for back-extraction was 0.025M.

Exp No.	Extraction Procedure:	Procedure Efficiencies in %:			Overall Efficiency in %
		Extraction	Back-Ext	HTiO	
CC5	2×(50ml of 0.05M HDEHP in kerosene) Each left pumping for 30 minutes	93±5	66±4	36±2	22±2
CC7	50ml of 0.1M HDEHP in kerosene Each left pumping for 30 minutes	85±13	66±8	78±16	44±5
CC8	2×(50ml of 0.05M HDEHP in kerosene) Each left pumping for 20 minutes	90±13	68±8	80±5	49±5

Table 5.6: *Results for the three stage secondary concentration of ^{228}Th from 2 litres of mock SUF eluate.*

The results of these experiments obtained by fitting several gamma counting measurements of samples taken at different times after the experiment to give the initial activities of ^{212}Bi, ^{212}Pb, ^{224}Ra and ^{228}Th in each sample as is explained in Appendix B are given in Table 5.6. These results show that thorium extraction efficiencies of about 90% can be obtained using either 0.05M or 0.1M HDEHP in kerosene and pumping times of more than 20 minutes. These results also show that the back-extraction efficiency from 0.025M HDEHP in kerosene is around 70%. This can be compared to the 100% efficiency when back-extracting from a 0.05M HDEHP solution and the 30% efficiency from a 0.07M HDEHP solution which were measured in Section 5.4.3 on page 77. There appears to be some variation in this efficiency which is difficult to explain, however good back-extraction efficiencies were obtained by using HDEHP concentrations less than 0.05M in kerosene.

It can also be seen from the results in Table 5.6 that the HTiO stage gives good efficiencies of around 80% for ^{228}Th when individual elution times of 10 minutes are used (experiments CC7 and CC8) but this efficiency drops to 40% when only a few minutes are used for each elution (experiment CC5). It can therefore be deduced that the elution of thorium from HTiO takes more than a few minutes when using 0.5M hydrochloric acid.

5.5.5 Conclusions of the Three Stage Concentration Technique

The results in this section show that the ^{212}Pb and ^{228}Th in 2 litres of a solution which is chemically similar to the SUF eluate, can be extracted and concentrated into a sample that can be counted on a single $\beta - \alpha$ counter. The overall efficiency for this three stage procedure for ^{228}Th is about 50% and for ^{212}Pb is as much as 80% if all the stages are optimised together.

Unfortunately there is a problem when the results of these experiments are scaled to extracting from 20 litres volumes, because the time required to concentrate the ^{212}Pb from such a volume would be far too long. In the most efficient experiment for ^{212}Pb (experiment CC8), four extractions each lasting 8 minutes were carried out. With 20 litres this means that forty, 8 minute extractions are needed which makes over 5 hours of processing time which would cause large losses of ^{212}Pb due to decay.

One method of speeding up the continuous extraction would be to use a higher pumping speed but one would expect this to also decrease extraction efficiencies since the contact between the phases would be less and thus it does not solve the difficulty in producing a fast and efficient extraction. It was clear that a quicker method was needed for performing a solvent-solvent extraction when volumes of up to 20 litres are involved.

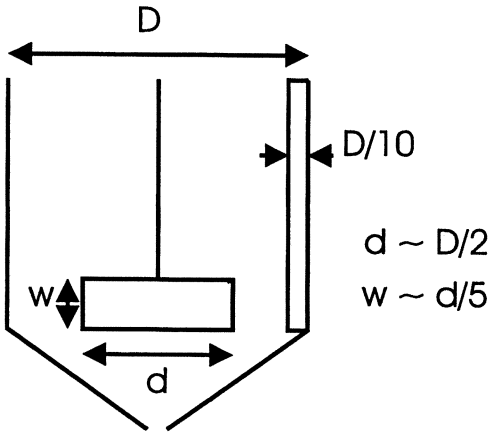

Figure 5.3: *Diagram of a large volume mixer including appropriate relative dimensions for the baffle and stirrer paddle in relation to the diameter, D, of the mixer.*

5.5.6 Alternative Methods for Large Volume Solvent-Solvent Extraction

Since solvent-solvent extractions using volumes greater than 20 litres are used in industry, the literature was consulted and expertise was sought. This effort produced a number of possible alternative methods resulting in good extraction efficiencies in a small amount of time. Two of these are discussed below:

- A counter-current continuous extraction column:

  This involves pumping two phases past each other in a column in a similar, if more sophisticated way to the 2 litre experiments detailed in the last section. The lighter phase is pumped in near the bottom of the column, the heavier near the top. One phase is then dispersed and the two allowed to mix for most of the length of the column. The lighter phase then collects at the top of the column and the heavier phase at the bottom from where each is pumped away. The different types of counter-current columns are described in the section beginning on page 672 in volume 9 of [Kir84]. Unfortunately the equipment needed to use this technique is both bulky and costly.

- A large scale batch extraction system:

  This method was previously disregarded as it was felt that good mixing between 20 litres of aqueous phase and a small volume of organic phase would be very difficult to achieve in one vessel. However, advice from Dr R.C.Darton of the Engineering Department at Oxford University, a chemical engineer, suggested that this presupposition is not true. A system using mechanical stirrers in large, drainable vessels is used in industrial applications to produce good mixing and allow adequate separations when phase volume ratios of up to 20 are used.

  A design of a large volume mixer for solvent-solvent batch extractions is shown in Figure 5.3. The mixing vessel shows the presence of a baffle which is needed to introduce turbulence in order to obtain good mixing. It was suggested that using such apparatus mixing times of only a few minutes would be required to produce high extraction efficiencies.

In the next section this second method of using a large scale batch extraction and a mechanical stirrer is developed into a Prototype Rig which was then tested for ^{212}Pb and ^{228}Th extraction efficiencies.

5.6 Large Scale Studies Using Mechanical Stirrers

5.6.1 Experimental Details and the Construction of the Prototype Rig

The previous section suggested apparatus for large scale solvent-solvent extractions using a mechanical stirrer. Using polypropylene, a Prototype Rig was constructed which would use this technique both for the solvent-solvent extraction of ^{212}Pb and ^{228}Th and for their back-extraction.

It was known that polypropylene is not fully resistant to 2-octanone and that fluorinated plastics should be used for a durable system, however to test the feasibility of the method the Prototype Rig was constructed out of the cheaper plastic.

The Prototype Rig had an 8 litre mixer to perform the solvent-solvent extraction which could be filled by a pump from a reservoir. The mixer could then drain either back to the reservoir or into a 1 litre separating funnel where the back-extraction would be carried out. Both of these mixers had baffles and stirrers of suitable dimensions.

The speed of mixing in the main vessel was adjusted until visual inspection indicated that good, uniform mixing had been obtained. After mixing for 2 minutes the phases were left to stand for a period of about 5 minutes before separating the organic phase and performing a back-extraction.

Two experiments were carried out to extract ^{212}Pb and ^{228}Th from 8 litres of 0.5M hydrochloric acid which also contained 1 gram of titanium. In the first experiment two sequential extractions, each using 0.2 litres of organic phase, were carried out. In the second experiment, just one extraction using 0.4 litres of organic phase was carried out.

To extract ^{212}Pb a 2% w/v DDDC solution in 2-octanone was used and this was back-extracted by mixing the organic phase, for two minutes, with 25 millilitres of concentrated nitric acid. For the ^{228}Th extractions an organic phase consisting of 0.05M HDEHP in kerosene was used and the ^{228}Th back-extracted into a few hundred millilitres of 6M hydrochloric acid.

The Prototype Rig was not sealed from the atmosphere and so only high level experiments were carried out as it was expected that airborne contamination would dominate any low level ^{212}Pb results. (See Appendix F for more details about airborne ^{212}Pb contamination.) Therefore about a kilobecquerel of ^{228}Th in equilibrium with its daughters was added to the aqueous phase prior to extractions and samples were measured using gamma counting, as before.

Exp No	Lead Results:			Thorium Results:		
	Vol of DDDC sol	Extraction Eff (%)	Back-Ext Eff (%)	Vol of HDEHP sol	Extraction Eff (%)	Back-Ext Eff (%)
MA1	2× 200ml	88±12	53±6	2×200ml	89±9	83±7
MA2	400ml	88±17	99±20	400ml	81±7	21±4

Table 5.7: *The results for the extraction and back extraction of both lead and thorium from 8 litres of mock SUF eluate using the Prototype Rig.*

5.6.2 Results of Experiments using the Prototype Rig

The overall results for the ^{212}Pb and ^{228}Th extractions and back-extractions using the Prototype Rig, with their statistical errors obtained after fitting many individual measurements, are given in Table 5.7.

The two experiments differed in how the back-extractions were carried out, as the results suggest. In experiment MA1 a mechanical stirrer was used in the 1 litre separating funnel to provide the required mixing for the back-extraction. This worked very well for the back-extraction of thorium, giving an 80% efficiency, but unfortunately in the lead back-extraction a much smaller aqueous phase was present, and the stirrer did not agitate the bottom of the funnel sufficiently to give good mixing between the two phases.

In experiment MA2, the back-extractions were performed by pumping air up into the bottom of the separating funnel after a suggestion by Dr R.K.Taplin. The air was seen to form large bubbles on emergence from the stop-cock and was then channelled to the surface by the curved shape of the separating funnel and it can be seen from the results of experiment MA2 in Table 5.7 that this method of mixing gave good back-extraction efficiencies for lead but not for thorium. It is not clear why the back-extraction efficiency for thorium was so low when using this mixing method but it may have been due to a slower reaction rate.

It can be seen that in both experiments good extraction efficiencies of around 90% for both ^{212}Pb and ^{228}Th were obtained after only 2 minutes of stirring.

5.6.3 Conclusions from the Prototype Rig Experiments

It is clear from the results in Table 5.7 that a quick and efficient method has been found to extract kilobecquerel quantities of both ^{212}Pb and ^{228}Th from 8 litres of a solution chemically similar to the SUF eluate into 0.4 litres of an organic phase. It is also clear that there are very efficient methods for the back-extraction of both lead and thorium, even if two different mixing techniques are needed.

If the results of these experiments are scaled to using 20 litres of SUF eluate then the ^{212}Pb and ^{228}Th can be extracted at about 90% efficiency into 1 litre of organic phase and then back-extracted with near 100% efficiency for ^{212}Pb, and 85% efficiency for ^{228}Th, into an acidic aqueous phase. Using the HTiO stage as tested in Section 5.5 on page 79 the ^{212}Pb and ^{228}Th could then be concentrated efficiently to produce a sample to be measured on a single $\beta - \alpha$ counter.

The time required to complete the ^{212}Pb extraction and back-extraction was under 1 hour in both experiments using the Prototype Rig but with the additional time required by the HTiO stage, and when 20 litres instead of 8 litres are used, the total time would be greater. It was noticed that the overwhelming contribution to the time of the extractions came from the filling of the large mixer using a Peristaltic pump with a flow rate of 1 litre per minute and the draining of the vessel under gravity through two 6 millimetre diameter pieces of tubing. It is clear that the flow rates involved in these two processes need to be increased to meet the time requirements for the secondary concentration of ^{212}Pb and this is also a good reason to limit the final procedure to just one solvent-solvent extraction.

5.7 Further Investigations into the Extraction Techniques

5.7.1 Experiments using very Small Amounts of ^{212}Pb and ^{228}Th

The previous experiments detailed in this chapter all used kilobecquerel quantities of ^{228}Th and ^{212}Pb to determine extraction and back-extraction efficiencies. In Section 3.2.1 on page 29 it was stated that the amount of ^{228}Th and ^{212}Pb in the heavy water of the SNO experiment is hoped to produce less than 1 decay per day per tonne. In the entire 1000 tonnes of heavy water this corresponds to about 10 millibecquerels of ^{228}Th and ^{212}Pb. Three small scale experiments were carried out to verify that the extraction and back-extraction techniques for ^{212}Pb and ^{228}Th developed using kilobecquerel amounts of activity also work for millibecquerel amounts of activity. The measurements for these experiments were all made using the $\beta - \alpha$ delayed coincidence scintillation counters, the details of which were discussed in Section 3.2.1 on page 30 with more details in Appendix D.

The first experiment was a blank run in which no activity was added so that any background contribution from the reagents themselves could be measured. A second experiment had about 10 millibecquerels of ^{228}Th in equilibrium with its daughters added to the original aqueous phase, and a third experiment had about 100 millibecquerels of ^{228}Th in equilibrium with its daughters added to the aqueous phase.

These experiments were all carried out in a 1 litre separating funnel and the solvent-solvent extractions used 0.5 litres of aqueous phase and 10 millilitres of organic phase. As usual the aqueous phase contained several milligrams of titanium and was 0.5M in hydrochloric acid. All the mixing of the two phases was carried out by shaking the separating funnel by hand.

These were low level experiments and thus required careful and clean experimental procedure and so all reagents and apparatus that were used were either new or previously had only been used for low level work. Since samples produced were to be measured by the $\beta - \alpha$ delayed coincidence scintillation counters it was known that each sample could be only 12 millilitres in volume and less than about 0.5M in acid or salt concentration and so all the samples were made to be 0.5M in hydrochloric acid and known fractions were taken for counting.

It was found, during the second experiment, that the scintillator cocktail is actually quite sensitive to 0.5M hydrochloric acid since one sample, when mixed with scintillator cocktail, turned cloudy and could not be measured for activity whereas all of the other samples were fine. Therefore, for the third experiment this was corrected by ensuring that counting samples were no more than 0.25M in hydrochloric acid.

Low Level Results for ^{212}Pb:

In each experiment for ^{212}Pb only one extraction was carried out using a 2% w/v solution of DDDC in 2-octanone. The back extraction was performed by mixing the organic phase with 1 millilitre of concentrated nitric acid for 2 minutes, leaving to stand for 2 minutes and then washing the ^{212}Pb out with a low molarity hydrochloric acid solution.

A sample of this low molarity hydrochloric acid solution and of the initial solution were immediately measured for ^{212}Pb activity using the $\beta - \alpha$ counters. The number of $\beta - \alpha$ delayed coincidence events that the counters recorded between times T_1 and T_2 for each sample are shown in Table 5.8.

It should be noted that the value given for the stock of experiment DF3 is not a measured value as this sample could not be measured by the $\beta - \alpha$ counters due to incompatibilities with the scintillator cocktail, as described in the section above. The value given is derived from the stock of experiment DF4 since it was known that this experiment used ten times the activity used in experiment DF3.

Experiment	Sample	Fraction of Sample Measured	Time Interval T_1 in hrs	Time Interval T_2 in hrs	Integration Factor (I)	Total Counts in Interval for Fraction	Total Rate in cts/hr for Sample
Background	Back-Ext	1/10th	1.12	45.93	13.45	5	3.7±0.2
DF3	Stock	-	-	-	-	DF4/10	21±1
DF3	Back-Ext	1/20th	1.12	45.93	13.45	16-2.5=13.5	20±6
DF4	Stock	1/20th	1.68	70.57	-	709	206±8
DF4	Back-Ext	1/20th	1.68	70.57	13.55	127-2.5=124.5	184±16

Table 5.8: *The results of three ^{212}Pb extractions and back-extractions. The extractions used 10 millilitres of 2% DDDC solution in 2-octanone and extracted from 0.5 litres of 0.5M hydrochloric acid. The back-extraction was completed by adding 1ml of concentrated nitric acid and then rinsing with water.*

The count rate for ^{212}Pb can be determined, if it is assumed that there is no ^{224}Ra present, by dividing the total number of counts recorded in a given time interval by the integrating factor, I, as given in Equation 5.2.

$$I = \int_{T_1}^{T_2} e^{-\lambda_{Pb} t} dt \tag{5.2}$$

The background experiment gave about 4 counts per hour above a counter background of one count per day and this is assumed to be due to airborne contamination since although steps were taken to minimise this background it was impossible to completely seal the apparatus from the air.

The overall efficiency of the second experiment was 95±29% and for the third experiment, with more activity and better statistics, it was 90±9%. These efficiencies are actually higher than those seen in similar scale experiments which used high-level activity whose results are given in Tables 5.1 and 5.2 on pages 76 and 78 respectively. This difference is believed to have been due to differences in the procedures used to collect the phases.

Low Level Results for ^{228}Th:

In each experiment for ^{228}Th only one extraction was carried out using a 0.05M solution of HDEHP in n-dodecane, the main constituent of kerosene. The back-extraction was performed by mixing the organic phase with 10 millilitres of 6M hydrochloric acid for 2 minutes, leaving to stand for 2 minutes and then, after being separated, it was diluted with water.

A sample of this low molarity hydrochloric acid solution and of the initial aqueous phase before and after the extraction were measured for activity using the $\beta - \alpha$ counters after the ^{228}Th had time to grow in and these results are shown in Table 5.9. More samples could be measured for ^{228}Th than for ^{212}Pb because the counting did not have to occur at the same time and so there was no limit as to how many $\beta - \alpha$ counters could be used.

It should be noted that the stock for experiment DF3 is the measured value, unlike that given for the ^{212}Pb results, since after two weeks the sample lost its cloudiness and could be measured by the $\beta - \alpha$ counters. Finally, no integration is needed to evaluate results as after 2 weeks all the samples should be in radioactive equilibrium. Therefore the $\beta - \alpha$ coincidence rate gives a direct measurement of the amount of ^{228}Th in each sample.

The background result for the first ^{228}Th extraction indicates no reagent contamination of ^{228}Th since the sample had the same count rate as the counter background.

Experiment	Sample	Fraction of Sample	Time(hrs)	Counts	Total Rate(cts/hr)
Background	Back-Ext	1/10th	67.1	1	at bkg
DF3	Stock	12/488th	67.1	37	22.4±3.7
DF3	Aqueous	12/488th	67.1	1	at bkg
DF3	Back-Ext	1/20th	67.1	32	9.5±1.7
DF4	Stock	1/20th	48.4	443	183.1±8.7
DF4	Aqueous	6/494th	48.4	11	18.7±5.6
DF4	Back-Ext	1/20th	48.4	195	80.6±5.8

Table 5.9: *The results of three ^{228}Th extractions and back-extractions. The extractions used 10 millilitres of 0.05M HDEHP in n-dodecane and extracted from 0.5 litres of 0.5M hydrochloric acid. The back-extraction was completed by mixing with 6M hydrochloric acid.*

By considering the amount of ^{228}Th left in the aqueous phase after the extraction, the efficiency for the extraction can be determined. This was around 100% for the second experiment and around 90% for the third. The overall efficiencies however were only 42±10% for the second experiment and 44±4% for the third which indicates that the back-extraction efficiency was only about 40%. This is lower than the 100% that was achieved in similar high level back-extractions but it should be noted that a different bottle of HDEHP was used for this experiment and in Section 5.7.3 on page 91 it will be explained why this might have caused differences in efficiencies.

5.7.2 Experiments to Reduce the Cost of Required Reagents

If the results of the 8 litre experiments in the previous section are scaled to give the amounts of reagents required to concentrate ^{212}Pb and ^{228}Th from 20 litre volumes, the predicted costs can be calculated. In each concentration one Media-Kap filter is expected to be required which costs about £14 (including taxes) and this is the majority of the cost in the case of a ^{228}Th concentration. However for a ^{212}Pb concentration the main cost is the £33 (including taxes) for the 25 grams of DDDC needed to make a saturated solution in 1 litre of 2-octanone.

To try to reduce the cost of concentrating ^{212}Pb from 20 litre volumes an experiment was carried out to determine whether or not a lower concentration solution of DDDC in 2-octanone could be used. This experiment consisted of five, 2 minute ^{212}Pb extractions with an aqueous phase equal to ten times the volume of the organic phase. The efficiencies of these extractions were measured, as usual, by gamma counting however it was found that the most accurate efficiency measurements were determined by examining the amount of ^{212}Pb that disappeared from the aqueous phase during the extraction. These extraction efficiencies, as measured by disappearance, for the different concentrations of DDDC that were used are given in Table 5.10 and show no decrease in extraction efficiency when the DDDC concentration is reduced from a saturated solution, about 2.5% w/v, to 0.5% w/v. It was therefore decided that, in order to reduce costs, extractions from 20 litre volumes would use 0.5% w/v DDDC solutions in 2-octanone.

The breakdown of the costs to concentrate ^{212}Pb and ^{228}Th from 20 litres of SUF eluate when a 0.5% w/v solution of DDDC in 2-octanone is used are shown in Tables 5.11 and 5.12 respectively. It can be seen that the total cost for ^{212}Pb is about £41 (including taxes) whereas the total cost for ^{228}Th is about £24 (including taxes).

Concentration of DDDC in w/v	Extraction Efficiency and Statistical Error
0.5%	75±12%
1.0%	75±09%
1.5%	79±12%
2.0%	74±10%
2.5%	72±10%

Table 5.10: *The extraction efficiencies, as determined by the disappearance of ^{212}Pb activity from the aqueous phase, when using varying concentrations of DDDC and an aqueous phase ten times larger than the organic phase.*

Consumable	Amount	Company	Number	Cost
2-octanone	1 litre	Aldrich	O-470-9	£14
DDDC	5 grams	Aldrich	31, 811-6	£8
Acids/Alkalis	2 litres	-	-	£5
Media-Kap 10 filter	one	Microgon	ME2M-100-18S	£14
			Total	£41

Table 5.11: *The breakdown of the cost of concentrating ^{212}Pb from 20 litres of an SUF eluate as of early 1997, including taxes.*

Consumable	Amount	Company	Number	Cost
kerosene	1 litre	Merck	28673LJ	£4
HDEHP	20ml	Sigma	D 1509	£1
Acids/Alkalis	2 litres	-	-	£5
Media-Kap 10 filter	one	Microgon	ME2M-100-18S	£14
			Total	£24

Table 5.12: *The breakdown of the cost of concentrating ^{228}Th from 20 litres of an SUF eluate as of early 1997, including taxes.*

Conc. of HDEHP	Extraction Eff	Back-Extraction Eff	Overall Eff
0.10M	100±23	10±5	10±5
0.05M	95±17	41±11	39±9
0.04M	99±21	64±18	63±13
0.02M	79±15	89±17	70±14
0.01M	80±12	90±18	72±11

Table 5.13: *The measured results for thorium extractions using HDEHP from 0.5M hydrochloric acid and back-extractions using 5M hydrochloric acid. The organic phase was a varying molarity solution of HDEHP in kerosene. In the extraction the aqueous phase volume was ten times the organic phase volume whereas in the back-extraction the phases had the same volume.*

Conc. of	Extraction:			Back-Extraction:			Overall
HDEHP	V/v	D	E(%)	V/v	D	1-E(%)	Efficiency
0.10M	10	105	91%	1	0.6	62%	56%
0.05M	10	2.7	21%	1	0.12	89%	19%
0.02M	10	0.35	3%	1	0.02	98%	3%

Table 5.14: *The calculated expected efficiencies using values of D, the partition coefficient taken from Figure 5.1 on page 74. The phase volume ratio, V/v, is the volume of the aqueous phase divided by the volume of the organic phase. The efficiency of extracting thorium into the organic phase in both extraction and back-extraction is calculated using Equation 5.1 given on page 70.*

5.7.3 A Final Investigation into the HDEHP System

To try to characterise the HDEHP extraction and back-extraction system a final experiment was performed in which extractions and back-extractions were carried out using a solution of HDEHP in kerosene whose molarity varied from 0.10M down to 0.01M. The extractions were all from an aqueous phase which was made similar chemically to the SUF eluate but which also contained a few kilobecquerels of ^{228}Th and the volume of this aqueous phase was always ten times the volume of the organic phase. The back-extractions were performed using a volume of 5M hydrochloric acid equal to the volume of the organic phase. The acid used in the back-extractions was therefore less acidic than the prescribed 6M hydrochloric acid and this was because it was known that it would be easier to obtain sufficient quantities of radioactively clean 5M hydrochloric acid for large scale extractions and back-extractions.

The extraction, back-extraction and overall efficiencies when using the different molarities of HDEHP in kerosene, as measured by gamma counting, are given in Table 5.13. These results show that reasonable overall efficiencies can be achieved when using a 0.01-0.04M solution of HDEHP in kerosene.

Measurements of the variation of the partition coefficient with hydrochloric acid molarity has been studied in the literature and were reproduced earlier in this chapter in Figure 5.1 on page 74. From this figure, values of the partition coefficient when using 0.10M, 0.05M and 0.02M HDEHP in kerosene can be deduced when the aqueous phase is 0.5M and 5M in hydrochloric acid. The knowledge of these partition coefficients allows expected extraction and back-extraction efficiencies for the experiments whose results are shown in Table 5.13 to be be calculated using Equation 5.1 given on page 70. These calculated, expected efficiencies are shown in Table 5.14 and by comparing them to the measured efficiencies as given in Table 5.13 it can immediately be seen that the measured extraction efficiencies are much higher than expected and the back-extraction efficiencies are generally lower than expected.

It seems that there are two difficulties with this HDEHP system. Firstly, it has been observed that the efficiencies are not very reproducible from one experiment to another especially when using different bottles of HDEHP, eg see Section 5.7.1 on page 88. Secondly, the measured efficiencies are very different from those calculated using published values of partition coefficients.

Both of these difficulties can be explained by the presence of mono-ester impurities within the HDEHP reagent itself. It has been noted previously, in Section 5.3.2 on page 75, that the HDEHP was not purified prior to use and so these impurities were present to a lesser or greater extent in all of the experiments. The literature states that mono-ester impurities in HDEHP have been seen to greatly enhance extraction efficiencies for thorium [Pep60], which is what has been observed. These mono-esters occur to a varying degree in every sample of HDEHP which could explain why the results of experiments using different bottles of HDEHP are not in agreement.

All of the impurities in the HDEHP can be removed using a purification technique given in the literature and then one would expect to see extraction and back-extraction efficiencies similar to those calculated in Table 5.14. Using these calculated values schemes for extracting and back-extracting ^{228}Th from 20 litres of 0.5M hydrochloric acid using pure HDEHP can be suggested, but without the mono-ester impurities the overall efficiency will never be more than about 60%. A known amount of mono-ester could be added to the purified HDEHP before its use to increase the overall efficiency but this would need much further investigation.

5.8 Conclusions

The experimental results of this chapter have led to the development of procedures for the secondary concentration of ^{212}Pb and ^{228}Th from the SUF eluate which have been shown to be unaffected by an initial presence of large quantities of titanium. The procedure for ^{212}Pb and for ^{228}Th both have three stages and these are:

1. A solvent-solvent extraction using a solution of diethylammonium diethyldithiocarbamate (DDDC) in 2-octanone for lead and a solution of di-(2-ethylhexyl)phosphoric acid (HDEHP) in kerosene for thorium.

2. A back-extraction using concentrated nitric acid for lead and 5M or 6M hydrochloric acid for thorium.

3. A final concentration stage using the HTiO ion-exchange to produce a sample which can be measured by a single $\beta - \alpha$ delayed coincidence scintillation counter.

These procedures have been shown to be relatively successful in concentrating kilobecquerel quantities of ^{212}Pb and ^{228}Th from 2 litres of a solution chemically similar to the SUF eluate into a 12 millilitre sample. The first two stages have also been shown to be very efficient at extracting and back-extracting kilobecquerel quantities of ^{212}Pb and ^{228}Th from 8 litres of mock SUF eluate using the Prototype Rig. This rig used the method of large scale batch extractions and mechanical stirrers which were successful in carrying out fast extractions. These techniques have also been verified using amounts of ^{212}Pb and ^{228}Th close to those that it is hoped will be present in SUF eluates that are produced by eluting the HTiO coated SUF membranes after they have been used in an extraction from the heavy water in the SNO experiment.

Unfortunately some final research into comparing measured efficiencies of the HDEHP system with those in the literature have shown some difficulties. The conclusion from this research is that much more work is needed to produce a reliably efficient method for the secondary concentration of thorium from the SUF eluate. In Section 2.5.3 on page 27 it was explained why the most important isotope in the thorium decay chain to assay is ^{212}Pb. This is because ^{212}Pb can be in disequilibrium with ^{224}Ra and ^{228}Th in the heavy water due to sources emanating ^{220}Rn. It was therefore decided that work should cease on developing procedures for the secondary concentration of thorium and instead be directed toward finalising procedures for the secondary concentration of lead.

It can be noted that the amount of ^{228}Th in an SUF eluate can be measured indirectly using the secondary concentration procedures for ^{212}Pb. This can be done by leaving the SUF eluate isolated from radioactive sources for two weeks and then measuring the amount of ^{212}Pb that it contains. After two weeks have passed any ^{212}Pb in the solution will be in radioactive equilibrium with the ^{228}Th. This method will allow the HTiO SUF assay system to measure the amount of ^{228}Th in the heavy water but with much lower statistics than would be expected if the ^{228}Th itself could be concentrated.

In the next two chapters the results of numerous experiments to concentrate ^{212}Pb from 20 litres of mock SUF eluate using the procedures developed in this chapter are detailed.

Chapter 6

The Evaluation of the Solvent-Solvent Extraction Rig

6.1 Introduction

In the last chapter techniques to extract lead from up to 20 litres of 0.5M hydrochloric acid into a 12 millilitre sample which can be measured by a single $\beta - \alpha$ counter were developed. These techniques are in three stages. Firstly, a solvent-solvent extraction using 1 litre of 2-octanone containing 5 grams of diethylammonium diethyldithiocarbamate (DDDC), secondly a back-extraction of the lead into an aqueous phase using concentrated nitric acid and a final concentration stage using HTiO.

The research that is discussed in this chapter is of the design, construction and evaluation of a full scale Solvent-Solvent Extraction Rig to carry out concentrations of ^{212}Pb from 20 litres of SUF eluate. To be used in the SNO experiment the procedures carried out on this rig must meet the following three requirements:

1. The overall efficiency of extracting and concentrating ^{212}Pb from 20 litres of SUF eluate to a 12 millilitre sample must be reproducibly high.

2. The procedural ^{212}Pb background must be low with respect to the extremely low levels of ^{212}Pb that it is hoped will be present in the heavy water of the SNO detector.

3. The total time it takes to carry out the concentration of ^{212}Pb must be less than about one hour to prevent losses in the overall processing time due to decay.

The first version of the Solvent-Solvent Extraction Rig was constructed in the middle of 1996 and the research in this chapter details the evaluation and development of this rig that was carried out during the next year.

6.2 Methods of Evaluating the Solvent-Solvent Extraction Rig

The three aims of the Solvent-Solvent Extraction Rig detailed in the introduction to this chapter are evaluated in the rest of this chapter using both stable lead and the ^{212}Pb sources that were manufactured to be free from any ^{224}Ra and ^{228}Th in the experiments detailed in Chapter 4. Efficiencies and backgrounds were therefore measured both by analysing samples for stable lead and for ^{212}Pb activity. The stable lead measurements were carried out by Mr C.Jackson of the Geography Department at Oxford University using Atomic Emission Spectroscopy. The ^{212}Pb measurements were carried out using the $\beta - \alpha$ delayed coincidence scintillation counters whose operation was described in Section 3.2.1 on page 30 with more details in Appendix D.

In order to evaluate the ^{212}Pb background of the rig, as compared to that required to measure the neutral current background in the SNO experiment, a ratio, $\mathcal{R}$, is defined. This is a comparison of the measured background to the procedures to concentrate ^{212}Pb, as carried out by the Solvent-Solvent Extraction Rig, to the expected ^{212}Pb signal.

In Section 3.2.1 on page 29 it was explained why it is hoped that the amount of ^{212}Pb in the 1000 tonnes of heavy water in the SNO detector will produce less than 1 decay per day per tonne. In a 15 hour assay with a flow rate of 200 litres per minute, as was suggested in Chapter 3, about 180 tonnes of heavy water can be processed by the HTiO SUF assay system. The amount of ^{212}Pb expected to be in the 20 litres of SUF eluate after such an assay can therefore be estimated to be that which would produce about 2 counts per hour on the $\beta - \alpha$ counters if it were all concentrated into a 12 millilitre sample.

Hence to determine $\mathcal{R}$, the background to signal ratio, the measured background for any full ^{212}Pb concentration from 20 litres was divided by the overall efficiency and then also divided by 2 $\beta - \alpha$ counts per hour. To be useful to the SNO experiment this value of $\mathcal{R}$ must be shown to be less than 1.

6.3 The Original Design of the Solvent-Solvent Extraction Rig

6.3.1 Introduction

The original design for the Solvent-Solvent Extraction Rig which indicates the positions of all of the individual components and valves is shown in Figure 6.1.

In the rest of this chapter the details and results of numerous experiments designed to evaluate the Solvent-Solvent Extraction Rig are given. Some experimental results led to adaptations and alterations of the original design producing two other distinct versions of the rig that were eventually used. Hence, the original version is labelled Version A, and the next two are labelled Versions B and C respectively. It should be noted that these other versions were not newly constructed rigs but upgrades of the original version.

In the following sections the individual components of the original version (Version A) of the Solvent-Solvent Extraction Rig are discussed and a description of the procedure to concentrate ^{212}Pb using this version of the rig is given.

6.3.2 The Main Reaction Vessels

The two main reaction vessels of the Solvent-Solvent Extraction Rig are shown in Figure 6.1 and are labelled M1 and M2. The first of these, M1, is a 20 litre mixer in which the initial solvent-solvent extraction is carried out. The second, M2, is a 2 litre mixer in which the back-extraction is performed. The use of two mixers to perform large extractions and back-extractions was verified using the Prototype Rig which was described in the last chapter in Section 5.5.6 on page 83. The use of 2-octanone required

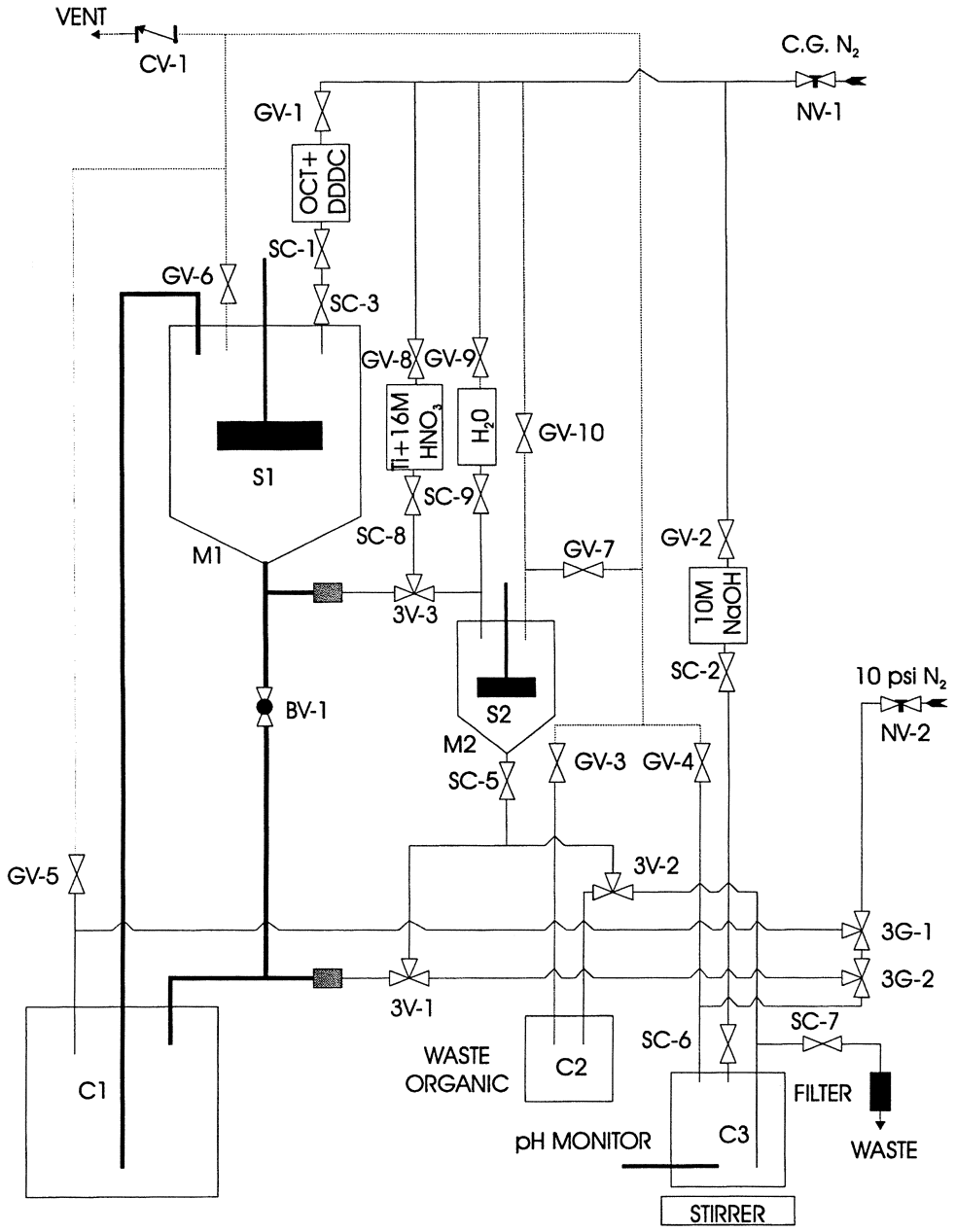

Figure 6.1: *The original design (Version A) of the Solvent-Solvent Extraction Rig. The two inputs to the diagram are for nitrogen cover gas and pressurised nitrogen, the output is for waste fumes. The thick lines show half inch diameter pipework whereas the thin lines show quarter inch diameter tubing. The 20 litres of SUF eluate starts in vessel C1 and is then forced into vessel M1, the large mixer, where the solvent-solvent extraction is carried out. The organic phase passes to M2 which is the small mixer for the back-extraction. The final HTiO stage is carried out in container C3 and the waste organic phase is drained to vessel C2 for disposal. The individual valves are labelled according to their type: needle valve (NV), ball valve (BV), gas valve (GV), three way gas valve (3G), stop cock (SC), three way liquid valve (3V) and check valve (CV).*

that both mixers be made of fluorinated plastics. They also had to be sealed to the air since it was known that there is a ^{212}Pb background due to ^{220}Rn emanating from the concrete in walls. (See Appendix F for more details about airborne ^{212}Pb contamination.)

The smaller mixer, M2, was purchased as a standard 2 litre Teflon FEP separating funnel from Fisher[1] but the larger mixer for the extraction from 20 litres of liquid had to be constructed specially from sheet stainless steel which was then coated with Halar (a fluorinated plastic) by Plastic Coatings[2].

This coating of the 20 litre mixer was not translucent which meant that it could not be used to perform careful phase separations. The careful phase separation of the 1 litre of organic phase and the 20 litres of aqueous phase after the solvent-solvent extraction was therefore designed to be carried out in two stages. Firstly, after leaving the phases to separate for a few minutes, 19 litres of liquid is drained from M1 to C1 using valve BV-1 as shown in Figure 6.1 and then the remaining 2 litres of liquid is drained to M2 using valve 3V-3. Since the 2 litre mixer, M2, is translucent a careful separation of the two phases can be made using the stop-cock SC-5. The 1 litre of aqueous phase transfered to M2 along with the organic phase can then be added to the 19 litres drained to C1 using valve 3V-1.

These two mixers required stirrers, labelled S1 and S2. This introduced a further difficulty since these stirrers needed seals resistant to 2-octanone and air tight. This was accomplished by purchasing the PTFE bearings made for the stirrer shafts and then adapting the lids of the two mixers to accept this fitting. These stirrers and bearings were purchased from Safelab[3].

Finally, it can be seen from Figure 6.1 that the bottom of the 2 litre mixer, M2, can be attached (via a number of valves) to a source of pressurised nitrogen gas. This is to allow the back-extraction mixing to be performed as it was in the Prototype Rig which was discussed in the last chapter in Section 5.5.6 on page 83. This mixing method bubbles gas through the lower acidic solution into the upper organic phase. This method was found to be a very efficient method for mixing a small volume of acid with a large volume of organic phase.

6.3.3 The Movement of Liquids around the Rig

In order to minimise contamination by airborne ^{212}Pb, the entire movement of liquids around the rig was designed to be carried out using sealed tubing and pipe work which drained under gravity.

One of the main requirements for ^{212}Pb concentrations carried out on the rig is that they have to be completed in a time short compared to the 10.6 hour half-life of ^{212}Pb. In Section 5.5.6 on page 83 of the last chapter, experiments using the Prototype Rig showed that to obtain short processing times it is important that the 20 litre mixer is filled and drained quickly. It was decided that the cheapest way of doing this, since fluorinated pumps are very expensive, would be to fill the 20 litre mixer using nitrogen pressure and to drain it using gravity. It was clear that the draining time is a function of the drainage pipe of the mixer and so a calculation was made which showed that for a 20 litre vessel to drain under gravity in only a few minutes a half inch diameter drainage pipe is required. This calculation is detailed in Appendix E.

Therefore, as can be seen from Figure 6.1, the 20 litre mixer is designed with a half inch drainage pipe. The Teflon valve with a half inch bore used to control this draining without slowing down the drainage rate (BV-1) was purchased from a specialist supplier, Production Techniques[4]. The part of the rig which deals with the back-extraction was designed to use quarter inch tubing to reduce costs since the volumes that are moved around this part of the rig are much smaller and so draining times are not as

[1]Fisher Scientific UK, Bishop Meadow Road, Loughborough, Leicestershire, LE11 ORG

[2]Plastic Coatings Limited, Southern Division, Woodbridge Industrial Estate, Guildford, Surrey, GU1 1BG

[3]Safelab Systems Limited, 2 Vines Industrial Centre, High Street, Nailsea, Bristol, BS19 1BW

[4]Production Techniques Limited, 13 Kings Road, Fleet, Hants, GU13 9AU

important. The valves for the quarter inch tubing were purchased as standard items from Cole Palmer[5]. The half inch pipe, valve and connections all used compression fittings whereas the quarter inch tubing system used flare fittings and so the two systems were joined using standard thread pipe adapters.

6.3.4 Details of the Final HTiO Stage

Since it had already been decided that pressurised nitrogen gas was going to be used on the rig both to fill the large mixer, M1, and to perform the mixing in the back-extraction it was also decided to use nitrogen pressure to push the back-extracted solution, after the precipitation of the HTiO in the final HTiO concentration stage, through a 0.2 micron Media-Kap 10 filter. It can be seen from Figure 6.1 that the solution back-extracted in M2 can drain into vessel C3. There titanium will be precipitated in solution as HTiO by raising the pH of the solution to between 8 and 9 using the 10M sodium hydroxide from a stock tank on the rig.

In Section 5.5.3 on page 81 this HTiO stage has been shown to be very efficient at extracting ^{212}Pb. It was also shown that when three samples of 4 millilitres of 0.5M hydrochloric acid were used, for a few minutes each, most of the ^{212}Pb could be eluted from the filter. Experiments in Section 5.7.1 on page 86 which used the $\beta - \alpha$ counters showed that 0.5M hydrochloric acid can be too acidic for the scintillator cocktail, so instead of using three 4 millilitre samples to elute the filter, it was decided to use two 4 millilitre samples for 8 minutes each.

6.3.5 The Addition of Reagents

Most of the reagents used to concentrate the ^{212}Pb are placed in stock tanks on the rig and are connected to a nitrogen cover gas to prevent the addition of air with the reagents. However, special treatment was required for DDDC solutions since the reagent can decompose on standing. A way was needed to allow the addition of the organic reagent to the large mixer, M1, which would not involve opening the rig up to the air. To accomplish this task two Teflon vessels were purchased from Techmate Limited[6]. The design of these vessels is shown in Figure 6.2. They have a 1 litre volume, a drain port at the bottom controlled by a stopcock and a port for the nitrogen cover gas at the top. The solution of DDDC in 2-octanone is made in one of these vessels and added to M1 through a further stopcock, SC-3, as is shown in Figure 6.1.

6.3.6 The Total Cost of the Rig

The components needed to construct the initial version of the Solvent-Solvent Extraction Rig were all purchased, as discussed in the preceding sections, and the costs incurred are shown in Table 6.1. The total cost of constructing the Solvent-Solvent Extraction Rig was £3640 (including taxes).

[5]Cole Palmer Instrument Company Limited, PO BOX 22, Bishops Stortford, Hertfordshire, CM23 3DX

[6]Techmate Limited, 10 Bridgeturn Avenue, Old Wolverton, Milton Keynes, MK12 5QL

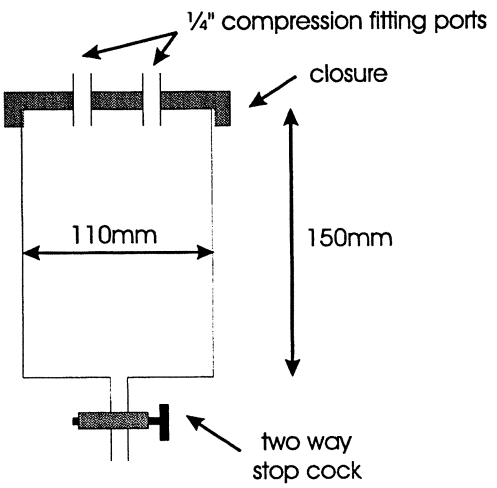

Figure 6.2: *The 1 litre container for dispensing the solution of DDDC in 2-octanone to the 20 litre mixer.*

Item	Cost	Item	Cost
20 litre mixer	£330	2 litre mixer	£190
Other Containers	£110	Teflon Stock Vessels	£500
1/2" Valves and piping	£760	1/4" Valves and tubing	£620
Stirrers and bearings	£340	Magnetic Stirrer	£200
pH meter and probe	£200	Gas regulators	£300
Stirrer motors	£90		

Table 6.1: *The breakdown of the costs of the Solvent-Solvent Extraction Rig as purchased in early 1996, including taxes.*

6.3.7 Overview of the Procedure to Concentrate ^{212}Pb

The procedures used to extract and concentrate ^{212}Pb from 20 litres of SUF eluate using Version A of the Solvent-Solvent Extraction Rig are given below.

Firstly, the 20 litres of SUF eluate which starts in vessel C1 is forced up into the 20 litre mixer, M1, using 10 psi nitrogen gas. A 1 litre solution of 2-octanone containing 5 grams of DDDC (a 0.5% w/v solution) is then made up in its special container as shown in Figure 6.2 and attached to the rig as shown in Figure 6.1 so that the organic phase can drain into M1.

The solvent-solvent extraction is then carried out by mixing the 1 litre of DDDC solution and the 20 litres of SUF eluate in M1 for 2 minutes using stirrer, S1. After standing for 10 minutes the two phases are separated in the two stages that were discussed in Section 6.3.2 on page 96. The first stage drains 19 litres of liquid directly from M1 to C1 and the second stage is the fine separation of the remaining 2 litres which is carried out in the translucent mixer, M2. This extraction stage is expected to take about 20 minutes to complete.

The back-extraction is performed in M2 by the addition of 0.1 litres of concentrated nitric acid which also contains 3 milligrams of titanium for use in the final HTiO stage. The concentrated acid and the 1 litre of DDDC solution is then mixed for 2 minutes by passing nitrogen gas at 10 psi into the bottom of M2. The concentrated acid is then be diluted to 1 litre using ultra-pure water while continuing to mix for 10 minutes using both the nitrogen gas and stirrer, S2. After leaving the solutions in M2 to stand for 5 minutes the aqueous phase is then drained into vessel C3 to perform the final HTiO concentration stage. This back-extraction stage is expected to take about 10 minutes to complete.

The precipitation of the titanium in the final HTiO stage is completed by adding 10M sodium hydroxide from a stock tank on the rig to the back-extracted solution in C3 until the pH of the solution is measured to be between 8 and 9. Once this is achieved the solution is forced through a Media-Kap 10 filter by pressurising vessel C3 with nitrogen gas. Any lead extracted onto the HTiO is held up on the filter and it is eluted back into solution by using two 4 millilitre samples of 0.5M hydrochloric acid left in the filter for 8 minutes each. A 12 millilitre sample for a $\beta - \alpha$ counter is made from 10 millilitres of 0.5M hydrochloric acid containing these elutions and 2 millilitres of ultra-pure water. It is expected that it will take about 20 minutes to produce a $\beta - \alpha$ source from the 1 litre of acid using the HTiO stage.

The expected overall processing time needed to extract and concentrate lead from 20 litres of SUF eluate to a single $\beta - \alpha$ counting sample is about 50 minutes.

6.4 Details of Experiments Using Version A of the Rig

6.4.1 Description of Experiments

Two experiments were carried out using Version A of the Solvent-Solvent Extraction Rig, shown in Figure 6.1 on page 95. Both of these experiments started from the same 20 litres of mock SUF eluate in vessel C1. This mock SUF eluate used 20 litres of ultra-pure water made to be 0.5M in hydrochloric acid and to contain about 2 grams of titanium.

In the first experiment, experiment SSR1, 1 milligram of stable lead was added to the 20 litres of mock SUF eluate and an entire lead concentration was carried out. The final sample that was produced was analysed for both stable lead and for ^{212}Pb to determine the efficiency and the background of the procedure. Unfortunately it was found that the Media-Kap filters blocked and each one could only filter about a third of the back-extracted solution. Three filters were therefore used to process the entire volume and these were eluted producing 32 millilitres of 0.5M hydrochloric acid.

A second experiment, experiment SSR2, used the same 20 litres of mock SUF eluate after a further 100 milligrams of stable lead had been added and performed just the solvent-solvent extraction. Samples of the 20 litres were taken before and after the extraction for stable lead analysis to determine the stable lead efficiency of the extraction stage.

6.4.2 Results of Experiments

The amount of stable lead that was found in the final eluate of experiment SSR1 was 77±3 micrograms. Since 1 milligram of lead had been initially added to the 20 litres this gives an overall rig efficiency of just 7.7±0.3%. In experiment SSR2 the 20 litres of mock SUF eluate initially contained 5.1±0.1 parts per million (ppm) of stable lead and after the extraction this was reduced to 4.6±0.1ppm. This means that the extraction efficiency in experiment SSR2 was only 10±3% which explains why the overall efficiency measured in experiment SSR1 was so low.

The ^{212}Pb background for experiment SSR1 was found to be quite high at 30 counts per hour. Together with the very low efficiency of this experiment this gives a value for $\mathcal{R}$ (as defined in Section 6.2 on page 94) of around 160. However it should be noted that the ^{212}Pb in the final eluate contained no observable ^{224}Ra or ^{228}Th, which means that the background could have been entirely due to airborne ^{212}Pb contamination.

The time needed to concentrate ^{212}Pb from the 20 litres in experiment SSR1 was 97 minutes which was longer than the expected 50 minutes due to the unforeseen problems in the HTiO stage.

6.4.3 Conclusions and Design Improvements

The overall efficiency of Version A of the Solvent-Solvent Extraction Rig was measured to be less than 10% which is very poor when compared to the 80% which had been measured using the Prototype Rig of the last chapter, see Section 5.5.6 on page 83. The source of this problem was located to be in the extraction stage. The reason for this poor extraction efficiency was suspected to be due to inadequate mixing of the two phases in M1 and so the stirrer speed was examined.

The stirrer speed for the 8 litre Prototype Rig was about 400 revolutions per minute, however this motor had failed before the construction of the Solvent-Solvent Extraction Rig and a new motor was used. It was found that this new motor was not the same as the first, as had been assumed, since it had a maximum speed of only 220 revolutions per minute. It was decided that this speed was too low for good mixing and so a new motor with a maximum speed of 2000 revolutions per minute was purchased and mounted in its place. It was found experimentally that this motor produced much more effective mixing and that the phases separated after standing for only five minutes, instead of 10 minutes.

Apart from the low extraction efficiency, the other difficulty that needed to be resolved was the practical one of why the Media-Kap filters kept blocking. It was thought that this problem could have been due to the high pH of the solution which was pumped through the filter since it is known that the filters are damaged by solutions which have a pH greater than about 11. The intention was to raise the pH of the solution to between 8 and 9 but it was very difficult to accurately control the pH using 10M sodium hydroxide and it in fact ended being above pH 10.

Therefore, it was decided that a known quantity of 10M sodium hydroxide would be added to vessel C3 via a syringe to raise the pH to about 3 and then final adjustments to the pH would be made using 1M sodium hydroxide added from a stock tank. It was observed that the back-extraction seemed to occur quite quickly with 100 millilitres of concentrated acid and so it was decided that less acid would be used in future experiments. It was also decided to add the titanium directly to vessel C3, via a syringe, rather than to the nitric acid before the back-extraction in order to avoid some unnecessary possible complications such as the settling of the titanium in the stock tank.

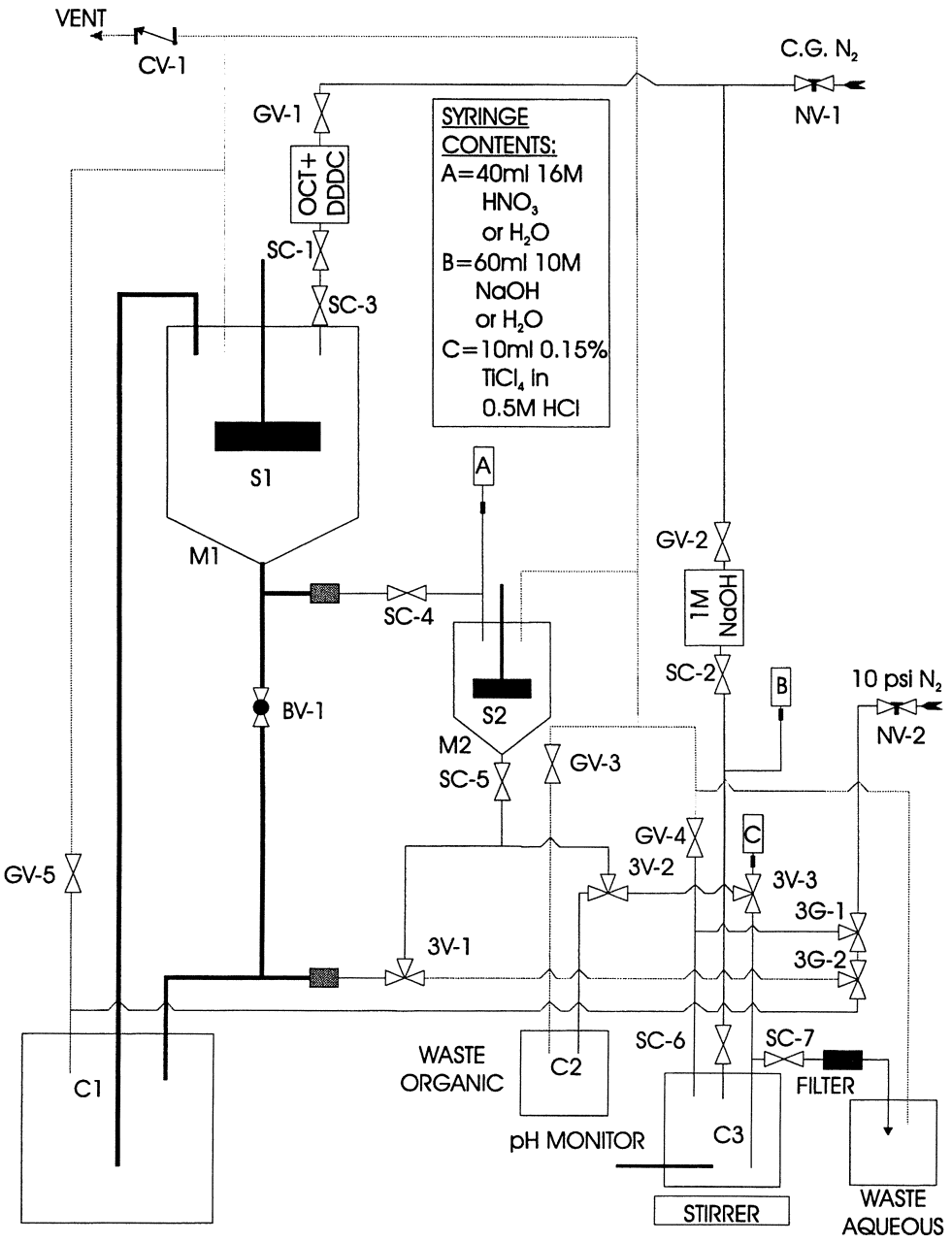

Figure 6.3: *Version B of the Solvent-Solvent Extraction Rig. The main differences to Version A are the syringe ports labelled A, B and C. Through these ports different chemicals can be added directly into vessels M2 and C3 to perform the back-extraction and the HTiO extraction.*

A further experimental concern arose related to the addition of the concentrated nitric acid through the valve labelled 3V-3 on Figure 6.1. It was observed that some of the concentrated nitric acid could end up in vessel M1 during the procedure and so the tubing was altered so that the nitric acid could be added, via a syringe, directly into the second mixer, M2. Finally, for safety purposes, some of the gas valves were removed so that it would be impossible to pressurise M1 or M2 by accident.

All of these alterations were made to the existing version of the rig and a new version, Version B was produced which is shown in Figure 6.3. The procedure to carry out a ^{212}Pb concentration from 20 litres of SUF eluate using Version B of the rig is very similar to that used on Version A.

One main difference with the procedure for Version B is the use of only 40 millilitres of concentrated nitric acid in the back-extraction of the lead from the DDDC solution which is added, via a syringe, directly to M2 rather than from a stock tank. Also, the titanium needed for the final HTiO stage is no longer added together with the nitric acid but is added in the form of 0.1 millilitres of a 15% titanium chloride solution directly to the 1 litre of back-extracted solution after it has drained to vessel C3. Finally, the pH of the solution in vessel C3 is increased firstly by adding a fixed quantity of 10M sodium hydroxide to raise the pH to about 3 and then by carefully adding 1M sodium hydroxide to adjust the pH to be between 8 and 9.

6.5 Details of Experiments Using Version B of the Rig

6.5.1 Description of Experiments

The first experiment of the two that were carried out using Version B of the Solvent-Solvent Extraction Rig was designed to test the efficiency, background and practicality of just the final HTiO stage. The second experiment tested the ^{212}Pb background and the stable lead efficiency of the entire process and the efficiency of just the extraction stage. The details of these experiments are given below and the results are shown in Table 6.2.

- Experiment SSR3:

  Three runs were performed sequentially for this experiment and each of these runs started from 40 millilitres of 16M nitric acid containing 0.1 milligrams of stable lead. This was diluted to 1 litre with ultra-pure water and then the HTiO concentration was carried out. After each run the final eluate was measured for stable lead and in the last run it was also analysed for ^{212}Pb. These eluates are labelled SSR3a, SSR3b and SSR3c respectively.

- Experiment SSR4:

  In this experiment three runs were performed sequentially, the first two runs tested all of the stages of the rig whereas the final run just tested the initial solvent-solvent extraction. The solvent-solvent extractions were carried out using 1 litre of a 0.5% w/v solution of DDDC in 2-octanone.

  The first run used a completely blank 20 litres of mock SUF eluate, as in experiment SSR1. The second run used the same 20 litres of mock SUF eluate but prior to extraction 0.1 milligrams of stable lead was added so that an efficiency could be determined. For these first two runs the final eluates (labelled SSR4a and SSR4b) were analysed for both ^{212}Pb activity and stable lead. In the third run a further 100 milligrams of stable lead was added to the same 20 litres of mock SUF eluate and a solvent-solvent extraction was performed. Samples of the 20 litres were taken before and after the extraction for stable lead analysis to determine the extraction efficiency.

6.5.2 Results of Experiments

These experiments showed that the pH of the solution in the HTiO stage could be far more easily controlled using Version B of the Solvent-Solvent Extraction Rig than had been the case with Version A and just one filter was needed to process the total neutralised volume for each run in experiment SSR3 and the first run of experiment SSR4. Unfortunately, the blocking of the filters returned in the second overall run of experiment SSR4 and three filters were once again needed. It was noted that the pH of the solutions in all of the runs was in the range 10.6 to 10.9 when it was forced through the filter and this included the last run where three filters were needed. Although all of the solutions had a pH above that

Name of Eluate	Description of Eluate	Initial Activity in cph of			Stable Lead	
		^{212}Pb	^{224}Ra	^{228}Th	Added	Recovered
SSR3a	The eluate after HTiO stage only	-	-	-	100μg	94±1μg
SSR3b	The eluate after HTiO stage only	-	-	-	100μg	96±1μg
SSR3c	The eluate after HTiO stage only	15	6	4	100μg	100±1μg
SSR4a	The eluate after all 3 stages	40	24	12	0μg	14±2μg
SSR4b	The eluate after all 3 stages	15	12	12	100μg	82±4μg
SSR5	The eluate after HTiO stage only	7	1	0.3	-	-

Table 6.2: *The stable lead and activity measurements for the elutions of the Media-Kap filters used in experiments SSR3, 4 and 5. The three runs of experiment SSR3 were identical runs with the same amount of stable lead added to each run. The two runs shown for experiment SSR4 both used the overall procedure to concentrate lead from the same 20 litres but 100 micrograms of stable lead was added before the extraction in the second run. Experiment SSR5 was a measurement of the background to the HTiO stage after some cleaning and alterations of the rig.*

which had been intended the fact that they were all so similar indicates that the high pH of the solutions is probably not the reason for the filters blocking.

The results of experiment SSR4 showed that the total time needed to concentrate lead from 20 litres of SUF eluate using Version B of the rig was about 65 minutes, whether or not there was a problem of filters blocking. This is a reduction of about a third from the time that it took using Version A of the rig and is quite close to the original 50 minutes that was expected.

The stable lead and activity measurements for the elutions of the Media-Kap filters used in experiments SSR3 and 4 are given in Table 6.2. The stable lead results for the three runs of experiment SSR3 show that the efficiency of the HTiO stage is virtually 100%, within errors. The fact that more lead is recovered on later runs is due to a small amount of stable lead being carried over from one run to another because the apparatus was not rinsed sufficiently between runs.

By assuming the same efficiency for the two runs in experiment SSR4, the carry over of stable lead between the runs can be determined to give an overall efficiency for the concentration of lead using Version B of the rig of 80±10%. In the final run of experiment SSR4 the mock SUF eluate was found initially to contain 6.2±0.1ppm lead and after a single solvent-solvent extraction this was reduced to 1.0±0.1ppm, thus indicating an extraction efficiency of 84±4%. The back-extraction efficiency and the efficiency of the final HTiO stage must therefore have both been nearly 100%.

The results for the initial activity of ^{212}Pb in the eluates show similar amounts to the 30 counts per hour which were measured using Version A of the rig. However, since the efficiency of the overall process has increased this lowers the background to signal ratio, $\mathcal{R}$, (as defined in Section 6.2 on page 94) from 160 when using Version A to around 30 when using Version B. Unfortunately, the radioactive contamination that was found when using Version B contained large amounts of both ^{224}Ra and ^{228}Th as well as ^{212}Pb and so it could no longer be attributed purely to ^{212}Pb airborne contamination.

6.5.3 Conclusions and the Cleaning of the Rig

It is clear from the results that some of the problems incurred when using Version A of the rig were resolved when using Version B. Firstly, the total time needed to concentrate lead from 20 litres of SUF eluate into a 12 millilitre sample was reduced by a third to an acceptable length of time. Secondly, the HTiO stage was, although still not ideal, much easier to control and the blocking of filters was reduced. Thirdly, the overall efficiency for concentrating the lead using Version B of the Solvent-Solvent Extraction

Rig was now, as originally expected, about 80%.

The outstanding problem of the rig was now one of a long-lived component to the radioactive contamination. This contamination must have been introduced during the rig alterations since they were not present when Version A of the rig was evaluated. The source of the ^{224}Ra and ^{228}Th contamination had to be physically near the HTiO stage because, unlike the solvent-solvent extraction stage, the HTiO stage extracts radium and thorium as well as lead. It was therefore suspected that the background sources were in the tubing and connectors added during the rig alterations which are located near vessel C3.

An attempt was made to clean the rig which involved leaving it filled with 0.5M hydrochloric acid for one week and replacing all of the non-Teflon tubing, connectors and valves. There were also some further alterations to the rig. Firstly, the addition of titanium was changed so that it could be added through the same syringe port as the 10M sodium hydroxide. Secondly, a 3-way valve was introduced so that the 16M nitric acid could be added directly to M2 without any losses in tubing.

After these minor alterations, and the attempted cleaning of the rig, the HTiO stage was tested for background activity by doing a single experiment, experiment SSR5. This was performed in the same way as experiment SSR3 but no stable lead was added since the efficiency had been seen to be reproducibly high. The fitted $\beta - \alpha$ measurements of the produced eluate showed a rig background of about 7 counts per hour ^{212}Pb, about 1 count per hour ^{224}Ra and about 0.3 counts per hour ^{228}Th. These results are shown in Table 6.2 for a comparison to the results prior to the cleaning.

These results show that the acid soak and the replacement of non-Teflon components reduced ^{212}Pb background by a factor of two and, more importantly reduced the background due to ^{224}Ra and ^{228}Th by a much larger factor. The remaining excess of ^{212}Pb activity when compared to that of ^{224}Ra and ^{228}Th means that the major source of activity is either due to airborne ^{212}Pb contamination or it is due to some thorium embedded in the material making up the rig which itself is emanating ^{220}Rn. The remaining radium and thorium activity could have been due to contaminated reagents or, more probably, it could have been some residual contamination of components of the rig.

Experiment SSR5 showed that the pH of the solution in the HTiO stage could be more easily controlled by adding the low molarity alkali via a syringe directly into C3 rather than from a stock tank. This minor alteration to the rig together with the other alterations made to Version B of the rig between experiments SSR4 and SSR5 led to the production of a new version of the rig, Version C, and this is shown in Figure 6.4.

The procedure to concentrate ^{212}Pb from 20 litres of SUF eluate using Version C is very similar to that when using Version B as the only difference is that all of the reagents needed in the final HTiO stage are added to vessel C3 directly through the same syringe port.

6.6 Details of Experiments Using Version C of the Rig

6.6.1 The First Set of Experiments Performed on Version C

The experiments that used Version B of the Solvent-Solvent Extraction Rig showed that the HTiO stage had ^{224}Ra and ^{228}Th as well as ^{212}Pb contamination. Most of this long-lived contamination was reduced by the cleaning of the rig prior to experiment SSR5 but some residual contamination remained. The objectives of this set of experiments were to eliminate the long-lived activity from the rig and to reduce further the ^{212}Pb background.

The first two experiments performed on Version C of the Solvent-Solvent Extraction Rig (experiments SSB1 and SSB2) investigated whether the nitrogen gas supply or container C3 were sources of contamination. These experiments were performed using lower strength chemicals than are needed to perform a back-extraction and so the next experiments (experiments SSB3, SSB4 and SSB5) investigated the effect of using the full strength chemicals and also of any possible contamination from the mixing vessel M2.

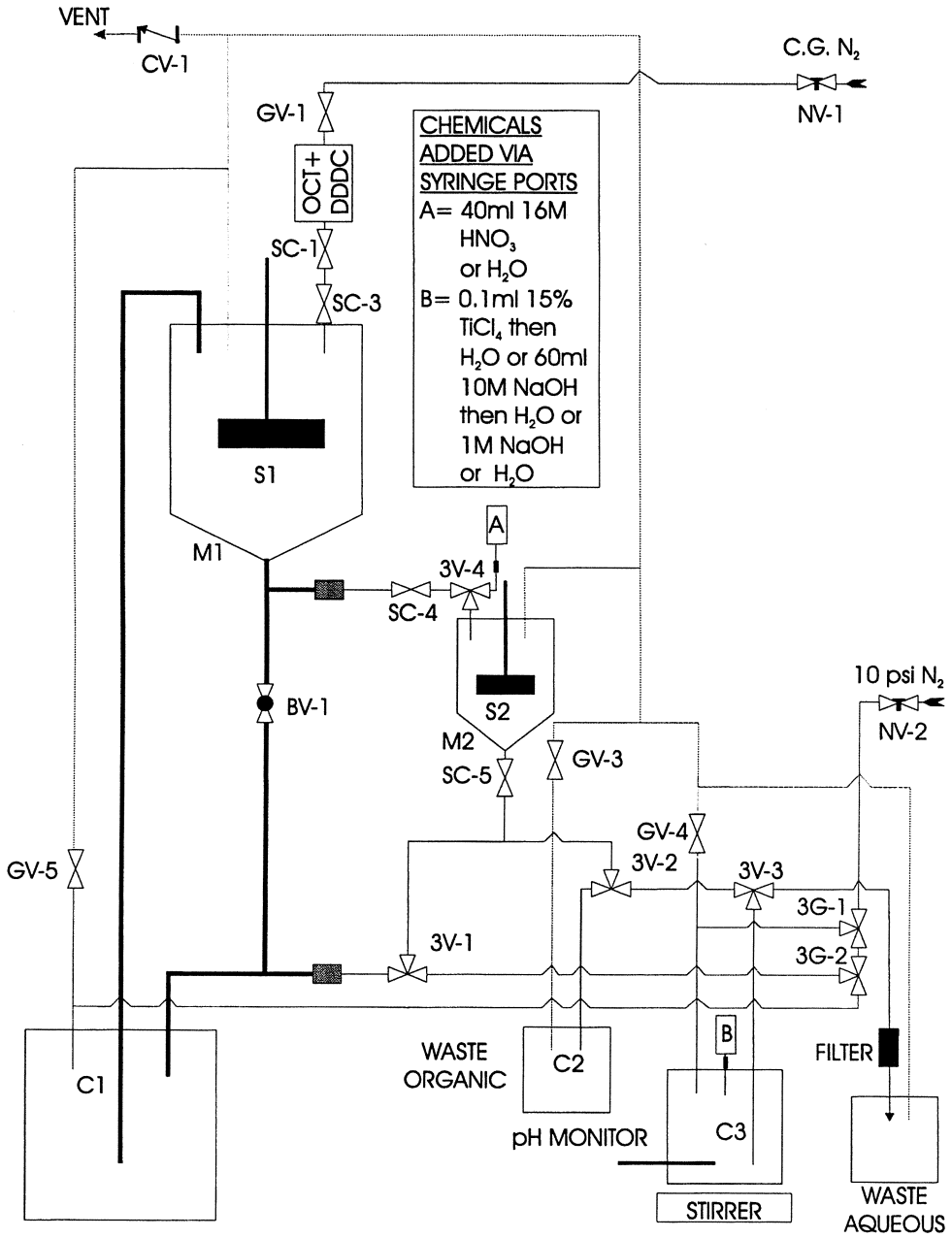

Figure 6.4: *Version C of the Solvent-Solvent Extraction Rig. In this version all of the stock tanks have been removed and all reagents apart from the organic phase are added via syringes which can be attached at just the two ports labelled A and B in the diagram.*

Sample Name	Summary of Experiment:				Activity of sample for: in cph		
	Starting Container	Pumping Gas	Reagents Used	Reagent Addition	^{212}Pb	^{224}Ra	^{228}Th
SSB1(1)	old C3	air	less	normal	3.5±0.5	1.3±0.3	<0.3
SSB1(2)	new C3	air	less	normal	1.8±0.4	<0.4	<0.2
SSB2(1)	old C3	N_2	less	normal	2.2±0.4	<0.7	<0.2
SSB2(2)	new C3	N_2	less	normal	<1.2	<0.3	<0.2
SSB3(1)	new C3	N_2	less	normal	1.4±0.3	<1.0	<0.2
SSB3(2)	new C3	N_2	normal	normal	<1.3	<0.3	<0.1
SSB3(3)	M2	N_2	normal	normal	1.5±0.3	<0.8	<0.1
SSB3(4)	M2	N_2	normal	normal	1.3±0.3	<0.6	<0.2
SSB4(1)	M2	N_2	normal	clean	1.2±0.3	<0.7	<0.2
SSB4(2)	M2	N_2	normal	clean	1.0±0.3	<0.8	<0.2
SSB5(1)	M2	N_2	clean	clean	1.3±0.3	<0.8	<0.3

Table 6.3: *Results of the first set of experiments performed on Version C of the Solvent-Solvent Extraction Rig which measured the backgrounds of the HTiO stage. The rates shown are in counts per hour and were estimated from the number of counts recorded by the $\beta - \alpha$ counters in 24 hour time slots at different times after the experiment, as described in Appendix D. In the experiments which started in vessel M2 only the new C3 vessel was used to carry out the HTiO stage. The normal method of adding reagents was to reuse pipettes but in the last three runs only new, clean pipettes were used. Also, in the final run the reagents were freshly made up and can therefore be assumed to be free from contamination.*

The details of these experiments are given below and are summarised along with the measured ^{212}Pb backgrounds in Table 6.3. Unless stated otherwise, all the runs in a particular experiment were performed in the order they are listed with a negligible time delay between them.

- Experiments SSB1 and SSB2

  The first run of experiment SSB1 used the old C3 container which was left sealed with 1 litre of ultra-pure water for a day so that any unsupported ^{212}Pb would have time to decay. To this container 5 millilitres of 16M nitric acid and 0.1 millilitres of a 15% w/v titanium tetrachloride solution was added and the pH of the solution adjusted using 1M sodium hydroxide. This solution was then forced through a Media-Kap filter using a peristaltic pump which fed air into vessel C3 at about 200 millilitres per minute. This air was taken directly from the room in which the experiments were being conducted and air could only enter this room through dust filters. This Media-Kap 10 filter was eluted using two samples of 4 millilitres of 0.5M hydrochloric acid to produce sample SSB1(1) for measurement on a $\beta - \alpha$ counter. The same procedure was carried out using a new C3 container to produce sample SSB1(2).

  In experiment SSB2 a similar procedure was carried out except that, instead of pumping air into the C3 container, the nitrogen gas supply was connected and 10 psi pressure used to force the solution through the Media-Kap filter. Sample SSB2(1) was produced using the old C3 container and sample SSB2(2) was produced using the new C3 container.

  The results in Table 6.3 for experiments SSB1 and 2 show that the old C3 container gave a contamination of ^{212}Pb which was reduced by about a count per hour when using the new C3 container. It was therefore decided that the old vessel should be discarded and the new C3 container used in its place.

The difference between the ^{212}Pb activities in samples SSB1 and SSB2, shows that using air to push the liquid through the filter, rather than nitrogen gas does add to the ^{212}Pb background, as one would expect if there is an airborne ^{212}Pb contamination.

- Experiments SSB3, SSB4 and SSB5

  These experiments used only the new C3 container. In each experiment, 1 litre of acid was produced and the HTiO concentration stage was carried out. Sample SSB3(1) was prepared using an initial acid concentration which was lower than that expected to be produced by a back-extraction, whereas sample SSB3(2) used the correct amount of acid. After a few hours two more samples were prepared using full strength chemicals but starting in M2 and transferring liquids into the new C3 container before carrying out the HTiO concentration. Concerns were raised over the cleanliness of the pipettes that were being used and so in experiment SSB4 samples were prepared using clean, disposable syringes and two HTiO extractions were completed. A further concern was that the acids and alkalis may have become contaminated and so in a final experiment, experiment SSB5, a sample was produced using freshly prepared reagents and clean pipettes.

  The results for experiments SSB3, 4 and 5 are shown in Table 6.3 and can all be seen to give similar levels of activity which indicates that the source of this remaining activity is not due to the acid or alkali reagents or the pipettes that were used. The ^{212}Pb background to the HTiO stage, as measured in these experiments, was less than 2 counts per hour which shows a reduction from the 7 counts per hour which was measured in experiment SSR5 and given in Section 6.5.3 on page 104. This reduction was achieved primarily by replacing the C3 container which at some point must have become contaminated with ^{228}Th.

6.6.2 The Second Set of Experiments Performed on Version C

The purpose of this set of experiments was to evaluate the overall operation of Version C of the rig while continuing to try to lower backgrounds and increase efficiencies. The efficiencies in these experiments were not normally measured using stable lead since the analysis for stable lead carried out at Oxford took at least a week to produce results and this did not allow the analysis of one experiment before starting another. Instead, sources of ^{212}Pb manufactured free from any ^{224}Ra and ^{228}Th as detailed in Chapter 4 were added to the 20 litres before an extraction. Efficiencies were calculated by measuring the activity of the ^{212}Pb source itself and the ^{212}Pb activity recovered in the final 12 millilitres. Listed below are the details and results of experiments which tested the overall procedure of the rig.

- Experiments SSC1 and SSC2

  For both of these experiments ^{212}Pb was concentrated from 20 litres of a mock SUF eluate into 12 millilitres.

  In experiment SSC1, the first run used a blank 20 litres of mock SUF eluate to allow a measurement of the overall background. The second run used the same 20 litres of mock SUF eluate but about 10 millibecquerels of ^{212}Pb was added to it prior to the extraction so that the efficiency of the procedure could be determined.

  In experiment SSC2, the first run used 20 litres of mock SUF eluate which also contained 0.1 milligrams of stable lead but no ^{212}Pb. The second run had a further 0.1 milligrams of stable lead added to the same 20 litres and also about 100 millibecquerels of ^{212}Pb. This would allow a determination of the background of the process and its efficiency as measured using both stable lead and ^{212}Pb.

Unfortunately the spike of 10 millibecquerels of ^{212}Pb used in experiment SSC1 was too small to determine the efficiency of the procedure since the ^{212}Pb background was relatively high. For experiment SSC2 the efficiency was measured by stable lead to be 52±3%, for the first run, and 43±2% for the second run. The efficiency for the second run was also measured by ^{212}Pb and found to be 42±5% which is in good agreement with that which was measured by the stable lead and is good evidence that stable lead does act an effective carrier for extremely small amounts of ^{212}Pb. It is reasonable to assume that the efficiency in experiment SSC1 was also about 45% since the procedure was identical.

The efficiency of these experiments is lower than the expected 80%, at only 45±5%. This was found to be due to the slipping of the motor on the shaft of stirrer S1 and this fault was rectified before the next experiments were performed.

The ^{212}Pb background for experiment SSC1 was 4.0±0.6 counts per hour and for SSC2, 3.6±1.6 counts per hour which are in good agreement.

- Experiments SSC3 and 4

  Experiment SSC3 was designed to measure the efficiencies of both the extraction and back-extraction stages of the rig. Therefore a large ^{212}Pb spike of about 10 becquerels was added to 20 litres of mock SUF eluate before two sequential solvent-solvent extractions were performed. The extraction efficiencies were determined by measuring the ^{212}Pb content of samples taken from the SUF eluate before and after each extraction. A back-extraction stage was performed for both extractions and the efficiency of the back-extraction stage was determined by weighing the final solution to accurately determine its volume and measuring the ^{212}Pb content in a sample of it.

  The extraction efficiency in the first run was measured to be 79±5% and on the second run, 71±16% thus giving an average value of 78±5%. This efficiency compares very well to the 84±4% extraction efficiency given in Section 6.5.2 on page 103 which was measured using stable lead in experiment SSR4 performed using Version B of the rig. The fact that these efficiency measurements agree is evidence that large quantities of stable lead and extremely small quantities of ^{212}Pb behave the same. The back-extraction efficiency for both runs was consistent with 100%.

  Experiment SSC4 measured the overall efficiency by adding 40 millibecquerels of ^{212}Pb to the 20 litres of SUF eluate and performing two sequential runs of the overall procedure. This gave an overall efficiency of 78±6% for the first run and 70±19% for the second, hence an average of 77±6%. This efficiency also compares very well to the 80±10% overall efficiency measured using stable lead in experiment SSR4 performed using Version B of the rig and given in Section 6.5.2 on page 103.

  By comparing this overall efficiency to the 78±5% extraction efficiency, as measured in experiment SSC3, the HTiO stage must, like the back-extraction stage, be virtually 100% efficient which agrees with the measurements of the HTiO stage efficiency using stable lead in experiment SSR3 performed using Version B of the rig and given in Section 6.5.2 on page 103.

- Experiments SSC5 and 6

  Experiment SSC5 used three runs and measured the background of ^{212}Pb in the different stages of the rig. The first run measured the HTiO stage only by adding 40 millilitres of 16M nitric acid together with 0.96 litres of ultra-pure water to M2 and performing an HTiO concentration. This gave a ^{212}Pb background of 2.1±0.4 counts per hour which, as expected, is comparable to the 1.3±0.3 counts per hour found in the similar experiment, experiment SSB5 whose results are listed in Table 6.3. The second run passed an organic phase, which had not been used in an extraction, into M2 and then performed a back-extraction and HTiO concentration. This gave a ^{212}Pb background of 9.6±1.0 counts per hour indicating that the organic reagent itself adds a ^{212}Pb background of

several counts per hour. The final run of experiment SSC5 measured the background of all three stages of the procedure using a completely blank 20 litres of mock SUF eluate. This gave a ^{212}Pb background of 12.7±1.2 counts per hour which indicates that a further 3 counts per hour are added by mixing with the 20 litres of mock SUF eluate.

Experiment SSC6 used the same 20 litres of mock SUF eluate as had been used in experiment SSC5 several days after the initial experiment had been carried out to determine the overall background to the process. The difference between this experiment and the last run of experiment SSC5 was that the DDDC and 2-octanone were measured out and left sealed for 3 days before mixing in order to reduce any ^{212}Pb background which had accumulated from the air. This was found to reduce the overall background to 4.2±0.7 counts per hour from the 12.7±1.2 counts per hour which was measured in experiment SSC5. This reduction is good evidence that airborne ^{212}Pb contamination getting into the DDDC solution is a major source of ^{212}Pb background.

- Experiments SSC7, 8 and 9

  These three experiments all concentrated ^{212}Pb from the 20 litres of mock SUF eluate which had been used in experiment SSC5 but the DDDC solutions were prepared by mixing the DDDC and 2-octanone a period of time before it was used to further minimise the effect of airborne ^{212}Pb. It was known that DDDC decomposes when it is left in solution, however small scale solvent-solvent batch experiments, which used a few kilobecquerels of ^{212}Pb, showed that a 0.5% w/v DDDC solution can be left for at least a few days without any observable loss of extraction efficiency.

  In experiment SSC7 the organic phase was left mixed for 3 days and then two background runs of the entire procedure were carried out. The first run of experiment SSC8 was the same as the runs in experiment SSC7 but in the second run of experiment SSC8 about 100 millibecquerels of ^{212}Pb was added to the 20 litres so that the overall efficiency of the procedure could be measured. Unexpectedly this efficiency was found to be only 24±2% which was much lower than the 80% which was measured in experiment SSC4. It was thought that this could have been due to the DDDC decomposing with time even though the small scale experiment had suggested this to be unlikely and so in the next experiment, experiment SSC9, the DDDC and 2-octanone were mixed and left for only 24 hours before being used. In this experiment three runs were carried out, the first two measured the ^{212}Pb background of the process and the third run used a spike of ^{212}Pb to measure the overall efficiency which was found, again, to be only 27±2%.

The ^{212}Pb background and efficiency results measured in this second set of experiments performed on Version C of the Solvent-Solvent Extraction Rig are summarised in Table 6.4. The experiments whose efficiencies are marked by an asterisk denote values which are assumed from other experiments. For experiment SSC1 it was clear that the efficiency had to have been the same as in experiment SSC2, however for experiments SSC5, SSC6 and SSC7 it was not clear whether the efficiency had been the 80% which was measured in experiment SSC4, or the 25% which was measured in experiment SSC8, therefore the two possible efficiencies for these experiments are listed.

For all of the experiments listed in Table 6.4 the value for $\mathcal{R}$, the background to SNO signal ratio as defined in Section 6.2 on page 94, is calculated and listed alongside the other results in the table. By considering these calculated values of $\mathcal{R}$ and assuming that it was roughly the same in all of the experiments means that it is likely that the loss of efficiency occurred after experiment SSC5 and before experiment SSC6.

The low efficiency measured in experiment SSC2 has already been discussed as it was due to a failure of the stirrer. When the stirrer operated correctly, in experiment SSC4, the efficiency for lead extraction returned to the expected value of about 80%. However, the reason for the drop of efficiency in experiments SSC8 and 9 is unknown. It was concluded not to be due to the fact that the DDDC solution was left

Experiment Number	Time the Organic Phase was Left	Measured Background in cph of:			^{212}Pb Efficiency	$\mathcal{R}$
		^{212}Pb	^{224}Ra	^{228}Th		
SSC1	no time	4.0±0.6	<0.19	<0.13	45%*	5
SSC2	no time	3.6±1.6	<0.42	<0.86	45±2%	4±2
SSC5	no time	12.7±1.2	<0.24	<0.19	25% or 80%*	25 or 8
SSC6	3 days, unmixed	4.2±0.7	<0.40	<0.11	25% or 80%*	8 or 3
SSC7(1)	3 days, mixed	2.9±0.5	<0.22	<0.08	25% or 80%*	6 or 2
SSC7(2)	3 days, mixed	1.4±0.3	<0.04	<0.09	25% or 80%*	3 or 1
SSC8	3 days, mixed	4.1±0.6	<0.21	<0.08	24±2%	8±2
SSC9(1)	1 day, mixed	4.5±0.6	<0.14	<0.13	27±2%	8±2
SSC9(2)	1 day, mixed	3.4±0.5	<0.04	<0.07	27±2%	7±2

Table 6.4: *The results of the second set of experiments performed on Version C of the Solvent-Solvent Extraction Rig. The values for the activities of each isotope were found by fitting the output of the $\beta - \alpha$ counters as is explained in Appendix D. The background to SNO signal ratio, $\mathcal{R}$, is defined in Section 6.2 on page 94 and calculated by dividing the measured background by both the efficiency and the 2 counts per hour expected signal from the SNO detector. The efficiencies which are marked by an asterisk are assumed efficiencies from other experiments since they were not measured directly in these experiments and the reasons for giving two efficiencies for some experiments is discussed in the text.*

to stand for a number of days prior to use since there was no increase in efficiency in either experiment SSC9, where the DDDC solution was only left for 24 hours, or in a further rig experiment which used a freshly prepared DDDC solution. The reason for this drop in efficiency had to be investigated before work on the rig could continue and the results of this investigation are given in the next section.

The time to perform the secondary concentration of ^{212}Pb in this set of experiments was between 70 and 80 minutes which is an acceptable time compared with the half-life of ^{212}Pb but was longer than had been expected due to some outstanding problems with the final HTiO stage. In this series of experiments 16 full ^{212}Pb concentrations were completed and each of these produced about 1.5 litres of a back-extracted solution with a pH of about 10 which was pushed through Media-Kap filters using nitrogen pressure. In total, 38 Media-Kap filters were used which means that, on average, 2 or 3 filters are needed to concentrate ^{212}Pb from 20 litres of SUF eluate. These filters were eluted by using the acids of the first elutions in the second elutions so that a sample small enough to be measured on a single $\beta - \alpha$ counter was produced, but this is obviously not an ideal solution.

Alongside the difficulties with the HTiO stage and the unexplained drop in efficiency measured in experiments SSC8 and 9, it can be seen from the values of $\mathcal{R}$ in Table 6.4 that there is still a ^{212}Pb background on the rig which is about 8 times larger than the expected signal from the SNO detector. In experiment SSC5 it was found that about 2 counts per hour of ^{212}Pb activity is produced in the final HTiO stage and a large amount is introduced through making up the DDDC solution in air. In experiments SSC6 through SSC9 attempts were made to reduce the amount of ^{212}Pb in the organic phase but it can be seen that these results are inconclusive due to the unexpected loss of efficiency in these experiments.

6.7 An Investigation into the Unexpected Loss of Rig Efficiency

6.7.1 Small Scale Solvent-Solvent Batch Extraction Experiments

The unexpected drop in efficiency experienced in the last experiments conducted using Version C of the Solvent-Solvent Extraction Rig was investigated by performing small scale batch extraction experiments with 0.5 litres of mock SUF eluate and 25 millilitres of organic phase. The extractions were carried out in a 1 litre separating funnel and the phases were mixed by shaking the funnel for 2 minutes. This was the same procedure as that which had been used in the preliminary tests detailed in Chapter 5 and, as in those experiments, about a 1 kilobecquerel of ^{228}Th in equilibrium with its daughters, including ^{212}Pb was added to the aqueous phase before extractions so that efficiencies could be determined using gamma counting.

The first experiment used a 0.5% w/v DDDC solution in 2-octanone and this produced less than 1% ^{212}Pb extraction and so more experiments were carried out to trace the cause by a process of elimination. Firstly, the DDDC was taken from an old batch and secondly the ultra-pure water source was changed but neither of these changes had any effect upon the extraction efficiency. However, when the DDDC concentration in the 2-octanone was increased to 2% w/v, a good extraction efficiency of 87±3% was measured. Initial experiments had used this concentration of DDDC but the concentration was lowered to reduce costs for rig experiments since an experiment had shown that the lower concentration would work just as well, see Section 5.7.2 on page 88.

This experiment was repeated and efficiencies measured by observing the disappearance of ^{212}Pb from the aqueous phase are compared directly to those of the previous experiment in Table 6.5. It should be noted that in the extractions carried out in the present experiment the aqueous phase volume was twenty times larger than the organic phase volume. Furthermore, in the present experiment much greater care was taken to ensure the complete collection of the phases and this is probably the explanation of the higher measured efficiencies when the DDDC concentration was greater than 1.5% w/v. The major differences between the previous and present experimental results are when the DDDC concentration is less than 1.5% w/v. In the previous experiment good extraction efficiencies were measured when the DDDC concentration was reduced to 0.5% w/v but in the present experiment the measured extraction efficiency was found to decrease rapidly to a poor 7±8% at a DDDC concentration of 0.5% w/v.

Concentration of DDDC in 2-octanone	^{212}Pb Extraction Efficiency:	
	Previous Exp	Recent Exp
0.5% w/v	75±12%	7±8%
1.0% w/v	75±09%	24±10%
1.5% w/v	79±12%	97±5%
2.0% w/v	74±10%	97±4%
2.5% w/v	72±10%	>98%

Table 6.5: *A comparison to compare the results of two experiments designed to measure the extraction efficiency of ^{212}Pb when using varying concentrations of DDDC 2-octanone. The results of the previous experiment are taken from Section 5.7.2 on page 88. The differences between the results of the two experiments are discussed in the text.*

These results suggest that the reagents used in this present experiment have changed from those used in the previous experiment. It was found that when high purity, 99+%, 2-octanone was used high extraction efficiencies with a 0.5% w/v solution of DDDC were once again achieved. It must therefore be concluded that different batches of the 98% 2-octanone contain varying amounts of some unknown impurity that inhibits lead extractions using DDDC.[7]

The solution to the decrease in efficiency was clearly to use only the high purity 2-octanone but it should be noted that it is more expensive than the low purity 2-octanone. The 99+% 2-octanone can be purchased from Acros[8] and 1 litre costs about £28 (including taxes). This is about twice the cost of the 98% 2-octanone sold by Aldrich and so this increases the cost to concentrate ^{212}Pb from 20 litres of SUF eluate from the £41 quoted in Section 5.7.2 on page 88 to about £55, assuming that only one Media-Kap filter is used.

6.7.2 A Rig Experiment Using High Purity 2-Octanone

The previous section suggested that if high purity 2-octanone is used, high extraction efficiencies for ^{212}Pb can be obtained when using a 0.5% w/v solution of DDDC. It was decided that this should be verified by performing a single experiment consisting of two complete ^{212}Pb concentrations using Version C of the Solvent-Solvent Extraction Rig. Firstly, a complete, blank ^{212}Pb concentration from 20 litres of mock SUF eluate was carried out to measure the ^{212}Pb background of the rig and then immediately afterwards a known quantity of ^{212}Pb was added to the same 20 litres and a further ^{212}Pb concentration conducted to measure the rig efficiency.

It should be noted that in this experiment the HTiO stage failed to produce a sample that could be measured by a single $\beta - \alpha$ counter and this was due to the Media-Kap filters blocking at an even higher rate than previously noted. In the first run five filters, and almost 30 minutes, were required to filter the back-extracted solution after the HTiO had been precipitated. The total elution volume for these five filters was too large to be measured by a single $\beta - \alpha$ counter and so a sample of it was taken and the result multiplied by a volume ratio. In the second run the filtration was stopped after three filters had been used and about a third of the back-extracted solution had been filtered. These three filters were eluted and the eluate measured using a $\beta - \alpha$ counter. The overall efficiency was then determined by accurately measuring the volume of the total back-extracted solution and comparing it to the amount that was actually filtered.

The efficiency of Version C of the rig when using the high purity 2-octanone was calculated to be 73±5% which is in good agreement with the 77±6% efficiency as measured in experiment SSC4, when the rig was also functioning correctly. The background measurement showed very little ^{224}Ra or ^{228}Th and a ^{212}Pb activity of 8±1 counts per hour. Combining these measurements gives a value of $\mathcal{R}$, the background to SNO signal ratio, of 5±1 which is a similar figure to those found in the last set of experiments.

[7]Independent experiments by Dr K.Rowley of the Brookhaven National Laboratory showed that 2-octanol is such an inhibitor. However the 98% 2-octanone used at Oxford was not found to contain large enough quantities of 2-octanol to account for the lower efficiencies and so another inhibitor must have been present.

[8]Acros Organics, Fisher Scientific UK, Bishop Meadow Road, Loughborough, Leicestershire, LE11 5RG

The difficulties that were found in these experiments in completing the final HTiO stage were very concerning since the number of filters was too great to produce a sample small enough to be measured by a single $\beta - \alpha$ counter and the time taken to complete this stage was much too long. It is interesting to note that the problem of blocking filters was not seen in experiments SSB1-5 performed on Version C of the rig in Section 6.6.1 on page 104 when a back-extraction from an organic phase had not been completed and it was also seen to get worse as more experiments were carried out. This indicates that the possible source of the problem is trace amounts of 2-octanone which make their way through the phase separation in the back-extraction and build up in vessel C3. It is known that the cellulose fibres of the Media-Kap filters are not resistant to 2-octanone and even trace amounts could cause the fibres to swell which would lead to the observed blocking.

If the blocking of the filters is indeed due to trace amounts of 2-octanone then a simple solution to the problem will be hard to find since there will always be trace amounts of 2-octanone present in the solution after the back-extraction. The entire suitability of the HTiO to perform the final concentration of the ^{212}Pb must therefore be brought into question.

6.8 Conclusions

The results of this chapter indicate that, generally, the chemical techniques used on the Solvent-Solvent Extraction Rig, as developed in Chapter 5, efficiently concentrate lead from a solution chemically similar to the SUF eluate into a sample which can be measured by a single $\beta - \alpha$ counter in an appropriate amount of time. However some difficulties still remain and these are discussed below.

Firstly, the efficiency of the initial extraction stage was found to drop considerably both when the SUF eluate and the organic phase were not mixed sufficiently and when certain 2-octanone was used. These drops in efficiency were resolved by fixing the stirrer in the 20 litre mixer and by using high purity 2-octanone, however these efficiency reductions were unexpected and not identified as soon as they occurred which raises concerns over the reproducibility of the efficiencies of the procedures carried out on the rig.

Secondly, the experiments of this chapter showed a major difficulty arising in the final HTiO stage. This stage, previously measured to have a very high efficiency, underwent many changes trying to improve it but the problem of the Media-Kap filters blocking has not been resolved. This raises concerns over the suitability of HTiO to perform the final concentration of ^{212}Pb.

The final difficulty with the Solvent-Solvent Extraction Rig, as used in this chapter, is that the procedural ^{212}Pb background is larger than the expected ^{212}Pb signal from the SNO detector. It should be noted that much successful work was completed to both lower the background on the rig and increase the efficiency for concentrating ^{212}Pb. Indeed the background to SNO signal ratio, $\mathcal{R}$, has been decreased from 160, as measured using Version A of the rig, to around 8, as measured using Version C, but this is still at least an order of magnitude too high.

In the next chapter are details of the further research that was carried out to determine solutions to the difficulties that are outlined above.

Chapter 7

The Final Development of a ^{212}Pb Assay For the SNO Detector

7.1 Introduction

In the last two chapters procedures have been developed to perform the secondary concentration of lead from up to 20 litres of SUF eluate using the Solvent-Solvent Extraction Rig. The completion of these procedures will enable the HTiO SUF assay system to measure the amount of ^{212}Pb in the heavy water of the SNO detector.

The three outstanding difficulties with these procedures are:

1. The final HTiO stage has to either be modified or replaced to solve the problem of blocking filters.
2. The overall efficiency of the rig has to be shown to be reproducibly high.
3. The ^{212}Pb procedural background of the rig has to be reduced by an order of magnitude.

The results of experiments described in the last chapter clearly show the difficulties in investigating the backgrounds to the secondary concentration procedures when the efficiency of these procedures were later found to have changed. It was decided that it would have been highly beneficial to measure the efficiency of the these procedures while simultaneously measuring the ^{212}Pb background. This could have been achieved by adding a stable lead carrier to each experiment and measuring the stable lead yield in the final eluate. Unfortunately the analysis for stable lead carried out at Oxford took at least a week to produce results and this did not allow the analysis of one experiment before starting another which is why the technique was not extensively used.

The need for immediate stable lead analysis, amongst other reasons, led to the transportation of the Solvent-Solvent Extraction Rig to the Brookhaven National Laboratory (BNL), New York, USA, which is a co-collaborator in the SNO experiment. Numerous experiments were carried out at BNL in the latter half of 1997 under the supervision of Dr K.Rowley to develop a reliable secondary concentration procedure for ^{212}Pb using the Solvent-Solvent Extraction Rig and the results of these are detailed in this chapter.

The first area of research that is discussed in this chapter is that of finding an alternative final concentration stage to replace the HTiO method. This involved the development of an alternative back-extraction technique and the use of an ion-exchange column to produce a sample suitable for measurement by a single $\beta - \alpha$ counter. Secondly an investigation into airborne ^{212}Pb activity is made in order to try to reduce ^{212}Pb backgrounds. Lastly, the final version of the Solvent-Solvent Extraction Rig together with the new techniques is evaluated using several experiments to measure efficiencies and backgrounds.

7.2 The Development of an Alternative Final Concentration Stage

7.2.1 Possible Methods

The previous chapter explained the difficulties in using HTiO as the final concentration stage for ^{212}Pb. These were mainly due to the fact that the Media-Kap filters, used to collect the HTiO, were found to be unsuitable when filtering solutions containing trace amounts of 2-octanone. Initial research was therefore directed at finding an alternative method to back-extract and concentrate the lead from the DDDC solution into a 12 millilitre sample which is less that 1M in either salt or acidity and can therefore be measured by a single $\beta - \alpha$ delayed coincidence scintillation counter.

Some small scale experiments had shown that 6M nitric acid instead of 16M concentrated nitric acid could be used to back-extract lead from DDDC very effectively, however 6M nitric acid is, like 16M nitric acid, not measurable by a single $\beta - \alpha$ counter and so even when using the lower strength acid a reduction in acid content is likely to be needed. Furthermore, it seemed infeasible to try to perform an effective back-extraction from the 1 litre of DDDC solution into a volume less than about 40 millilitres. Therefore a method reducing both the volume and acidity of the back-extracted solution was required.

Due to the presence of the strong nitric acid in the back-extracted solution it was difficult to find chemical methods to extract and concentrate the lead. One possibility that was considered was to evaporate the liquid to dryness and then dissolve residues in a small quantity of low molarity nitric acid. The use of such a procedure would produce small volume samples suitable for measurement by a single $\beta - \alpha$ counters however it would take a few hours to evaporate the 40 millilitres to dryness in a controlled fashion and this would lead to losses of ^{212}Pb due to decay.

The difficulty in further concentrating the lead from a solution of strong nitric acid led to a search for an effective alternative back-extraction procedure which would leave the lead in 40 millilitres of a solution suitable for further chemical processing. It was noticed by Mr B.Knox that the order of decreasing stability of various metal diethyldithiocarbamates has been determined to be: mercury(II), palladium(II), silver(I), copper(II), thallium(III), nickel(II), bismuth(III), lead(II), cadmium(II), thallium(I), zinc(II), indium(III), antimony(III), iron(III), tellurium(IV) and manganese, see [Sta64] and [Bod57]. This suggests that if enough copper(II) or nickel(II) were present in an aqueous phase which was mixed with a DDDC solution, the DDDC would become saturated and any lead would be displaced into the aqueous phase. The use of copper to displace metal ions from their dithiocarbamates is a known procedure, see [Sěd52].

A small scale test experiment was performed using both copper and nickel to investigate whether this procedure would be useful to back-extract lead from a 0.5% DDDC solution in high purity 2-octanone. Since two DDDC molecules react with each divalent ion, see Section 5.2.4 on page 73, half the number of copper ions or nickel ions are needed to saturate a given number of molecules of DDDC. The amount required was calculated and added to an aqueous phase which was then shaken with a small volume of DDDC solution after it had undergone an extraction of lead from 0.5M hydrochloric acid. Unfortunately nickel was observed to not displace the lead which indicates that nickel might be lower than lead in the stability order when 2-octanone is used as the solvent. However, copper was found to be extremely efficient at displacing the lead into the aqueous phase.

Since the aqueous phase used to back-extract the lead can be made more or less concentrated with copper as needed, the results of this preliminary experiment suggested that it would be likely that, using an excess of copper, the lead could be back-extracted from 1 litre of a DDDC solution into about 40 millilitres of aqueous phase. Since this 40 millilitres must also contain a large amount of copper needed to saturate the DDDC, it would be preferential to extract the lead from this solution to make a 12 millilitre

sample which can be measured by a single $\beta - \alpha$ counter. Research into the literature on ion-exchange materials suggested that the lead in a copper solution could be extracted and then collected into a smaller volume using an ion-exchange column containing a strong base anion-exchange resin, Dowex-I, provided that the original copper solution was made to be 1M in hydrochloric acid. Since the back-extraction using copper was relatively insensitive to the acid molarity in the aqueous phase it seemed possible that a copper back-extraction followed by an ion-exchange stage would obtain the required final concentration of ^{212}Pb.

In the next two sections experiments investigating the reliability of the copper back-extractions and the feasibility of a final ion-exchange concentration are detailed.

7.2.2 Feasibility Studies for Copper Back-Extractions

Several small scale experiments were performed to try to understand and characterise the back-extraction of lead from DDDC using copper. In each experiment a solvent-solvent extraction from 0.5 litres of 0.5M hydrochloric acid was performed using 25 millilitres of a solution of DDDC in 2-octanone. These were shaken in a 1 litre separating funnel for 2 minutes and then the two phases were separated and the back-extraction carried out in a 100 millilitre separating funnel by adding a solution of copper and shaking for 2 minutes.

These experiments were therefore very similar to the original small scale feasibility studies detailed in Chapter 5, however there were a few differences. Firstly, the 2-octanone used was the high purity 2-octanone purchased from Acros since in the last chapter it had been shown that using lower purity 2-octanone could cause decreases in efficiency, see Section 6.7.1 on page 112. Secondly, no titanium was added to the 0.5M hydrochloric acid since it had previously been shown that titanium does not play a role in the extraction of lead using DDDC. Thirdly, all of these experiments were conducted in glass apparatus, using appropriately sized separating funnels and a standardised rinsing procedure to eliminate losses of efficiencies due to incomplete phase collection as had been observed in the small scale feasibility experiments in Chapter 5.

The results of these experiments were determined by adding 104 micrograms of stable lead to each aqueous phase before an extraction and measuring the amount of stable lead in the back-extracted solution. The amount of copper extracted was determined by adding a known quantity of copper to perform the back-extraction and then measuring the amount remaining in the aqueous phase. These measurements were made using Atomic Absorption Spectroscopy using the 283.3 nanometer absorption line for lead and the 324.9 nanometer absorption line for copper.

The results of several such experiments using copper back-extractions are shown in Table 7.1. The results show that although the lead recovery is always above 95%, there is quite a large variation in the amount of copper that was extracted during the back-extraction. Interestingly, the amount of copper that was extracted is not enough to saturate the initial amount of DDDC that was present since one would expect a DDDC/Cu molar ratio of 2 and the results show molar ratios of between 10 and 20.

The likely explanation for the observed high molar ratios is that some of the DDDC in the 2-octanone decomposes before or during the back-extraction. If it is assumed that the DDDC has decomposed and that the remaining DDDC is fully saturated with copper then the amount of DDDC remaining as a percentage of that initially added can be calculated and these percentages are shown in Table 7.1 alongside the other results.

It is unclear exactly where the decomposition of DDDC was occurring but in Section 7.4.4 on page 134 experimental results show that some of the DDDC decomposes during the extraction stage. There is also some evidence for decomposition within the back-extraction in the results in Table 7.1 itself since there appeared to be more DDDC remaining when 0.1M nitric acid was used in the back-extraction (experiments BMB2-4) than when 1M hydrochloric acid was used (experiments BMB6-10). Naively one would expect

Exp No	Organic Phase	Aqueous Phase	Ext/Back-Ext Efficiency	Copper Extracted	Molar Ratio	DDDC Left
BMB2	0.5% DDDC	0.1M HNO_3	94±1%	2.5mg	14	14%
BMB3	0.5% DDDC	0.1M HNO_3	97±1%	4.1mg	9	23%
BMB4	0.5% DDDC	0.1M HNO_3	95±2%	4.6mg	8	26%
BMB6	0.5% DDDC	1M HCl	99±1%	1.2-3.2mg	11-30	7-18%
BMB7	0.5% DDDC	1M HCl	95±1%	1.6-1.8mg	20-22	9-10%
BMB8	0.5% DDDC (in CCl_4)	1M HCl	98±1%	2.7mg	13	15%
BMB9	1.0% DDDC	1M HCl	97±1%	3.7mg	19	10%
BMB10	0.5% DDDC (in 4 day old 2-oct)	1M HCl	95±1%	2.2mg	16	12%

Table 7.1: *The results of several lead back-extractions using copper. In all of the experiments 105 micrograms of stable lead was extracted from 0.5 litres of 0.5M hydrochloric acid into 25 millilitres of an organic phase and the lead was then displaced from the DDDC with copper using 1-2 millilitres of aqueous phase. The overall extraction and back-extraction efficiencies for these experiments were determined by analysing the final back-extracted solution for stable lead.*

more decomposition in the stronger acid, as was observed.

It is interesting to see that when carbon tetrachloride was used as the solvent and a similar copper back-extraction carried out (experiment BMB8) the amount of copper needed was not significantly higher than that when 2-octanone was used. This is strange because this is a well understood system and it is known that the DDDC decomposition in this system takes times much longer than the few minutes of mixing used in this experiment [Bod59]. This indicates that there must be more complicated effects taking place.

In experiments BMB6 and BMB7 a small amount of copper was initially added to try to back-extract the lead and then successive back-extractions were carried out each containing an additional amount of copper. The results of these experiments showed that the lead was released over a very small range of added copper. For example, in experiment BMB7, only 7% of the lead was released when 1.6 milligrams of copper was added but by adding a further 0.2 milligrams 88% of the lead was released. The remaining few percent of lead were released on adding a further 0.2 milligrams of copper.

The results of experiments BMB7 and BMB9 can be compared to see the effect of increasing the amount of DDDC in the original organic phase. In the first experiment the usual 0.5% w/v solution was used whereas in the second a 1.0% w/v solution was used. In both experiments good lead recovery was found and the amount of copper needed was found to increase approximately in proportion to the amount of DDDC present. This result suggests that the findings of these small scale experiments can successfully be scaled to experiments at the 20 litre scale. Finally, in experiment BMB10 the DDDC solution was left, mixed for 4 days prior to the experiment and the results imply that no further DDDC decomposition takes place during this time. This is in agreement with the results of an experiment conducted at Oxford which was discussed in Section 6.6.2 on page 109.

A final small scale back-extraction using copper was carried out in Oxford which measured the back-extraction efficiency by adding a kilobecquerel of ^{228}Th in equilibrium with all of its daughters, including ^{212}Pb, to the aqueous phase before the extraction. The efficiencies for ^{212}Pb were measured using gamma counting, as described in Appendix B. The back-extraction was performed with about the same amount of copper as had been needed in the experiments at BNL and the back-extraction efficiency was found to be 98±3%. This showed that the copper back-extraction technique is very effective even when the

amount of lead present in the organic phase is reduced by several orders of magnitude.

It should be noted that the distinctive brown colouring of the copper-DDDC complex made it easy to see when the copper was extracted and that this extraction seemed to occur very quickly. Furthermore in all of the experiments it was found that if a blue colouring remained in the aqueous phase this indicated that there was a copper excess and hence that the lead had been displaced.

In the above experiments the amount of copper that was needed to perform the back-extraction of lead was calculated by observing the disappearance of copper from the aqueous phase. A brief investigation was conducted to determine whether the copper extracted by the DDDC could be quantitatively recovered. Firstly, the acid back-extraction method that had been used for lead was used for copper. This involved shaking the organic phase left from experiment BMB9 with a few millilitres of 6M nitric acid for 2 minutes. Unfortunately this was found to recover only about a third of the copper and further water rinses of the organic phase continued to show a green colouring which indicated that the back-extraction was not complete. So, for experiment BMB10 the acid was initially shaken with the organic phase for 2 minutes and then the mixture was left to stand for 1 hour to allow the reaction to proceed before a final shaking for 2 minutes and a separation of the phases. It is interesting to note that during this hour the dark brown colour of the copper-DDDC complex changed to a green colour which then faded to a persistent yellow colour which was not removed from the organic phase despite several water rinses. The hour long method of back-extracting copper from DDDC was found to be very effective and the amount of copper recovered was in good agreement with the amount calculated to have disappeared from the aqueous phase.

A further experiment, experiment BRT1, was conducted to verify the copper back-extraction method at full scale. A solvent-solvent extraction from 20 litres of 0.5M hydrochloric acid containing 400 micrograms of stable lead was performed using 1 litre of 0.5% w/v solution of DDDC in high purity 2-octanone. This extraction was performed using mixer, M1 and stirrer, S1 of Version C of the Solvent-Solvent Extraction Rig as shown in Figure 6.4 on page 105. The extraction lasted for 5 minutes and then the phases were left to stand for a further 5 minutes before the organic phase was separated into mixer, M2. To this 1 litre of 2-octanone, 40 millilitres of 1M hydrochloric acid containing about 80 milligrams of copper was added and the phases mixed for 5 minutes by bubbling nitrogen gas into the bottom of M2. The phases were separated and then a second, identical back-extraction was carried out. Both of the 40 millilitres of back-extracted solutions were analysed for stable lead and copper content using Atomic Absorption Spectroscopy, as before.

After both extractions the copper was back-extracted from the organic phase by adding 200 millilitres of 6M nitric acid, mixing for 5 minutes then standing for 1 hour. After this time the phases were once again mixed for 5 minutes before the acid was removed, evaporated down and analysed for copper. All of the copper and stable lead measurements for this experiment are shown in Table 7.2.

These results show that the overall extraction and back-extraction efficiency for lead was virtually 100%. The amount of copper found in the organic phase was 34 milligrams which is consistent with that which disappeared from the aqueous phase in the first lead back-extraction. The copper results show that only 0.54 millimoles of copper were needed to completely back-extract the lead from 22.5 millimoles of DDDC. This is a molar ratio of 42 which would indicate that only 4.8% of the DDDC that was initially added to the 2-octanone was present after the back-extraction. This is a much lower fraction than that measured in the small scale experiments but this is to be expected if DDDC decomposition is occurring in the extraction stage since the mixing time had been increased from 2 minutes to 5 minutes and the method of mixing was significantly different.

Sample	Lead Content	Copper Content
1st back-extraction using copper	406μg	44mg
2nd back-extraction using copper	7.2μg	75mg
final back-extraction using 6M nitric acid	-	34mg

Table 7.2: *The results of a 20 litre extraction into 1 litre of a 0.5% w/v DDDC solution using high purity 2-octanone followed by two back-extractions using 40 millilitres of 1M hydrochloric acid containing about 80 milligrams of copper. The acid back-extraction was carried out after the two copper back-extractions by leaving 200 millilitres of 6M nitric acid with the 1 litre of organic phase for over 1 hour. The initial 20 litres of acid contained 400 micrograms of stable lead and so the overall efficiency can be seen to be virtually 100%.*

7.2.3 Ion-Exchange Feasibility Studies

In the introduction to this section it was explained that the Dowex-I anion-exchange resin offers the possibility of separating lead from a 1M hydrochloric acid solution containing a large amount of copper. The literature states that the Dowex-I anion-exchange material extracts lead from 1M hydrochloric acid solutions but does not extract copper. This can be seen in Figure 7.1 which contains the two relevant figures from [Kra53] and [Kra54]. This figure shows that from 1M hydrochloric acid the Dowex-I material has a distribution coefficient for lead of about 24 suggesting that about 10 column volumes of 1M hydrochloric acid can be passed through a column before the lead begins to breakthrough. The figure also shows, from the low elution constant for copper, that copper in 1M hydrochloric acid is hardly absorbed at all by an ion-exchange column made from Dowex-I.

The combination of these two results would seem to suggest that, using a 4 millilitre column of Dowex-I, the lead in 40 millilitres of 1M hydrochloric acid would be adsorbed by the column whereas the copper would pass straight through.

This theory was put to the test by an experiment which used 90 millilitres of 1M hydrochloric acid containing both half a milligram of stable lead and one milligram of copper. This 90 millilitres was passed, in 10 millilitre samples, through a 4 millilitre ion-exchange column made up with 100-200 mesh Dowex-I X8 resin. Each 10 millilitres which passed through the column was analysed for stable lead and copper so that the cumulative breakthrough as a percentage of the amount of the ion passed into the column could be calculated. The results of this experiment are shown graphically in the top plot of Figure 7.2. This figure shows that after 10 millilitres all of the copper passes through the column whereas only after about 40 millilitres does a significant amount, about 7%, of the lead pass through the column. This significant breakthrough of lead after only ten column volumes of 1M hydrochloric acid indicates a lower distribution coefficient than that which is suggested in [Kra54]. This difference may have been due to using a coarser mesh material.

This experiment showed that the lead from 1M hydrochloric acid could be held up on a Dowex-I ion-exchange column and so the next stage was to demonstrate that the lead could be recovered into a 12 millilitres sample suitable for counting on a $\beta - \alpha$ counter. To ensure that the lead is well separated from the copper the first step was to wash the column with a **small volume of** 1M hydrochloric acid to remove any remaining copper. This was tested experimentally by firstly passing 30 millilitres of 1M hydrochloric acid containing 105 micrograms of stable lead and 1 milligram of copper through a 4 millilitre column. All but a few percent of the lead remained on the column whereas about 90% of the copper was found to have passed through the column. The column was then eluted using three 2 millilitre samples of 1M hydrochloric acid and these were measured for stable lead and copper content.

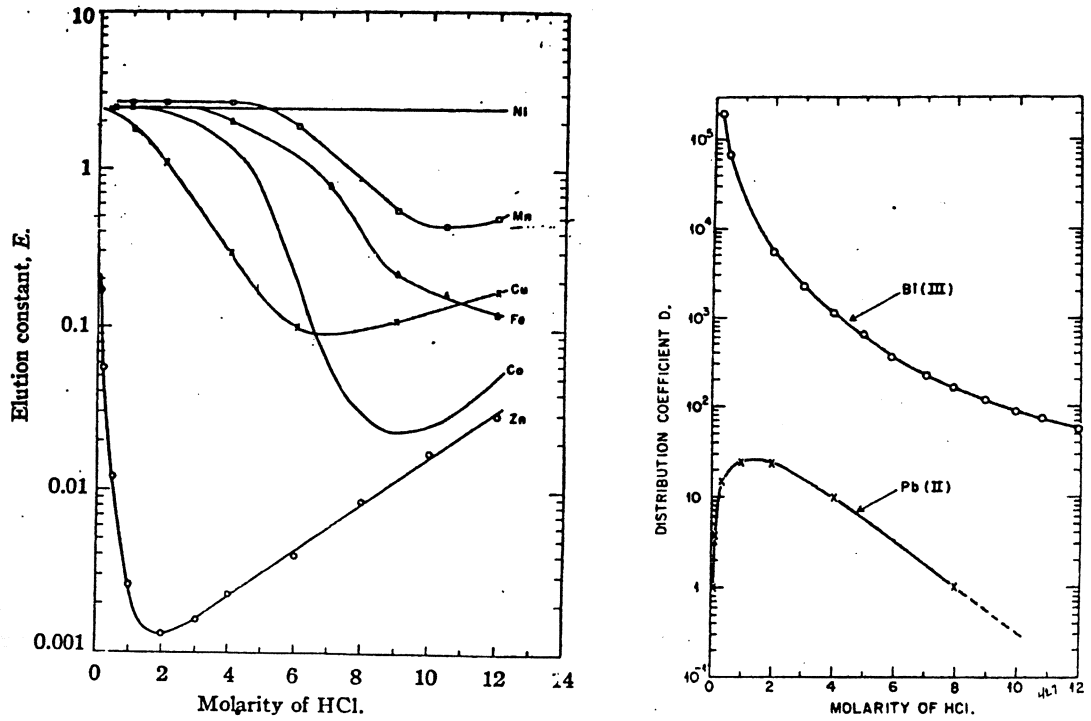

Figure 7.1: *The plot on the left is taken from [Kra53] which gives the elution constants of some divalent transition elements for a Dowex-I column in hydrochloric acid. This figure includes the curve for copper and this gives an elution constant, E, of about 1.7 for copper in 1M hydrochloric acid. The plot on the right is from [Kra54] which gives the adsorption of lead and bismuth on Dowex-I from hydrochloric acid in terms of the distribution coefficient. The distribution coefficient, D, for lead in 1M hydrochloric acid can be seen to be about 24. It should be noted that* $E = 1/(i+D)$ *where i is the fractional interstitial space of the column which is usually about 0.4. This means that 40% of the column volume is not occupied by the anion-exchange resin.*

The results of these three copper elutions, in terms of the percentage of the lead and copper that had been left on the column, are shown graphically in the middle plot of Figure 7.2. It can be seen that after just 4 millilitres almost 90% of the copper left on the column was eluted along with only about 3% of the lead.

A method for removing the lead from the column had been suggested in [Kra54] but this involved an elution with 8M hydrochloric acid which would not produce a sample which could be measured by a single $\beta - \alpha$ counter. However, if one observes carefully the curve for lead against hydrochloric acid molarity in Figure 7.1, it can be seen that the distribution coefficient for lead reduces greatly both at high hydrochloric acid molarity and at very low hydrochloric acid molarity. Therefore, it seemed possible that an elution of a Dowex-I column with water would successfully remove any lead which had been extracted onto it. This was tested experimentally using the same column as that which had had the copper elutions by eluting the column next with six 2 millilitre samples of water and analysing each for copper and lead. The results of this experiment, in terms of the percentage lead and copper left on the column before the copper elutions, are shown graphically in the bottom plot of Figure 7.2. This plot shows that after about 8 millilitres of water over 90% of the lead is eluted and that this elution contains less than 3% of the copper that had been left on the column after the 30 millilitres of sample had passed through it. Since only about 10% of the copper in the 30 millilitres of 1M hydrochloric acid was left on the column this means that only 0.3% of the copper initially present ends up with the lead after this ion-exchange stage.

The results of these experiments were encouraging as they seemed to suggest that lead can indeed be separated from a copper solution in 1M hydrochloric acid into a small volume of weak hydrochloric acid. (The final sample ends up being about 0.1M in hydrochloric acid due to the washing off of some acid left in the column.) Indeed, when initially using 30 millilitres of 1M hydrochloric acid, after a 6 millilitre 1M hydrochloric acid wash, a lead yield of 90% was achieved by washing the column with 12 millilitres of water. Unfortunately, increasing the initial volume from 30 millilitres was seen to produce large reductions in the overall efficiency due to the lead breakthrough from the ion-exchange column. For example, when 40 millilitres were passed through the column the overall efficiency decreased to 85% and when 50 millilitres was passed through the column the overall efficiency was reduced further to just 75%. It is clear that although promising this column itself was not ideal for the final concentration of the lead from the back-extracted solution since a back extraction into a volume less than 40 millilitres from 1 litre has already been discussed as infeasible.

Further development work was completed by Dr K.Rowley and a new column was made which used 5 millilitres of 200-400 mesh Biorad AG I-X8. This is the same material as Dowex-I but a larger amount of a smaller mesh size was used. The results of experiments using this column were similar to those using the old column but larger initial volumes could be passed through the column before lead breakthrough was observed. Typically, virtually 100% overall efficiencies for the extraction and elution of lead were found when starting from a 40 millilitres volume, using a 5 millilitre 1M hydrochloric acid copper wash and eluting the lead with 12 millilitres of water.

Unfortunately, it was found that under gravity the flow rates through the column were too slow for the concentration of ^{212}Pb and so the column was adapted so that it could be pressurised to give flow rates of about 3 millilitres per minute and this allowed the entire ion-exchange procedure to be completed in about 20 minutes. Further experiments of Dr K.Rowley showed that flow rates between 2 and 5 millilitres per minute could be tolerated without any major losses in efficiency. A diagram of the pressurised column which was used in these, and future, experiments is shown in Figure 7.3.

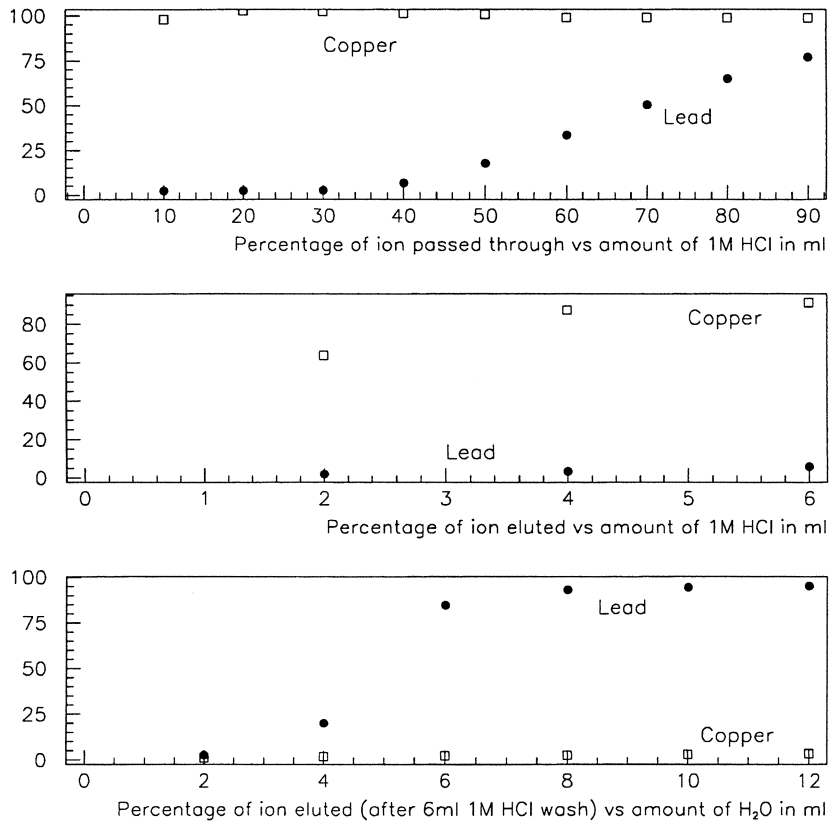

Figure 7.2: *The results of the characterisation of the ion-exchange column. The top plot gives the results of a breakthrough experiment. It shows how much lead (circles) and copper (squares) is passed through a 4 millilitres Dowex-I column when different volumes of 1M hydrochloric acid containing lead and copper are used. The middle and lower plots give the results of two elution experiments performed one after the other on a pre-loaded ion-exchange column. The middle plot shows how much copper and lead are eluted using different volumes of 1M hydrochloric acid. The bottom plot shows how much lead and copper are eluted using different volumes of water.*

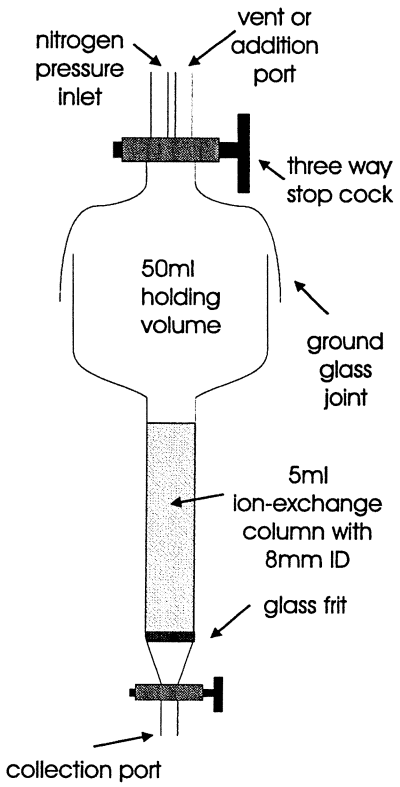

Figure 7.3: *The pressurised ion-exchange column which was used in the final concentration of lead to produce a 12 millilitre sample suitable for $\beta - \alpha$ counting.*

7.2.4 An Investigation into the Compatibility of Copper with Scintillation Counting

The previous two sections have shown that lead can be back-extracted from 1 litre of a DDDC solution and concentrated into a 12 millilitres sample which, in terms of acidity, is chemically suitable for counting on a single $\beta - \alpha$ counter. However it is expected that this sample will contain some copper and due to the blue colouring of copper salts it was not clear whether or not small amounts of copper would effect the efficiency of detecting a $\beta - \alpha$ coincidence using scintillation counting. Therefore an investigation was conducted to determine any systematic effect of copper on the counting efficiency of the $\beta - \alpha$ counters which were described in Section 3.2.1 on page 30 with more details in Appendix D.

It is expected that 80 milligrams of copper will be added to the organic phase for the back-extraction of lead from 1 litre of a 0.5% w/v solution of DDDC in 2-octanone. However, only about half of that is extracted, the rest remains in the back-extracted solution along with the lead. The ion-exchange separation has been shown to reduce the amount of copper in the final 12 millilitres volume to less than a percent of that which was originally present and so it is not expected that a sample for measurement by the $\beta - \alpha$ counters will contain more than about 1 milligram of copper.

Three samples for measurement on the $\beta - \alpha$ counters at Oxford were prepared each of which contained the same amount (about 70 millibecquerels) of ^{228}Th and either no copper, 2 milligrams of copper or 4 milligrams of copper in the form of a copper chloride solution diluted to be 0.4M in hydrochloric acid. Each sample was measured on three $\beta - \alpha$ counters and the results of these measurements are given in Table 7.3.

$\beta - \alpha$ Counter	Copper Content		
	blank	2mg	4mg
3	132±4	124±5	126±3
4	125±4	124±4	126±5
5	149±5	162±4	159±4

Table 7.3: *The results of measuring samples with the same amount of ^{228}Th but different amounts of copper on the $\beta - \alpha$ counters in Oxford. The count rates are in counts per hour and the errors quoted assume $\sqrt{N}$ errors.*

Any effect on counter efficiency of the copper can be calculated by determining the ratio of the count rate when copper was present to that when there was no copper present for each counter. An average of all three counters can be made for the sample containing 2 milligrams of copper and for the sample containing 4 milligrams of copper. These average ratios come to 1.01±0.03 for 2 milligrams and 1.01±0.02 for 4 milligrams which indicate that there was no effect due to the presence of the copper. It can therefore be concluded that the $\beta - \alpha$ counters can tolerate at least 4 milligrams of copper with no noticeable effect on the efficiency of detecting a delayed $\beta - \alpha$ coincidence.

7.3 Investigations of ^{212}Pb Backgrounds

7.3.1 The ^{212}Pb Background in the Ion-Exchange Stage

The final ion-exchange stage was evaluated for backgrounds and efficiencies by carrying out two identical experiments, experiments BRT4A and BRT4B. These experiments performed a mock back-extraction from 1 litre of 2-octanone which had been used previously in an extraction and back-extraction. This mock back-extraction was performed in mixer M2 of Version C of the Solvent-Solvent Extraction Rig (see Figure 6.4 on page 105) and used 35 millilitres of 1M hydrochloric acid containing both 75 milligrams of copper and 1 milligram of stable lead. After mixing with the 2-octanone the aqueous phase was transferred by beaker to the pressurised ion-exchange column as shown in Figure 7.3 on page 124. This column was then washed with 5 millilitres 1M hydrochloric acid to remove most of the remaining copper from the column and finally the lead was removed by eluting twice, each time with 12 millilitre samples of water.

All of the samples that were taken, along with a rinse of M2, were measured for stable lead and copper content using Atomic Absorption Spectroscopy, as before. The first lead elutions were also measured for ^{212}Pb activity using the $\beta - \alpha$ delayed coincidence scintillation counters which were set up at BNL (see Appendix D for details). This first lead elution was weighed and then divided into two samples, a 1 millilitre sample for Atomic Absorption Spectroscopy and an 11 millilitre sample for measurement on a $\beta - \alpha$ counter. This process of dividing the final 12 millilitre sample to allow a measurement of both its stable lead content and its ^{212}Pb content is used extensively in the rest of this chapter.

The results of all of the measurements made in experiments BRT4A and BRT4B are shown in Table 7.4. It can be seen that the overall lead recovery is very high at 97-99% and that more than 90% of the lead was recovered in the first lead elution. The ^{212}Pb background results for these two experiments showed that the first lead elution in experiment BRT4A contained 2.5±0.4 counts per hour of ^{212}Pb and the first elution from experiment BRT4B contained 2.1±0.5 counts per hour of ^{212}Pb. Since these backgrounds were higher than expected two pairs of experiments were performed to try to determine their cause. These experiments all started from 40 millilitres of 1M hydrochloric acid containing 1 milligram of stable lead. The lead was then extracted using the ion-exchange column and eluted from it using 12 millilitres of water.

The first pair of experiments, experiments BRT5 and BRT6, operated the ion-exchange column in the usual way using standard experimental equipment. This meant that the column was opened up to the air to add reagents which were decanted from stock bottles in the air and the lead elutions were collected in loosely covered beakers. In the second pair of experiments, experiments BRT7 and BRT8, steps were

Sample	BRT4A		BRT4B	
	Stable Lead	^{212}Pb	Stable lead	^{212}Pb
Copper fraction	0.7%	-	1.1%	-
1st lead elution	91.3%	2.5±0.4cph	92.5%	2.1±0.5cph
2nd lead elution	0.8%	-	0.6%	-
Rinse of M2	4.3%	-	4.6%	-

Table 7.4: *The stable lead efficiency results and the ^{212}Pb background results for experiments BRT4A and BRT4B. The ^{212}Pb results are for the initial activity of ^{212}Pb in the sample in $\beta - \alpha$ counts per hour (cph). In these experiments a full scale mock back-extraction and an ion-exchange stage were carried out. The sample labelled 'copper fraction' in the table is the analysis of the 35 millilitre solution which passed through the column along with the 5 millilitre 1M hydrochloric acid wash of the column. The lead elutions both consisted of 12 millilitres of water.*

Description of Sample	^{212}Pb Activity in $\beta - \alpha$ cph:			
	No syringes		Syringes	
	BRT5	BRT6	BRT7	BRT8
1st lead elution	2.3±0.7	0.9±0.3	0.1±0.2	0.4±0.2
2nd lead elution	0.2±0.3	1.5±0.4	0.3±0.1	0.0±0.2

Table 7.5: *The ^{212}Pb background results of two pairs of experiments which used just the ion-exchange concentration stage. The ^{212}Pb results are for the initial activity of ^{212}Pb in the sample in $\beta - \alpha$ counts per hour (cph). In experiments BRT5 and BRT6 a standard procedure was carried out which involved some air contact whereas in experiments BRT7 and BRT8 syringes were used to transfer liquids thus virtually eliminating any air contact and any backgrounds due to airborne ^{212}Pb contamination.*

taken to try to virtually eliminate any contact to the air in the experiments.

Firstly, all of the required chemicals were prepared three days in advance and left in sealed syringes so that any ^{212}Pb introduced in making up the solutions would have decayed away before the experiment. Secondly, these solutions were added to the column using these same syringes and the addition port shown in Figure 7.3 on page 124 so that the column never had to be opened up to the air. Finally, the lead elutions were collected in 20 millilitre syringes by using the nitrogen pressure to force the 12 millilitres of water through the column and directly into the syringe.

In all four experiments two lead elutions of the ion-exchange column were made and each of these was measured for ^{212}Pb activity on the $\beta - \alpha$ counters at BNL and these results are shown in Table 7.5.

It can be seen from these results that when the air contact was virtually eliminated by using the syringes the measured ^{212}Pb background in the elutions were all very low whereas when syringes were not used some samples had a low ^{212}Pb background but some had a very large ^{212}Pb background. Furthermore the sample with a high ^{212}Pb background in experiment BRT5 does not correspond to the sample with a high ^{212}Pb background in experiment BRT6 which was performed identically. This random distribution of ^{212}Pb backgrounds could indicate that ^{212}Pb atoms are being transported in clusters on particles of dust in the air which sometimes drop into samples giving a high ^{212}Pb background and sometimes do not. Whatever the exact mechanism of airborne ^{212}Pb the results of experiments BRT5-8 clearly show that airborne ^{212}Pb is a serious problem in performing procedures to concentrate ^{212}Pb when the expected signal of ^{212}Pb is only about 2 counts per hour as measured by the $\beta - \alpha$ counters, see Section 6.2 on page 94.

The efficiency of the ion-exchange column using the syringe method was determined by stable lead using a separate experiment and this gave an efficiency of 91% for recovering the lead in the first 12 millilitre elution for lead. This, together with the results of experiments BRT7 and BRT8, as given in Table 7.5 show that high efficiencies together with reproducible, low ^{212}Pb backgrounds can be achieved for the ion-exchange stage if syringes are used to transfer liquids to and from the column.

7.3.2 Measurements of Airborne ^{212}Pb Contamination

In the previous section it was shown that a large ^{212}Pb background is introduced when apparatus is not completely sealed from the air and so a brief series of experiments were conducted to examine the problem of airborne ^{212}Pb contamination at different institutions more closely. The main experimental method was to add 10 millilitres of dilute hydrochloric acid to a $\beta - \alpha$ counting pot and leave it open to the air for a period of a few hours. This pot was then filled with scintillator cocktail in the usual way and any ^{212}Pb collected was measured on a $\beta - \alpha$ delayed coincidence scintillation counter. (It should be noted that these measurements were carried out using the $\beta - \alpha$ counters at Oxford, BNL and Sudbury but that any systematic differences between counting efficiencies are expected to be small.)

Institute Name	Time of Exposure in hrs	^{212}Pb activity Measured in cph	Deposition Rate in atoms of ^{212}Pb per hr	Average Rate
Sudbury	3	0.3	3	7±5
	3	0.9	10	atoms/hr
BNL	1	20	630	410±250 atoms/hr
	1.17	25	680	
	1.25	9	230	
	2	9	150	
	4	82	700	
	8	33	170	
	74	150	300	
Oxford	0.3	0.5	51	30±20 atoms/hr
	1	0.3	10	
	2	1.6	25	
	5	2.7	20	
	5	19	53	
	6	3	19	
	7.5	2.3	10	
	13.5	16	54	
	23	15	39	

Table 7.6: *The measurements of the deposition rate of ^{212}Pb as measured at experimental areas in different institutions. These values are shown graphically in Figure 7.4. The errors on each individual measurement are not listed since the spread of measurements indicate a much larger systematic error.*

The results of such experiments carried out in experimental areas at three different institutes are given in terms of ^{212}Pb counts per hour in Table 7.6. The measurements made at Sudbury were performed by Dr M.Moorhead in the surface chemistry laboratory where the secondary concentration of ^{212}Pb is expected to take place. The measured activities can be converted to ^{212}Pb deposition rates, in atoms of ^{212}Pb per hour, by solving the same differential equation as was used in Section 4.4.4 on page 59 to describe the amount of ^{212}Pb produced when emanating ^{220}Rn at a constant rate. This equation is reproduced in Equation 7.1 and the solution to it, assuming no initial ^{212}Pb, in Equation 7.2.

$$\frac{dN(t)}{dt} = R - \lambda_{Pb} N(t) \tag{7.1}$$

$$R = \lambda_{Pb} N(T)(1 - e^{-\lambda_{Pb} T})^{-1} \tag{7.2}$$

Since $\lambda_{Pb} N(T)$ is the initial activity of ^{212}Pb in the counting pot as measured by the $\beta - \alpha$ counters, after T hours of exposure divided by their 50% counting efficiency, it is clear that the deposition rate, R, can be calculated from the measured count rates. Using Equation 7.2 deposition rates, in atoms of ^{212}Pb per hour, for all of the measurements given in Table 7.6 have been calculated and are listed alongside. These deposition rates are also shown graphically in Figure 7.4 on a logarithmic scale to show the differences between the airborne ^{212}Pb backgrounds in the experimental areas at different institutes.

The results of these measurements show a wide variation between the amount of airborne ^{212}Pb in the experimental areas at different institutions. To put these deposition rates in context it should be remembered that the total amount of ^{212}Pb in the SUF eluate is hoped to produce just 2 counts per hour on the $\beta - \alpha$ counters which is the counting rate that would be seen if a $\beta - \alpha$ counting pot was left

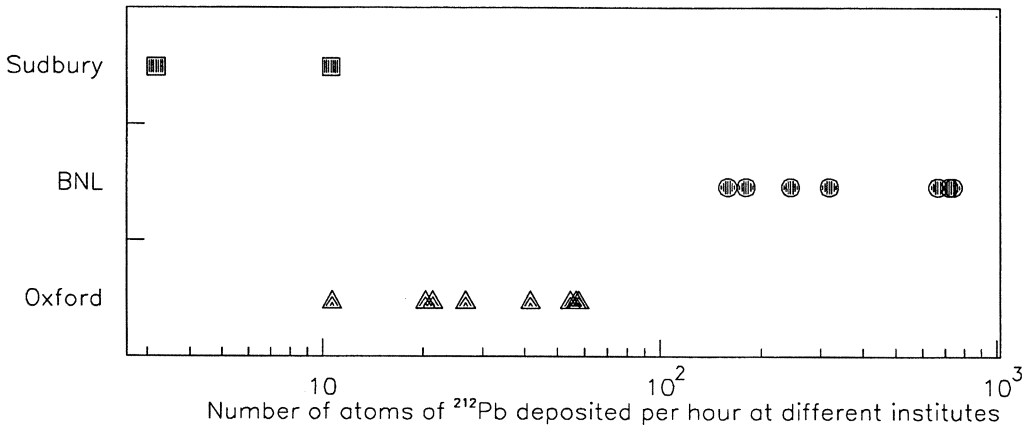

Figure 7.4: *A figure displaying the results given in Table 7.6 of several measurements of airborne ^{212}Pb contamination at experimental areas in different institutes. It should be noted that this figure has a logarithmic x-axis. The rate of deposition is given in atoms of ^{212}Pb per hour and this was found by leaving $\beta - \alpha$ counting pots containing a few millilitres of dilute acid open to the air for a known amount of time and then calculating the average rate of deposition during this time taking into account the half-life of ^{212}Pb.*

uncovered at the surface chemistry laboratory in Sudbury for about 10 hours, at the experimental area in Oxford for about 2 hours and at the experimental area in BNL for only a few minutes!

These large differences are probably due to differences in the materials which make up the walls of the experimental areas. In Sudbury care was taken to construct the surface chemistry laboratory out of materials which contain very low amounts of thorium and uranium, whereas at BNL and Oxford the experimental areas used were rooms inside concrete buildings and it is known that concrete contains relatively high amounts of both thorium and uranium.

One further measurement regarding ^{212}Pb airborne contamination was carried out at BNL and this was to determine whether the ^{212}Pb atoms were simply dropping into the $\beta - \alpha$ counting pots or whether they were being attracted to the pots by electrostatic forces. In this experiment two empty $\beta - \alpha$ counting pots were left open in air for 80 minutes. One of the pots was placed on a bench facing upwards and the other was turned upside down and held in a clamp. After filling these pots with acid and scintillator in the usual way the following count rates were obtained: 9 ± 2 counts per hour for the pot facing upwards and 0.7 ± 0.3 counts per hour for the pot turned upside down. This is very good evidence that the majority of ^{212}Pb falls out from the air and deposits itself on available surfaces.

In Appendix F it is shown that the large amount of ^{212}Pb that must be in the air at these institutions can be accounted for by the thorium content of building materials in the walls surrounding the various experimental areas.

7.4 The Final Secondary Concentration Procedures for ^{212}Pb

7.4.1 The Final Design and Procedure

The final design of the Solvent-Solvent Extraction Rig is shown in Figure 7.5 which is simply Version C of the rig where the apparatus used to perform the HTiO stage has been removed. This means that after a copper back-extraction in M2, instead of passing the aqueous phase into another vessel on the rig, the solution is removed from the rig and taken to a pressurised ion-exchange column which is shown in Figure 7.3 on page 124.

This ion-exchange column contains 5 millilitres of 200-400 mesh Biorad AG I-X8 and it should be prepared before use by washing it with strong hydrochloric acid to remove any organic residues and water to remove any lead which may have been left on the column from previous experiments. Finally, the column has to be primed with 1M hydrochloric acid before sealing a few days in advance of its use in order to reduce ^{212}Pb backgrounds due to air which gets into the column during its preparation.

A 0.5% w/v solution of DDDC in high purity 2-octanone should also be prepared at least one day in advance of its use in order to allow any ^{212}Pb backgrounds introduced into this solution by air during its preparation to decay away. Similarly if a mock SUF eluate needs to be used the 20 litres of 0.5M hydrochloric acid should also be made a number of days in advance and left sealed to reduce ^{212}Pb backgrounds.

The first stage to concentrate ^{212}Pb from 20 litres of SUF eluate is a solvent-solvent extraction into 1 litre of a 0.5% w/v solution of DDDC in high purity 2-octanone. This is carried out in the same way as that which was used in all the previous versions of the Solvent-Solvent Extraction Rig, although in these experiments the mixing time was increased from 2 minutes to 5 minutes to try to increase efficiencies. After mixing in M1 the contents of M1 is left to stand for 5 minutes before draining 19 litres of liquid directly into C1 and the final 2 litres to mixer M2. In M2 the organic phase is completely separated from the aqueous phase.

Once the organic phase has been separated, the back-extraction by the copper displacement of the lead can be carried out by adding 35 millilitres of 1M hydrochloric acid containing about 70 milligrams of copper in the form of copper chloride. This copper solution is added to M2 using a syringe as is indicated in Figure 7.5. This copper solution is then mixed with the organic phase in M2 by pumping nitrogen gas into the bottom of the separating funnel for 5 minutes and then the phases are left for a few minutes to separate. The back-extracted solution can then be collected from M2 using another syringe, again as indicated in Figure 7.5.

This back-extracted solution is then added to the ion-exchange column via the addition port shown in Figure 7.3 on page 124 and then using pressurised nitrogen gas it is passed though the column at a flow rate of about 3 millilitres per minute. Since this solution is 1M in hydrochloric acid the column extracts the lead but allows the majority of the copper to pass straight through. While the aqueous phase is being passed through the column, the organic phase which is left in M2 should be rinsed sequentially with two 5 millilitre samples of 1M hydrochloric acid, using syringes, to ensure the full recovery of the back-extracted solution. These two samples can then be used, in the same order as they were produced, to wash most of any residual copper from the ion-exchange column after the main back-extracted solution has passed through the column.

Finally, the lead is eluted from the column using a 12 millilitre sample of water which is added and recovered from the ion-exchange column using syringes. This sample ends up being about 0.1M in hydrochloric acid which is suitable for measurement by a single $\beta - \alpha$ counter.

One of the main difficulties which occurred while using Version C of the Solvent-Solvent Extraction Rig was the inability to simultaneously measure the efficiency for concentrating lead and the ^{212}Pb background. It was therefore decided that stable lead would be used as a carrier in all full scale lead

Experiment Number	Procedural Comment	Stable Lead Efficiency	^{212}Pb Background in cph	$\mathcal{R}$ ratio
BRT2	Syringes not used	88.8%	5.6±0.8	3.2±0.5
BRT9	One Rinse of Organic	79.5%	2.4±0.4	1.5±0.3
BRT13	Two Rinses of Organic	83.5%	1.2±0.5	0.7±0.3
BRT14	Two Rinses of Organic	80.4%	1.1±0.6	0.7±0.4
BRT15	1% DDDC used	87.2%	3.4±0.8	1.9±0.5
BRT16	1% DDDC used	87.3%	2.0±0.4	1.1±0.2
BRT22	6min Extraction Time	86.4%	3.2±0.7	1.9±0.4
Average of all except BRT2:		84±3%	2.1±0.2	1.2±0.1

Table 7.7: *The results of concentrating ^{212}Pb from 20 litres of 0.5M hydrochloric acid into a 12 millilitre sample using the final version of the Solvent-Solvent Extraction Rig and a 5 millilitres ion-exchange column. The stable lead and ^{212}Pb content of the final solution was calculated from that measured in samples of the 12 millilitres. From these figures the stable lead efficiency could be determined and the SNO background to signal ratio, $\mathcal{R}$ as defined in Section 6.2 on page 94, is calculated for each experiment. For a full explanation of the procedural comments which describe small differences in procedures between experiments see the main text.*

concentrations and that the final 12 millilitre sample would be measured for both stable lead and ^{212}Pb as was done in experiments BRT4A and BRT4B of Section 7.3.1 on page 126. Hence, 1 millilitre was taken for Atomic Absorption Spectroscopy and 11 millilitres for $\beta - \alpha$ counting. In order to have good sensitivity for the overall efficiency as measured by stable lead, 1 milligram of stable lead needs to be added to the 20 litres of SUF eluate prior to the extraction with the DDDC solution.

7.4.2 The Background and Efficiency of Full Scale Concentrations

The efficiency and background results for concentrating ^{212}Pb from 20 litres of 0.5M hydrochloric acid containing 1 milligram of stable lead are given in Table 7.7. This table also gives comments as to some of the small procedural differences between the procedure as given in the last section and that which was actually used in each of the experiments and these differences are fully explained in the paragraphs below.

The first experiment, experiment BRT2, has a higher ^{212}Pb background than the other experiments because this experiment did not use syringes to transfer solutions to and from apparatus, instead beakers were used which were kept covered to minimise air contact. Since this experiment did not use the syringes to minimise airborne ^{212}Pb contamination its results are not included in the average results given in Table 7.7.

It should be noted that experiments BRT14 and BRT16 were conducted immediately after experiments BRT13 and BRT15 and used the same 20 litres of 0.5M hydrochloric acid in the initial extraction stage. This meant that any carry over of stable lead from one experiment to the next had to be taken into account when calculating overall efficiencies. It was found that there was about 11% of the 1.004 milligrams of stable lead left in the 20 litres after experiment BRT13 and about 7% left after experiment BRT15. The lower figure in experiment BRT15 may be explained by the increased amount of DDDC that was used in this experiment. The use of a 1% w/v solution of DDDC in experiments BRT15 and BRT16 also shows a few percent increase in the overall efficiency of the ^{212}Pb concentration however, this increase is not as large as would be expected by doubling the DDDC concentration.

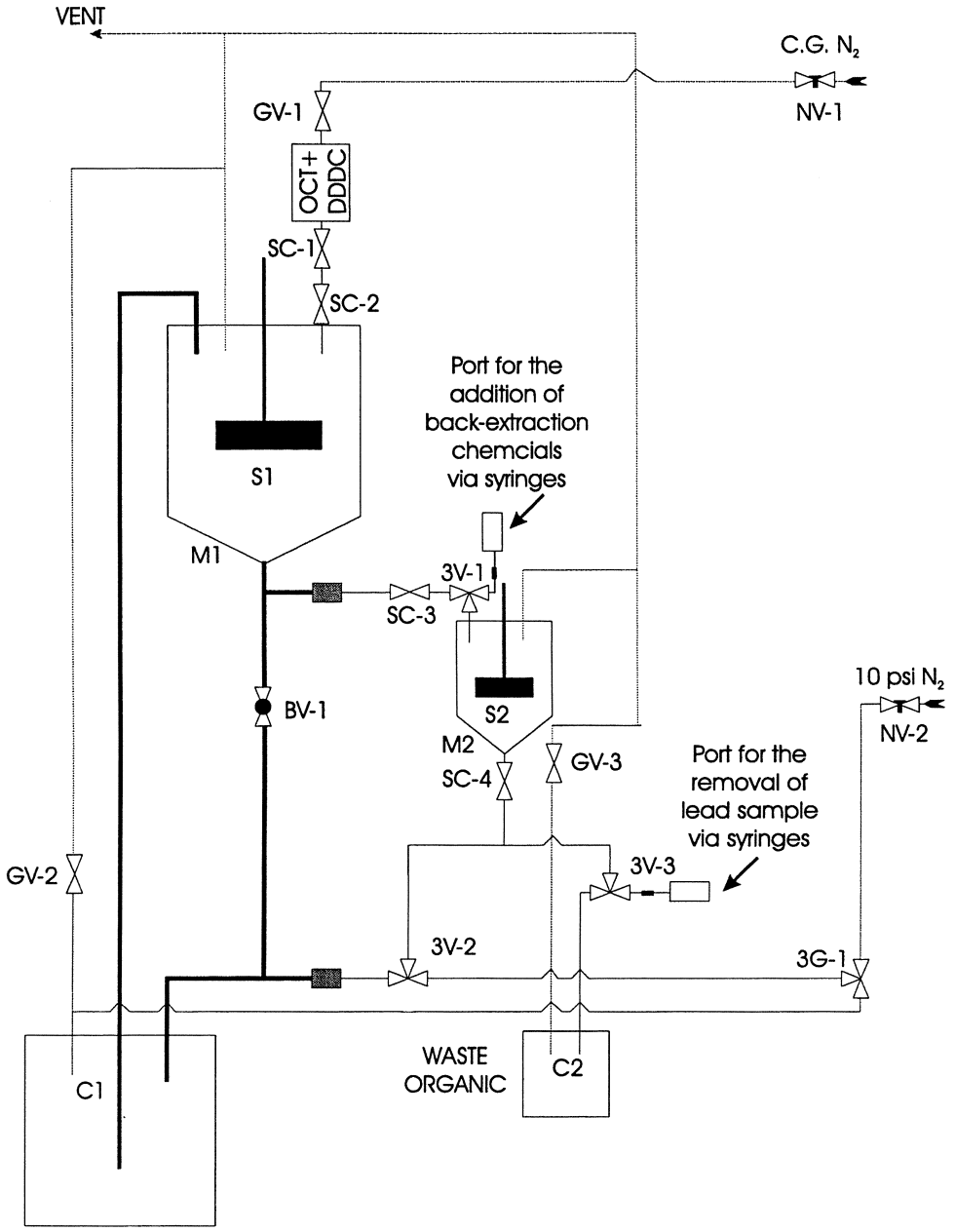

Figure 7.5: *The final design of the Solvent-Solvent Extraction Rig. The two inputs to the diagram are for nitrogen cover gas and pressurised nitrogen, the output is for waste fumes. The 20 litres of SUF eluate starts in vessel C1 and is then forced through half inch diameter pipework into vessel M1, the large mixer. Here the solvent-solvent extraction using 1 litre of a 0.5% w/v solution of DDDC in 2-octanone is carried out. The organic phase then passes to M2, the small mixer, through quarter inch diameter tubing. Here the back-extraction is carried out which displaces the lead ions from the DDDC by adding an excess of copper ions. The sample is then removed from the rig using a syringe and transferred to the ion-exchange column as shown in Figure 7.3 on page 124.*

In Table 7.7 it is indicated that the extraction time in experiment BRT22 was 6 minutes rather than the standard 5 minutes. The results for this experiment do not suggest any obvious difference in extraction efficiencies by increasing the mixing time by just one minute, however a large decrease in efficiency was observed when a mixing time of 10 minutes was used and this is discussed in Section 7.4.4 on page 134.

Other small differences in the overall efficiency of experiments may have been due to differences in the rinsing procedures of the organic phase in M2. In experiment BRT2 there were no rinses of the organic phase in M2 and in experiment BRT9 there was only one rinse. In all of the other experiments two rinses were used according to the procedure detailed in the previous section.

It can be seen from Table 7.7 that the overall efficiency of the process, as measured by stable lead, is very reproducible and the average efficiency of the experiments (ignoring experiment BRT2) comes to 84±3%. The measured ^{212}Pb backgrounds were all significantly lower than those measured using other versions of the Solvent-Solvent Extraction Rig which were detailed in the last chapter. It is expected that this decrease in ^{212}Pb backgrounds has been achieved both by the removal of the impractical HTiO stage and by a better understanding of the consequences of airborne ^{212}Pb.

The SNO background to signal ratio, $\mathcal{R}$, as defined in Section 6.2 on page 94, is given for each experiment in Table 7.7 and the average value (ignoring experiment BRT2) can be calculated to be 1.2±0.1. This means that the ^{212}Pb procedural background for concentrating ^{212}Pb from the SUF eluate is about the same size as the expected signal from the SNO detector. Although ideally this value of $\mathcal{R}$ should be smaller still this value would allow the detection of the SNO signal and is a major improvement on the values of around 8 which were measured in the last chapter.

The measurements given in this chapter show that the Solvent-Solvent Extraction Rig together with an ion-exchange column provides the secondary concentration procedures required to perform ^{212}Pb assays from the heavy water of the SNO experiment using the HTiO SUF assay system.

7.4.3 Comparing Measurements of Efficiencies using Stable Lead and ^{212}Pb

Three experiments were carried out to examine any differences between efficiencies measured using stable lead and those measured using ^{212}Pb. This was done by adding a known amount of ^{212}Pb, manufactured by the procedure detailed in Chapter 4, to 20 litres of 0.5M hydrochloric acid along with a carrier of stable lead and then concentrating both the ^{212}Pb and the stable lead into a 12 millilitre sample for measurement using the procedures described in Section 7.4.1 on page 131.

The first two experiments, experiments BRT18 and BRT19, were carried out in sequence using the same initial 20 litres and so the carry over of lead which was not extracted from the 20 litres of experiment BRT18 had to be taken into account when calculating the efficiency of experiment BRT19. The efficiency results of these two experiments and one other experiment, experiment BRT22, measured both by stable lead and ^{212}Pb are compared in Table 7.8.

Experiment	Stable Lead Efficiency	^{212}Pb Efficiency	Difference
BRT18	89.2%	109±7%	+2.8σ
BRT19	89.5%	92±6%	+0.4σ
BRT22	81.0%	69±4%	-3.0σ

Table 7.8: *The results of three experiments designed to compare the efficiency of Version C of the Solvent-Solvent Extraction Rig as measured by both stable lead and, at the same time,* ^{212}*Pb.*

The results of these experiments show no overall systematic difference between measuring the efficiency with stable lead or ^{212}Pb but there are differences in the measurements of the individual experiments. In experiments BRT18 and BRT19 a low activity ^{212}Pb source was used and the usual ^{212}Pb background

reducing steps were not taken so there is some suspicion that a large ^{212}Pb background was responsible for elevating the measured ^{212}Pb efficiency above 100%. It is not understood why the ^{212}Pb efficiency in experiment BRT22 was much lower that that measured using the stable lead.

It would obviously have been beneficial to carry out more experiments to verify that ^{212}Pb does indeed behave the same as the stable lead in this process, as would be expected, but unfortunately there was not time to carry out further experiments at BNL. In Section 6.6.2 on page 107 the results of experiments using Version C of the Solvent-Solvent Extraction Rig showed no differences between efficiencies measured using ^{212}Pb and stable lead in the same, acidic conditions as the experiments discussed here. It therefore seems that the most reasonable conclusion to make is that these differences are caused by underestimating systematic errors.

7.4.4 The Measured Decomposition of DDDC in the Extraction Stage

While carrying out experiments to evaluate the secondary concentration procedures for ^{212}Pb the time of mixing in the extraction stage in some experiments was varied between 2 minutes and 10 minutes. The overall stable lead efficiency was measured to decrease from 80% when a 2 minute extraction was used to 50% when a 10 minute extraction was used. One possible explanation for this drop in efficiency is that the DDDC in the 2-octanone decomposes while it is being mixed with the 0.5M hydrochloric acid. The decomposition of DDDC in acidic conditions is a known phenomena. In Section 5.2.4 on page 73 it was noted that when equal phase volumes of DDDC in carbon tetrachloride and 1M hydrochloric acid are mixed together it requires 20 minutes of mixing to reduce the concentration of the dithiocarbamate ion in the organic phase by a factor of two [Bod59]. Also, in Section 5.5.3 on page 81 losses of efficiency attributed to DDDC decomposition in 2-octanone were observed after 20 minutes of mixing with 0.5M hydrochloric acid. Therefore it is not unreasonable to expect some DDDC decomposition after 10 minutes of mixing a solution in 2-octanone with 0.5M hydrochloric acid.

In Section 7.2.2 on page 117 it was suggested that the amount of copper used in the back-extraction can allow the determination of the amount of DDDC left after the back-extraction. In summary this can be done by assuming that two DDDC molecules are needed to extract one copper ion and that after the back-extraction any DDDC left is saturated with copper. The amount of copper needed to back-extract the lead in all of the solvent-solvent extractions which used a 5 minute extraction mixing time was found to be very similar and showed that only about 4% of the 22.5 millimoles of DDDC that was initially added to each litre of 2-octanone was left after the back-extraction.

If the DDDC does decompose with the time of extraction mixing it would be expected that there would be an exponential relationship between the time of extraction and the deduced amount of DDDC left after the back-extraction. Therefore, in Table 7.9 the results of experiments which concentrated lead from 20 litres of 0.5 M hydrochloric acid in which the extraction time was varied are listed alongside the measured amount of copper used in the back-extraction and the deduced amount of DDDC left after the back-extraction. This deduced amount of DDDC is plotted against the time of extraction mixing in Figure 7.6 and fitted to an exponential in time. The results of this fit are shown in the figure and confirm that the DDDC seems to be decomposing exponentially in time with a half-life of 3.2±0.4 minutes.

Unfortunately, the fit also suggests that if there was no mixing there would still only be about 11% of the DDDC left after the back-extraction and so it is clear that there is more than one method by which the DDDC decomposes. In Section 7.2.2 on page 117 there was some evidence that further decomposition is occurring within the back-extraction stage itself but only further experimentation could verify this.

Experiment Number	Time of Extraction	Stable Lead Efficiency	Amount of Cu used		Amount of DDDC Left	
			in mg	in mmol	in mmol	in %
BRT20	2 minutes	86.4%	55.2	0.869	1.738	7.8
BRT19	5 minutes	89.5%	25.8	0.406	0.812	3.6
BRT22	6 minutes	81.0%	18.0	0.283	0.566	2.6
BRT21	10 minutes	50.3%	9.4	0.148	0.296	1.4

Table 7.9: *The results of the copper back-extractions in four full scale ^{212}Pb concentrations which used different times of mixing in the extraction stage. In each experiment 1 litre of a 0.5% w/v solution of DDDC in 2-octanone was used which means that initially there was 22.5 millimoles of DDDC present. The calculated amount of DDDC left after the extraction stage assumes that two DDDC molecules are needed to combine with one copper molecule and that any DDDC left after the back-extraction is saturated with copper.*

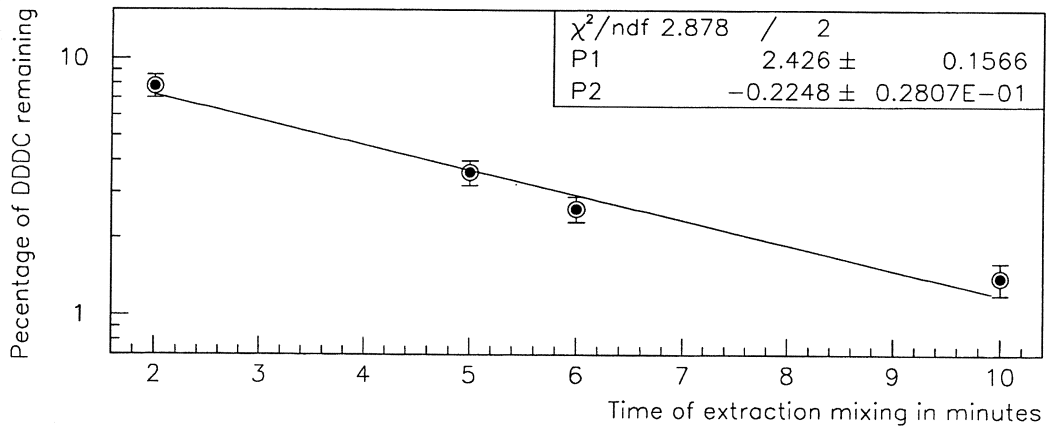

Figure 7.6: *The above figure takes the calculated values of the amount of DDDC left during the back-extraction of four different experiments, as given in Table 7.9, assumes 10% errors and plots it against the time of mixing in minutes used in the extraction stage. The fit values displayed in this figure are for the following exponential: $Y = e^{(P1+P2X)}$, where $-P2$ is the decay constant for the decomposition in minutes^{-1}.*

Experiment Number	Time of Extraction	Lead Efficiency	Amount of Cu used		Amount of DDDC Left	
			in mg	in mmoles	in mmoles	in %
BRT11	10 minutes	31.9%	6.1	0.096	0.192	0.9
BRT12	5 minutes	83.4%	23.0	0.362	0.724	3.2
BRT17	5 minutes	81±6%	25.6	0.403	0.806	3.6

Table 7.10: *The results of full ^{212}Pb concentrations using recycled 2-octanone. The overall efficiency of experiments BRT11 and 12 were measured using the stable lead carrier whereas for experiment BRT17 it was measured using a source of ^{212}Pb. The loss of extraction efficiency in experiment BRT11 was due to the 10 minutes of mixing in the extraction stage and is similar to that which was observed in experiment BRT21 which used fresh 2-octanone and also had 10 minutes of mixing.*

7.4.5 The Possibility of Recycling 2-Octanone

In Section 6.7.1 on page 112 it was found that there was a need to use only high purity (99+%) 2-octanone for solvent-solvent extractions due to the fact that the low purity (98%) 2-octanone can contain a poison which inhibits lead extractions with DDDC. Unfortunately, the high purity 2-octanone is not as readily available as the low purity 2-octanone and this produced a shortage of 2-octanone at BNL during the research which is detailed in this chapter. Since this is a possible occurrence at the SNO experiment some investigations were made into the possibility of reusing the high purity 2-octanone in successive ^{212}Pb concentrations.

The first experiment using 2-octanone which had been previously used in a DDDC extraction was a small scale experiment similar to those described in Section 7.2.2 on page 117. This experiment used 25 millilitres of 2-octanone which had gone through an entire process of lead extraction, copper back-extraction and an hour long acid back-extraction to remove the copper. This 2-octanone was rinsed several times with water before the addition of more DDDC. It was then used to perform a second extraction and back-extraction under similar conditions to the first. The efficiency of the extraction and back-extraction was determined by stable lead analysis to be 100±1% which is the same as the efficiency obtained in experiments using fresh 2-octanone. However, there was a difference in the deduced amount of DDDC left after the back-extraction. By measuring the amount of copper extracted in the back-extraction it was seen that when using this rinsed 2-octanone only about 4% of the DDDC remained after the back-extraction and this can be compared to between 10 and 20% when using fresh 2-octanone in small scale experiments. This result implies that there was some acid or other impurity left in the 2-octanone which speeded up the DDDC decomposition.

Since the small scale experiment had given a good efficiency, three full scale experiments to concentrate ^{212}Pb were completed using 2-octanone from a previous ^{212}Pb experiment. This 2-octanone had been used for just one DDDC extraction, copper back-extraction and acid back-extraction. It was then rinsed with a large amount of water and dried using magnesium sulphate by Dr K.Rowley before having some more DDDC added and being used in a further DDDC extraction. The overall lead efficiency in each of the experiments which used the recycled 2-octanone, along with the amount of copper used in the back-extraction and the deduced amount of DDDC left after the back-extraction, are given in Table 7.10.

By comparing the result of experiment BRT11 in Table 7.10 with that of experiment BRT21 in Table 7.9 it can be seen that 10 minutes of mixing in the extraction stage when using recycled 2-octanone shows a similar loss of efficiency as was seen when using fresh 2-octanone. It is possible that the decomposition of DDDC is greater in the recycled 2-octanone than in new 2-octanone but it is hard to be certain without more experimental results. The results of experiments BRT12 and BRT17, as given in Table 7.10, both give very similar efficiencies and DDDC decomposition when compared to experiments using fresh 2-octanone, for example compare to the results of experiment BRT19 given in Table 7.9.

It is interesting to note some of the colour changes that are observed when using recycled 2-octanone. Firstly, the recycled 2-octanone contained a yellow colouring which is very different to the colourless fresh 2-octanone. This yellow colouring was seen to change to a pinkish colouring on the addition of DDDC and finally to a dark brown colouring after it was used to extract lead from 0.5M hydrochloric acid. Since these colours were not observed with fresh 2-octanone it can only be concluded that they are due either to some residual copper in the 2-octanone or, more likely, they are due to some decomposition products of DDDC which remain in the 2-octanone. To produce such colours these decomposition products are unlikely to be simply carbon disulphide and an amine as was suggested in Section 5.2.4 on page 73.

One other possibility for recycling the 2-octanone which was not investigated would be to use re-distillation which would be expected to remove any impurities within the 2-octanone that it gains from taking part in a solvent-solvent extraction using DDDC.

The conclusion of these few experiments is that it is possible, if necessary, to recycle 2-octanone. However, it should be noted that in these three experiments the 2-octanone was only recycled once and if the same 2-octanone was to be recycled for several extractions there may be the possibility for the accumulation of impurities which could effect both efficiencies and ^{212}Pb backgrounds. It is, of course, far more preferable to continue to use new, fresh, high purity 2-octanone for each full scale solvent-solvent extraction if the amounts required can be purchased from a chemical supplier.

7.5 Final Conclusions

In this chapter final procedures have been developed using the Solvent-Solvent Extraction Rig which take about an hour to extract lead from 20 litres of 0.5M hydrochloric acid into a 12 millilitre sample which can be measured for ^{212}Pb activity by a single $\beta - \alpha$ delayed coincidence scintillation counter. In Chapters 5 and 6 it was shown that these methods are not affected by a large amount of titanium in the 20 litres of 0.5M hydrochloric acid and so they can be used to perform the secondary concentration of lead from the elutions of the membrane pairs used by the HTiO SUF assay system.

In this chapter it has been shown, by using stable lead as a carrier, that the amount of ^{212}Pb in an SUF eluate can be concentrated into a 12 millilitre sample with a known, reproducible efficiency of 84±3%. The ^{212}Pb procedural background to this process when carried out in the experimental area at BNL has been shown to be about the same as the amount of ^{212}Pb it would expect to extract from the SUF eluate if the amount of ^{212}Pb in the heavy water of the SNO detector is at the level which will produce neutrons at a rate equal to about one tenth of the rate with which they are expected to be produced by NC neutrino interactions. It is suspected that the remaining source of ^{212}Pb background is due to airborne ^{212}Pb. The amount of airborne ^{212}Pb has been measured in the different experimental areas and has been found to be much lower at the actual site of the chemical processing in Sudbury that at the experimental area used at BNL. It is therefore hoped that the ^{212}Pb procedural background to measuring the amount of ^{212}Pb in the SUF eluate at the SNO experiment in Sudbury will be much lower.

The three procedures to perform the secondary concentration of ^{212}Pb from up to 20 litres of SUF eluate into a 12 millilitre sample are:

1. A solvent-solvent extraction using 1 litre of a 0.5% w/v solution of diethylammonium diethyldithiocarbamate (DDDC) in high purity (99+%) 2-octanone.

2. A back-extraction into 35 millilitres of 1M hydrochloric acid using 70 milligrams of copper.

3. A final concentration using a 5 millilitre, pressurised ion-exchange column made from 200-400 mesh Biorad AG I-X8.

These procedures make up the final stage of a ^{212}Pb assay from the heavy water of the SNO detector using the HTiO SUF assay system. The first stage of this ^{212}Pb assay is the extraction of the ^{212}Pb from the heavy water using ultra-filtration membranes coated with hydrous titanium oxide (HTiO) placed on the SUF Rig. The second stage is the elution of the ^{212}Pb from the HTiO by circulating 20 litres of 0.5M hydrochloric acid through the membranes for 20 minutes using the Elution Rig. The details of these two procedures are given in Chapter 3 where it was also stated that these stages will need to be calibrated. This can be done using either stable lead or sources of ^{212}Pb manufactured by the procedure given in Chapter 4 to be free from long-lived activity.

If radioactive backgrounds to all of these chemical procedures can be kept low then, by using them, it should be possible to assay the amount of ^{212}Pb within the heavy water of the SNO detector through the methods described in the analysis of Chapter 3. Such a ^{212}Pb assay should enable the SNO experiment to determine the contribution to the neutral current background due to isotopes from the ^{232}Th decay chain in the heavy water.

When this result is combined with the results of other background measuring techniques which were discussed in Chapter 2, the SNO experiment should be able to determine the total NC background. Once this is achieved it will then be possible for the SNO experiment to find the ratio of the rate of neutrino neutral current (NC) interactions to charged current (CC) interactions. The value of this CC/NC ratio can show if the neutrinos coming from the Sun are oscillating between flavours. If neutrino oscillations are observed then this means that neutrinos have a small, finite mass which was discussed in Chapter 1.

Appendix A

Mathematical Model of a Double Membrane System

A.1 Introduction

In this appendix there are details of the analysis of the HTiO SUF assay system, the results of which are used in Chapter 3. This analysis starts by solving the coupled differential equations that were given in Section 3.3.2 on page 34 to give expressions for the activity of ^{228}Th, ^{224}Ra and ^{212}Pb on each membrane pair after a certain time of extraction. The method by which the HTiO SUF assay system will measure these activities is then modelled and finally exact algebraic expressions to calculate the amount of ^{228}Th, ^{224}Ra and ^{212}Pb in the heavy water together with many of the parameters which describe the system are derived.

A.2 Solutions to the Differential Equations

The equations given in Section 3.3.2 on page 34 can be solved by substituting trial solutions to produce expressions for the amount of activity of ^{228}Th, ^{224}Ra and ^{212}Pb on each membrane pair as functions of the extraction time. These expressions are given in terms of the feed activity flow rates of ^{228}Th, ^{224}Ra and ^{212}Pb (F_{Th}, F_{Ra} and F_{Pb}) and the various parameters which describe the system which are defined in Section 3.3.2 on page 33. Relatively simple expressions for the activity of ^{228}Th on both membrane pairs as a function of the time of extraction, t, can be found quite easily. Unfortunately, for ^{224}Ra and ^{212}Pb the decays of parent isotopes have to be taken into account which means that solutions are rather complicated.

In order to simplify the algebra, without losing the symmetry of the problem, six new constants and six new time dependent variables are defined. The first three constants: K_1, K_2 and K_3, are three ratios of the decay constants for ^{228}Th, ^{224}Ra and ^{212}Pb and are defined in Equation A.1. The second set of three constants: X, Y and Z, are combinations of the parameters describing the system and they are defined in Equation A.2. The first three variables: T_1, T_2 and T_3, are time dependent functions of the decay exponentials for each isotope, they have the dimension of time and are defined in the same way for each isotope as shown in Equation A.3. The second set of three variables: R_1, R_2 and R_3, are the three time dependent dimensionless ratios of T_1, T_2 and T_3 and are defined in Equation A.4.

$$K_1 \equiv \frac{\lambda_{Ra}}{\lambda_{Ra}-\lambda_{Th}} = 1.0053 \quad ; \quad K_2 \equiv \frac{\lambda_{Pb}}{\lambda_{Pb}-\lambda_{Th}} = 1.0006 \quad ; \quad K_3 \equiv \frac{\lambda_{Pb}}{\lambda_{Pb}-\lambda_{Ra}} = 1.1372 \tag{A.1}$$

$$Z \equiv \alpha_{Ra}\eta(1-\delta) + \delta(1-\alpha_{Th}) \quad ; \quad Y \equiv \alpha_{Pb}\mu(1-\epsilon) + \epsilon(1-\alpha_{Ra}) \quad ; \quad X \equiv \alpha_{Pb}\mu(1-\epsilon)\delta + \epsilon Z \tag{A.2}$$

$$T_{Th}(t) \equiv \frac{1-e^{-\lambda_{Th}t}}{\lambda_{Th}} \quad ; \quad T_{Ra}(t) \equiv \frac{1-e^{-\lambda_{Ra}t}}{\lambda_{Ra}} \quad ; \quad T_{Pb}(t) \equiv \frac{1-e^{-\lambda_{Pb}t}}{\lambda_{Pb}} \tag{A.3}$$

$$R_1(t) \equiv 1 - \frac{T_{Ra}(t)}{T_{Th}(t)} \quad ; \quad R_2(t) \equiv 1 - \frac{T_{Pb}(t)}{T_{Th}(t)} \quad ; \quad R_3(t) \equiv 1 - \frac{T_{Pb}(t)}{T_{Ra}(t)} \tag{A.4}$$

The full expressions using these definitions for the activity of ^{228}Th, ^{224}Ra and ^{212}Pb on the first and second membrane pairs after an extraction of t hours are shown in Equations A.5 to A.10. Using these equations the activities of ^{228}Th, ^{224}Ra and ^{212}Pb on either membrane pair can be calculated for a given extraction time if the parameters describing the system and the amount of each isotope in the heavy water are known.

$$A_{Th}^{M1}(t) = T_{Th}(t)\alpha_{Th}F_{Th} \tag{A.5}$$

$$A_{Ra}^{M1}(t) = T_{Ra}(t)\alpha_{Ra}F_{Ra} + T_{Th}(t)\alpha_{Th}F_{Th}\delta K_1 R_1(t) \tag{A.6}$$

$$A_{Pb}^{M1}(t) = T_{Pb}(t)\alpha_{Pb}F_{Pb} + T_{Ra}(t)\alpha_{Ra}F_{Ra}\epsilon K_3 R_3(t) + T_{Th}(t)\alpha_{Th}F_{Th}\epsilon\delta K_1[K_3(R_1(t)-R_2(t)) + K_2 R_2(t)] \tag{A.7}$$

$$A_{Th}^{M2}(t) = T_{Th}(t)\alpha_{Th}(1-\alpha_{Th})F_{Th} \tag{A.8}$$

$$A_{Ra}^{M2}(t) = T_{Ra}(t)\alpha_{Ra}(1-\alpha_{Ra})F_{Ra} + T_{Th}(t)\alpha_{Th}F_{Th}ZK_1R_1(t) \tag{A.9}$$

$$A_{Pb}^{M2}(t) = T_{Pb}(t)\alpha_{Pb}(1-\alpha_{Pb})F_{Pb} + T_{Ra}(t)\alpha_{Ra}F_{Ra}YK_3R_3(t) + T_{Th}(t)\alpha_{Th}F_{Th}XK_1[K_3(R_1(t)-R_2(t)) + K_2R_2(t)] \tag{A.10}$$

A.3 Details of Modelling the Chemical Processing and Counting

The expressions of the last section allow the activities of ^{228}Th, ^{224}Ra and ^{212}Pb on each membrane pair after an assay of a given time to be calculated for a wide range of initial conditions. The HTiO SUF assay system will not directly measure these activities but will strip the activities from the membrane pairs, concentrate it into a small volume and measure the activity on low level counters. This introduces two main errors: the error on the efficiency for the chemical concentration procedures and the statistical counting error. In this section the details of modelling the chemical processing and counting techniques will be described.

The first effects to model were the time delays in performing the chemical processing. It is expected that it will take about 1 hour to remove the two membrane pairs from the SUF Rig situated underground

at the SNO experiment and transport them above ground to the Elution Rig. During this time the activities of ^{228}Th, ^{224}Ra and more significantly ^{212}Pb will be reduced by their half-lives, however decays of ^{228}Th on each membrane will add to the activity of ^{224}Ra and decays of ^{224}Ra will add to the activity of ^{212}Pb and so both of these effects have to be taken into account to calculate the overall effect of this, first time delay. After the three isotopes have been removed from the membrane pairs it is expected that there will be a further, second time delay of about 1.5 hours before the start of counting. During this time the activities of ^{228}Th, ^{224}Ra and, more significantly, ^{212}Pb will simply be reduced by their half-lives since during this delay the isotopes can be assumed to have been isolated from each other.

The second effects to model were the overall chemical processing and counting efficiencies for ^{228}Th, ^{224}Ra and ^{212}Pb. It was assumed that the overall chemical processing for radium is that which was discussed in Section 3.2.3 on page 31 which consists of a 90% efficient elution, a 75% efficient secondary concentration procedure and a 50% counting efficiency making an overall efficiency of 35%. It was assumed that a similarly efficient secondary concentration procedure for lead and thorium will be developed. This gives overall efficiencies for lead and thorium of 35% and 25% respectively taking into account the different elution efficiencies for lead and thorium. These overall efficiencies are expressed by the following three quantities:

$$\beta_{Th} = 0.25 \quad ; \quad \beta_{Ra} = 0.35 \quad ; \quad \beta_{Pb} = 0.35$$

Finally, it was necessary to model the total number of counts expected to be measured for each sample of ^{212}Pb, ^{224}Ra and ^{228}Th which is obviously dependent upon the length of time that samples can be measured. A reasonable time period for measurement is one week and so to calculate a time factor for each isotope an expression for the number of ^{212}Bi decays as a function of time due to a pure sample of that isotope was integrated for one week. The resulting time factors allow the conversion of initial count rates in counts per hour into total numbers of measured counts and these conversion factors have the following values for each isotope:

$$D_{Th} = 64.3 \quad ; \quad D_{Ra} = 88.6 \quad ; \quad D_{Pb} = 13.7$$

The total number of counts of ^{228}Th, ^{224}Ra and ^{212}Pb for the first and second pairs of membranes after an assay can be calculated from the time delay adjusted activity of that isotope on each pair of membranes, the $\overline{A_i^{Mj}}$'s, by multiplying by the overall chemical processing and counting efficiencies, the β_i's, and by the conversion factors, the D_i's, as is shown in Equation A.11.

$$C_i^{Mj} = D_i \beta_i \overline{A_i^{Mj}} \qquad j = 1, 2; i = Th, Ra, Pb \tag{A.11}$$

To model a 10% systematic error of knowing the secondary concentration efficiencies (β_{Th}, β_{Ra} and β_{Pb}) the value of each β_i used in Equation A.11 was selected randomly from a Gaussian shaped distribution centred around the true β_i values with a width equal to $\beta_i/10$.

Integer measured values of the total numbers of counts for each isotope on each membrane pair were then modelled by randomly selecting values for the C_i^{Mj}'s from Gaussian distributions centred around the exact C_i^{Mj} values with a width equal to the square root of this exact value. Obviously this is only valid for total count numbers greater than about 20 since Poisson statistical errors should be used for small numbers. However, for the purposes of this analysis the approximation to Gaussian errors is reasonable.

Using these modelled total numbers of counts, measured values for the activities of each isotope on each membrane pair after an assay were calculated by carrying out the reverse of the process described above using exact values for the β_i's.

In the next section it will be described how the amount of ^{228}Th, ^{224}Ra and ^{212}Pb in the heavy water flowing into the HTiO SUF system can be calculated from measurements of the activity of these isotopes extracted onto each pair of membranes.

A.4 Expressions to Calculate Feed Activities and Parameters from Measured Values

The primary aim of the HTiO SUF assay system is to be able to calculate the amount of ^{228}Th, ^{224}Ra and, especially, ^{212}Pb in the heavy water from measured values after an extraction. The double membrane design of the SUF system allows the possibility of the simultaneous determination of the extraction probabilities and the loss parameters which describe the system. Obviously the values of these parameters are not expected to vary greatly between different extractions and so after several extractions average values will eventually be obtained. However, it would be highly beneficial, especially in the initial understanding of the system, to be able to monitor the values of these parameters in each extraction.

Using Equations A.5 to A.10 given in Section A.2 on page 140 it is possible to calculate expressions for the feed activity flow rates of ^{212}Pb, ^{224}Ra and ^{228}Th (F_{Th}, F_{Ra} and F_{Pb}) and the extraction probabilities (α_{Th}, α_{Ra} and α_{Pb}) in terms of the loss parameters (δ and ϵ) and the activities of ^{212}Pb, ^{224}Ra and ^{228}Th on the first and second membrane pairs after an extraction from the heavy water.

Expressions for α_{Th} and F_{Th} can be obtained simply in terms of the activity of ^{228}Th on the first and second membrane pair after an extraction, A_{Th}^{M1} and A_{Th}^{M2}. These expressions are shown in Equation A.12 and they allow F_{Th} and α_{Th} to be calculated simultaneously after a single extraction.

$$\alpha_{Th} = 1 - \frac{A_{Th}^{M2}}{A_{Th}^{M1}} \quad ; \quad F_{Th} = \frac{A_{Th}^{M1}}{T_{Th}(t)\alpha_{Th}} \tag{A.12}$$

Expressions for α_{Ra} and F_{Ra} can be obtained in terms of δ, η and the activities of ^{224}Ra and ^{228}Th on the first and second membrane pairs after an extraction and these are shown in Equations A.13 and A.14 respectively. In these equations approximate expressions for α_{Ra} and F_{Ra} are also given which are valid for extractions lasting a short time compared to the 87.8 hour half-life of ^{224}Ra. These approximate expressions are found by assuming that at small times $K_1R_1(t) \to 0$ which can be justified by observing the time dependence of $K_1R_1(t)$ as shown in Figure A.1.

$$\alpha_{Ra} = \frac{K_1R_1(t)(A_{Th}^{M1} - A_{Th}^{M2})\delta - (A_{Ra}^{M1} - A_{Ra}^{M2})}{K_1R_1(t)(1-\eta)A_{Th}^{M1}\delta - (A_{Ra}^{M1} - \eta K_1R_1(t)A_{Th}^{M1})} \overset{t \ll 87.8}{\longrightarrow} 1 - \frac{A_{Ra}^{M2}}{A_{Ra}^{M1}} \tag{A.13}$$

$$F_{Ra} = \frac{A_{Ra}^{M1} - \delta K_1R_1(t)A_{Th}^{M1}}{T_{Ra}(t)\alpha_{Ra}} \overset{t \ll 87.8}{\longrightarrow} \frac{A_{Ra}^{M1}}{T_{Ra}(t)\alpha_{Ra}} \tag{A.14}$$

The exact expressions for α_{Ra} and F_{Ra} show that if δ is unknown then for one extraction there are three unknowns and only two equations which means that α_{Ra}, F_{Ra} and δ cannot be simultaneously calculated after a single extraction. However, if a short extraction time is used then the approximate expressions are valid and they have no terms involving δ which means that by using short extraction times α_{Ra} and F_{Ra} can be simultaneously calculated. To be able to calculate δ the results of two extractions will have to be combined and the two simultaneous equations for δ and α_{Ra} solved.

The solutions for lead are even more complicated than that for radium, but exact expressions for α_{Pb} and F_{Pb} can be found. These exact expressions are shown in Equations A.15 and A.16 respectively in terms of a new time dependent variable, $V(t)$, which is defined in Equation A.17.

The value of $-V(t)$ at different times has been calculated and is shown in Figure A.1. This shows that at all times $V(t)$ is negative and very small and so approximate expressions for α_{Ra} and F_{Pb} can be found by setting $V(t) \to 0$ and these are given alongside the exact expressions in Equations A.15 and A.16.

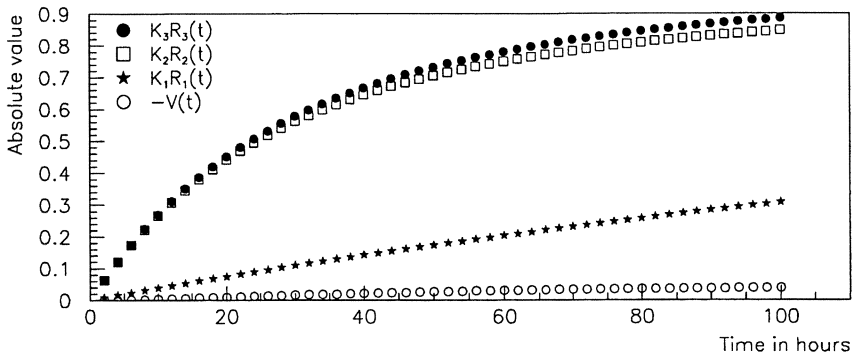

Figure A.1: *This figure gives calculated values of several variables that are used in the analysis of the HTiO SUF assay system at different times. The definitions of these variables can be found in Equations A.1, A.4 on page 140 and Equation A.17 on page 143.*

$$\begin{aligned}\alpha_{Pb} &= \frac{\{K_3R_3(t)(A_{Ra}^{M1}-A_{Ra}^{M2})+V(t)[\delta(A_{Th}^{M1}-A_{Th}^{M2})-\alpha_{Ra}\eta(1-\delta)A_{Th}^{M1}]\}\epsilon-(A_{Pb}^{M1}-A_{Pb}^{M2})}{\{(K_3R_3(t)A_{Ra}^{M1}+\delta V(t)A_{Th}^{M1})(1-\mu)\}\epsilon-(A_{Pb}^{M1}-\mu K_3R_3(t)A_{Ra}^{M1}-\mu\delta A_{Th}^{M1}V(t))} \\ &\cong \frac{K_3R_3(t)(A_{Ra}^{M1}-A_{Ra}^{M2})\epsilon-(A_{Pb}^{M1}-A_{Pb}^{M2})}{K_3R_3(t)(1-\mu)A_{Ra}^{M1}\epsilon-(A_{Pb}^{M1}-\mu K_3R_3(t)A_{Ra}^{M1})} \end{aligned} \tag{A.15}$$

$$F_{Pb} = \frac{A_{Pb}^{M1}-\epsilon K_3R_3(t)A_{Ra}^{M1}-\epsilon\delta V(t)A_{Th}^{M1}}{T_{Pb}(t)\alpha_{Pb}} \cong \frac{A_{Pb}^{M1}-\epsilon K_3R_3(t)A_{Ra}^{M1}}{T_{Pb}(t)\alpha_{Pb}} \tag{A.16}$$

$$V(t) \equiv K_1[K_3(R_1(t)-R_2(t))+K_2R_2(t)]-K_1R_1(t)K_3R_3(t) \tag{A.17}$$

The expressions for α_{Pb} and F_{Pb} show that if ϵ is unknown then for one extraction there are three unknowns and only two equations which means that α_{Pb}, F_{Pb} and ϵ cannot be simultaneously calculated after a single extraction. Unfortunately, unlike in the equations for radium, a further approximation to remove terms containing ϵ cannot be made since it can be seen from Figure A.1 that the term $K_3R_3(t)$ is never very small.

It is clear that more information is needed to calculate F_{Pb}, the feed activity flow rate for ^{212}Pb, and hence the amount of ^{212}Pb in the heavy water after a single extraction. This can be obtained by calibrating for α_{Pb}, the lead extraction efficiency. If this lead extraction efficiency is calibrated the radon breakthrough parameter, ϵ, can be calculated from α_{Pb} and the activities of isotopes on the membrane pairs after a single extraction by rearranging the expressions given in Equation A.15. An approximate expression to calculate ϵ can be found by setting $V(t) \to 0$ and this is given in Equation A.18.

$$\epsilon \cong \frac{(A_{Pb}^{M1}-\mu K_3R_3(t)A_{Ra}^{M1})\alpha_{Pb}-(A_{Pb}^{M1}-A_{Pb}^{M2})}{K_3R_3(t)(1-\mu)A_{Ra}^{M1}\alpha_{Pb}-K_3R_3(t)(A_{Ra}^{M1}-A_{Ra}^{M2})} \tag{A.18}$$

Appendix B

Gamma Counting

B.1 Introduction to Gamma Ray Detectors

Gamma ray photons are detected through their three main interactions with matter: photo-electric absorption, Compton scattering and pair production. These interactions can be detected using either a scintillation detector or a solid state detector. The solid state detectors produce far better energy resolution than scintillation detectors because they require much lower energy to produce an electron-hole pair. Both silicon and germanium can be used in solid state gamma detectors but germanium has a higher absorption coefficient for gamma rays which explains its preferred use. One difficulty in using germanium detectors is that at room temperature thermal dark currents can occur due to the very low energy band gap of germanium of 0.67eV. To eliminate such dark currents germanium detectors are always operated at low temperatures, typically 77K.

In the past it was not possible to produce large germanium crystals with no impurities and so germanium detectors were made with lithium drifted into the crystal to compensate for these impurities. These, so called Ge(Li), detectors act in a very similar way to the more commonly used intrinsic germanium detectors but because the lithium can diffuse at room temperature the Ge(Li) detectors have to be kept at 77K even when not in operation.

B.2 The Measurement of Gamma Decays from ^{232}Th

The decay chain for ^{232}Th was shown in Figure 2.3 on page 24 of this thesis where it was explained that for the purposes of the SNO experiment it is only important to measure the presence of isotopes lower than ^{228}Th in the decay chain. These isotopes have many gamma decays of energies in a suitable range for detection using germanium counters and in Table B.1 these are listed together with values for the branching ratios to these decays from both their immediate parent and from isotopes of the main decay chain assuming equilibrium in the decay chain.

These gamma decays were measured for the research detailed in this thesis using both a Ge(Li) detector situated at Oxford and an intrinsic germanium detector at the Brookhaven National Laboratory (BNL), New York, USA. The samples to be measured for gamma activity at both institutions were usually in the form of aqueous or organic solutions. These solutions were diluted to a constant volume of 50 or 60 millilitres at Oxford and 20 millilitres at BNL. They were then measured for gamma activity in counting bottles of a standard geometry placed in a constant position relative to the detector. These standard techniques were used to eliminate effects caused by the scattering and absorption of gamma rays between comparing measurements of samples contained in different geometries. In Section 4.4.1 on page 52 there are some details of an investigation into the effect of measuring sources of different geometry.

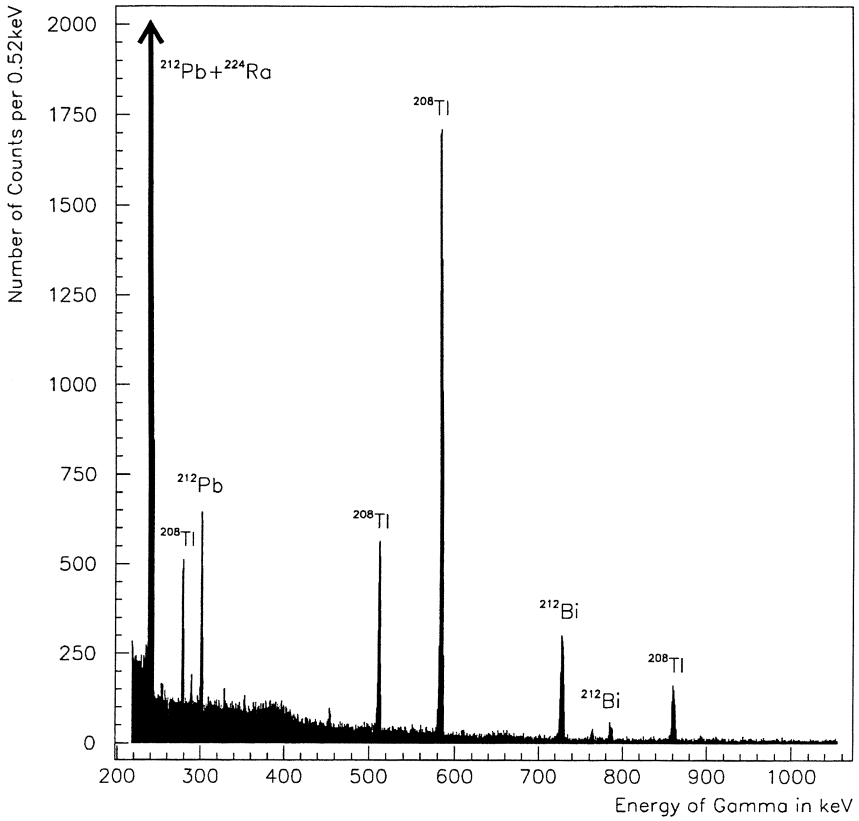

Figure B.1: *An example of a gamma spectrum from a equilibrated source of ^{228}Th as measured by an intrinsic germanium detector. The peaks due to isotopes of the ^{232}Th decay chain are all labelled. The 240keV peak, which is a combination of gamma decays from ^{212}Pb and ^{224}Ra, has not been shown at its full height so that the other peaks can be more easily identified. In fact the height of the peak at 240keV for this source was about 12,500 counts per channel which is about seven times higher than the next largest peak which can be seen at 583keV.*

Energy in keV	Isotope Parent	Branching Ratio in %	
		of parent	from main chain
238.6	^{212}Pb	43.3±0.4	43.3±0.3
241.0	^{224}Ra	3.97±0.04	3.97±0.04
277.4	^{208}Tl	6.31±0.09	2.27±0.03
300.1	^{212}Pb	3.28±0.03	3.28±0.03
510.8	^{208}Tl	22.6±0.3	8.13±0.11
583.2	^{208}Tl	84.5±0.7	30.4±0.2
727.3	^{212}Bi	6.58±0.05	6.58±0.05
785.4	^{212}Bi	1.10±0.01	1.10±0.01
860.6	^{208}Tl	12.4±0.1	4.47±0.04

Table B.1: *The energies and branching ratios of the gamma decays from daughters of ^{228}Th. The branching ratios listed give the probability that a decay of the parent produces this gamma decay and also the probability that a decay of either ^{212}Pb, ^{224}Ra or ^{228}Th produces this gamma decay assuming equilibrium within the decay chain. The values listed in this table are all taken from [Fir96].*

The Ge(Li) detector and the intrinsic germanium detector were both used to measure an acidic source of ^{228}Th which had been left isolated from other radioactivity for several half-lives of ^{224}Ra so that equilibrium within the decay chain could be assumed. The gamma spectrum of this source as measured by the intrinsic germanium detector is shown in Figure B.1. Using the results of this spectrum, and other measurements, the resolution, linearity and efficiency of the detectors as a function of energy could be found.

The energy resolution for both the intrinsic germanium detector and the Ge(Li) detector, in terms of the full width at half maximum (FWHM), was found to vary between about 2 and 4keV. In the case of the intrinsic germanium detector it could be seen that this resolution varied with the square root of the energy of the peak, as would be expected since this is the statistical fluctuation on the number of electron-hole pairs produced by a photon. In fact the following relationship was found to hold quite accurately: FWHM$\simeq$ $0.15 \pm 0.01\sqrt{E}$, where all the values are in keV. Thus for the 240keV peak the FWHM was about 2.3keV and for the 860keV peak the FWHM was about 4.4keV.

The top plots in Figures B.2 and B.3 show the linearity of the detectors as a function of energy and it can be seen that both the Ge(Li) detector and the intrinsic germanium detector have good linearity, with the intrinsic detector's linearity being excellent. The lower plots in Figures B.2 and B.3 show the efficiency of detecting gamma rays as a function of their energy on log-log plots. The result of the fits and the observation of straight lines on the log-log plots suggest that the general dependence of this variation of efficiency with energy is reasonably modelled by a power law, as would be expected from the variation of the Compton cross-section with energy.

It should be noted that the activity of the source of ^{228}Th that was used for the efficiency measurements was not precisely known and so these results are not accurate calibrations. Such accurate calibrations were not necessary since measurements were almost always examining relative not absolute activities. The low overall efficiencies of only a few percent did mean that large amounts of ^{228}Th, typically a few kilobecquerels, had to be added to experiments whose results were to be measured using gamma detectors. This amount of activity is much higher than the amounts expected in the SNO detector. (For a discussion of this see Section 5.7.1 on page 86.)

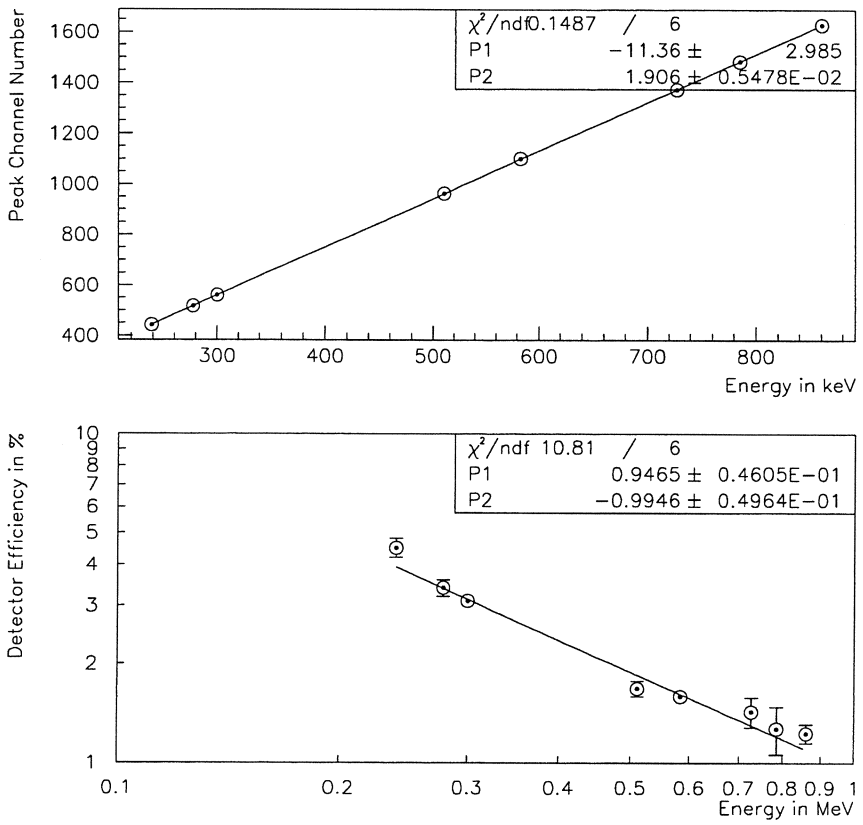

Figure B.2: *The energy and efficiency measurements of the intrinsic germanium detector used at BNL. In the top figure the fit is to a first degree polynomial whereas in the bottom figure, which is a log-log plot, the fit is to* $P1 \times Energy^{P2}$, *a power law.*

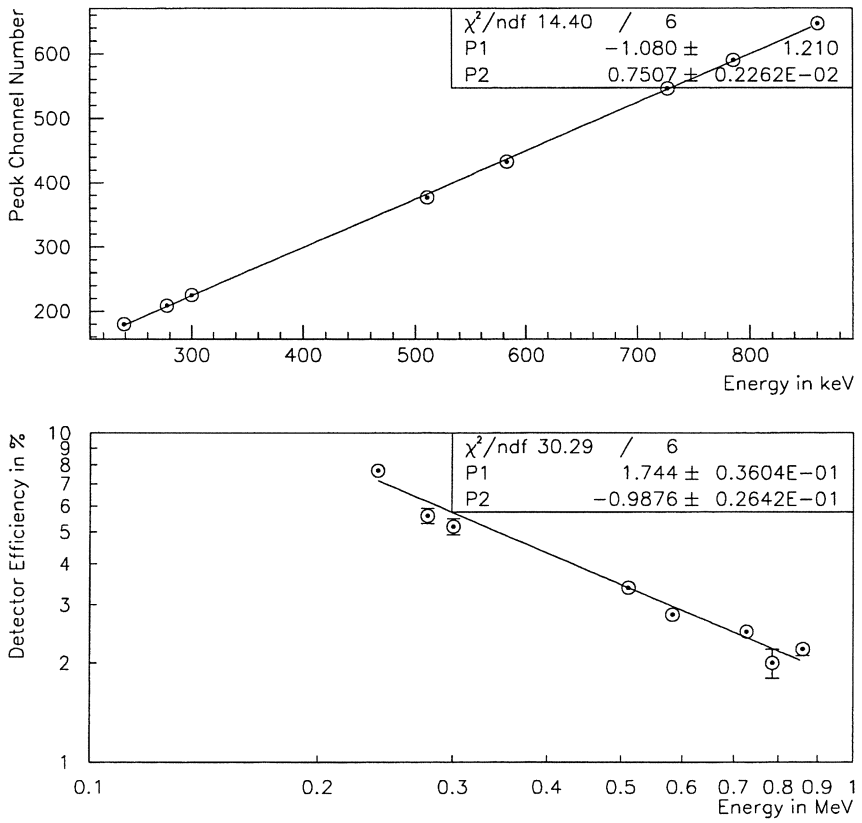

Figure B.3: *The energy and efficiency measurements of the Ge(Li) detector used at Oxford. In the top figure the fit is to a first degree polynomial whereas in the bottom figure, which is a log-log plot, the fit is to* $P1\times$ *Energy*^{P2}*, a power law.*

Finally it should be noted that when obtaining measurements by gamma counting the decay rate of all of the ^{228}Th peaks that are shown in Figure B.1 were not measured since sufficient accuracy could be achieved by measuring the decay rate of just one peak. This chosen peak was the 583keV gamma decay from ^{208}Tl. This peak gives the highest counting efficiency for a peak consisting of gamma decays from just one isotope.

In the next section it is explained how the initial activities of ^{212}Bi, ^{212}Pb, ^{224}Ra and ^{228}Th in a sample can be determined by measuring the decay rate of ^{208}Tl, using the 583keV gamma decay, at different times after the sample is produced.

B.3 Determining Initial Activities from the Decay Rate of ^{208}Tl

B.3.1 An Approximate Method

In the small scale batch extraction feasibility experiments detailed in Section 5.3.1 on page 75 the amount of ^{212}Pb and ^{228}Th that was in each sample was estimated by measuring the decay rate of ^{208}Tl, using the 583keV gamma decay, at different times after the sample was produced.

The initial activity of ^{228}Th in a sample was estimated by measuring the decay rate of ^{208}Tl two weeks after the sample was produced. Since the samples were always sealed at production they can be assumed to be in isolation from external sources of radioactivity during this time and so after two weeks the decay rate of ^{208}Tl should be the same as the original decay rate of ^{228}Th.

The initial activity of ^{224}Ra in a sample was estimated by measuring the decay rate of ^{208}Tl three days after the sample was produced. This time was chosen to minimise the effects of ^{212}Pb, which has a half-life of 10.6 hours, while maximising sensitivity to ^{224}Ra which has a half-life of 3.66 days.

Finally, the initial activity of ^{212}Pb in a sample was estimated by measuring the decay rate of ^{208}Tl two hours after the sample was produced. This time was chosen to minimise the effects of ^{212}Bi, which has a half-life of 60.6 minutes and ^{224}Ra while maximising sensitivity to ^{212}Pb. If the ^{212}Bi and ^{212}Pb act in the same way, as they do in extractions using diethylammonium diethyldithiocarbamate (DDDC), the error on estimating the initial activity of ^{212}Pb in a sample by assuming it to be the same as the decay rate of ^{208}Tl two hours after its production is quite small. However, an exact method which allows the initial activity of both ^{212}Pb and ^{212}Bi to be accurately determined is explained in the next section.

B.3.2 An Exact Method

In Appendix B of [Tap95b] there is an expression for the decay rate of ^{208}Tl as a function of time in terms of the initial activities of ^{212}Pb, ^{224}Ra and ^{228}Th. However, the derivation of this expression ignores the presence of ^{212}Bi in the decay chain and to be sure to accurately determine the initial activity of ^{212}Pb it is necessary to include the effects of this isotope.

In order to find an expression for the decay rate of ^{208}Tl as a function of time in terms of the initial activities of ^{228}Th, ^{224}Ra, ^{212}Pb and ^{212}Bi an additional differential equation to the ones considered in Appendix B of [Tap95b] needs to be considered. Equations B.1 to B.4 are the four coupled differential equations that need to be solved to find the decay rate of ^{212}Bi which is always proportional to the decay rate of ^{208}Tl for times greater than a few minutes.

$$\frac{dN_{Th}(t)}{dt} = -\lambda_{Th} N_{Th}(t) \tag{B.1}$$

$$\frac{dN_{Ra}(t)}{dt} = -\lambda_{Ra} N_{Ra}(t) + \lambda_{Th} N_{Th}(t) \tag{B.2}$$

$$\frac{dN_{Pb}(t)}{dt} = -\lambda_{Pb} N_{Pb}(t) + \lambda_{Ra} N_{Ra}(t) \tag{B.3}$$

$$\frac{dN_{Bi}(t)}{dt} = -\lambda_{Bi} N_{Bi}(t) + \lambda_{Pb} N_{Pb}(t) \tag{B.4}$$

Equations B.1 to B.4 are given in terms of the decay constants of ^{228}Th, ^{224}Ra, ^{212}Pb and ^{212}Bi and in units of seconds^{-1} the values of these decay constants are given in Equation B.5.

$$\lambda_{Th} = 1.15 \times 10^{-8} \quad ; \quad \lambda_{Ra} = 2.20 \times 10^{-6} \quad ; \quad \lambda_{Pb} = 1.82 \times 10^{-5} \quad ; \quad \lambda_{Bi} = 1.91 \times 10^{-4} \tag{B.5}$$

An expression for the decay rate of ^{212}Bi as a function, assuming that $\lambda_{Th} \simeq 0$, is given in Equation B.6. This expression is in terms of three constants: α, β and γ, which are defined in Equation B.7 and four coefficients: $\mathcal{W}$, $\mathcal{X}$, $\mathcal{Y}$ and $\mathcal{Z}$, which are defined in terms of the initial activities of the four isotopes: A_{Bi}, A_{Pb}, A_{Ra} and A_{Th}, in Equations B.8 and B.9.

$$\lambda_{Bi} N_{Bi}(t) = \mathcal{W} e^{-\lambda_{Bi} t} + \mathcal{X} \alpha e^{-\lambda_{Pb} t} + \mathcal{Y} \beta \gamma e^{-\lambda_{Ra} t} + \mathcal{Z} \tag{B.6}$$

$$\alpha = \frac{\lambda_{Bi}}{\lambda_{Bi} - \lambda_{Pb}} = 1.11 \quad ; \quad \beta = \frac{\lambda_{Bi}}{\lambda_{Bi} - \lambda_{Ra}} = 1.01 \quad ; \quad \gamma = \frac{\lambda_{Pb}}{\lambda_{Pb} - \lambda_{Ra}} = 1.14 \tag{B.7}$$

$$\mathcal{Z} = A_{Th} \quad ; \quad \mathcal{Y} = A_{Ra} - A_{Th} \quad ; \quad \mathcal{X} = A_{Pb} - A_{Ra}\gamma + A_{Th}(\gamma - 1) \tag{B.8}$$

$$\mathcal{W} = A_{Bi} - A_{Pb}\alpha + A_{Ra}\gamma(\alpha - \beta) + A_{Th}(\beta\gamma - \alpha(\gamma - 1) - 1) \tag{B.9}$$

These expressions taken together allow the initial activities of ^{212}Bi, ^{212}Pb, ^{224}Ra and ^{228}Th in a sample to be obtained by fitting measurements of the decay rate of ^{208}Tl. The minimum number of measurements for each sample to achieve this fit is four and these need to be made at particularly sensitive times such as at about 1 hour, 6 hours, 3 days and more than two weeks after the sample was produced. These fits were made using the PAW fitting routine called MINUIT[1], with bounded parameters, for the majority of gamma counting measurements discussed in this thesis. In Figures 4.3, 4.5 and 4.6, which can be found on pages 55, 58 and 59 respectively, the results of such fits are displayed.

[1]MINUIT, CERN Program Library entry D506.

Appendix C

Alpha Counting

C.1 Introduction to Alpha Counters

Alpha particles are commonly detected through their energy deposition in solid state detectors. To be optimised for alpha spectroscopy these solid state detectors need to have a very thin layer of material through which the alpha particles have to pass before reaching the active region of the detector. This is achieved using surface barrier detectors which are made by etching an extremely thin p-type layer onto the surface of n-type silicon. A very thin layer of gold is finally evaporated onto the front of the detector to provide the electrical contact for the bias voltage which, at about 100V, typically gives a depletion layer of about 170 microns in thickness. Since the typical range of a 5MeV alpha particle in silicon is only 20 microns, all alpha particles are absorbed by such a depletion layer. Finally, because of the presence of ions in air it is necessary to operate these alpha sources in a vacuum.

C.2 The Measurement of Alpha Decays from ^{232}Th

The decay chain for ^{232}Th was shown in Figure 2.3 on page 24 of this thesis where it was explained that for the purposes of the SNO experiment it is only important to measure the presence of isotopes lower than ^{228}Th in the decay chain. These isotopes have many alpha decays which are expressed in terms of their Q-values. The energy carried away from each alpha decay can be calculated roughly from these Q-values using the expression: $T_\alpha = Q(1 - 4/A)$, where A is the atomic number of the parent isotope, as is explained on page 248 of [Kra88].

The measured energies of the alpha particles produced in each of these decays are listed in Table C.1 together with values for the branching ratios to these decays from both their immediate parent and from isotopes of the main decay chain assuming equilibrium in the decay chain.

These alpha decays were measured for the research detailed in Chapter 4 of this thesis using silicon detectors at the Brookhaven National Laboratory (BNL), New York, USA, with the assistance of Dr R.Hahn. The sources measured were, so called, 'thin alpha sources' prepared on platinum disks of about 1 centimetre in diameter. These disks were cleaned before use by placing in a solution of 1M hydrochloric acid, then water and finally acetone before drying and storing. When a liquid sample was to be measured by alpha counting 10-100 microlitres of the liquid was placed in the centre of one of these disks by Dr R.Hahn. The liquid was then evaporated by placing the disk under a heat lamp for several minutes. In order to measure volumes larger than 100 microlitres this process of evaporation was repeated a number of times. Finally, the disk was flamed so that it glowed red hot to adhere the residues to the disk.

Energy in MeV	Isotope Parent	Branching Ratio in %	
		of parent	of main chain
5.34	^{228}Th	28.2±1.0	28.2±1.0
5.42	^{228}Th	71.1±0.1	71.1±0.1
5.45	^{224}Ra	5.06±0.04	5.06±0.04
5.69	^{224}Ra	94.94±0.04	94.94±0.04
6.05	^{212}Bi	69.9±0.2	25.12±0.07
6.09	^{212}Bi	27.1±0.1	9.74±0.04
6.29	^{220}Rn	99.89±0.02	99.89±0.02
6.79	^{216}Po	100	100
8.78	^{212}Po	100	64.0

Table C.1: *The energies and branching ratios of the alpha decays from daughters of ^{228}Th. The branching ratios listed give the probability that a decay of the parent produces this alpha decay and also the probability that a decay of either ^{212}Pb, ^{224}Ra or ^{228}Th produces this alpha decay assuming equilibrium within the decay chain. The values listed in this table are all taken from [Fir96].*

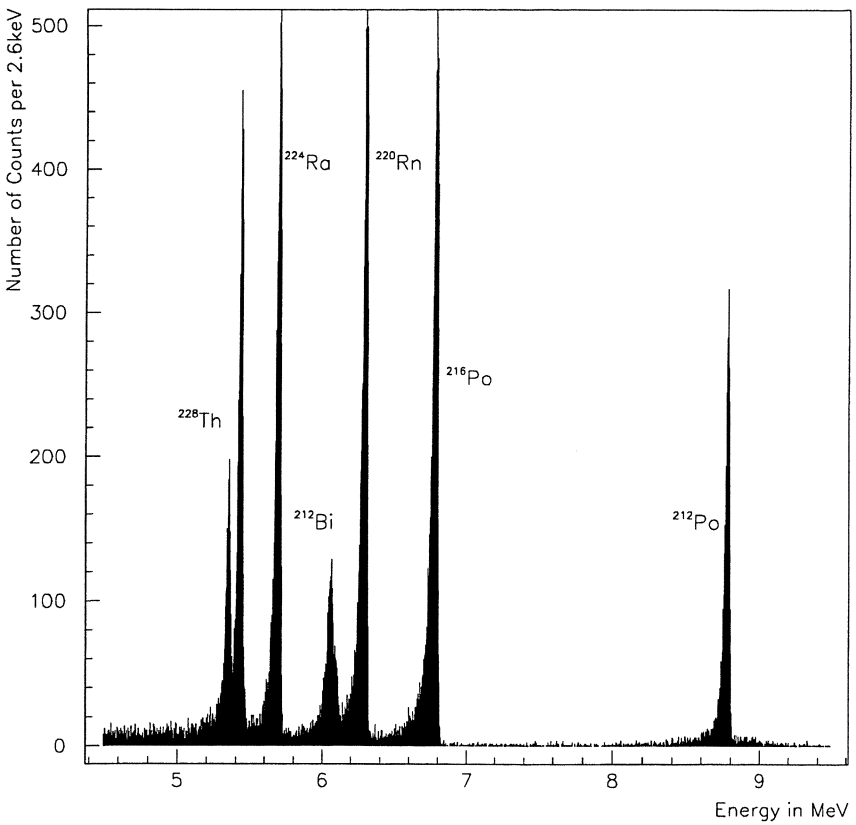

Figure C.1: *An example of an alpha spectrum from an equilibrated source of ^{228}Th as measured by an alpha detector at BNL.*

Peak Energy in MeV	Main Isotope in Peak	Main Chain Equivalent Activity in Bq:	
		Shelf 5 (Efficiency =0.92%)	Shelf 6 (Efficiency=0.67%)
5.1-5.5	^{228}Th	16.7	16.7
5.5-5.7	^{224}Ra	16.4	15.9
5.9-6.1	^{212}Bi	17.5	17.0
6.1-6.3	^{220}Rn	16.6	16.5
6.5-6.8	^{216}Po	17.1	17.7
8.1-9.5	^{212}Po	17.6	16.6
Average:		17.0±0.5	16.7±0.6

Table C.2: *The activity of a ^{228}Th source as measured at two calibrated positions from an alpha detector. It can be seen that all six of the peaks give very similar values for the main chain activity as do the measurements taken at the different distances from the detector.*

The efficiency of measuring alpha decays from sources placed at different distances from the detector were determined by Dr R.Hahn using a calibrated source of ^{241}Am. Measuring sources at the furthest distance, called Shelf 6, was found to have a 0.67% efficiency whereas measuring sources at the slightly nearer distance, called Shelf 5, was found to have a 0.92% efficiency. Thin sources of ^{228}Th were measured using this detector and a typical spectrum is shown in Figure C.1. The full width at half maximum (FWHM) resolution of this detector was found to be independent of energy at 31±3keV.

The activity of the ^{228}Th source was determined by measuring the number of counts in each of the six fully resolvable alpha peaks in a known amount of time, subtracting a reasonable background and calculating the main chain activity that would give these counts. The results of such calculations made for two measurements of the same source placed at different distances from the detector are shown in Table C.2.

These results show that all of the peaks give very similar figures for the ^{228}Th activity of the source and that measurements made at different distances from the detector are also in good agreement. The accurate measurement of this source of ^{228}Th allowed it to be used to calibrate the $\beta - \alpha$ counters that were set up at BNL which are discussed in Appendix D.

C.3 The Problem of Nuclear Recoils in Alpha Counting ^{228}Th Sources

One difficulty with alpha counting ^{228}Th sources is due to the fact that detectors can easily become contaminated with activity due to nuclear recoils. This effect was observed at BNL by counting a thin source of ^{228}Th for several hours very close to the detector, removing this source and continuing to measure the decay rates of ^{220}Rn, ^{216}Po, ^{212}Bi and ^{212}Po. These decay rates were measured at different times after the removal of the ^{228}Th source by measuring the number of counts in each alpha peak after a short time of counting. The main chain activity that would cause the observed decay rates in each of these peaks was then calculated and these activities, in counts per second, are shown in Figure C.2 plotted against the time, in hours, after the ^{228}Th was removed when the measurement was made.

The plots for the ^{212}Bi and ^{212}Po peaks clearly show two components of different half lives whereas the ^{220}Rn and ^{216}Po peaks show just one component. The results for all of the peaks have been fitted to the decay of ^{212}Bi as a function of time, as detailed in Appendix B, to give the initial activities of ^{212}Bi, ^{212}Pb, ^{224}Ra and ^{228}Th. These fitted results show that the alpha peaks of isotopes below ^{212}Pb in the decay chain indicate a large radioactive contamination of the detector which decays with the ^{212}Pb half-life and that the alpha peaks of all of the isotopes indicate a much smaller radioactive contamination which decays with the ^{224}Ra half-life. This is all consistent with contamination due to nuclear recoils since no ^{228}Th contamination was observed.

The ^{228}Th source which had been measured by the detector produced 1.85±0.13 alpha decays per second and so the amount of ^{224}Ra contamination can be calculated to be about 1.5% of this activity and the ^{212}Pb contamination about 20%. The larger ^{212}Pb contamination is probably caused by the extra mobility of ^{220}Rn. These percentages will of course depend upon geometrical effects and the exact distance between the ^{228}Th source and the detector but these results indicate the scale of the problem.

Instead of waiting for this contamination to decay away a new detector was used to measure the clean ^{212}Pb sources produced by the method given in Chapter 4. This new detector had not been used to count ^{228}Th sources and so had not been contaminated by nuclear recoils. It is clear that by only counting ^{212}Pb sources this detector could be kept free from long-lived contamination since nuclear recoils from ^{212}Pb can only lead to ^{212}Bi contamination which decays with a half-life of 60.6 minutes. This detector was specifically chosen to have a very high efficiency for the purpose of counting these ^{212}Pb sources and this was optimised to be 30% by Dr R.Hahn by using thin alpha sources placed as close to the detector as possible.

Alpha spectra produced using this high efficiency detector did not differ greatly from those produced with the previously used detector. However, because sources were measured at a much closer distance this did have the effect of adding a high energy tail to the ^{212}Po peak. This high energy tail can be clearly seen in the top spectrum shown in Figure 4.9 on page 67 and it is caused by the detection of $\beta - \alpha$ coincidences from the decays of ^{212}Po and ^{212}Bi. When sources were measured some distance away from the detector the number of $\beta - \alpha$ coincidences that were detected was reduced by using a small magnetic field but this had little effect when the source was being measured very close to the detector.

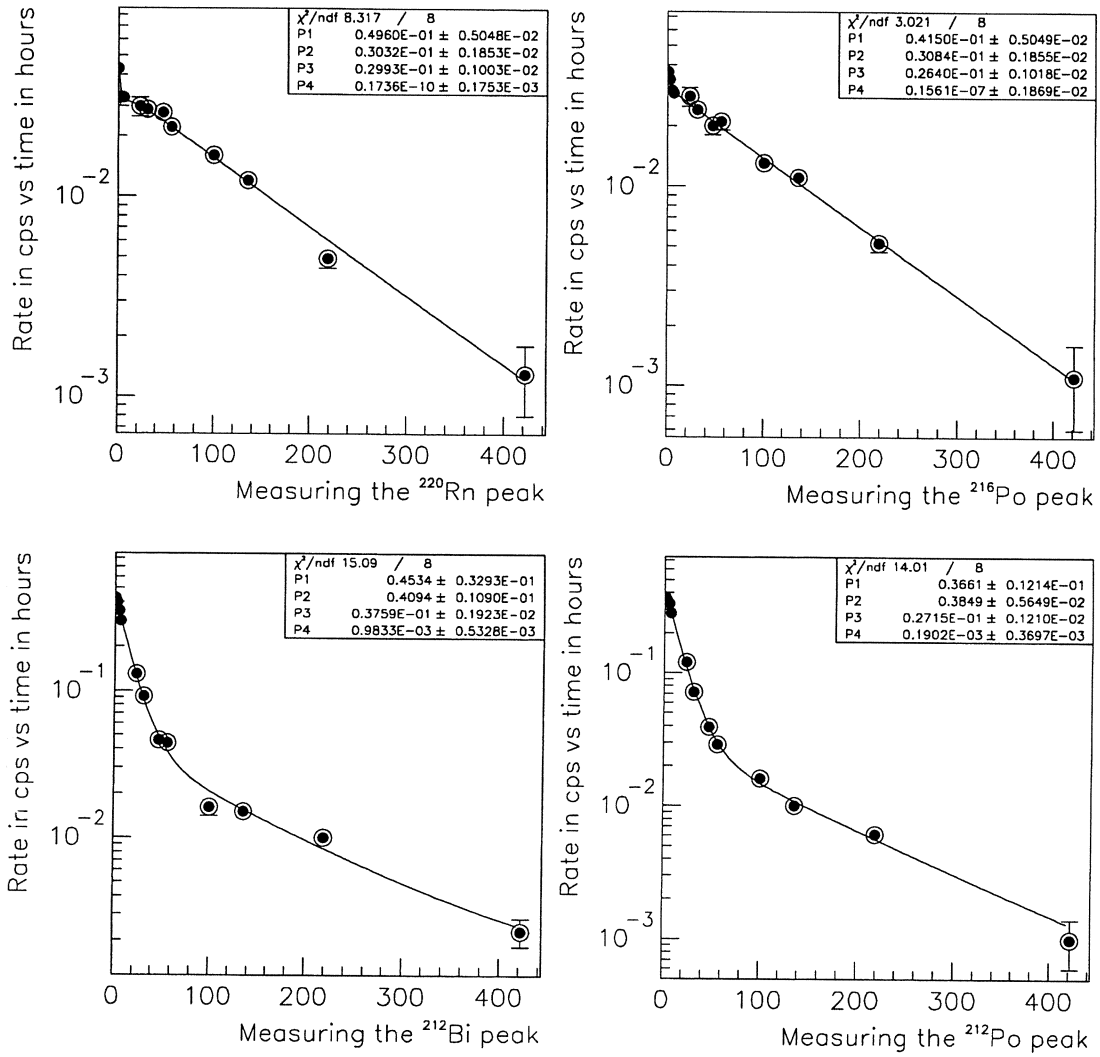

Figure C.2: *The time dependence, in hours, of the contamination of an alpha detector used to measure a source of ^{228}Th after the source is removed. The contamination shown is the calculated main chain activity, in counts per second, that would cause the observed decay rates in the alpha peaks from ^{220}Rn, ^{216}Po, ^{212}Bi and ^{212}Po. The fitted parameters are for the initial activity of ^{212}Bi (P1), ^{212}Pb (P2), ^{224}Ra (P3) and ^{228}Th (P4). Since ^{220}Rn and ^{216}Po are above ^{212}Bi and ^{212}Pb in the ^{232}Th decay chain the fitted values for P1 and P2 in the top two plots have no meaning.*

Appendix D

The Beta-Alpha Delayed Coincidence Liquid Scintillation Counters

D.1 The Beta-Alpha Counters used at Oxford

In Section 3.2.1 on page 30 it was explained why the $\beta - \alpha$ delayed coincidence liquid scintillation counters were developed for use in the SNO experiment by Dr R.K.Taplin. The main advantage that they have over other counting techniques is their very high efficiency for measuring ^{212}Po decays in a small aqueous sample and the very low background rate due to the coincidence requirement.

The $\beta - \alpha$ counting performed in the experiments detailed in Chapters 4 to 6 of this thesis used the set of counters which were set up in Oxford by Dr R.K.Taplin. The details and the operation of these $\beta - \alpha$ counters are explained in Chapter 4 of [Tap95b] but a simple overview of the process is shown in the form of a flow diagram in Figure D.1. It can be seen in this flow diagram that the measured quantities are: the full charge of the start pulse, the full charge of the stop pulse, the tail charge of the stop pulse and the time of the coincidence. These first three quantities are measured by analogue to digital converters (ADCs) and the last with a time to digital converter (TDC). The tail charge of the stop pulse is a measure of the shape of this pulse which allows $\beta - \alpha$ coincidences to be distinguished from $\beta - \beta$ or $\beta - \gamma$ coincidences.

The $\beta - \alpha$ counters set up at Oxford had been previously calibrated for absolute efficiency and this was quoted to be 50% in Chapter 4 of [Tap95b]. The relative calibrations of all six counters were measured and the results are shown in Table D.1. It can be seen that there were small differences between the relative counting rates but compared to the statistical errors on measured activities these systematic errors are very small and so they were ignored.

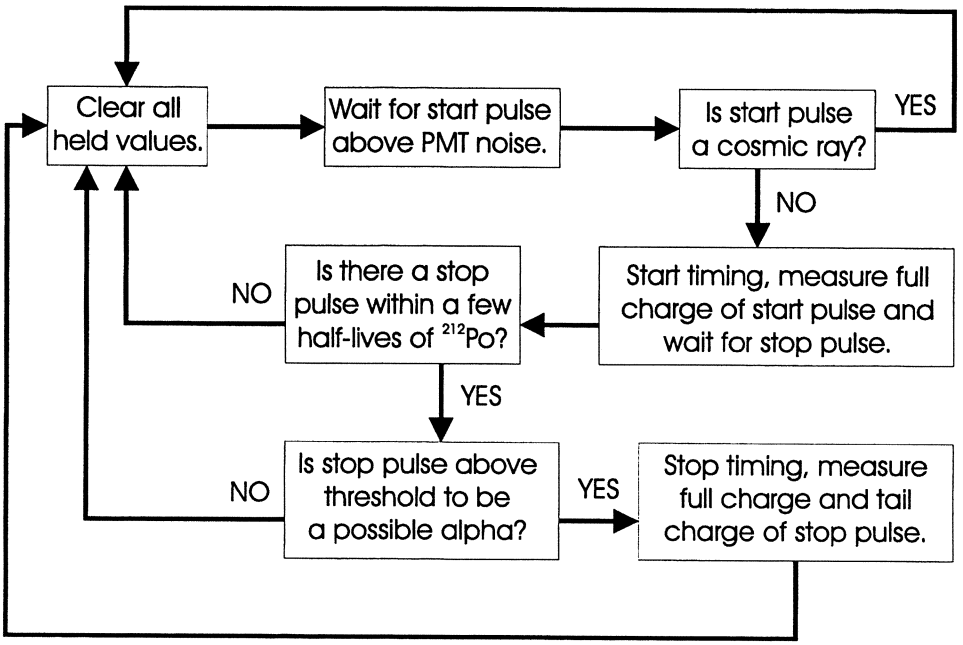

Figure D.1: *Starting from the top left corner this flow diagram gives a simple overview of the processes involved in using a $\beta-\alpha$ counter to measure coincidences from the ^{232}Th decay chain which are generated by the short lived ^{212}Po isotope.*

Counter	Count Rate	Efficiency
1	0.401±0.002	54.2±0.3%
2	0.353±0.002	47.7±0.3%
3	0.349±0.002	47.2±0.3%
4	0.360±0.002	48.7±0.3%
5	0.401±0.002	54.2±0.3%
6	0.353±0.002	47.7±0.3%

Table D.1: *The relative calibration of the $\beta-\alpha$ delayed coincidence scintillation counters set up at Oxford. Measurements were made of the same source of ^{228}Th and the errors quoted are statistical errors on the number of measured counts. The relative efficiencies are calculated by assuming a 50% efficiency for the mean measured count rate.*

The initial activity of ^{212}Pb, ^{224}Ra and ^{228}Th in a sample, measured by $\beta - \alpha$ counting at Oxford, was often estimated by recording the total number of $\beta - \alpha$ coincidences in a period of time, at different times after the sample was produced. The initial activity of ^{212}Pb in a sample was estimated by recording the total number of $\beta - \alpha$ coincidences measured in the first 24 hours after its production and dividing by a time factor to calculate the initial activity of ^{212}Pb that would produce this integrated number of counts. This is a similar calculation as was performed in Section 5.7.1 on page 86.

The initial activity of ^{228}Th in a sample was estimated by recording the total number of $\beta - \alpha$ coincidences measured in a few days, two weeks after the sample was produced. Finally, the initial activity of ^{224}Ra in a sample was estimated by recording the total number of $\beta - \alpha$ coincidences measured in a few days, three days after each sample was produced and subtracting any expected $\beta - \alpha$ coincidences due to the initial, known activity of ^{212}Pb.

The errors on these estimates were found by assuming either $\sqrt{N}$ errors on the measured number of counts or by using 95% upper level confidence limits using Poisson statistics.

In some of the experiments detailed in Chapter 6 of this thesis a more accurate method to determine the initial activities of ^{212}Pb, ^{224}Ra and ^{228}Th in a sample was used. This method was to fit the data from the $\beta - \alpha$ counters to an expression giving the decay of ^{212}Bi as a function of time in terms of the initial activities of ^{212}Pb, ^{224}Ra and ^{228}Th. The details of this method are given in Chapter 4 and Appendix B of [Tap95b]. A fit of the measured numbers of $\beta - \alpha$ counts, binned by hour, to this ^{212}Bi decay rate was performed by assuming Poisson distributed bin heights and by using the log-likelihood method to obtain values for errors.

It should be noted that samples for $\beta - \alpha$ counting were rarely measured immediately after production and this, together with binning the counts by hour, means that the presence of the ^{212}Bi isotope, which has a half-life of 60.6 minutes, between the ^{212}Pb isotope and the $\beta - \alpha$ coincidence can be safely ignored in the fitting process.

D.2 The Beta-Alpha Counters used at BNL

The $\beta - \alpha$ counting carried out in the experiments detailed in Chapter 7 of this thesis was performed at the Brookhaven National Laboratory (BNL), New York, USA, where some $\beta - \alpha$ counters were set up with the assistance of Dr J.Boger. These $\beta - \alpha$ counters differed from the Oxford counters only in the actual electronic units that were used. In particular the TDC unit used was not a long-range LRS 4208 unit but a short-range LRS 2228 unit which had been suggested as an alternative in [Tap97].

One of the counters that was set up at BNL was used to measure $\beta - \alpha$ coincidences from a source of ^{228}Th so that the full charge distributions of the start and stop pulses could be compared to those measured by Dr R.K.Taplin at Oxford. These distributions are shown in Figure D.2 and can be compared favourably to those given in Chapter 4 of [Tap95b].

The distributions shown in Figure D.2 were obtained by reading data from the CAMAC crate every time the TDC unit holds a value. This means that data is read after every singles event as well as every coincidence event since if the TDC has been started by a start pulse it will always hold a value. If no stop pulse arrives before the TDC reaches its full range the value that it holds will be a maximum which indicates a singles event. This method of reading data from the CAMAC crate was the one used by Dr R.K.Taplin. However it was found at BNL to be inefficient because of the shorter range of the TDC unit. It was found that a proportion of coincidences were being misidentified as singles events because they had a coincidence time longer than the range of the TDC unit.

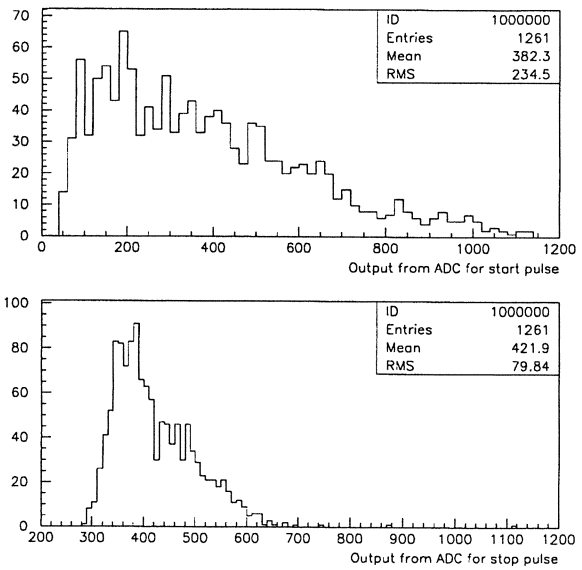

Figure D.2: *The charge distributions for the start and stop pulses of $\beta - \alpha$ coincidences from ^{212}Po as measured by a $\beta - \alpha$ counter at BNL.*

^{228}Th source strength in Bq	Using Electronics:		Using CAMAC crate:		
	Rate of all pulses $N_s + 2N_c$	Rate of stop pulses N_c	Reading when ADC has value: Coinc Rate n_c^A	Reading when TDC has value: Coinc Rate n_c^T	Reading when TDC has value: Singles Rate n_s^T
31	229±2	17.3±0.5	10.2±0.2	2.24±0.08	30.8±0.3
3.1	21.8±0.6	1.79±0.10	1.61±0.07	0.80±0.05	12.8±0.2
0.31	2.72±0.12	0.175±0.009	0.161±0.007	0.122±0.006	2.25±0.03

Table D.2: *The results of measuring both singles and coincidence rates in counts per second using the electronics directly or via the CAMAC crate. It can be seen that rates measured using the electronics scale with the activity of the ^{228}Th source whereas rates measured via the CAMAC crate do not and this is an indication of dead-times associated with processing events through the CAMAC crate.*

An alternative method to read out the CAMAC crate was to read data only when the stop pulse ADC unit holds a value. This ensures that only data from coincidences is read out but it has the disadvantage that the values of the full charge for the start pulse held in the start pulse ADC unit and the coincidence time held in the TDC unit are taken from an earlier singles event and are not associated with the coincidence.

The effects of using these two different methods to read data from the CAMAC crate can be seen from the results in Table D.2 which shows rates measured by various methods using three high activity sources of ^{228}Th and a $\beta - \alpha$ counter at BNL. These results give the coincidence rate (subscript c) and the singles event rate (subscript s) as measured via the CAMAC crate (n) and as measured using a scaler directly from the electronic gating units (N).

The ^{228}Th sources used in this experiment were later accurately calibrated and by comparing this activity to the coincidence rate measured using the electronic units, N_c, the detection efficiency for $\beta - \alpha$ coincidences can be calculated. Removing the 64% branching ratio of ^{212}Bi to ^{212}Po this gives detection efficiencies for $\beta - \alpha$ coincidences of: 87±3%, 90±5% and 88±5% for each of the three ^{228}Th sources that were measured. The average is therefore 88±2% and this indicates a 10% loss due to the start pulse discriminator threshold and timing delays.

The singles rates measured by the electronic units, N_s, can be calculated for each ^{228}Th source to be 194±2, 18.2±0.6 and 2.37±0.12 counts per second respectively. This seems to vary roughly with the activity of the ^{228}Th source which would indicate that the majority of these singles events are beta decays from isotopes in the ^{228}Th decay chain.

The coincidence rates measured using the CAMAC crate do not increase in proportion to the activity of the ^{228}Th source, especially when reading data whenever the TDC unit holds a value. This is due to the dead-times involved in processing singles events, τ_s, and coincidence events, τ_c. The coincidence rate measured when reading data whenever the TDC unit holds a value is further lowered due to a proportion, K, of coincidences that would be measured being misidentified as singles events because the coincidence time is longer than the TDC range, as has already been discussed. Equations D.1 to D.3 give expressions to connect the rates measured using the CAMAC crate to the rates measured directly from the electronics in terms of the values of τ_s, τ_c and K by taking into account the probability of one event occurring when another is being processed and the extra loss of misidentifying a coincidence event as a singles event.

$$N_c - n_c^A = N_c n_c^A \tau_c \tag{D.1}$$

$$N_c - n_c^T = N_c n_c^T \tau_c + N_c n_s^T \tau_s + K n_c^T \tag{D.2}$$

$$N_s - n_s^T = N_s n_s^T \tau_s + N_s n_c^T \tau_c \tag{D.3}$$

Using the results of measuring the highest activity ^{228}Th source for N_c, N_s, n_c^A, n_c^T and n_s^T as given in Table D.2, the values of τ_s, τ_c and K can be determined and these are given in Equation D.4.

$$\tau_s = 0.024 \pm 0.001 sec \quad ; \quad \tau_c = 0.040 \pm 0.003 sec \quad ; \quad K = 0.23 \pm 0.06 \tag{D.4}$$

The values for the dead-times, τ_s and τ_c, explain why the rates measured via the CAMAC crate are lower than those measured directly from the electronics when the coincidence rate is higher than about 25 events per second and singles rate is higher than about 40 events per second. These dead-times give an upper level limit of a few becquerels for the activity of ^{228}Th sources that can be measured by this system without having to take these dead-times into account. The calculated value of K means that about one quarter of the $\beta - \alpha$ coincidences had coincidence times greater that the maximum time that could be measured by the TDC unit. The full range of the TDC unit can therefore be calculated to be 650±100 nanoseconds by integrating an exponential decay with the ^{212}Po half-life. This can be compared to a measurement of the full range of the TDC unit obtained by fitting the actual data from the TDC unit with the ^{212}Po half-life. This fit is shown in the top plot of Figure D.3 which shows that the 2048 channels of the TDC unit must correspond to 650±50 nanoseconds.

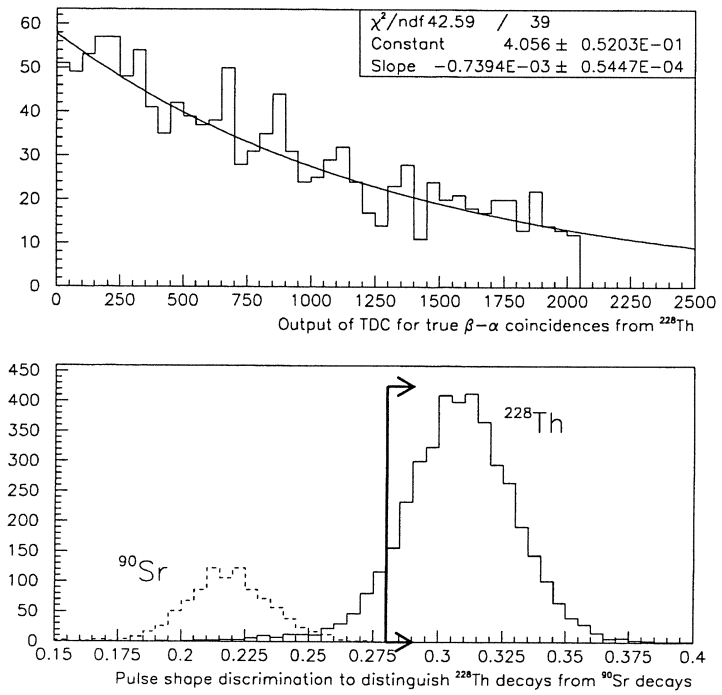

Figure D.3: *These plots show some analysis on data taken using a $\beta - \alpha$ counter at BNL. The top plot shows the measured coincidence time for $\beta - \alpha$ coincidences from ^{212}Po with a fit to an exponential decay. The fit result can be used to calculate the full range of the TDC unit using the following calculation: Slope$\times 2048/\lambda_{Po} = 650 \pm 50$ nanoseconds. The bottom plot shows the different measured distributions of the tail charge to full charge ratio for sources of ^{228}Th and ^{90}Sr.*

To remove the in-built loss of efficiency caused by reading data from the CAMAC crate whenever the TDC unit holds a value it was decided to always use the alternative method of only reading data when the stop pulse ADC holds a value. As has already been explained this has the disadvantage that the values held in the TDC unit and the start pulse ADC unit have to be ignored since they will not correspond to the coincidence event. Since the $\beta - \alpha$ counters were only being used to measure ^{212}Po coincidences, not ^{214}Po coincidences as well, the timing information and the start pulse information was not essential to obtain accurate results. The full charge and tail charge of the stop pulse are required in order to distinguish signals caused by alpha particles from those caused by gamma or beta particles using pulse shape discrimination as detailed in Chapter 4 of [Tap95b].

The power of this pulse shape discrimination can be seen from the lower plot of Figure D.3 which shows the measured values of the tail charge to full charge ratio for sources of ^{228}Th and ^{90}Sr. The ^{90}Sr source is a pure beta emitter and so this figure shows that the tail charge to full charge ratio is much smaller for $\beta - \beta$ coincidences than for $\beta - \alpha$ coincidences. In Figure D.3 a low level cut for the tail charge to full charge ratio of 0.28 is shown and by only selecting coincidences which have a value greater than 0.28 the chance of measuring a $\beta - \beta$ coincidence by mistake is eliminated by accepting a slight loss of efficiency for measuring a $\beta - \alpha$ coincidence. After adding in this pulse shape discrimination separately for each $\beta - \alpha$ counter at BNL they were calibrated for absolute efficiency using a 0.31Bq source of ^{228}Th whose activity had been accurately determined using both alpha and gamma detectors. The results of this absolute calibration are shown in Table D.3 and by taking into account the 64% branching ratio of ^{212}Bi to ^{212}Po this gives an average detection efficiency of 77±3% which is very similar to that found in Oxford by Dr R.K.Taplin, see Chapter 4 of [Tap95b].

Counter	Absolute Efficiency:
1	49±1%
2	48±1%
3	52±2%
4	48±1%

Table D.3: *The calibration of the $\beta - \alpha$ delayed coincidence scintillation counters as used at BNL.*

Unfortunately it was not possible to spend a large amount of time reducing and analysing residual backgrounds on the $\beta - \alpha$ counters at BNL which were the order of a few decays per day. To eliminate the effect of this counter background, in measuring the initial activity of ^{212}Pb sources, the data from the $\beta - \alpha$ counters was always fitted to a constant counter background together with a component with a 10.6 hour half-life. A fit of the measured numbers of $\beta - \alpha$ counts, binned by hour, to this function was performed by assuming Poisson distributed bin heights and by using the log-likelihood method to obtain values for errors.

Appendix E

Calculation of Reservoir Drainage Time

In this appendix a simple calculation is made in order to estimate the time that it would take to drain 20 litres from the mixer of the Solvent-Solvent Extraction Rig under gravity using either half inch (1.27×10^{-2} metres) or quarter inch (6.35×10^{-3} metres) diameter pipe.

A diagram of the apparatus involved in draining a reservoir is given in Figure E.1 along with a number of definitions. The mixer of the Solvent-Solvent Extraction Rig was designed to have a drainage pipe of length, $l = 1.5$ metres, a reservoir diameter, D, of 0.3 metres and an initial head height of water in the reservoir, $h(0) = H$, of 0.3 metres to give a volume of 20 litres.

The conservation of volume leads immediately to the two simple relationships which are given in Equations E.1 and E.2. The first equation, Equation E.1, equates the volume of water which flows out of the pipe in a small time, dt, to the volume of water lost from the reservoir in terms of a small decrease in the head height, $-dh$. These two volumes are shown by the shaded regions in Figure E.1. The second equation, Equation E.2, gives a relationship between the velocities of the water at the top of the reservoir, V_1, and in the flow out of the exit pipe, V_2.

$$-D^2 dh = d^2 V_2 dt \tag{E.1}$$

$$V_1 = V_2 \left(\frac{d}{D}\right)^2 \tag{E.2}$$

To estimate the velocity of water leaving the pipe as a function of the head height, $h(t)$, it is necessary to use the Bernoulli equation for two points on a streamline assuming a quasi steady state during the draining. The Bernoulli equation, which is given in Equation E.3, connects the pressure, p, velocity, V and the height, z, of points on a streamline in terms of the acceleration due to gravity, g, and the specific weight, $\gamma = \rho g$.

$$\frac{p_1}{\gamma} + \frac{V_1^2}{2g} + z_1 = \frac{p_2}{\gamma} + \frac{V_2^2}{2g} + z_2 \tag{E.3}$$

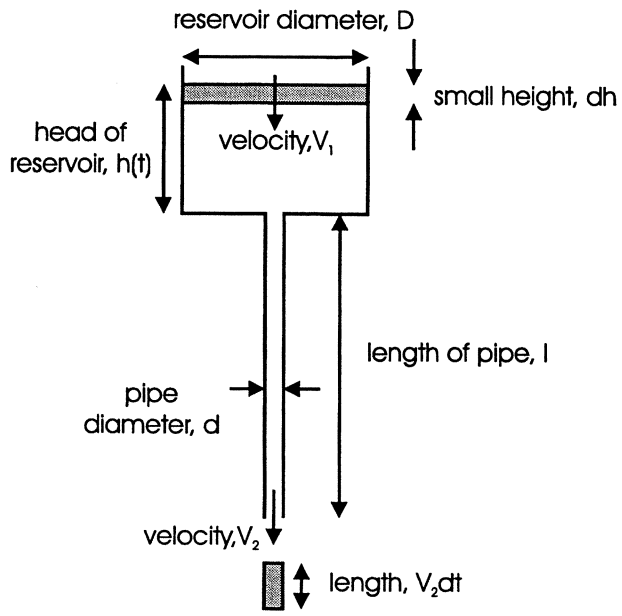

Figure E.1: *A diagram showing the apparatus involved in draining the reservoir on the Solvent-Solvent Extraction Rig. The shaded areas indicate the two volumes which are equated to give the differential equation shown in Equation E.1. When the reservoir is full* $h(0) = H$ *and when empty* $h(T) = 0$.

The Bernoulli equation for the situation shown in Figure E.1 can be constructed by choosing one point at the top level of the water in the reservoir and the other point at the end of the exit pipe. The difference in heights of these two points, $z_1 - z_2$, can be seen from Figure E.1 to be equal to $h(t)+l$. Also, the top of the reservoir is open to the atmosphere which makes $p_1 = 0$ and the water leaves the exit pipe as a free jet which makes $p_2 = 0$. Substituting these values into Equation E.3 leads to Equation E.4. By using the relationship between the velocities at these two points as given in Equation E.2, an expression for V_2 in terms of the head height in the reservoir can be found and it is given in Equation E.5.

$$\frac{V_1^2}{2g} + h(t) + l = \frac{V_2^2}{2g} \tag{E.4}$$

$$V_2 = \sqrt{\frac{2g(h(t)+l)}{1-(d/D)^4}} \tag{E.5}$$

Since $D \gg d$ it is clear that the term involving $(d/D)^4$ given in Equation E.5 can be ignored and then by substituting this equation into Equation E.1 a first order differential equation for $h(t)$ can be obtained as shown in Equation E.6. This differential equation is solved trivially in Equations E.7 and E.8 to give the time, T, that it takes to drain the reservoir by using the boundary condition that at time, t=0, the head of water in the reservoir, $h = H$.

$$-D^2 dh = d^2\sqrt{2g(h(t)+l)}dt \tag{E.6}$$

$$-\frac{1}{\sqrt{2g}}\int_H^0 \frac{dh}{\sqrt{h(t)+l}} = \left(\frac{d}{D}\right)^2 \int_0^T dt \tag{E.7}$$

$$T = \sqrt{\frac{2}{g}}\left(\frac{D}{d}\right)^2 \left[\sqrt{(H+l)} - \sqrt{l}\right] \tag{E.8}$$

Using Equation E.8 and the dimensions as were given above, the time that it would take to drain 20 litres from the mixer of the Solvent-Solvent Extraction Rig under gravity using half inch diameter pipe can be calculated to be about 30 seconds and when using quarter inch diameter pipe it can be calculated to be almost 2 minutes.

The expression for T given in Equation E.8 was obtained by neglecting any losses in the draining, in fact there are two important losses that need to be taken into account and these are expressed in terms of head height losses in Equations E.9 and E.10. (See [Mun90] or another text on Fluid Mechanics for the derivation of these expressions.)

$$h_p = f\frac{l}{d}\frac{V_2^2}{2g} \tag{E.9}$$

$$h_c = K_C\frac{V_2^2}{2g} \tag{E.10}$$

The first equation, Equation E.9, gives the loss due to friction within the pipe in terms of its dimensions, the velocity of water in it and a friction factor, f. The exact value of this friction factor can only be calculated if there is laminar flow within the pipe and this is not expected in this situation. However, for plastic, smooth pipes the value of f for turbulent flow can be estimated to lie in the range 0.01 to 0.04.

The second equation, Equation E.10, gives the loss due to the constriction between the reservoir and the exit pipe in terms of the velocity of water in the pipe and a geometrical factor, K_C. The value of the geometrical factor depends upon the exact nature of the constriction, however when going from a large diameter reservoir to a small diameter pipe it is reasonable to assume a limiting value of 0.5.

These head losses need to be added onto the right hand side of Equation E.4 to determine the effect upon the velocity, V_2, in the pipe. By including these terms and following the calculation as above a new expression for T can be found which includes the effect of the two main losses in the system and this expression is given in Equation E.11.

$$T = \sqrt{\frac{2}{g}}\left(\frac{D}{d}\right)^2\left[\sqrt{(H+l)} - \sqrt{l}\right]\left(1 + f\frac{l}{d} + K_C\right)^{1/2} \tag{E.11}$$

The correction due to the losses increases the calculated time that it would take to drain 20 litres from the mixer of the Solvent-Solvent Extraction Rig under gravity using half inch diameter pipe to 1 to 2 minutes and when using quarter inch diameter pipe to 4 to 7 minutes. It is clear that losses greatly effect drainage times and the inclusion of a valve in this draining will further slow the flow down. To ensure that this drainage time does not become long compared to other processing times involved in using the Solvent-Solvent Extraction Rig it can be concluded that half inch diameter pipe should be used.

The expression in Equation E.11 was tested experimentally by draining a large tank. This tank was actually square in its cross-section but its area corresponded to a diameter, D, of 0.4 metres. It was filled with water to a head height, H, of 0.15 metres and then placed 2 metres above the ground so that it could be drained using a length, $l = 2$ metres, of three eights inch diameter tubing, $d = 9.525 \times 10^{-3}$ metres. By substituting these values into Equation E.11 and assuming that the friction factor, f, lies in the range 0.01 to 0.04 a calculated drainage time of 80 to 130 seconds can be obtained. This compares very favourably to the measured value of 90 seconds and indicates that f had a value nearer 0.01 than 0.04.

Appendix F

A Model of Airborne ^{212}Pb Contamination

In this appendix a simple model will be used to estimate the deposition rates of ^{212}Pb in a $\beta - \alpha$ counting pot that would be expected in the experimental areas at Oxford and BNL due to the emanation of ^{220}Rn from the thorium which is expected to be present in concrete. The first step in this calculation is the need to determine the emanation of ^{220}Rn from a concrete wall containing a fixed amount of thorium. This can be done by assuming infinitely thick, flat walls by solving the diffusion equation given in Equation F.1. In this equation $n(x)$ is the concentration of ^{220}Rn atoms in the concrete a distance x from the surface of a wall, D is the diffusion coefficient of radon in concrete and N is the concentration of ^{220}Rn atoms a long way from the surface of the wall which is generated by thorium within the concrete. Finally, $\lambda_{Rn} = 44.88\text{hr}^{-1}$ is the decay constant for ^{220}Rn which has a half life of just 55.6 seconds.

$$D\frac{d^2n}{dx^2} - \lambda_{Rn}n = -\lambda_{Rn}N \tag{F.1}$$

The boundary conditions for this problem are that: $n(L) = N$, where L is large and $n(0) = 0$. The latter condition means that any ^{220}Rn at the surface of the concrete is immediately transported away by convection currents. With these boundary conditions the solution to Equation F.1 is shown in Equation F.2, where l has been defined to be the diffusion length of ^{220}Rn in concrete which is also given in Equation F.2.

$$n(x) = N(1 - \frac{\sinh(L-x)/l}{\sinh L/l}) \quad ; \quad l = \sqrt{D/\lambda_{Rn}} \tag{F.2}$$

The flux of ^{220}Rn in the concrete at any distance, x, from the surface of the wall can be found using the usual formula for flux as shown in Equation F.3. By evaluating this equation at $x = 0$ using Equation F.2, the flux of ^{220}Rn out of the surface of the concrete wall can be found and the expression for this flux is given in Equation F.4.

$$\mathbf{j} = -D\nabla n \tag{F.3}$$

$$|\mathbf{j}|_{x=0} = Flux = -D\frac{dn}{dx}\bigg|_{x=0} = \frac{ND}{l}\frac{\cosh(L-x)/l}{\sinh L/l}\bigg|_{x=0} = \frac{ND}{l\tanh L/l} \tag{F.4}$$

In the limit that the wall is thick compared to the diffusion length of ^{220}Rn, $L \gg l$, the flux can be reduced to a simple expression, given in Equation F.5, in terms of the diffusion coefficient, D, the concentration of ^{220}Rn in the concrete, N and the decay constant of ^{220}Rn, λ_{Rn}.

Institute Name	Estimated area in square metres of the:			Deposition Rate in atoms/hr	
	Concrete Walls	Floor Area	$\beta - \alpha$ pot	Calculated Rate	Measured Rate
Oxford	12	8	1.5×10^{-3}	100-300	30±20
BNL	112	49	1.5×10^{-3}	150-450	410±250

Table F.1: *A comparison of the calculated and measured ^{212}Pb deposition rates in experimental areas at Oxford and BNL. These calculations use the value of the flux of ^{220}Rn out of concrete to be 5-13$\times10^4$ atoms per square metre per hour which corresponds to a thorium content of the concrete of 1 part per million.*

$$Flux = \frac{ND}{l} = N\sqrt{D\lambda_{Rn}} \tag{F.5}$$

Using the formula in Equation F.5 the flux of ^{220}Rn out of a concrete wall can be estimated by choosing suitable values for the thorium concentration in concrete, the density of concrete and the diffusion coefficient of radon in concrete. A summary of measured values of the diffusion lengths for the 3.82 day half-life radon from the uranium decay chain, ^{222}Rn, in various concretes are given in [Zap83]. These values lie between 13 and 29 centimetres and so using the expression in Equation F.2 it can be deduced that the diffusion coefficient for radon in concrete lies between 4×10^{-4} and 18×10^{-4} squared centimetres per second or between 1×10^{-4} and 6×10^{-4} squared metres per hour. If it is assumed that the concrete contains 1 part per million ^{232}Th and has an average density of 2.5 grams per cubic centimetre this gives N, the concentration of ^{220}Rn atoms in the concrete, to be 8×10^5 atoms per cubic metre. Hence, the flux of ^{220}Rn out of a surface can be calculated to be somewhere between 5-13$\times10^4$ atoms per square metre per hour.

It is clear that the ^{220}Rn itself does not have time in its 55.6 second half-life to travel very far around a room, however it has been observed previously [Por78] that the daughters of ^{220}Rn are indeed found a long way from any source of ^{220}Rn. This is suggested as being due to the transport of ^{212}Pb on aerosols on which atoms of ^{212}Pb cluster together and this would explain the results seen in experiments BRT5-8 of Section 7.3.1 on page 127. It will therefore be assumed that this is indeed the case for this example calculation. The production rate of ^{212}Pb equals the production rate of ^{220}Rn, if equilibrium is assumed, and so it can be calculated for a given experimental area by multiplying the flux out of concrete by the relevant area of concrete walls.

In Section 7.3.2 on page 127 it was shown that the vast majority of the airborne ^{212}Pb background falls directly from the air into the counting pot in clusters. However, after long periods of time it is reasonable to make the assumption that on average the ^{212}Pb produced is evenly distributed on exposed surfaces. Hence, the deposition rate in a $\beta - \alpha$ counting pot can be found from the production rate of ^{212}Pb by scaling the production rate in proportion to the ratio of the area of the counting pot to the total surface area available for deposition. These calculated deposition rates are compared in Table F.1 to the average ^{212}Pb deposition rates as measured in the experimental areas at Oxford and BNL which are taken from the results of Table 7.6 on page 128. These results indicate that the measured ^{212}Pb backgrounds can be attributed to airborne ^{212}Pb caused by ^{220}Rn emanating from the concrete walls. The results also show that the backgrounds in Oxford appear to be much lower than one would expect and this could either be due to a lower thorium concentration in the concrete or, perhaps more probably, a much higher ventilation rate which may have prevented the ^{212}Pb from depositing.

Bibliography

[Abd94] Results from SAGE (The Russian-American Gallium Solar Neutrino Experiment).
J.N.Abdurashitov et al. Physics Letters B, Volume 328, Page 234, 1994.

[Ach95] Search for Neutrino Oscillations at 15, 40 and 95 metres from a Nuclear Power Reactor at Bugey.
B.Achkar et al. Nuclear Physics B, Volume 434, Page 503, 1995.

[Agl89] Experimental Study of Atmospheric Neutrino Flux in the NUSEX Experiment.
M.Aglietta et al. Europhysics Letters, Volume 8, Page 611, 1989.

[AlM88] Rapid Separation of ^{212}Pb - ^{212}Bi - ^{208}Tl by High-Performance Liquid Ion Chromatography.
I. Al Mahamid, J.M.Paulus. Journal of Radioanalytical and Nuclear Chemistry. Letters, Volume 127 (5), Page 357, 1988.

[Ans92] Solar Neutrinos observed by GALLEX at Gran Sasso.
P.Anselmann et al. Physics Letters B, Volume 285, Page 376, 1992.

[Apo97] Initial Results from the CHOOZ Long Baseline Reactor Neutrino Oscillation Experiment.
M.Apollonio et al. Preprint: hep-ex/9711002, November, 1997.

[Ass96] Upper Limit of the Muon-Neutrino Mass and Charged-Pion Mass from Momentum Analysis of a Surface Muon Beam.
K.Assamagan et al. Physical Review D, Volume 53 (11), Page 6065, 1996.

[Atc87] A Remote System for the Separation of ^{228}Th and ^{224}Ra.
R.W.Atcher, J.J.Hines, A.M.Friedman. Journal of Radioanalytical and Nuclear Chemistry. Letters, Volume 117 (3), Page 155, 1987.

[Ath96] Evidence for $\overline{\nu_\mu} \rightarrow \overline{\nu_e}$ Oscillations from the LSND Experiment at the Los Alamos Meson Physics Facility.
C.Athanassopoulos et al. Physical Review Letters, Volume 77, Page 3082, 1996.

[Ath97] Evidence for $\nu_\mu \rightarrow \nu_e$ Neutrino Oscillations from LSND.
C.Athanassopoulous et al. Preprint: nucl-ex/9709006, 16 September, 1997.

[Bah78] A Proposed Solar-Neutrino Experiment Using ^{71}Ga.
J.N.Bahcall et al. Physical Review Letters, Volume 40, Page 1351, 1978.

[Bah89] Neutrino Astrophysics.
J.N.Bahcall. Published by Cambridge University Press, 1989.

[Bah96] Status of Solar Models.
J.N.Bahcall. Proceedings of the 17th International Conference on Neutrino Physics and Astrophysics, Neutrino '96, Page 56. Published by World Scientific, 1997.

[Bah97] An Introduction to Solar Neutrino Research.
J.N.Bahcall. Proceedings of the XXV SLAC Summer Institute on Particle Physics, 'Physics of Leptons,' August, 1997.

[BP95] Solar Models with Helium and Heavy-Element Diffusion.
J.N.Bahcall, M.H.Pinsonneault. Reviews of Modern Physics, Volume 67, Page 781, 1995.

[Bau97] The Heidelberg-Moscow Experiment: Improved Sensitivity for ^{76}Ge Neutrinoless Double Beta Decay.
L.Baudis et al. Physics Letters B, Volume 407, Page 219, 1997.

[Bec92] Electron and Muon Neutrino Content of the Atmospheric Flux.
R.Becker-Szendy et al. Physical Review D, Volume 46, Page 3720, 1992.

[Bod57] Investigations of Distributed Dithiocarbamates. Communication VI. Displacement reactions between inner complexes of diethyl dithiocarbamates in an organic phase and metal ions in an aqueous phase.
H.Bode and K-J.Tusche. Zeitschrift für Analytische Chemie, Volume 157, Page 414, 1957.

[Bod59] Investigations of Distributed Diethyl Dithiocarbamates. Communication VII. The stability of diethyldithiocarbamic acid upon shaking CCl_4 and $CHCl_3$ solutions of diethylammonium diethyldithiocarbamate with aqueous mineral acids.
H.Bode and F.Neumann. Zeitschrift für Analytische Chemie, Volume 169, Page 410, 1959.

[Bod60] Investigations of Distributed Diethyl Dithiocarbamates. Communication VIII. Extractions with solutions of diethylammonium diethyldithiocarbamate in organic solvents.
H.Bode and F.Neumann. Zeitschrift für Analytische Chemie, Volume 172, Page 1, 1960.

[Bon96] Status and Perspectives of the Mainz Neutrino Mass Experiment.
J.Bonn. Proceedings of the 17th International Conference on Neutrino Physics and Astrophysics, Neutrino '96, Page 259. Published by World Scientific, 1997.

[Bor92] Search for Muon-Neutrino Oscillations $\nu_\mu \to \nu_e$ ($\overline{\nu_\mu} \to \overline{\nu_e}$) in a Wide-Band Neutrino Beam.
L.Borodovsky et al. Physical Review Letters, Volume 68, Page 274, 1992.

[Bri96] Monte Carlo and Analysis Techniques for the Sudbury Neutrino Observatory.
S.J.Brice, Balliol College, Oxford University. A thesis submitted in partial fulfilment of the requirements for the degree of Doctor of Philosophy, Trinity Term, 1996.

[Bro78] The letter that Pauli wrote is reproduced in English in: The Idea of the Neutrino.
L.M.Brown. Physics Today, Volume 31, Number 9 (September), Page 23, 1978.

[Che85] Direct Approach to Resolve the Solar Neutrino Problem.
H.H.Chen. Physical Review Letters, Volume 55, Page 1534, 1985.

[Chu98] Three Neutrino Δm^2 Scales and Singular Seesaw Mechanism.
E.J.Chun, C.W.Kim and U.W.Lee. Preprint: hep-ph/9802209, 1998.

[Cow56] Detection of the Free Neutrino: A Confirmation.
C.L.Cowan, F.Reines, F.B.Harrison, H.W.Kruse, A.D.McGuire. Science, Volume 124, Page 103, 1956.

[Cri97] Results of the whole GALLEX Experiment (GALLEX note GX-113).
M.Cribier. Proceedings of the 5th International Workshop on Topics in Astroparticle and Underground Physics (TAUP97), Gran Sasso, Italy, September, 1997.

[Dau95] Determination of the Atmospheric Neutrino Spectra with the Fréjus Detector.
K.Daum et al. Zeitschrift für Physik C, Volume 66, Page 417, 1995.

[Dav68] Search for Neutrinos from the Sun.
R.Davis, Jr., D.S.Harmer and K.C.Hoffman. Physical Review Letters, Volume 20, Page 1205, 1968.

[Dav97] A History of the Homestake Solar Neutrino Experiment.
R.Davis, Jr. et al. Proceedings of the 4th International Solar Neutrino Conference, 1997.

[Eit97] KARMEN: Neutrino Oscillation Limits and New Results with the Upgrade.
K. Eitel et al. Proceedings of the 5th International Workshop on Topics in Astroparticle and Underground Physics (TAUP97), Gran Sasso, Italy, September, 1997.

[Ell96] Outlook on Neutrino Physics.
J.Ellis. Proceedings of the 17th International Conference on Neutrino Physics and Astrophysics, Neutrino '96, Page 541. Published by World Scientific, 1997.

[Enq96] Proceedings of the 17th International Conference on Neutrino Physics and Astrophysics, Neutrino '96. Editors: K.Enqvist, K.Huitu, J.Maalampi. Published by World Scientific, 1997.

[Esk97] A Search for $\nu_\mu \rightarrow \nu_\tau$ Oscillation.
E.Eskut et al. Prepreint: CERN-PPE/97-149, November, 1997.

[Fer92] Radiogenic Background Suppression in a Heavy Water Solar Neutrino Detector.
A.P.Ferraris, Magdalen College, Oxford University. A thesis submitted in partial fulfilment of the requirements for the degree of Doctor of Philosophy, February, 1992.

[Fie97] Nucleosynthesis Limits on the Mass of Long Lived Tau and Muon Neutrinos.
B.D.Fields, K.Kainulainen, K.A.Olive. Astroparticle Physics, Volume 6, Page 169, 1997.

[Fir96] Table of Isotopes, 8th Edition.
R.B.Firestone, V.S.Shirley, C.M.Baglin, S.Y.F.Chu, J.Zipkin. Published by John Wiley and Sons, 1996.

[Gav97] Results taken from a talk given by V.N.Gavrin at the Brookhaven National Laboratory, New York, USA, 8th December, 1997.

[Gib61] The Radiochemistry of Lead (NAS-NS 3040).
W.M.Gibson. National Academy of Sciences, Nuclear Science Series, Bell Telephone Laboratories, August, 1961.

[Hal84] Quarks and Leptons: An Introductory Course in Modern Particle Physics.
F.Halzen and A.D.Martin. Published by John Wiley and Sons, 1984.

[Hee96] Probability of a Solution to the Solar Neutrino Problem within the Minimal Standard Model.
K.H.Heeger and R.G.H.Robertson. Physical Review Letters, Volume 77, Page 3720, 1996.

[Her93] Elution of HTiO.
H.Heron, W.Locke. Internal SNO Report, August, 1993.

[Hir88] Observation in the Kamiokande-II Detector of the Neutrino Burst from Supernovae SN1987A.
K.S.Hirata et al. Physical Review D, Volume 38, Page 448, 1988.

[Hir90] Results from One Thousand Days of Real-Time, Directional Solar-Neutrino Data.
K.S.Hirata et al. Physical Review Letters, Volume 65, Page 1297, 1990.

[How94] Ion Exchange Properties of Hydrous Titanium Oxide.
K.H.Howard, Magdalen College, Oxford University. A thesis submitted for the Honour School of Natural Science: Chemistry Part II, June, 1994

[Hyd60] The Radiochemistry of Thorium (NAS-NS 3004).
E.K.Hyde. National Academy of Sciences, Nuclear Science Series, University of California, January, 1960.

[Ino97] Results from Kamiokande and Status of Super-Kamiokande.
K.Inoue. Nuclear Physics B (Proceedings Supplements), Volume 59, Page 267, 1997.

[Kaf97] Result presented by T.Kafka at the 5th International Workshop on Topics in Astroparticle and Underground Physics (TAUP97), Gran Sasso, Italy, September, 1997.

[Kir84] Encyclopedia of Chemical Technology, 3rd Edition.
R.E.Kirk, F.F.Othmer. Published by John Wiley and Sons, 1984.

[Kla96] Double Beta Decay - Physics beyond the Standard Model.
H.V.Klapdor-Kleingrothaus. Proceedings of the 17th International Conference on Neutrino Physics and Astrophysics, Neutrino '96, Page 330. Published by World Scientific, 1997.

[Kra88] Introductory Nuclear Physics.
K.S.Krane. Published by John Wiley and Sons, 1988.

[Kra53] Anion Exchange Studies VI. The Divalent Transition Elements Manganese to Zinc in Hydrochloric Acid.
K.A.Kraus and G.E.Moore. Journal of the American Chemical Society, Volume 75, Page 1460, 1953.

[Kra54] Anion-exchange Studies XI. Lead(II) and Bismuth(III) in Chloride and Nitrate Solutions.
F.Nelson and K.A.Kraus. Journal of the American Chemical Society, Volume 76, Page 5916, 1954.

[Lan96] The Homestake Solar Electron Neutrino Detector Program: Chlorine and Iodine.
K.Lande. Proceedings of the 17th International Conference on Neutrino Physics and Astrophysics, Neutrino '96, Page 25. Published by World Scientific, 1997.

[LEP89] The 1989 results from LEP concerning the width of the Z^0 particle for L3, ALEPH, OPAL and DELPHI were published in Physics Letters B, Volume 231, Pages 509, 519, 530 and 539 respectively.

[Lob96] Status and New Results from the Experiment 'Troitsk ν-mass.'
V.M.Lobashev. Proceedings of the 17th International Conference on Neutrino Physics and Astrophysics, Neutrino '96, Page 264. Published by World Scientific, 1997.

[Lyo97] Neutron Transport in the Sudbury Neutrino Detector.
M.J.Lyons, Balliol College, Oxford University. A thesis submitted in partial fulfilment of the requirements for the degree of Doctor of Philosophy, Michaelmas Term, 1996.

[Mag81] Solvent Extraction Procedures Combined with Back-Extraction for Trace Metal Determinations by Atomic Absorption Spectrometry.
B.Magnusson and S.Westerlund. Analytica Chimica Acta, Volume 131, Page 63, 1981.

[McD87] Sudbury Neutrino Observatory Proposal (SNO-87-12).
A.B.McDonald et al. SNO Report, October, 1987.

[McF95] Limits on $\nu_\mu(\overline{\nu_\mu}) \rightarrow (\overline{\nu_\tau})\nu_\tau$ and $\nu_\mu(\overline{\nu_\mu}) \rightarrow (\overline{\nu_e})\nu_e$ Oscillations from a Precision Measurement of Neutrino-Nucleon Neutral Current Interactions.
K.S.McFarland et al. Physical Review Letters, Volume 75, Page 3993, 1995.

[Mez97] Recent Results from the NOMAD Experiment.
M.Mezzetto for NOMAD Collaboration. Proceedings of the 5th International Workshop on Topics in Astroparticle and Underground Physics (TAUP97), Gran Sasso, Italy, September, 1997.

[Mik85] Resonance Enhancement of Oscillations in Matter and Solar Neutrino Spectroscopy.
S.P.Mikheyev and A.Y.Smirnov. Soviet Journal of Nuclear Physics, Volume 42, Page 913, 1985.

[Moh91] Massive Neutrinos in Physics and Astrophysics.
R.N.Mohapatra and P.B.Pal. Published by World Scientific, 1991.

[Moo96] Design Description for the SUF Plant at Sudbury (SNO-STR-96-033).
M.Moorhead, N.Tanner, P.Trent, W.Locke, B.Knox, R.Taplin, R.Every, H.Heron. Internal SNO Report, September, 1996.

[Mun90] Fundamentals of Fluid Mechanics.
B.R.Munson, D.F.Young, T.H.Okiishi. Published by John Wiley and Sons, 1990.

[Nak97] Results from Super-Kamiokande.
M.Nakahata. Talk given at APCTP Workshop: Pacific Particle Physics Phenomenology, Seoul, Korea, October, 1997.

[Nob96] Scientific Review of SNO Water Systems by the SNO Water Group.
Edited by A.J.Noble. SNO Report, April, 1996.

[Nor91] Method and Generator for Producing Radioactive ^{212}Pb.
J.H.Norman, W.A.Wrasidlo, K.J.Mysels. United States Patent. Patent Number: 5,038,046. Date of Patent: 6th August 1991.

[Pas97] Direct Bounds on the Tau Neutrino Mass from LEP.
L.Passalacqua et al. Nuclear Physics B (Proceedings Supplements), Volume 55C, Page 435, 1997.

[Pep60] Extraction of Thorium(IV) by Di-Esters of Orthophosphoric Acid.
D.F.Peppard, G.W.Mason and S.McCarty. Journal of Inorganic and Nuclear Chemistry, Volume 13, Page 138, 1960.

[Por78] The Influence of Exhalation, Ventilation and Deposition Processes upon the Concentration of ^{222}Rn, ^{220}Rn and their Decay Products in Room Air.
J.Porstendörfer, A.Wicke and A.Schraub. Health Physics, Volume 34 (May), Page 465, 1978.

[Qur67] Radiochemical Separation of Lead by Amalgam Exchange.
I.H.Qureshi, F.I.Nagi. Talanta, Volume 14, Page 323, 1967.

[Rei64] Limits on Solar Neutrino Flux and Elastic Scattering.
F.Reines and W.R.Kropp. Physical Review Letters, Volume 12, Page 457, 1964.

[Ros87] An Introduction to Neutrino Oscillations and the Solar Neutrino Problem.
S.P.Rosen. Presented at the TASI Meeting, Santa Fe, New Mexico.

[Sat68] The Extraction of Thorium from Hydrochloric Acid Solutions by Di-2-Ethylhexyl Phosphoric Acid.
T.Sato. Zeitschrift für Anorganischen und Allgemeine Chemie, Volume 358, Page 296, 1968.

[Sěb74] Extraction Chromatography using Chelating Agents. VI. Separation of radiothorium (^{228}Th) and its daughter products on paper treated with di(2-ethylhexyl) phosphoric acid.
F.Sěbesta, I.Kron. Radiochemical Radioanalytical Letters, Volume 18 (4), Page 217, 1974.

[Sěd52] Indirect Colourimetric Determination of Lead, Bismuth and Thallium.
V.Sědivec and V.Vašák. Chemické Listy, Volume 46, Page 607, 1952.

[Sha77] Extraction and Separation of Uranium, Thorium and Cerium from Different Mixed Media with HDEHP.
R.Shabana, H.Ruf. Journal of Radioanalytical Chemistry, Volume 36, Page 389, 1977.

[Sta64] The Solvent Extraction of Metal Chelates.
J.Stary. Published by Pergamon, Oxford, 1964.

[Suz94] The Super-Kamiokande Project.
Y.Suzuki. Nuclear Physics B (Proceedings Supplements), Volume 35, Page 273, 1994.

[Tap95a] The Production of ^{228}Th-less ^{224}Ra Solutions using HTiO (SNO-STR-97-005).
R.K.Taplin, M.E.Moorhead. Internal SNO Report, January, 1995.

[Tap95b] The Use of Photomultipliers in SNO.
R.K.Taplin, Hertford College, Oxford University. A thesis submitted in partial fulfilment of the requirements for the degree of Doctor of Philosophy, Michaelmas Term, 1995.

[Tap96] The Elution of Lead and Thorium from HTiO.
R.K.Taplin. Internal SNO Report, April 24, 1996.

[Tap97] Design Description for the Beta Alpha Counters.
R.K.Taplin. Internal SNO Report, July 25, 1997.

[Tre96] The Secondary Concentration of Radium.
P.T.Trent. Private Communication, April, 1996.

[Whi61] Separations by Solvent Extraction with Tri-n-octylphosphine Oxide (NAS-NS 3102).
J.C.White and W.J.Ross. National Academy of Sciences, Nuclear Science Series (Radiochemical Techniques), Oak Ridge National Laboratory, February, 1961.

[Wol78] Neutrino Oscillations in Matter.
L.Wolfenstein. Physical Review D, Volume 17, Page 2369, 1978.

[Zap83] A Time-Dependent Method for Characterizing the Diffusion of ^{222}Rn in Concrete.
G.H.Zapalac. Health Physics, Volume 45 (2), Page 377, 1983.

[Xin98] Monte Carlo Simulations and Analyses of Backgrounds in the Sudbury Neutrino Observatory.
Xin Chen, Balliol College, Oxford University. A thesis submitted in partial fulfilment of the requirements for the degree of Doctor of Philosophy, Trinity Term, 1997.